

APPENDIX F

Attachments from Comment Letter U

APPENDIX F-1

EH City Creek Scour Analysis Final Report

City Creek

Scour Analysis for Inland Feeder Pipeline Crossing



Prepared for:

Black & Veatch
6300 South Syracuse Way, #300
Centennial, CO 80111

Table of Contents

INTRODUCTION.....	1
OBJECTIVE.....	3
PROJECT APPROACH.....	3
Problem Definition	3
Reach Degradation	3
Local Scour	5
Combined Effect.....	6
Approach.....	6
AVAILABLE DATA	7
METHODOLOGY	7
Geomorphic Characterization.....	7
Hydrology Analysis.....	7
Hydraulic Modeling.....	8
Bed Material Characterization	8
Scour Analyses.....	10
RESULTS	17
Geomorphic Characterization.....	17
Field Reconnaissance.....	17
Existing Topography	23
Historical Morphologic Analysis.....	25
Hydrology.....	26
Hydraulics	27
Material Characterization	30

Bed Material Gradation	30
Erosion Resistance	30
Scour Analysis	31
Reach Degradation	31
Local Scour	36
SUMMARY	38
DESIGN ALTERNATIVES	38
Channel Widening without Boundary Hardening	41
Riprap Chute.....	41
Single Vertical Drop Structure	42
Multiple Grade Control Structures	43
REFERENCES	44
APPENDIX A – HYDROLOGY CALCULATIONS	A-1
APPENDIX B – HEC-RAS MODEL	B-1
APPENDIX C – ERODIBILITY INDEX METHOD	C-1
APPENDIX D – ARMOR LAYER	D-1
APPENDIX E – STABLE SLOPE	E-1
APPENDIX F – BEND SCOUR	F-1
APPENDIX G – HEADCUT HYDRAULICS	G-1
APPENDIX H - BLACK & VEATCH RIPRAP GRADATION CALCULATIONS.....	H-1

LIST OF FIGURES

Figure 1. Site Location Map (Obtained From Google Earth)	2
Figure 2. Schematic of Lane's Stream Balance (Taken from Rosgen 1996 after Lane 1955).....	4
Figure 3. Erosion Threshold for Earth Materials with Erodibility Index $K > 0.1$ (Annandale 1995; 2006)	9
Figure 4. Erosion Threshold for Earth Materials With Erodibility Index $K < 0.1$ (Annandale 1996; 2006)	10
Figure 5. Pipeline Crossing Cross Section	13
Figure 6. Flow Around a Bend, Showing Spiraling Transverse Flow and Longitudinal Flow (Annandale 2006).....	14
Figure 7. Headcut Hydraulics (Annandale 2006)	15
Figure 8. City Creek Exiting San Bernardino National Forest.....	18
Figure 9. City Creek Entering Santa Ana River	19
Figure 10. Photo of the Pipeline Crossing (Upstream is on the Right).....	19
Figure 11. City Creek at Highland Ave Looking Downstream	20
Figure 12. Channelization of City Creek (Base Line St and Boulder Ave in Background), Looking Downstream.....	20
Figure 13. Schematic of Historic, Current, and Possible Future Geomorphic Conditions of City Creek.....	21
Figure 14. City Creek Downstream of Baseline Street	22
Figure 15. Headwall of Mining Pit In Floodplain Downstream of Baseline Street	22
Figure 16. City Creek Longitudinal Profile Indicating Head Cut Locations.....	24
Figure 17. Photograph of City Creek in 2003	25
Figure. 18 Photograph of City Creek in 2005	25
Figure 19. Location of USGS Stream Flow Gage 11055800	27
Figure 20. Pipeline Cross-sections Used for the HEC-RAS Models	28
Figure 21. Average Flow Velocities at Pipeline Crossing (Calculated with HEC-RAS).....	28
Figure 22. Shear Stress at Channel Bottom at Pipeline Crossing (Calculated with HEC-RAS)	29
Figure 23. Stream Power at Channel Bottom at pipeline crossing (Calculated with HEC-RAS)	29
Figure 24. Bed Material Gradation (Chang 1995)	30

Figure 25. Existing Grain Size Distribution and Calculated Armor Layer D50 for All Four Geometries Evaluated	32
Figure 26. Predicted Armor Layer Gradation Using Gessler (1970) Compared to Existing Bed Material Gradation at Pipeline Crossing.	33
Figure 27. Estimated Scour Depths Associated With Armor Layer Formation	34
Figure 28. Location and Dimensions of Bend Analyzed	37
Figure 29. Three-Dimensional Image of Calculated Bend Scour at the Pipeline Crossing.	37
Figure 30. Conceptual Configuration of Riprap Lined Rock Chute. Exact Dimensions to be Determined During Preliminary and Final Design.	42
Figure 31. Conceptual Sketch of Single Drop Structure.	42
Figure 32. Multiple Rock Chutes.	43

LIST OF TABLES

Table 1. Available Data	7
Table 2. City Creek Flood Peak Discharges	26
Table 3. Threshold Stream Power at Pipeline Crossing	30
Table 4. Armor Layer Particle Diameter and Associated Depth of Degradation Results at the Pipeline Crossing	32
Table 5. Armor Layer Particle Diameter and Associated Depth of Degradation Results at Existing Headcuts	33
Table 6. Base Level Information and Estimated Time for Stable Conditions to Establish if Median Bed Material Particle Size Dominates in the Determination of Quasi-Equilibrium Conditions	35
Table 7. Estimated Stable Slope, Depth of Degradation, and Rate of Scour at Pipeline Crossing Assuming Median Bed Material Diameter Control	35
Table 8. Comparison Between Stream Power in Bend and Erosion Threshold	36
Table 9. Backroller Stream Power Associated with Active Headcuts	38
Table 10. Optional Mitigation Measures	40
Table 11. Comparison of Erosive Capacity of Water for Design Flood Conditions and the Threshold Stream Power of an Armor Layer that is Expected to Form Under Such Conditions.	41

INTRODUCTION

The Inland-Feeder Pipeline runs beneath City Creek in the reach between Highland Avenue and Boulder Avenue in Southwest San Bernardino County, California (Figure 1). The 12-foot diameter pressurized pipeline was originally buried 20 feet below the City Creek thalweg (Chang 1995). The creek experienced relatively high discharges during the winter of 2004/2005, which led to flooding concerns. As a consequence, the conveyance capacity of the creek was increased by excavating an earthen trapezoidal channel in the stream reach of interest, with a length of about 1.5 miles. The excavation changed the channel morphology from a braided stream to a single-thread stream with a consequent change in hydraulic characteristics. The erosive capacity in the single-thread stream is greater than that of a braided stream, resulting in increased scour at the crossing. An initial rough estimate indicated that the amount of cover above the pipeline has decreased by 8 to 10 feet. At this time, it is not clear if this is due to construction activities or the new channelized conditions. Metropolitan Water District (MWD) requested Engineering & Hydrosystems Inc. (E&H) to evaluate the risk posed to the pipeline by the altered hydraulic and sediment transport regime and to propose mitigation measures, if necessary.

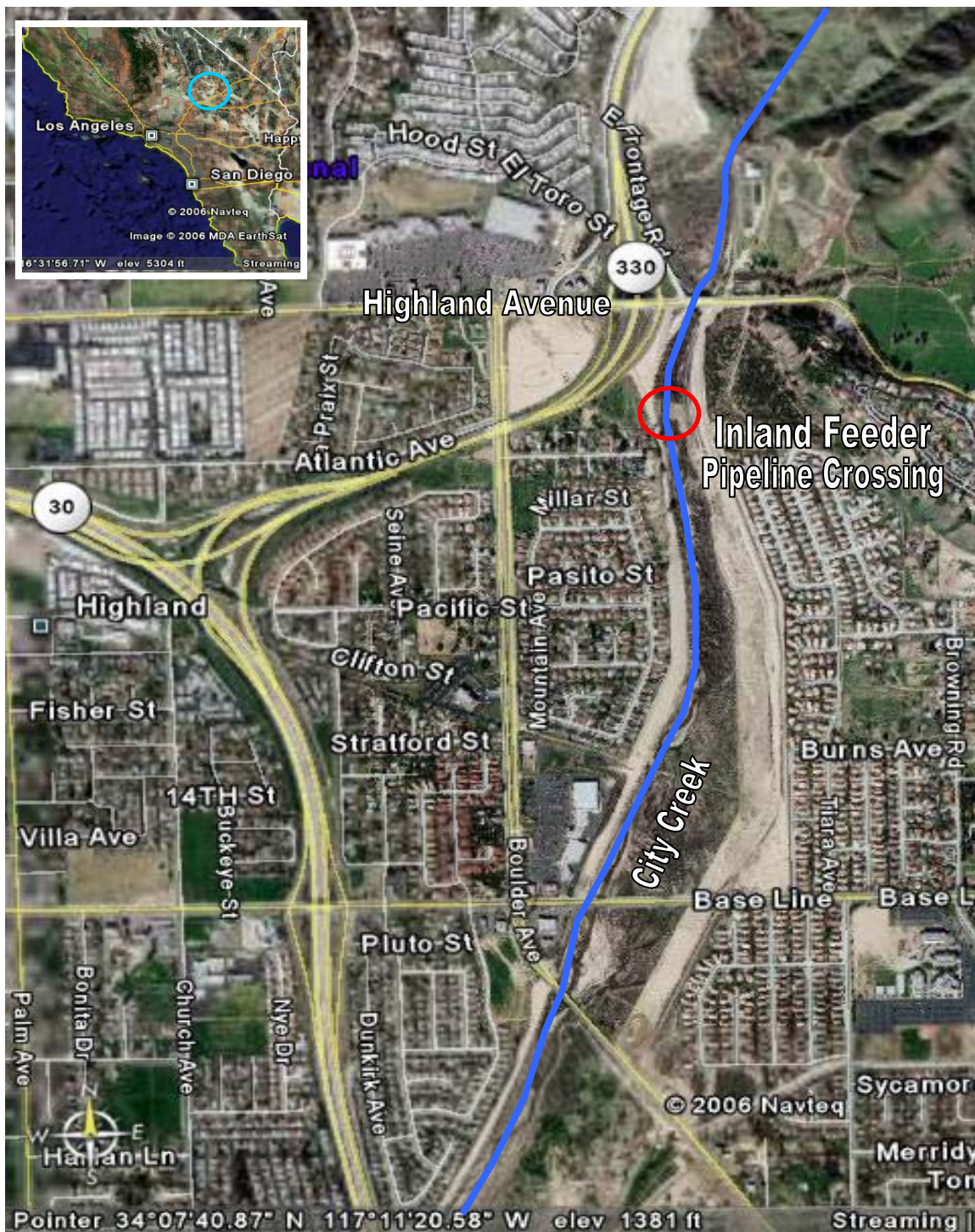


Figure 1. Site Location Map (Obtained From Google Earth)

OBJECTIVE

The objective of this investigation is to determine if the existing soil cover above the Inland Feeder Pipeline is adequate to protect it against future scour that may occur within City Creek. If the cover is inadequate mitigation measures are to be proposed and evaluated for fatal flaws.

PROJECT APPROACH

Problem Definition

Changing the fluvial geomorphologic characteristics of City Creek from a braided to a single-thread stream in the vicinity of the Inland Feeder Pipeline crossing concentrates the erosive capacity of the water on the bed of the excavated channel. This concentration in the water results in increased erosion, characterized as reach degradation and local scour. Reach degradation is the result of erosion along a stream reach, i.e. a general decrease in average reach elevations. Local scour is a response to hydraulic action at local stream irregularities. Such stream irregularities increase the local turbulence intensity in the flowing water, resulting in local lowering of the stream bed. By quantifying the reach degradation and local scour it is possible to assess the risk of stream degradation to the Inland Feeder Pipeline.

Reach Degradation

Reach degradation is the result of erosion manifested over a long river reach (say e.g. between Highlands Avenue and Baseline Avenue, or an even longer distance). When general erosion occurs over a stream reach the average bed elevations along the river reach decrease. Degradation will continue until the variables determining stream channel characteristics are in balance. This is known as a quasi-equilibrium condition, due to the fact that flow variability will always result in varying channel geometry, within certain limits.

The principal parameters determining stable reach conditions are water discharge, sediment properties and channel geometry. A simplified explanation of the relationship between stable reach conditions and the variables determining quasi-equilibrium is given by Lane (Figure 2). This simplification of fluvial geomorphic response to changes in hydrologic, geometric and sediment characteristics in river systems is useful for conceptually understanding and explaining river behavior.

Lane's balance indicates that a river is in quasi-equilibrium (i.e. in balance) for a particular combination of water discharge, sediment characteristics, and channel geometry. The sediment characteristics are represented by sediment load (shown on the left hand scale bucket) and by sediment diameter (represented by the scale on the left arm of the balance). The bucket containing the sediment load can be moved to the left or right along the left arm of the scale, depending on the representative diameter of the sediment. Coarsening of the sediment requires moving the scale pan containing the sediment to the left. If the sediment diameter decreases in size, the scale pan is moved to the right. A change in sediment load, i.e. either an increase or decrease in load, is represented by changing the amount of sediment on the scale pan.

Similarly, the amount of water discharging in the river is represented by the jug containing water on the right hand side of the balance. The geometric characteristics of a river or creek are represented by longitudinal slope. If the river or creek slope increases, the pan containing the

water is moved towards the right. If the slope decreases, the pan is moved towards the left. Additionally, if the discharge in the river or creek increases, the amount of water in the jug on the right hand scale pan is increased.

The anticipated fluvial geomorphologic response of a river or creek is determined by making observations on the movement of the indicator in the middle of the scale. If the scale tips towards the right, the indicator moves towards the left, indicating degradation. Alternatively, if the scale tips towards the left, the pointer moves towards the right indicating aggradation.

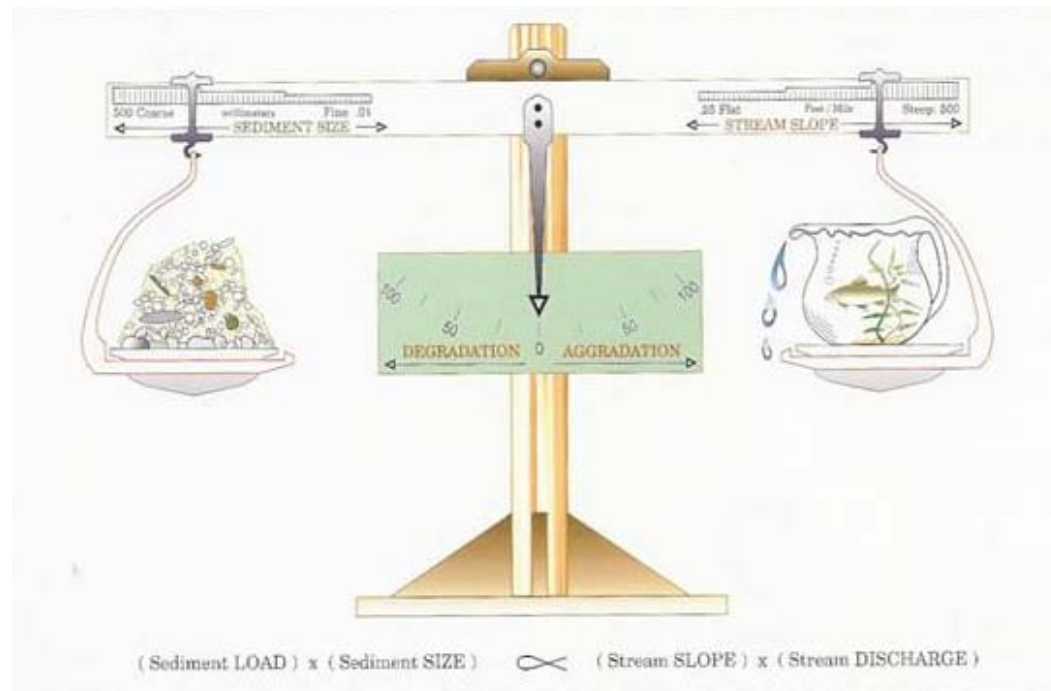


Figure 2. Schematic of Lane's Stream Balance (Taken from Rosgen 1996 after Lane 1955)

For example, to interpret the anticipated response of City Creek to the channelization project one proceeds as follows. By changing the channel characteristics from a braided channel to a single channel, the amount of discharge is effectively increased. This is deduced from the fact that the amount of discharge per channel in a braided system is less than the combined discharge in a single-thread channel. Additionally, the average channel slope has been increased because of the reduction in sinuosity. A braided channel is much more sinuous than the straight, channelized reach. Therefore, by increasing the amount of water in the jug shown in the Lane diagram (representing the increased concentration of flow in the channel) and by moving the scale pan containing the jug to the right (indicating an increase in slope), one expects the scale pointer to move towards the left; indicating degradation.

An important part of the reach analysis is to quantify the relationship between sediment characteristics, water discharge and channel slope. The objective of such an analysis is to quantify the long-term stable reach slope. Such an analysis assumes that the sediment and water discharge characteristics are known.

The water discharge characteristic is represented by the magnitude of what is known as the channel-forming discharge, which is normally defined as approximately equal to the 2-year

recurrence interval discharge (Annable1994 and Andrews1980). This is a discharge that occurs on a regular basis, regular enough to exert a dominant impact on the long term characteristics of a stream reach.

When considering the impact of sediment characteristics on the long term stable stream slope it is necessary to account for the characteristics of the bed material gradation. Stream bed material gradations can consist of fine material only, coarse material only, or a combination of fine and coarse material. Coarse material is defined, somewhat arbitrarily, as sediment particles that cannot be moved by the water flowing in the stream during channel-forming discharge.

From a stable slope analysis point of view, the scenarios where the bed material consists of almost uniformly distributed fine or coarse particles, the long term stable slope can be related to the median diameter of the bed material. This is done by making use of established techniques relating discharge, sediment particle diameter and channel slope. These methods are identified in the report section dealing with methodology.

Should the bed material gradation consist of both fine and coarse material, an additional analysis is required. In such cases it is possible that the coarse material can form an armor layer consisting of the coarsest sediment particles in the bed material mix. An armor layer develops when the fine sediment particles that can be removed by the flowing water have been removed and are no longer present in the top layer of the bed material. In such a case only the coarse material remains in the top stream bed material layer. The latter forms a continuous layer along the bed surface and protects the underlying fine material from scour. Experience has shown that the formation of armor layers is possible if the amount of coarse material in the sediment gradation equals 10% or more (Pemberton and Lara 1984).

Once it has been established that it is possible for an armor layer to form, it is necessary to determine the amount of scour that will occur before the layer is in place. This scour occurs due to the removal of fine particles from the upper layer of the bed material. If it is desired to know the stable slope of the stream once an armor layer has established, the amount of scour prior to armor layer formation at various locations along the stream reach is determined. Connecting these elevations it is possible to develop an estimate of the stable long section of the stream. Methods for determining the potential for armor layer formation and the amount of scour that will occur prior to armor layer formation are presented in the section dealing with methodology.

Local Scour

Local scour occurs due to increased flow turbulence developing in the immediate vicinity of an irregularity in stream geometry. Such irregularities include bridge piers, flow contraction due to the presence of bridge abutments, and irregularities in a stream bed profile, such as headcuts. A headcut is a sudden drop in a river bed. When a water jet discharges over a drop it can lead to the formation of a backroller between the upstream, vertical face of the headcut and the point of jet impact. If the erosive capacity of the water in the backroller is greater than the ability of the earth material in the headcut face to resist erosion, this material will erode and the headcut will move upstream. This action is known as headcut migration. The magnitude of the erosive capacity of water in the immediate vicinity of local irregularities is usually significantly greater than the erosive capacity of water merely flowing over a stream bed with a regular, continuous slope. Therefore, the rate of scour at irregularities is usually greater than that associated with reach degradation.

Combined Effect

The total scour at the pipeline crossing is the sum of the reach degradation and local scour. When combining the quantitative results of the analyses, appropriate interpretation of results is required. The long term elevations of the stream thalweg is represented by the maximum elevations of either the stable slope determined using the median particle diameter of the sediment gradation or that associated with the degradation of the stream bed associated with the formation of bed armoring.

The process of combining the local scour estimates with the long term stable thalweg depends on the kind of local scour. If the local scour is the result of bridge pier scour or contraction scour between bridge abutments, it is normally subtracted from the long term stable bed profile. This is justified if an armor layer that formed on the bed is unable to resist the increase in erosive capacity of the water at these irregularities.

If the local scour is due to the presence of headcuts these are normally not subtracted from the stable bed elevation. The reason for this is that headcuts are interpreted as geomorphic processes accelerating the river processes leading to long term stability. These processes are perceived to occur during the interim phases, prior to establishment of the long term stable reach slope.

Approach

The approach followed in this investigation entails combining fluvial geomorphologic and fluvial hydraulic expertise and experience to assess scour potential at the Inland Feeder Pipeline crossing at City Creek. As standard practice, E&H takes a watershed approach to geomorphic investigations. In order to understand the erosion/deposition processes at a single cross section, which in this case is the pipeline crossing, it is imperative to understand the processes occurring within the system, i.e. the watershed.

By following this approach the investigation included visiting the site, conducting a fly-over with a helicopter provided by MWD, and conducting detailed scour analyses using fluvial geomorphologic and fluvial hydraulic principles. This assessment entailed conducting a fluvial geomorphologic characterization of the watershed and the stream reach up to the confluence with the Santa Ana River, followed by hydrologic and hydraulic analyses, stream bed material characterization, and, finally, a scour analysis. The latter consisted of quantifying reach degradation and local scour as conceptually outlined in the previous section. Once the extent of long term erosion has been quantified, the risk of pipeline exposure was determined and optional protection techniques identified for safeguarding the pipeline crossing against the effects of scour.

AVAILABLE DATA

In order to conduct our analyses, the hydrology, geometry, bed material characteristics, and historical condition of the reach are required. Table 1 lists the data collected and used for our analyses.

Table 1. Available Data

Source	Data
MWD	Photographs of City Creek (pre and post channelization)
MWD	Chang, Howard H. 1995. Inland Feeder Pipeline, San Bernardino Segment (Contract 3): Fluvial Study of City Creek for Pipeline Placement. Prepared for Dames and Moore
MWD	Bridge surveys of Highland Avenue, Baseline Street, and Boulder Avenue
MWD	AutoCAD topographical map of site created from surveyed data
USGS	Annual peak stream flow data from USGS gage 11055800 for the period of record (1920-2004)

METHODOLOGY

Geomorphic Characterization

Geomorphic characterization of the watershed is critical for understanding the potential mechanisms for scour. A geomorphic analysis involves studying the current field conditions, site topography and historical site and watershed conditions. Current field conditions including vegetation, presence/absence of headcuts, condition of tributaries, bank shape and steepness, viewed in terms of the fluvial geomorphologic balance represented by Figure 2, allow an interpretation of the current channel stability. Topographic maps of the site enhance the field information by allowing detailed calculations of the stream morphometry. Historical analysis of stream channel plan form using current and historical aerial photographs and investigations of the changes in the longitudinal stream profile using current and historic topographic maps and surveys add to the interpretation of the condition of the creek or river, and potential future trends.

Hydrology Analysis

The scour analysis required peak discharge magnitudes associated with the 2- and 100-year recurrence intervals. Chang (1995) provides hydrologic data, i.e. peak discharges for the 10-year, 50-year, 100-year 3-hour, 100-year 24-hour, and the Standard Project Flood (SPF). For this investigation, the channel-forming discharge was also required.

Channel forming discharge is the discharge that is assumed to play the dominant role in determining the long-term morphology of a river or stream, which is of principal interest in this investigation. The channel-forming discharge for City Creek was assumed to be represented

by the 2-year recurrence interval flow. The selection of a 2-year recurrence interval flow implies that the long-term morphology of rivers is determined by flows that occur on a regular basis. This, of course, does not mean that major floods, such as a 50- or 100- year flood, will not affect morphometry. On the contrary, such floods affect short term response of river and creek morphometry and should be accounted for in infrastructure design.

The 2-yr discharge for City Creek was calculated using a log Pearson type III analysis. The log Pearson type III is a type of probability distribution used in the United States for relating flood-peak magnitude and probability of occurrence (Haan et al. 1994). Yearly peak discharge data was obtained from USGS gage 11055800, located on City Creek approximately one mile upstream of the Pipeline crossing. This gage provided 85 years of annual peak discharge data. The calculations are contained in Appendix A.

Hydraulic Modeling

It is necessary to quantify the hydraulic parameters associated with the 2-yr and 100-yr flows at the crossing and along the creek to calculate the potential scour depth. The hydraulic characteristics of the 2-yr flood were used to estimate long term stable creek conditions; while those of the 100-year flow are used to assess short term, i.e. event-based, impacts.

The HEC-RAS software was used to quantify the hydraulic parameters of the creek. HEC-RAS v. 3.1.3 (USACE 2005) is a software package that can perform one-dimensional steady flow and unsteady flow hydraulic calculations for networks of natural and constructed channels. Developed by the Hydrologic Engineering Center at the U.S. Army Corps of Engineers, the system comprises a graphical user interface, separate hydraulic analysis components, data storage and management capabilities, and graphics and reporting facilities. Data requirements include channel geometry, flow data and hydraulic boundary conditions. HEC-RAS model input and output are included in Appendix B.

Bed Material Characterization

Bed material characterization entails quantifying the physical properties and erosion resistance of the stream bed material. In the case of City Creek the bed material consists of non-cohesive sediment and physical characterization is accomplished by conducting gradation analyses on the earth material. Determination of the erosion resistance of the bed material can be accomplished by making use of acknowledged methods, such as the Shields (1936) diagram and the Erodibility Index Method (EIM) (Annandale 1995). The principal method for quantifying erosion resistance used during the course of this project is the EIM. This method has been used for a number of years and has been shown to correlate favorably with field experience (Annandale 2006). However, other methods, including the Shields diagram, are used to estimate reach degradation.

The EIM defines a threshold between erosion and non-erosion by relating the erosive capacity of water, expressed in terms of stream power, and the relative ability of earth material to resist erosion, expressed in terms of the erodibility index (Appendix C). The index is the scalar product of the values of its constituent parameters and takes the form:

$$K = M_s * K_b * K_d * J_s \quad (0.1)$$

M_s = mass strength number

K_b = particle/block size number = $1000 * (d \text{ (in meters)})^3$ for non-cohesive particulate matter

K_d = discontinuity or inter-particle bond shear strength number = tangent of the angle of internal friction in the case of non-cohesive particulate matter

J_s = relative ground structure number

d = characteristic particle size; = median particle size in the case of no armoring; = armor material size in the presence of armoring.

The numbers identified above are quantified by making use of tables in Annandale (1995, 2006). The Erodibility Index K for a particular earth material is used to determine the threshold stream power per unit area. If the stream power of the water is greater than the threshold stream power, the earth material will erode. If it is lower, the earth material will not erode. The erosion thresholds for earth materials with $K > 0.1$ and $K < 0.1$, respectively, are shown on Figure 3 and Figure 4.

The stream power exerted by the water can be obtained from the HEC-RAS model for open channel flow conditions. It is quantified by analytical means for other flow conditions, such as those present at bridge piers, headcuts and hydraulic jumps (Annandale 2006).

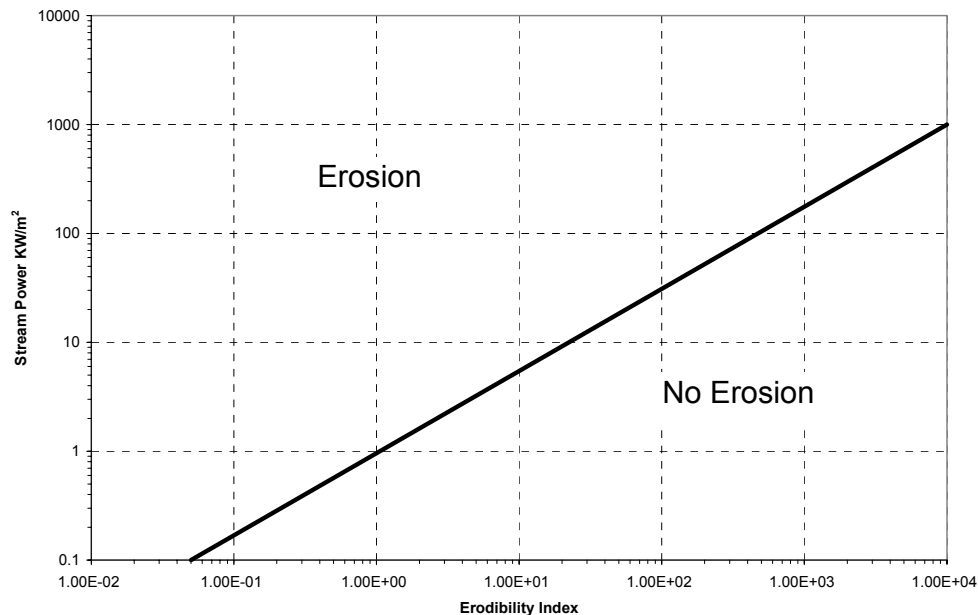


Figure 3. Erosion Threshold for Earth Materials with Erodibility Index $K > 0.1$ (Annandale 1995; 2006)

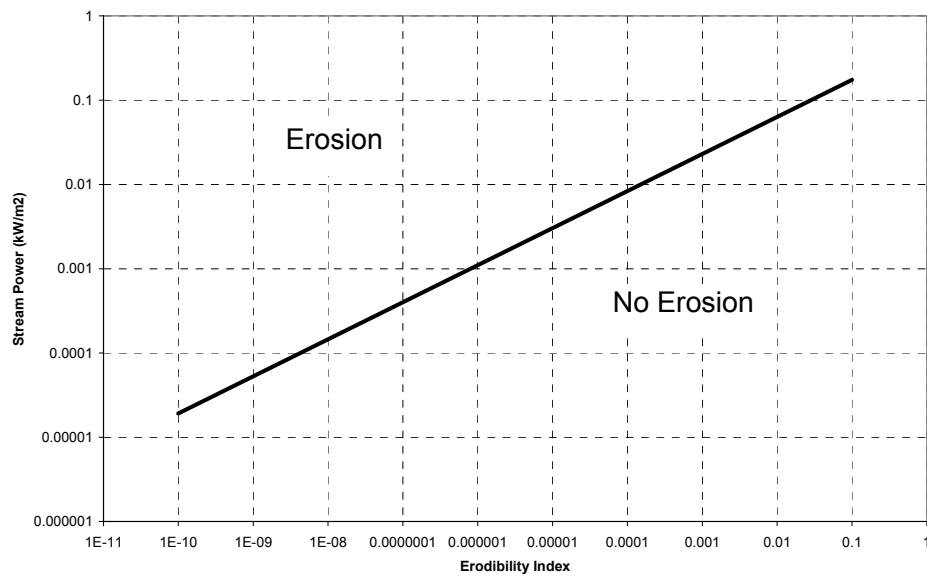


Figure 4. Erosion Threshold for Earth Materials With Erodibility Index $K < 0.1$ (Annandale 1996; 2006)

Scour Analyses

Reach Degradation

Pemberton and Lara (1984) outline an analytical approach for implementing the concept of the Lane balance (Figure 2) in practice, i.e. estimating reach degradation and quantifying the long term stable slope for quasi-equilibrium conditions. It is important to note that analytical techniques contained in this publication do not address streambed and/or valley controls such as rock outcrops, vegetation, or manmade changes. "A control in the channel may in some cases prevent any appreciable degradation from occurring above it. Conversely, a change or removal of an existing control may initiate the degradation process (Pemberton and Lara 1984)."

Reach Degradation Associated with Armor Layer Formation

The formation of an armor layer is associated with bed scour, which results due to the removal of fine bed material particles subject to erosion. Once the fine particles have been removed and the armor layer has established, scour ceases. Reach degradation associated with the formation of armor layers is therefore equal to the amount of overall degradation occurring prior to armor layer formation. Pemberton and Lara (1984) recommend using the following five methods for estimating the characteristic armor layer particle size (see Appendix D for detail):

1. Meyer-Peter, Muller sediment transport equation,
2. Competent bottom velocity method;
3. Lane's tractive force theory;
4. Shields diagram; and

5. Yang incipient motion

Gessler (1970) established a method that was found to be very useful for estimating armor layer characteristics. This method is more detailed and has been found to provide satisfactory results when compared to field observations (Oehy 1999). A unique feature of the Gessler method is that it results in a sediment gradation curve of the armor layer. This method has also been used to estimate the armor layer characteristics.

Once the physical characteristics of the armor layer are known, the amount of scour is calculated by making use of an equation recommended by Pemberton and Lara (1984), i.e.

$$y_d = y_a \left(\frac{1}{\Delta p} - 1 \right) \quad (0.2)$$

where y_d = amount of scour, measured in the vertical direction; y_a = thickness of the armor layer; Δp = percentage of material in the original bed material gradation that is equal to or exceeds the armor layer particle size.

Example calculations and results when implementing these six methods for determining armor layer size and using equation (0.2) to estimate scour associated with armor layer formation are included in Appendix D.

Reach Degradation in the Absence of Armor Layer Formation

Reach degradation associated with flow conditions in the absence of armor layer formation is a function of the difference between the stream slope prior to establishment of stable flow conditions and that after establishment of stable flow conditions, as previously outlined. Streams subject to degradation will decrease their longitudinal slope until a new level of equilibrium is reached. As degradation occurs the longitudinal slope of the river gradually decreases, and, with it, the erosive capacity of the water. Once the erosive capacity of the water is equal to the erosion threshold of the bed material a stable slope has been established.

The methods implemented by Pemberton and Lara (1984) for calculating stable slope include (see Appendix E for detail on implementing these methods):

1. Schoklitsch bedload equation;
2. Meyer-Peter Muller sediment transport equation;
3. Shields diagram; and
4. Lane's relationship for critical tractive force assuming clear water-flow in canals.

The results obtained by implementing the four methods listed above are interpreted and a long term stable slope for the stream assigned.

Local Scour

Mechanisms of local degradation include contraction scour, pier scour, abutment scour, bed form scour (dune formation and propagation), headcut migration, bend scour, and low-flow channel incisement. During the field investigation it was determined that contraction scour; pier

scour, abutment scour, bed form scour and low-flow channel incisement would not be the large-scale factors influencing bed stability at the Pipeline. The only two significant local scour features identified are bend scour and headcut migration.

Bridge pier and contraction scour were not considered due to the fact that these scour types do not currently affect scour at the pipeline. The Pipeline crossing is not within the limits of any pier or abutment scour associated with the Highland Avenue or Baseline Street bridges.

Additionally, the Highland Avenue Bridge crossing contains a concrete apron overlying the earth material. The crossing at Baseline Street is a concrete box culvert. The concrete linings will protect this infrastructure against the effects of scour as long as they remain in place. It is therefore important to prevent scour occurring just downstream of these concrete aprons from destroying the aprons themselves. Significant scour just downstream of the Highland Avenue Bridge is already present. Gravel mining downstream of the Baseline Street crossing (see discussion further on) may also have an adverse impact on the long term stability of this culvert. Should scour just downstream of the creek crossings destroy the protective layer provided by the concrete linings, the additional scour may have an adverse effect on scour at the Inland Feeder Pipeline crossing.

The particle sizes present in the bed are not prone to dune formation or dune migration. We therefore expect that dune formation will play an insignificant role.

Low-flow channel incisement can potentially pose problems if not taken into account in the mitigation design. Figure 5 indicates incision may have already occurred. However, although low-flow channel incisement currently appears to play a role, the channel is expected to assume a braided condition in the long term (decades from now), with relatively small channel depths. (This assessment is discussed below in GEOMORPHIC CHARACTERIZATION section.) Therefore, low-flow incisement would be a relatively insignificant amount of scour relative to the overall long-term degradation. When developing mitigation designs it should be prepared in a manner that will encourage formation of a braided channel configuration. Low-flow channel incisement potential has therefore not been investigated as it will be accounted for in the mitigation design.

The principal local scour features considered in this investigation are bend scour and headcut migration.

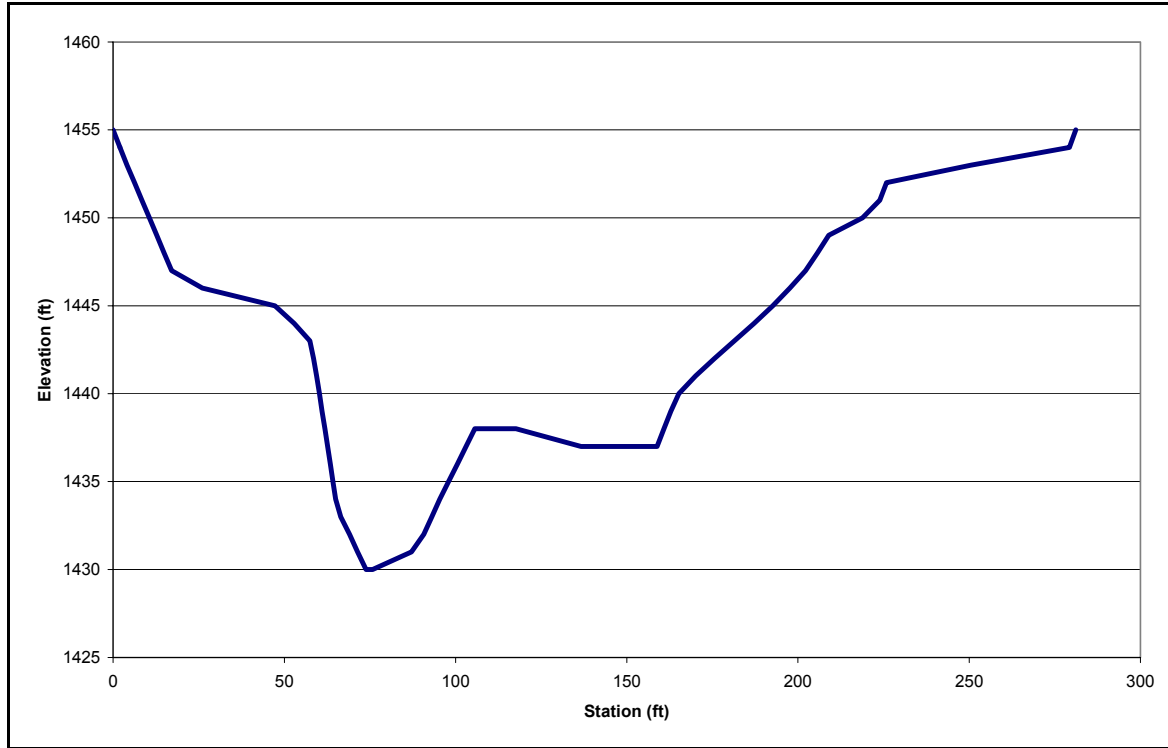


Figure 5. Pipeline Crossing Cross Section

Bend Scour

The potential for and the magnitude of bend scour are determined by first quantifying the magnitude of the stream power of the water flowing around the bend, and comparing it with the erosion threshold of the material in the stream bed. Once it has been established that the bed material can potentially scour, i.e. the erosion threshold is exceeded when water flows around the bend, then the magnitude of the scour is determined by making use of a three-dimensional analytical model.

The magnitude of the stream power flowing around a bend can be calculated by making use of a method described by Annandale (2006). The total stream power around a bend can be quantified as,

$$P_{\text{total}} = P_{\text{channel}} + P_{\text{bend}} \quad (0.3)$$

where P_{total} = total stream power around the bend; P_{channel} = stream power that would normally exist in a straight stream reach = $\gamma Q s_f$; γ = unit weight of water; Q = water discharge; s_f = energy slope of the flowing water.

The stream power caused by the spiraling flow as water discharges around a bend P_{bend} is calculated by solving the following integral, Chang (1992) (see Appendix F). The variables in the integral are defined on Figure 6.

$$P_{\text{bend}} = \int_{r_1}^{r_2} \int_0^D \rho v \frac{u^2}{r_c} dz \cdot dr \quad (0.4)$$

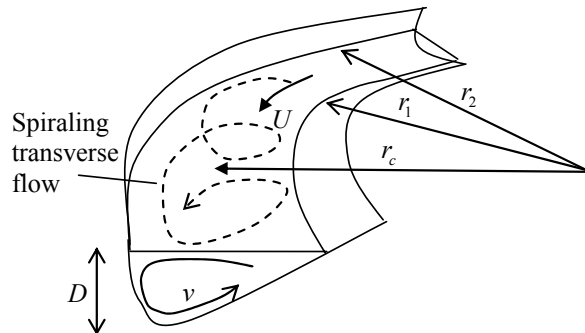


Figure 6. Flow Around a Bend, Showing Spiraling Transverse Flow and Longitudinal Flow (Annandale 2006)

If the comparison of the total stream power calculated with equations (0.3) and (0.4), and the threshold stream power of the earth material within the bend indicates scour potential, the magnitude of the bend scour is determined by making use of an analytical technique developed by Odgaard (1986). The method is not explained here, but an example of its application to City Creek is presented in Appendix F. It was considered necessary to estimate bend scour as the current configuration of flow over the Inland Feeder Pipeline occurs around a bend.

Headcut Migration Potential

Multiple, active head cuts were noted during the field visit. Headcut migration, as explained previously in the report, is a long term scour mechanism, which, over time, aids in achieving equilibrium in the channel. The potential for headcut migration was assessed on a local level by evaluating the existing headcuts and quantifying the stream power discharging over the drops in the stream bed (Figure 7) and comparing it with the erosion threshold stream power of the bed material. In particular, it is necessary to quantify the magnitude of the stream power of back-rollers forming upstream of the impingement point of the water jet discharging over the drop and impacting the drop face. Methods for quantifying the magnitude of the stream power at a headcut for both super- and sub-critical upstream flow are detailed in Annandale (2006).

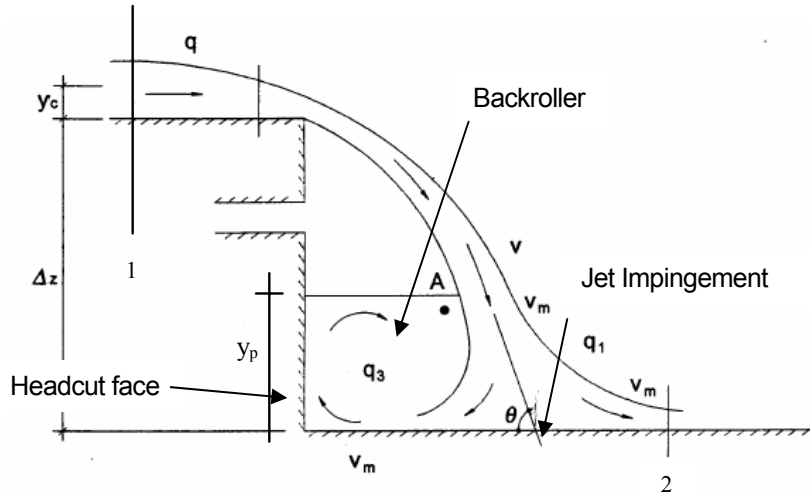


Figure 7. Headcut Hydraulics (Annandale 2006)

As the jet impinges onto the downstream bed of the stream at an angle θ it splits into two, part of it flowing upstream to form a backroller (unit discharge of backroller is q_3) and the rest flowing downstream. The unit discharge flowing in a downstream direction (q_1) is equal to the unit discharge q once equilibrium is reached. The discharge q_3 from the roller feeds back into the jet at A, with the same amount of water discharging back into it at the point of impingement. The discharge in the jet at the elevation of point A is therefore equal to $q + q_3$, leading to a local widening of the jet. It can be shown (Moore 1941) that the ratio between the flows is,

$$\frac{q_1}{q_3} = \frac{(1 + \cos \theta)}{(1 - \cos \theta)} \quad (0.5)$$

By applying the momentum equation Henderson (1966) shows that

$$V_m = \frac{V}{2} \cdot (1 + \cos \theta) \quad (0.6)$$

and that

$$\cos \theta = \frac{1.06}{\sqrt{\frac{\Delta z}{y_c} + \frac{3}{2}}} \quad (0.7)$$

Expressing the total energy head loss as

$$\Delta E = \Delta z + \frac{3}{2} \cdot y_c - y_1 - \frac{V_m^2}{2 \cdot g} \quad (0.8)$$

where y_1 = downstream depth, it can be shown that the total energy loss can be expressed in dimensionless form solely as a function of the drop height and critical depth at the drop, i.e.

$$\frac{\Delta E}{y_c} = \frac{\Delta z}{y_c} + \frac{3}{2} - \frac{y_1}{y_c} - \frac{1}{4} \cdot \left(\frac{3}{2} + \frac{\Delta z}{y_c} \right) \cdot \left[1 + \frac{1.06}{\sqrt{\frac{\Delta z}{y_c} + \frac{3}{2}}} \right]^2 \quad (0.9)$$

With this estimate of energy head loss at the base of a headcut known, it is now possible to estimate the total rate of energy dissipation per unit width of flow (and thus the stream power per unit width of flow) at the point of impingement (impact) at the base of a headcut.

$$SP_{impact} = \gamma \cdot q \cdot y_c \cdot \left[\frac{\Delta z}{y_c} + \frac{3}{2} - \frac{y_1}{y_c} - \frac{1}{4} \cdot \left(\frac{3}{2} + \frac{\Delta z}{y_c} \right) \cdot \left[1 + \frac{1.06}{\sqrt{\frac{\Delta z}{y_c} + \frac{3}{2}}} \right]^2 \right] \quad (0.10)$$

By using an equation derived by Henderson (1966) to calculate the portion of the energy loss in the backroller it is possible to calculate its rate of energy dissipation. This is the power per unit width of flow that will interact with the face of a headcut.

$$SP_{backroller} = \gamma q y_c \left[\frac{1}{4} \left(\frac{3}{2} + \frac{\Delta z}{y_c} \right) \left[1 + \frac{1.06}{\sqrt{\frac{\Delta z}{y_c} + \frac{3}{2}}} \right]^2 \right] \quad (0.11)$$

The stream power per unit area on the face of the headcut can therefore be determined by dividing equation (0.11) by the depth of the pool y_p that forms behind the jet. This can be calculated with an equation developed by Chamani and Beirami (2002).

$$\frac{y_p}{y_c} = \sqrt{\left(\frac{y_1}{y_c} \right)^2 + 2Fr_1^2 \left(\frac{y_c}{y_1} \right) - (2Fr_1^2 + 1)} \quad (0.12)$$

The authors tested this equation for both super- and sub-critical flow in the reaches upstream of the drop. The best agreement with experimental results was found for sub-critical flow. Example calculations are provided in Appendix G.

RESULTS

Geomorphic Characterization

Field Reconnaissance

The field reconnaissance took place at the end of September 2005. The investigation included both ground and aerial assessment. The headwaters of City Creek originate in the San Bernardino National Forest (Figure 8), resulting in high bed loads that are aggravated by forest fires. High sediment loads have been reported in the Creek, especially during post-fire conditions. The high bed load is maintained as the Creek passes over the Inland Feeder Pipeline. This reach is characterized by relatively steep slopes and large particles comprising the channel bed and banks (cobble and boulder).

The confluence between City Creek and the Santa Ana River is about 3.5 miles downstream of the Pipeline crossing (Figure 9). The Santa Ana River, with very high sediment loads and characterized by a wide, braided channel, acts as the local base level for City Creek. Therefore, if the Santa Ana River would experience a significant adjustment in bed elevation it will, in turn, adversely affect City Creek. No signs of adverse impacts on City Creek, originating from the Santa Ana River, have been observed during the site visit. Degradation in City Creek originates from other sources, particularly human intervention.

The largest man-made impact at the pipeline crossing (Figure 10) is the recent channelization, which commences at Highland Ave (Figure 11) and continues downstream towards Baseline Street (Figure 12). All vegetation in this part of the channel, which existed prior to channelization, has been removed (compare Figure 17 and Figure. 18). The channelization project resulted in a significantly decreased width and a trapezoidal channel shape with side-slopes graded at about 3H:1V.

This channelization has completely altered the erosion and deposition processes occurring between Highlands Ave and Baseline Street. Chang noted in 1995 that this reach “has been found to have a mild trend for sediment deposition.” Multiple headcuts migrating upstream were observed during the 2005 field investigation, which is indicative of an actively degrading reach.

By channelizing this reach, the depositional zone has been moved farther downstream (Figure 13). This reach has now become an erosional zone and the sediment is carried farther downstream. If no human intervention would be imposed on the creek from here onwards, through *geologic* time City Creek would return to the quasi-equilibrium conditions noted in 1995. However, in the near future, the Pipeline is in danger of being exposed and interim action is required to protect it against scour.

Further downstream, i.e. upstream of Boulder Avenue and downstream of Baseline Street, aggregate mining adversely impacts creek stability (Figure 14 and Figure 15). In this reach the channel flows along the right creek bank. The left bank of the small stream consists of small cobbles, about 2 feet high (Figure 14). The left floodplain has been completely excavated and currently forms a mine pit (see Figure 14 and Figure 15). If a large discharge were to flow down City Creek the presence of the pit could potentially lead to the initiation of a large headcut. The

headcut could threaten Baseline Street Bridge and could potentially cause significant degradation at the Pipeline Crossing if bridge road crossing failure occurs. For purposes of this study, we assumed that any headcut associated with the pit would be arrested at Baseline Street. This position is based on the assumption that the road will be maintained and kept in good condition.



Figure 8. City Creek Exiting San Bernardino National Forest



Figure 9. City Creek Entering Santa Ana River



Figure 10. Photo of the Pipeline Crossing (Upstream is on the Right)



Figure 11. City Creek at Highland Ave Looking Downstream



Figure 12. Channelization of City Creek (Base Line St and Boulder Ave in Background), Looking Downstream

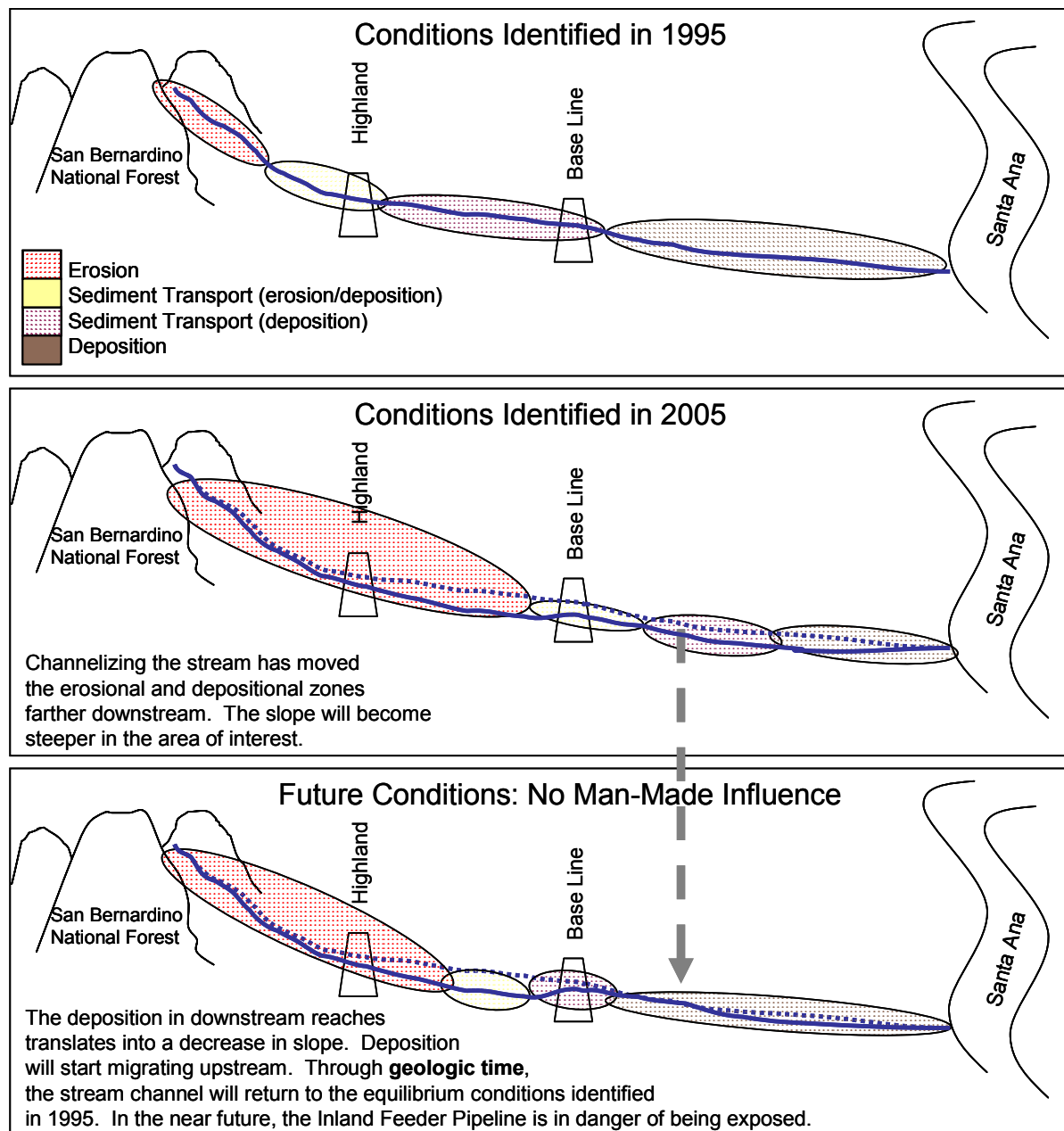


Figure 13. Schematic of Historic, Current, and Possible Future Geomorphic Conditions of City Creek

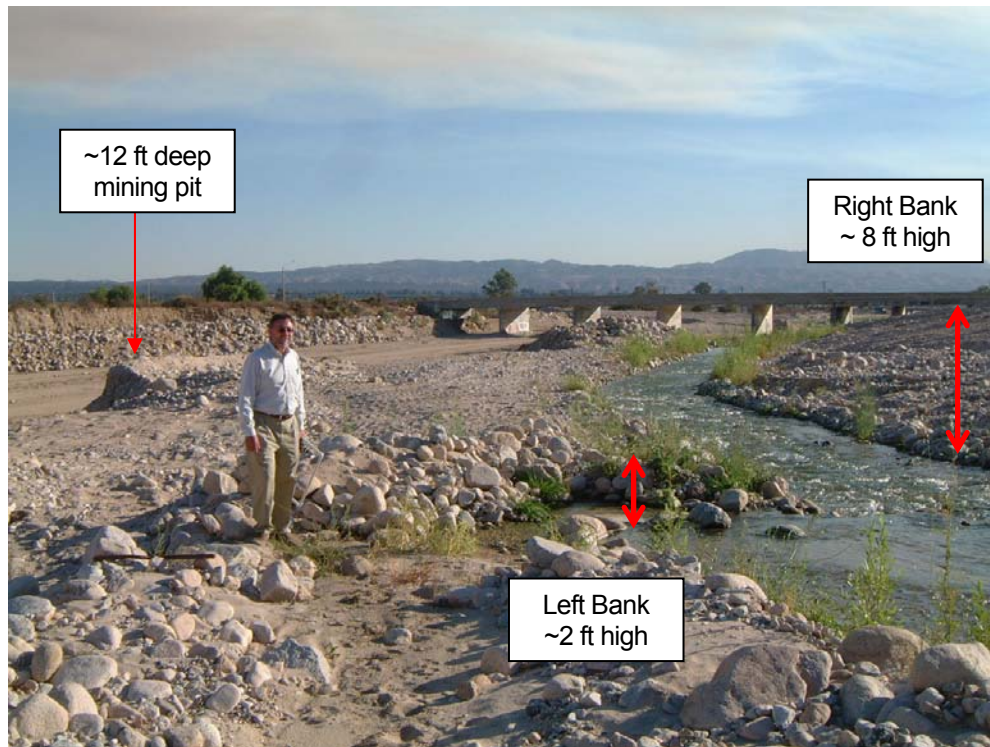


Figure 14. City Creek Downstream of Baseline Street



Figure 15. Headwall of Mining Pit In Floodplain Downstream of Baseline Street

Existing Topography

The site topography was obtained from drawings provided by MWD (Plate 1). The current average longitudinal slope of the creek is 0.027 ft/ft, while that in the vicinity of the pipe crossing is 0.039 ft/ft. The longitudinal profile of the main thalweg (Figure 16) illustrates the presence of headcuts throughout the reach. Most of these headcuts are actively migrating upstream.

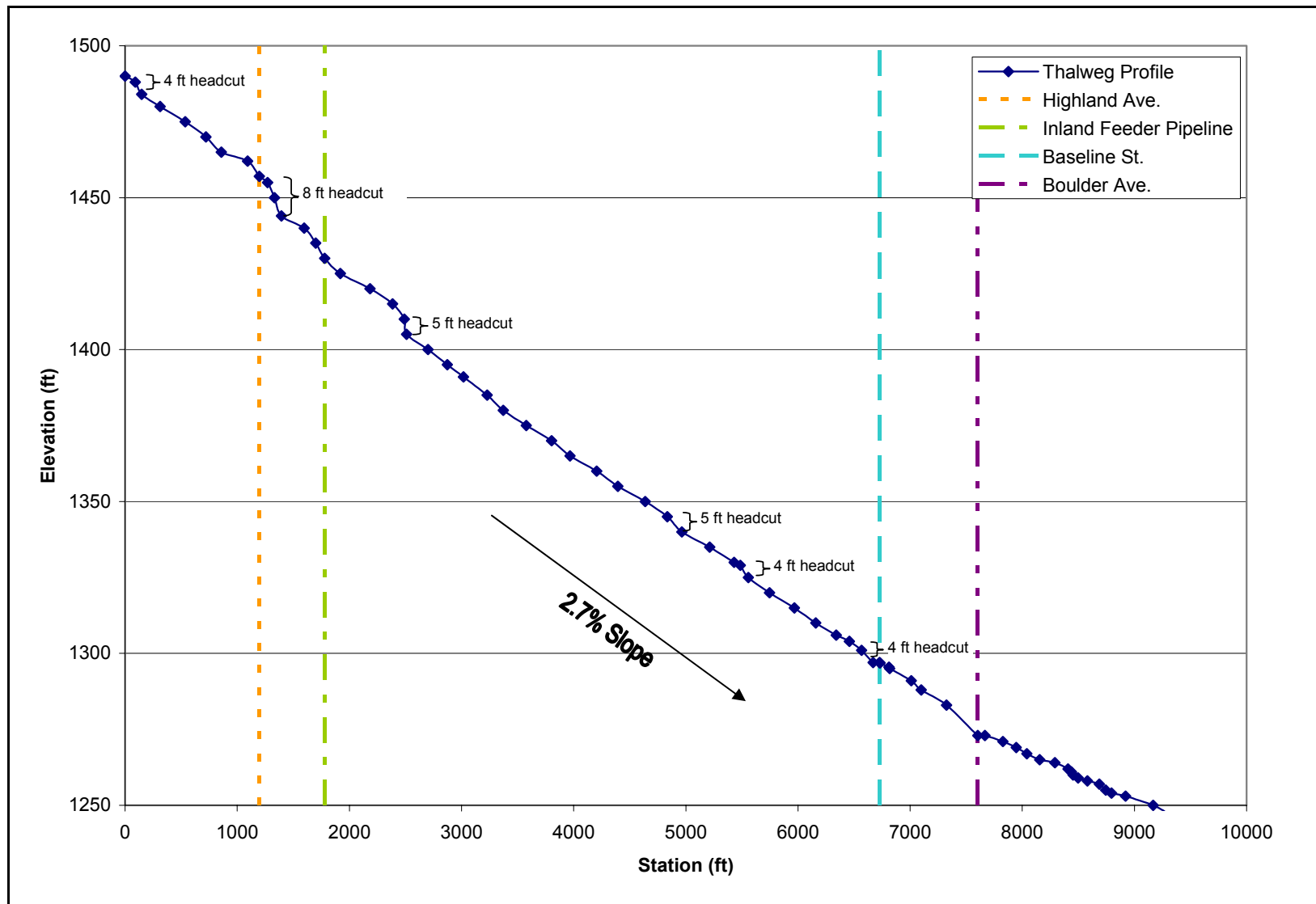


Figure 16. City Creek Longitudinal Profile Indicating Head Cut Locations



Figure 17. Photograph of City Creek in 2003



Figure. 18 Photograph of City Creek in 2005

Historical Morphologic Analysis

E&H did not conduct a full investigation into the historical morphology of the channel. The reason for this is that the recent alterations to the channel are deemed to have a more substantial impact on the hydraulics and sediment transport of the creek than what historical trends would show. This is readily apparent when comparing Figure 17 and Figure. 18. The removal of vegetation significantly increased the erosion potential of the channel, as did the channelization imposed on the creek.

Hydrology

The majority of the hydrologic data required for the analysis, i.e. the flood peak estimates for the 10-yr 24-hr, 50-yr 24-hr, 100-yr 3-hr, 100-yr 24-hr, and the Standard Project Flood are contained in the report by Chang (1995). Additionally, an estimate of the 2-yr recurrence interval flood, i.e. the assumed dominant flow, is also required for estimating stable creek conditions.

To estimate the magnitude of the 2-yr storm, the yearly peak discharge data was obtained from USGS gage 11055800 located on City Creek approximately one mile upstream of the Pipeline crossing (Figure 19). This gage provided 85 years of annual peak discharges. Using a log Pearson type III distribution, the 2-yr flood peak was calculated as 400 cfs (see Appendix A). The flood peak discharges obtained with the statistical analysis are compared with those from Chang (1995) – see Table 2. The highlighted discharges were used for analyzing scour in order to be consistent with previous studies.

Table 2. City Creek Flood Peak Discharges

	Log Pearson III	Chang (1995)
Recurrence	Discharge (cfs)	Discharge (cfs)
Standard Project Flood	N/A	15000
100-yr (24-hr storm)	8548	10500
100-yr (3-hr storm)	N/A	13000
50-yr	5983	6600
25-yr	4021	N/A
10-yr	2174	2150
5-yr	1221	N/A
2-yr	400	N/A
1.0101-yr	19	N/A

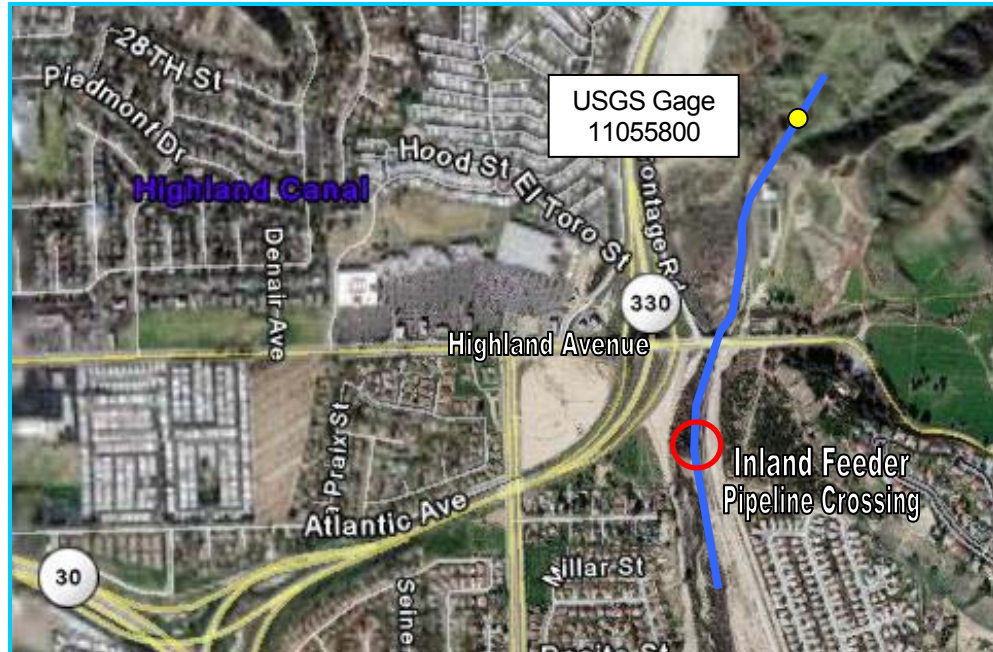


Figure 19. Location of USGS Stream Flow Gage 11055800

Hydraulics

The hydraulic parameters required for conducting the reach and local scour analysis were calculated by making use of a HEC-RAS model. The primary HEC-RAS model represents existing conditions (EXST). Additionally, three other HEC-RAS models to simulate construction of a trapezoidal channel with varying channel bottom widths of 50 ft (ALT50), 70 ft (ALT 70), and 100 ft (ALT100) were also developed. The results from these three models were used to evaluate potential design alternatives (see DESIGN ALTERNATIVES section). The cross-section for all four models at the pipeline crossing is shown on Figure 20. A steady-state solution procedure was used to simulate flow in the creek using the highlighted discharges in Table 2. The model information is included in Appendix C and results are summarized on Figure 21 - Figure 23.

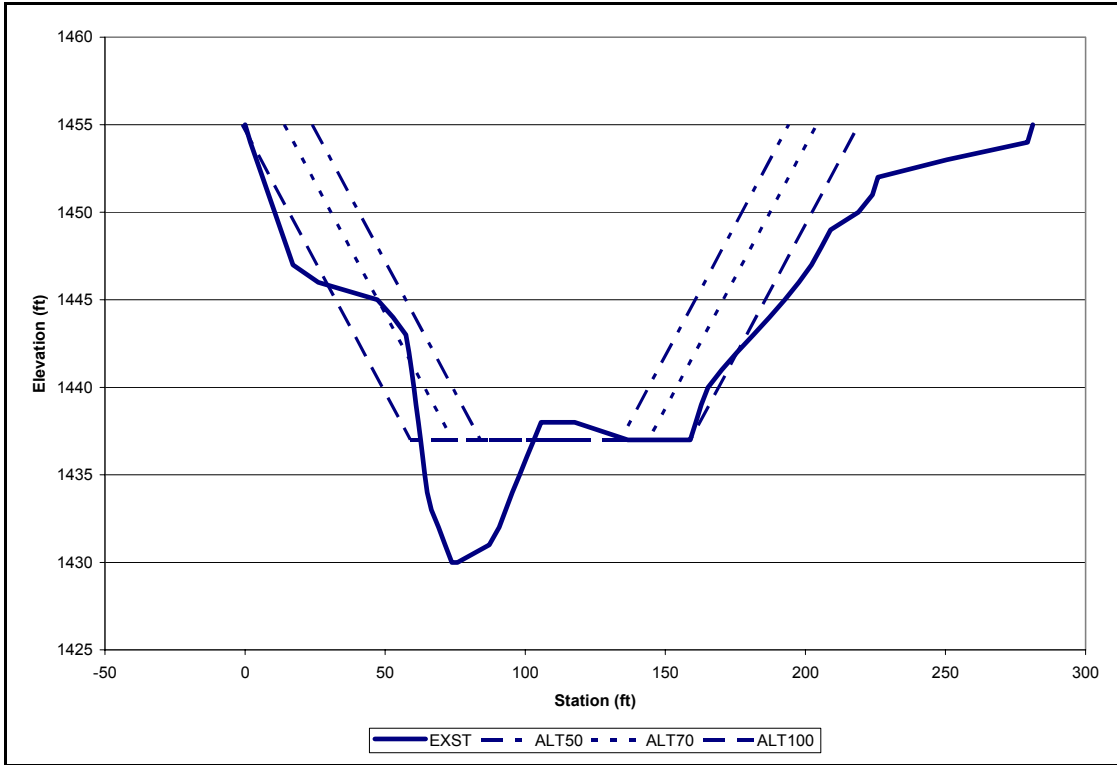


Figure 20. Pipeline Cross-sections Used for the HEC-RAS Models

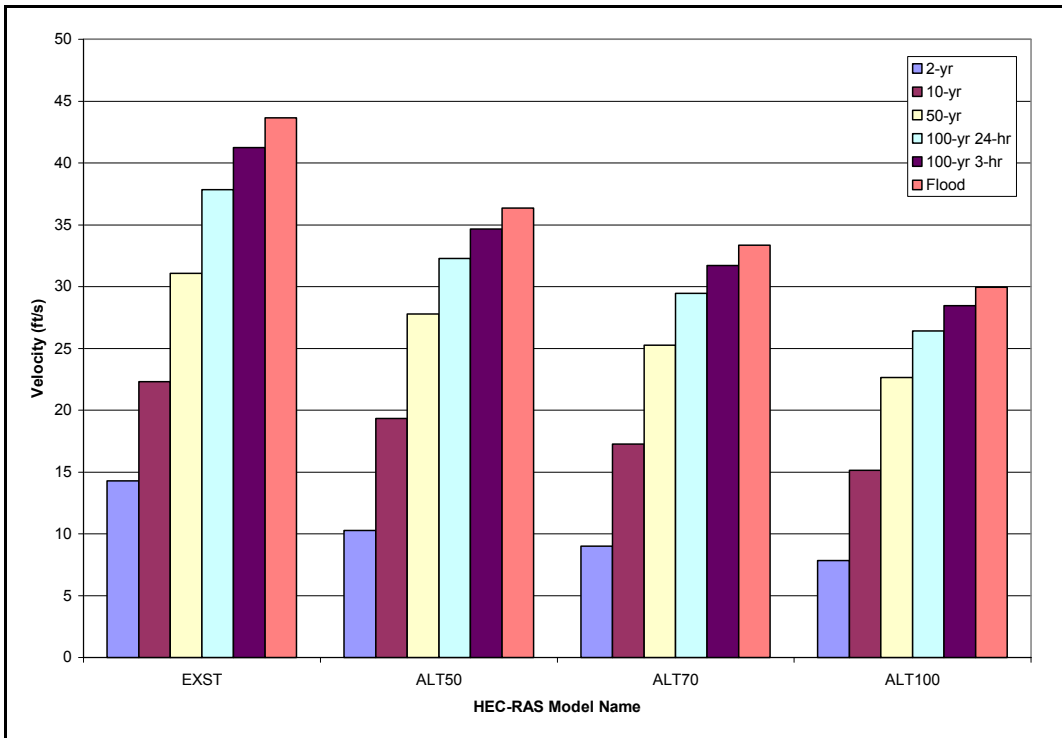


Figure 21. Average Flow Velocities at Pipeline Crossing (Calculated with HEC-RAS)

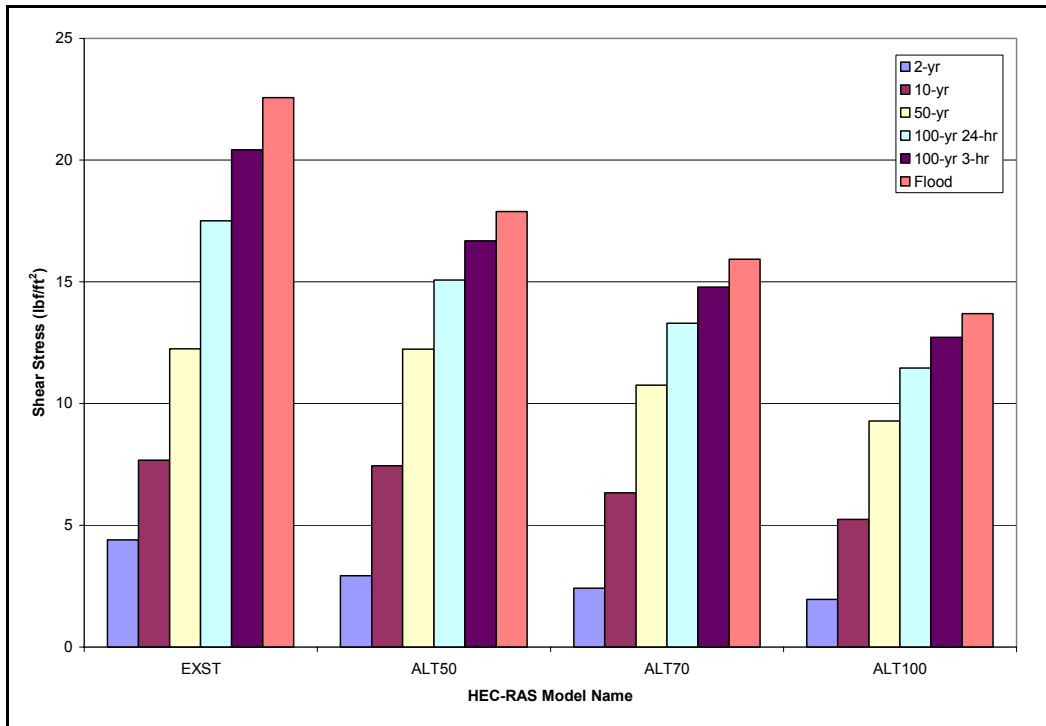


Figure 22. Shear Stress at Channel Bottom at Pipeline Crossing (Calculated with HEC-RAS)

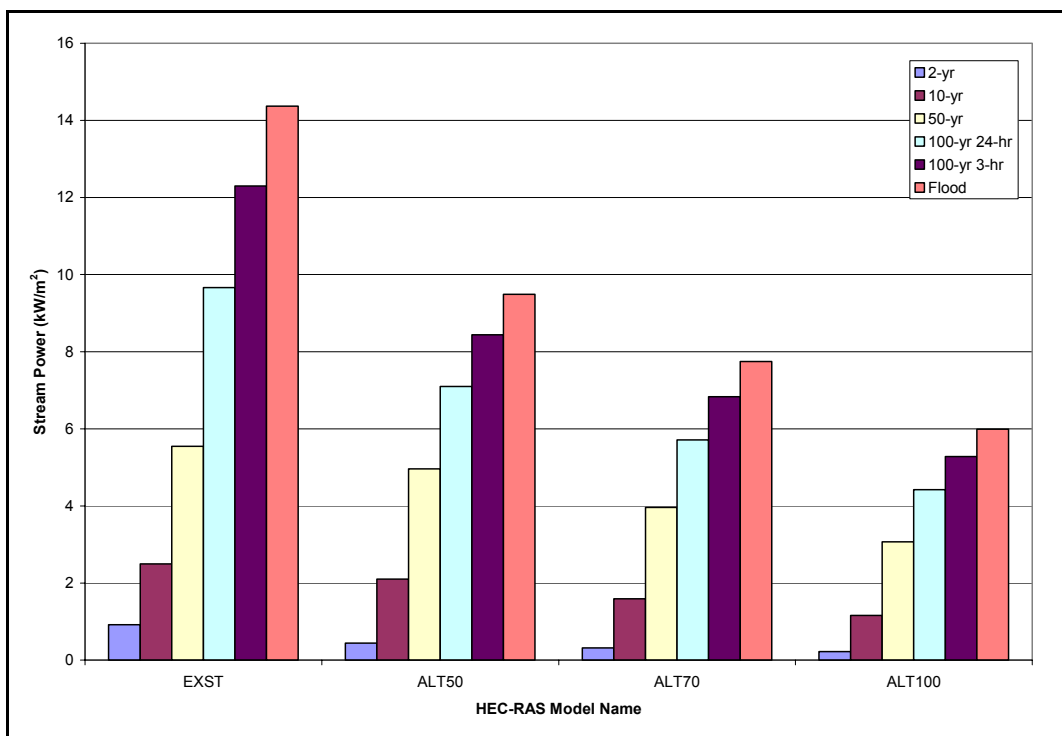


Figure 23. Stream Power at Channel Bottom at pipeline crossing (Calculated with HEC-RAS)

Material Characterization

Bed Material Gradation

The bed material gradation (Figure 24) for City Creek was obtained from Chang (1995). We found no reason to believe that the essential character of the bed material in City Creek changed since 1995 and therefore used the same gradation for execution of our study.

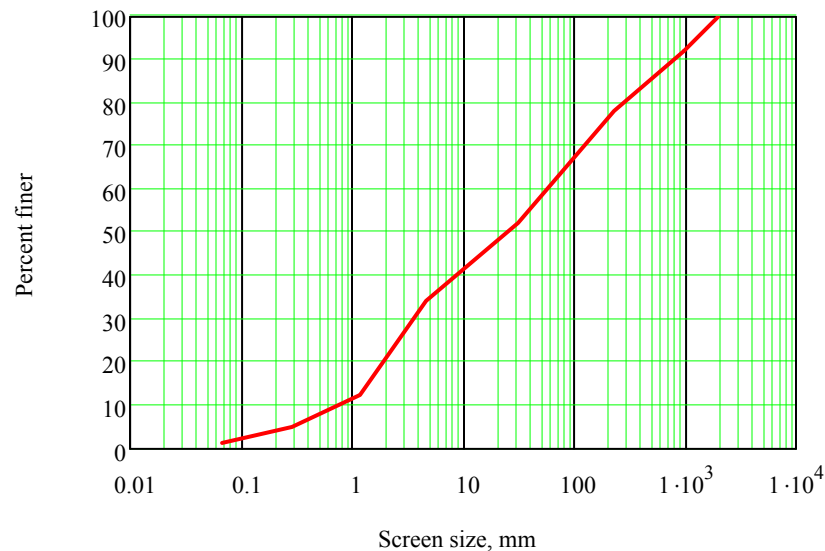


Figure 24. Bed Material Gradation (Chang 1995)

Erosion Resistance

The erosion resistance of bed material was estimated for both the median bed material particle size and the median armor layer particle size. The median particle size is determined as 25mm from Figure 24. The armor layer particle size range is estimated between 125mm and 435mm for dominant flow conditions at the pipeline crossing and other locations upstream of the Baseline Street Crossing. These are the armor layer sizes that are anticipated to develop over the long term. The erosion threshold stream powers for these particle sizes are shown in Table 3.

Table 3. Threshold Stream Power at Pipeline Crossing

Material Type	Median Size (mm)	Threshold Stream Power (W/m ²)
Bed material	25	15.5
Armor Layer (small)	125	181
Armor Layer (large)	435	3250

Scour Analysis

Reach Degradation

Armor Layer Formation

The hydraulic parameters for the 2-yr discharge in the EXST, ALT50, ALT70 and ALT100 HEC-RAS models were used to determine if an armor layer will form at the pipeline crossing and, if so, how much scour will occur until its complete formation. Table 4 summarizes the results of the analysis conducted at the pipeline crossing using the Meyer-Peter Muller; Competent Bottom Velocity; Lane's Tractive Force; Shields Diagram; Yang Incipient Motion, and Gessler methods.

Figure 25 compares the median armor layer diameter at the pipeline crossing with the original bed material gradation. This comparison indicates that it is possible for an armor layer to form from this bed material. All the calculated sizes are associated with percentage passing values indicating that 10% or more of the bed material is equal to or greater than the calculated particle size. This satisfies Pemberton and Lara's (1984) criterion.

Once the armor layer sizes were determined, the scour depth that will occur prior to formation of the armor layer was calculated using equation (0.2). Example calculations are presented in Appendix D and results at the pipeline are also summarized in Table 4.

Table 4 indicates that the median diameter of the armor layer can be as much as 17 in (435mm), with an associated scour depth prior to formation of 23 ft (7 m). Should it be possible to widen the channel and maintain this configuration when water discharges through the section, the armor layer diameter that will develop can be as small as 6 in (150 mm) and an associated scour depth of about 4 ft (1.2 m). Implementation of such widening should be conducted with care. If not implemented correctly, the same scenario found during the 2004 / 2005 floods will occur, i.e. deepening of the channel by low flow incisement. This will concentrate the flow, as is currently the case, essentially reverting back to current conditions.

Figure 26 shows the predicted armor layer gradation using the Gessler (1970) approach for existing conditions. It is compared with the stream bed material gradation curve and shows that the particle sizes required for armor layer formation are present in the virgin material.

In addition to investigating armoring at the pipeline crossing, the bed degradation subject to formation of an armor layer has also been calculated at four existing headcuts, located at stations 64, 48, 31, and 24 in the EXST HEC-RAS model, using the hydraulic parameters for the 2-yr discharge from the EXST model. The armor layer median size and associated depth of degradation for these locations can be seen in Table 4. Figure 27 indicates an increase in scour depth associated with armor layer formation in the upstream reaches, and lower values just upstream of the Baseline Street crossing. The reason for this is that the erosive capacity of the water in the vicinity of the pipeline is greater due to flow concentration in the incised channel, while damming of flow upstream of the Baseline Street bridge results in lower stream power, and therefore smaller armor layer size requirements to maintain channel bed stability.

Table 4. Armor Layer Particle Diameter and Associated Depth of Degradation Results at the Pipeline Crossing

Method	Armor Layer Particle Diameter (in)			
	EXST	ALT50	ALT70	ALT100
Meyer-Peter, Muller	20	10	9	7
Competent Bottom Velocity	15	7.5	6	4
Lane's Tractive Force	Out of range	4	4	4
Shields Diagram	14	7	6	5
Yang Incipient Motion	16	8	6	5
Gessler D ₅₀	20	16	13	12
Average Particle Diameter	17	9	7	6

Method	Depth of Degradation (ft)			
	EXST	ALT50	ALT70	ALT100
Meyer-Peter, Muller	28	9	7	5
Competent Bottom Velocity	18	6	4	2
Lane's Tractive Force	---	2	2	2
Shields Diagram	16	5	5	3
Yang Incipient Motion	21	6	4	3
Gessler D ₅₀	29	8	6	4
Average Depth of Degradation	23	8	6	4

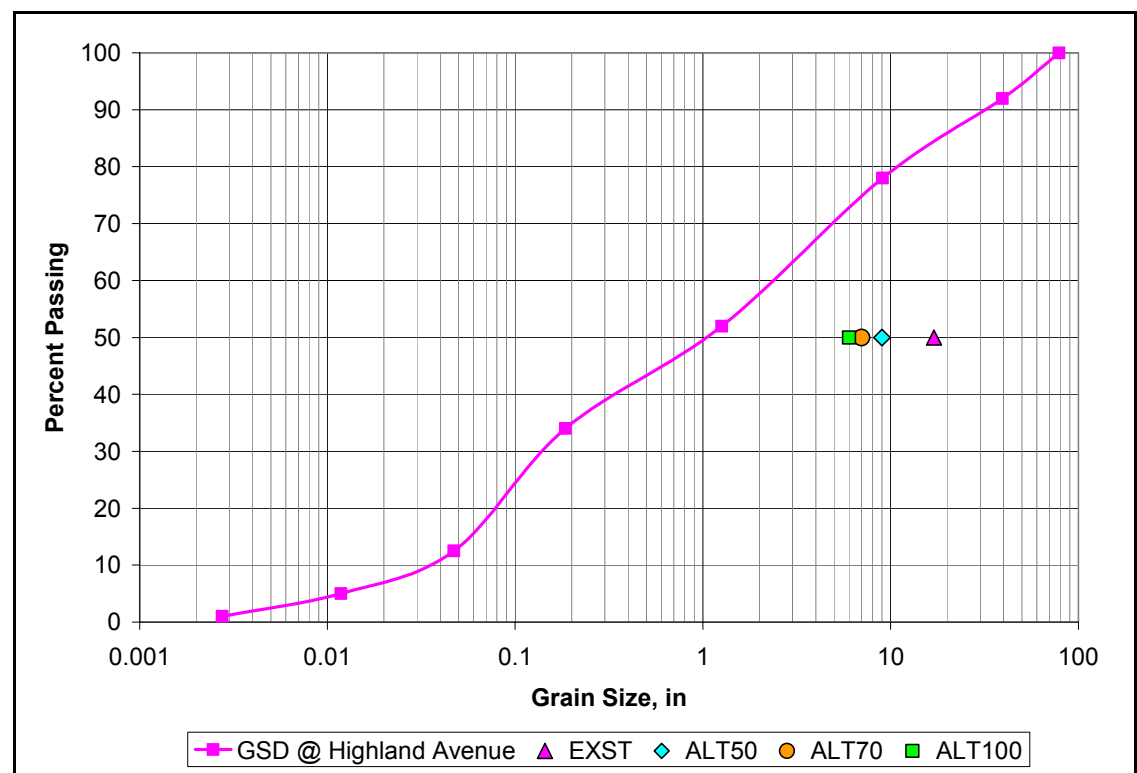


Figure 25. Existing Grain Size Distribution and Calculated Armor Layer D₅₀ for All Four Geometries Evaluated

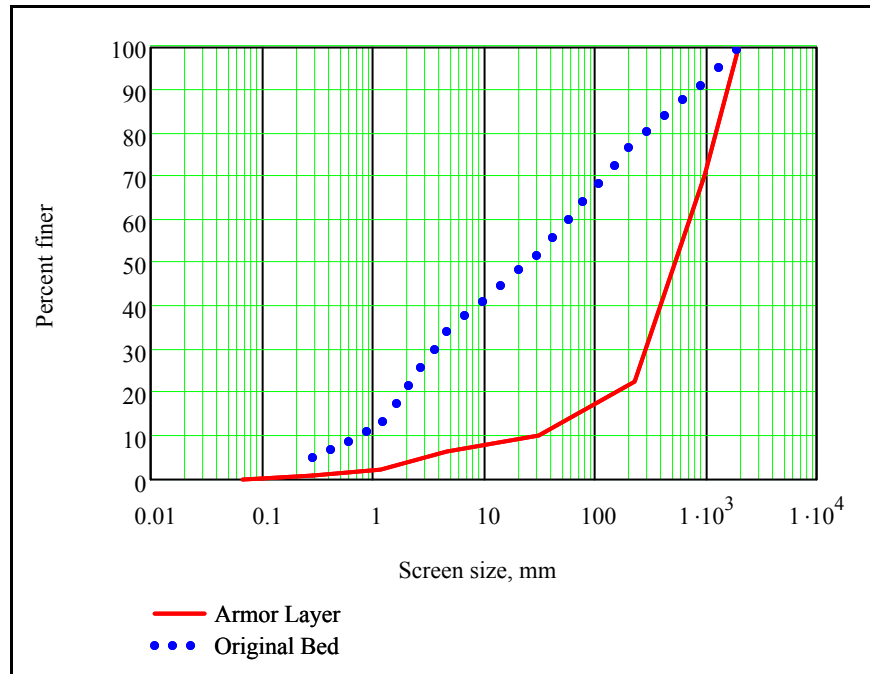


Figure 26. Predicted Armor Layer Gradation Using Gessler (1970) Compared to Existing Bed Material Gradation at Pipeline Crossing.

Table 5. Armor Layer Particle Diameter and Associated Depth of Degradation Results at Existing Headcuts

Station #	64	48	31	24
Chainage (ft)	90.6	2510.56	5485.74	6567.75
Thalweg Elevation (ft)	1488	1405	1329	1301
Method	2-yr Armor Layer Particle Diameter (mm)			
Meyer-Peter, Muller	12	20	6	8
Competent Bottom Velocity	7	9	4	3
Lane's Tractive Force	Out of range	Out of range	Out of range	Out of range
Shields Diagram	8	14	4	6
Yang Incipient Motion	7	9	5	3
Average	9	13	4	5

Method	Depth of Degradation (ft)			
Meyer-Peter, Muller	12	28	4	7
Competent Bottom Velocity	5	7	2	1
Lane's Tractive Force	---	---	---	---
Shields Diagram	7	16	2	4
Yang Incipient Motion	5	8	3	1
Average	7	15	3	3
Final Slope	0.0278	0.0223	0.0244	0.0099

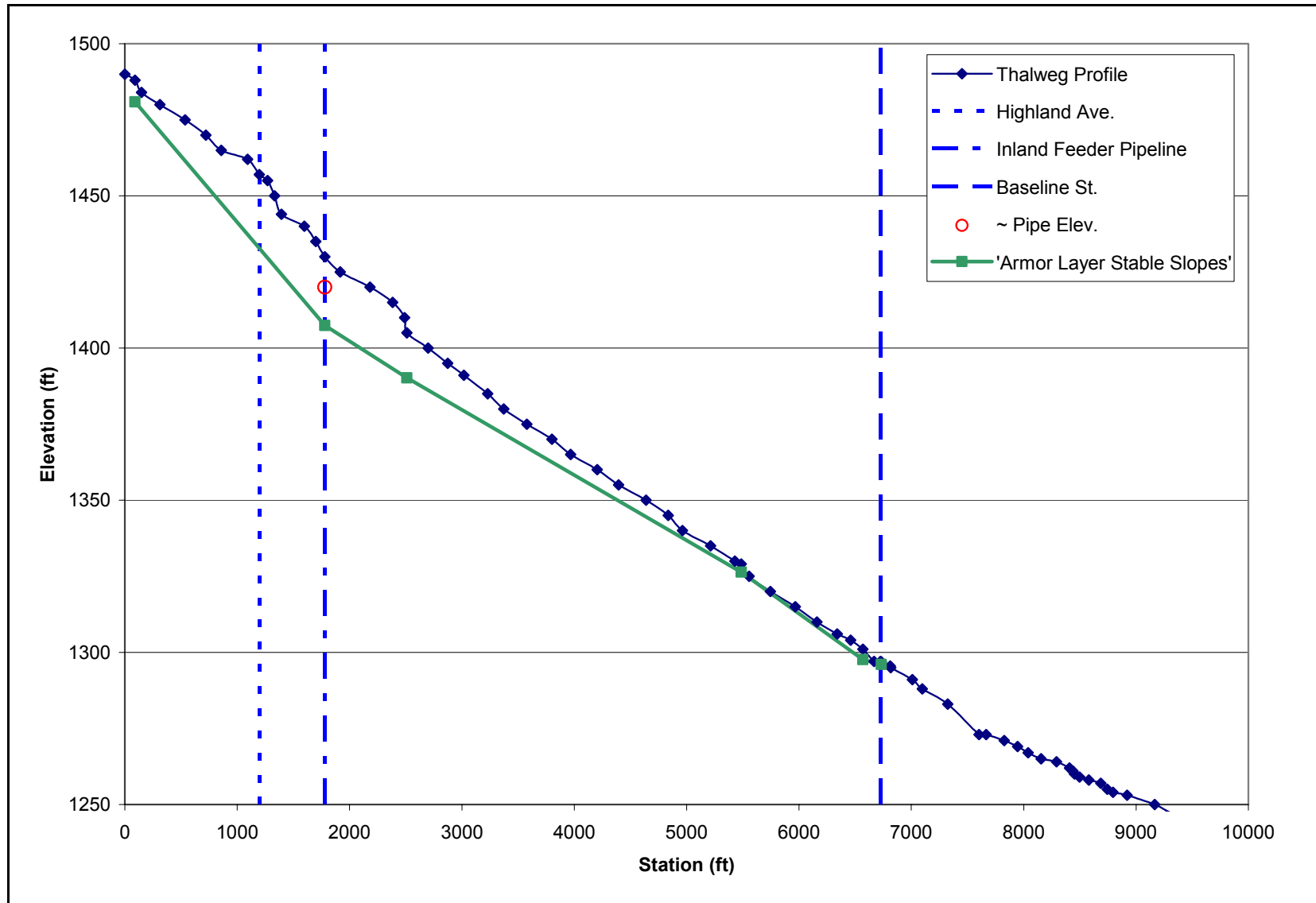


Figure 27. Estimated Scour Depths Associated With Armor Layer Formation

Stable Longitudinal Stream Slope associated with Median Particle Size

The potential for armor layer formation in City Creek indicates that the quasi-equilibrium creek slope will be subject to the formation of such a layer. Nevertheless, the stable slopes associated with the median grain size of the original bed material have been calculated in order to be complete.

The stable slope associated with the median particle size of the original bed gradation is likely to be much milder than that associated with the armor layer. The scour at the Pipeline, should stable slope conditions associated with the median particle size govern, is calculated by pivoting a line around the baselevel at the Baseline Street culvert. The relevant elevations and distances used in such a calculation are shown in Table 6. The estimated stable channel slopes for these conditions are presented in Table 7.

Table 6. Base Level Information and Estimated Time for Stable Conditions to Establish if Median Bed Material Particle Size Dominates in the Determination of Quasi-Equilibrium Conditions

Grade Control Structure Location:	Baseline St. Culvert
Elevation of Thalweg of Baseline St. Culvert:	1296 ft
Distance Between Pipeline and Baseline St.:	4947.18 ft
Current Thalweg Elevation at Pipeline Crossing:	1430 ft
Estimated Time for Stable Conditions to establish	100 yr

Table 7. Estimated Stable Slope, Depth of Degradation, and Rate of Scour at Pipeline Crossing Assuming Median Bed Material Diameter Control

	Bottom Width (ft)	EXST	ALT50	ALT70	ALT100
Stable Slope	Scholitsch	0.18%	0.41%	0.53%	0.69%
	Meyer-Peter, Muller	0.22%	0.60%	0.73%	0.88%
	Shields Diagram	0.30%	0.84%	1.00%	1.30%
	Lane's Tractive Force	0.31%	0.87%	1.10%	1.30%
	Average	0.26%	0.68%	0.84%	1.00%
Degradation @ Pipeline (ft)	Scholitsch	125	114	108	100
	Meyer-Peter, Muller	123	104	98	91
	Shields Diagram	119	92	85	70
	Lane's Tractive Force	119	91	80	70
	Average	121	100	93	85
Average Scour Per Year (ft/yr)*		1.21	1.00	0.93	0.85

*Assumes 100 years for full degradation depth

Although the total depth of degradation at the pipeline crossing for this method was calculated to be 121 ft, this is not the predicted total depth of erosion due to the presence of coarse material in the bed and the potential for armor layer formation.

Net Reach Degradation

The net amount of scour, in the absence of human intervention, at the pipeline crossing is controlled by an armor layer formation, if the necessary particle gradations are present in

the bed material, or the median particle size slope, if coarse materials are not present. The reason for this is that once the stable condition has established at a certain elevation in the stream bed, it is assumed not to degrade any further.

The estimated reach degradation depth at the pipeline crossing is therefore 23ft below the current bed elevation at the pipeline crossing assuming that armoring occurs (Table 4).

Local Scour

Bend Scour

Figure 28 shows the bend in current existence in the vicinity of the pipeline crossing. The additional scour that could occur as a result of flow around this bend was estimated for dominant flow conditions using the procedures outlined before for existing conditions. This entails calculating the total stream power around the bend and comparing it with the erosion resistance of the bed and bank material. If this comparison indicates scour potential, the next step is to calculate the additional scour depth around the bend resulting from bend flow.

Using the procedure by Chang (1992) for existing conditions and the 2-year recurrence interval discharge it is found that the maximum total stream power around the bend is 1470 W/m^2 . A comparison between earth material erosion resistance and the maximum stream power around the bend is provided in Table 8. This comparison indicates that it is possible for the stream bed material to erode prior to and after the formation of an armor layer.

The scour depth around the bend was estimated using the Odgaard (1986) three-dimensional analytical model. The result of the calculation is shown on Figure 29. Estimated scour depth, in addition to what would occur without the bend, is about 0.5m (18 inches).

Table 8. Comparison Between Stream Power in Bend and Erosion Threshold.

Material Type	Erosion Threshold (W/m^2)	Total Stream Power around Bend (W/m^2)	Erosion? (Yes / No)
Original Bed Material	15.2	1470	Yes
Armor Layer	944	1470	Yes

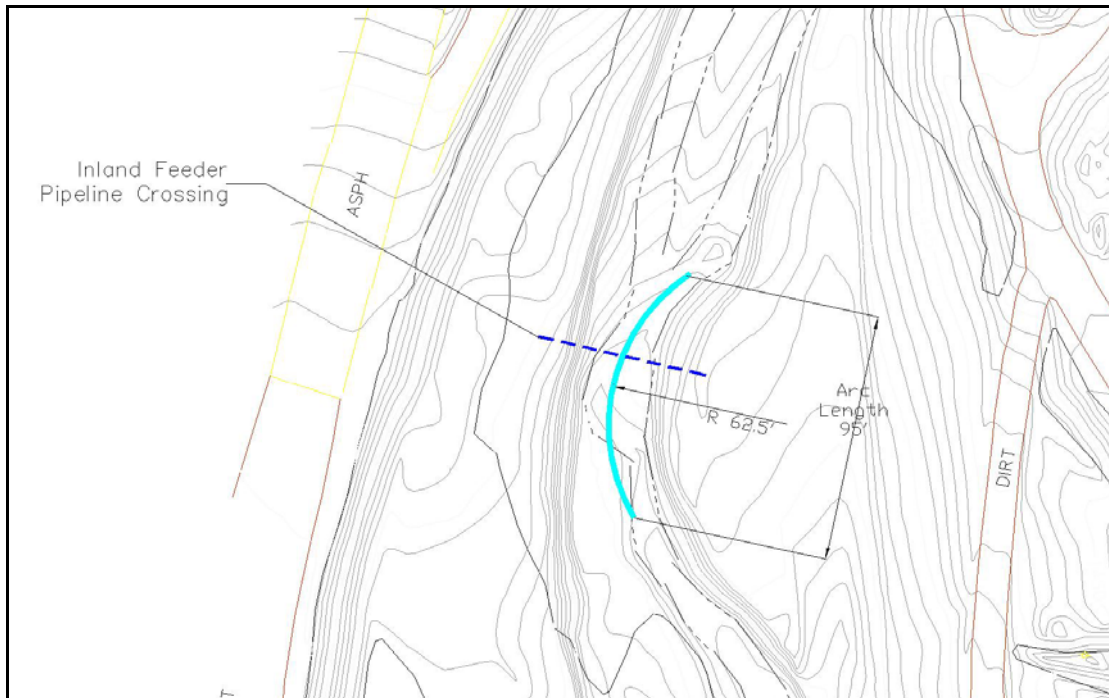


Figure 28. Location and Dimensions of Bend Analyzed

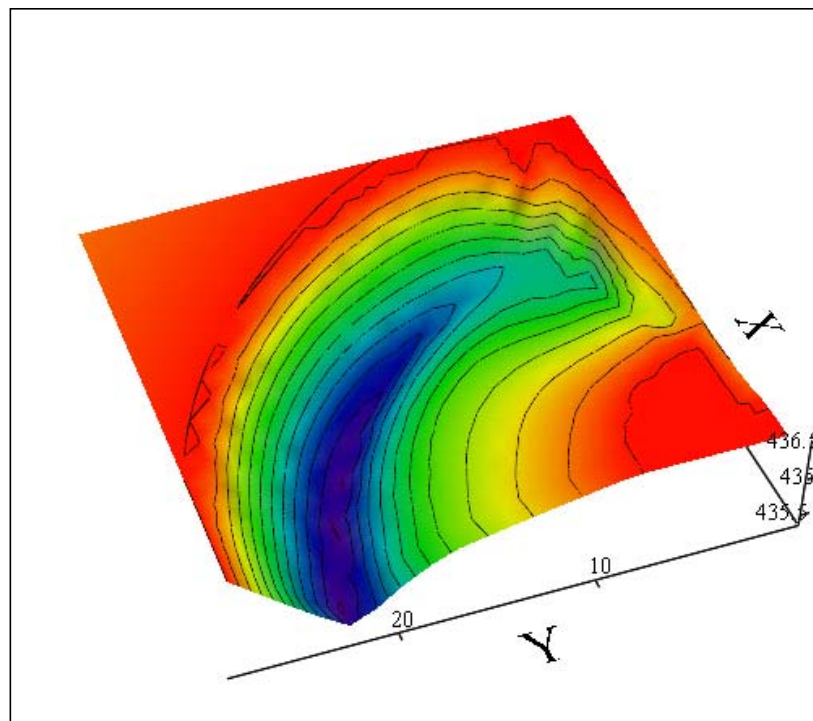


Figure 29. Three-Dimensional Image of Calculated Bend Scour at the Pipeline Crossing.

Headcut Migration

Headcuts were noted during the field visit. Headcut migration is a long term scour mechanism that over time aids in achieving equilibrium in the channel, at which time the channel bed will be armored. To illustrate that the current headcut will migrate upstream, we calculated the erosive capacity of the backroller at the base of the headcut drop and compared it with the threshold stream power of the base material. The results for the seven headcuts observed on site are presented in Table 9. The table illustrates that the stream power associated with the back roller is higher than the erosion threshold of the existing bed materials and that the headcuts will migrate upstream.

Table 9. Backroller Stream Power Associated with Active Headcuts

	Drop Height (ft)	Stream Power (W/m ²)	
		Back Roller	Threshold
64	4	2280	15.2
57	3	749	15.2
56	6	1989	15.2
48	5	2589	15.2
35	4	1300	15.2
31	4	1077	15.2
24	3	620	15.2

SUMMARY

It is concluded that the scour in City Creek will continue in the future in the absence of intervention. The scour process will be aided by headcut migration, and will stabilize once an armor layer has formed throughout the reach. This results in approximately 23ft of scour at the pipeline crossing, below the current elevation. It was found that bend scour at the pipeline crossing is on the order of about 18 inches, which makes the total predicted depth of erosion at the Pipeline to be 25ft.

It has also been shown that degradation of the river reach will continue even if the cross section is widened quite substantially. In order to mitigate the scour at the pipeline, the essential design approach should be to make the slope milder, while concurrently widening the channel section. Re-vegetation of the channel bed and banks will assist in further stabilizing the reach.

DESIGN ALTERNATIVES

The approach to the design of mitigation measures is based on the insight we developed during the course of the analysis. Our interpretation of the fluvial geomorphic nature of the reach indicates that it is possible for it to return to a depositional zone in the very long term (geologic time). However, in following the course to reverting back to a depositional zone, our analysis indicates that scour up to a maximum depth of about 23ft below current thalweg elevations will first occur. It is therefore necessary to protect the pipeline against the consequences of such an event. For design purposes we ignore the geologic time

scenario, i.e. the area eventually reverting back to a depositional zone. However, this insight is used to conceptualize a stable mitigation design.

The focus of the mitigation design approach should be to provide a design configuration that will accelerate the geomorphic process to revert the river reach containing the pipeline crossing back to a depositional zone. In principal this can be accomplished by designing mitigation elements that will reduce the river slope and prevent occurrence of low-flow channel incision.

The recommended design flood equals the 100-year, 3-hr design discharge. Should MWD require implementation of the Standard Project Flood, this discharge should replace our recommendation. The discharge for designing mitigation measures is considerably larger than the discharge used to estimate long term quasi-equilibrium conditions. This is for obvious reasons. When assessing long-term stability, it is appropriate to use the associated dominant discharge. However, for protection, it is necessary to use a large design flood, with an appropriate probability of occurrence to protect infrastructure and public safety.

The table below lists optional mitigation strategies and indicates our assessment of anticipated feasibility. A description of each measure is provided below the table. It should be noted that E&H's commission was to recommend potential mitigation measures in a conceptual manner. However, we have conducted preliminary analyses to identify potential fatal flaws. Exact sizing of structures can be accomplished once a preferred solution has been selected.

Table 10. Optional Mitigation Measures

Mitigation Measure	Feasible? (Yes / No)	Comment
Channel Widening; without boundary hardening	No	The current situation developed after a widened channel was created to pass a flood. The inability of a non-hardened widened channel bed to resist the erosive capacity of water led to the development of an incised channel. This is confirmed by comparing the erosive capacity of the water flowing for design flow conditions in wide channels to the erosion resistance of the bed material, even after armoring has occurred. The comparison indicates that the channel bottom will scour.
Riprap Chute	Yes	A riprap chute terminating in a riprap energy dissipater basin can be used to guide flows to lower elevations below the pipeline crossing. Feasible rock sizes are obtained when the chute is about 200ft to 250ft wide, with a slope of about 1V:5H. Rock sizes are roughly ½ ton rock.
Single Vertical Drop Structure	No	A structure consisting of a single, vertical drop is not considered be feasible. The drop height is anticipated to be too high. It poses engineering and construction problems, and is a potential public safety hazard.
Multiple Drops	Yes	Multiple drops, using a concept similar to the riprap chute is considered feasible. It adds redundancy and diminishes public safety concerns. Multiple drops using vertical walls (concrete or sheet piling) is considered less desirable from an engineering and construction, and public safety points of view.

Channel Widening without Boundary Hardening

It is not considered feasible to propose a concrete-lined channel to protect the pipeline against the effects of scour. This alternative mitigation design therefore entails widening the channel without boundary hardening.

Ideally, if flow is spread over a wider channel the erosive capacity of the water per unit area of the bed is expected to decrease. A comparison of the applied stream power to the channel bed during design flood conditions and the threshold stream power of an armor layer associated with a 100 ft wide channel is presented in Table 11. The comparison indicates that the channel bottom is likely to scour. Experience during the 2004 / 2005 floods indicate that this is a reasonable expectation. The bed of the trapezoidal channel that was created scoured and was incised. Channel widening without hardening of the boundary is not considered a feasible solution to the scour problem.

Table 11. Comparison of Erosive Capacity of Water for Design Flood Conditions and the Threshold Stream Power of an Armor Layer that is Expected to Form Under Such Conditions.

Erosive Capacity of SPF in ALT100 Armored Channel	12.3	kW/m ²
Erosive Threshold of Armor Layer for ALT100	0.24	kW/m ²

Riprap Chute

This mitigation design entails filling the area above and upstream of the pipeline crossing to create a mild slope and force a depositional area. The milder sloped channel reach terminates in a riprap-lined chute, which guides the water to a lower elevation to meet the thalweg of the downstream channel. The riprap in the chute protects the pipeline and the underlying earth material against scour. The mild slope upstream of the riprap chute forces deposition of sediment, and prevents formation of an incised channel. Chute slopes of 20% or less can feasibly be protected against scour with approximately ½ ton rock. This might be a feasible solution provided adequate availability of rock. The riprap rock size will be confirmed and more design detail provided if a decision is made to implement this potential design solution.

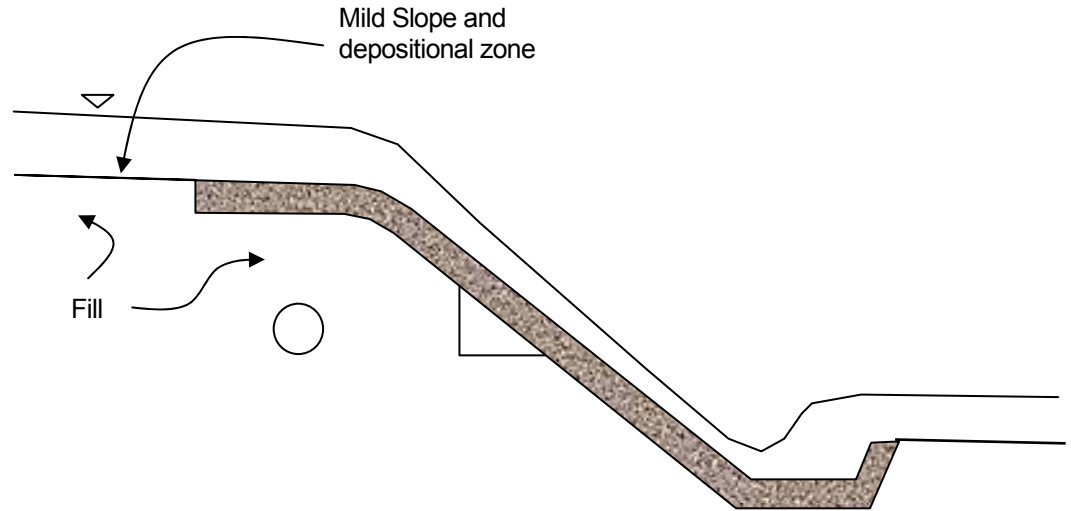


Figure 30. Conceptual Configuration of Riprap Lined Rock Chute. Exact Dimensions to be Determined During Preliminary and Final Design.

Single Vertical Drop Structure

The essential concept when implementing a single drop structure is to create a mild channel slope upstream of the drop structure by backfilling, establish sub-critical flow conditions, force deposition of sediment in the reach upstream of the drop, and prevent formation of an incised channel in this sub-reach of the channel. Our opinion is that the vertical drop associated with such a structure will be too great. This presents the designer with hydraulic, geotechnical and structural design problems that might be difficult to overcome, in addition to public safety concerns (Figure 31). Design details to facilitate construction of such a structure need resolving.

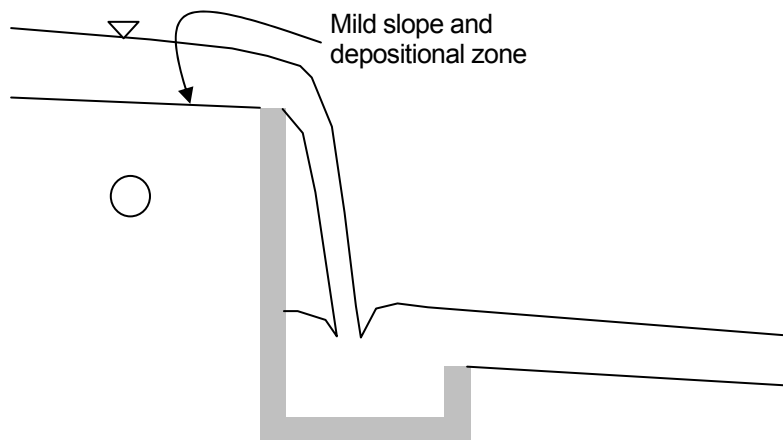


Figure 31. Conceptual Sketch of Single Drop Structure.

Multiple Grade Control Structures

The implementation of multiple grade control structures is a design mitigation approach with merit. Two optional approaches can be followed. The drop structures can be constructed of a hard material, i.e. vertical concrete walls or sheet piling; or it can be constructed of riprap, similar to the riprap design chute.

If a vertical drop structure is constructed E&H recommends against using drops in excess of 3ft. Such a design will require a large number of drop structures; approximately 20 to 40, depending on layout detail and is most probably not feasible.

Implementation of this concept becomes more feasible when using riprap chutes (Figure 32). The reason for this is that the individual drops that can be accommodated are greater than when using a vertical drop. As the water flows down the inclined slopes of these structures, it dissipates energy on a continuous basis.

A potential benefit of using multiple grade control structures is that they may exhibit greater overall stability. For example, if one of the structures fails the other may assist in preventing overall failure. Such a system is characterized by increased redundancy, making it safer. Additionally, the use of smaller drops reduces public safety concerns.

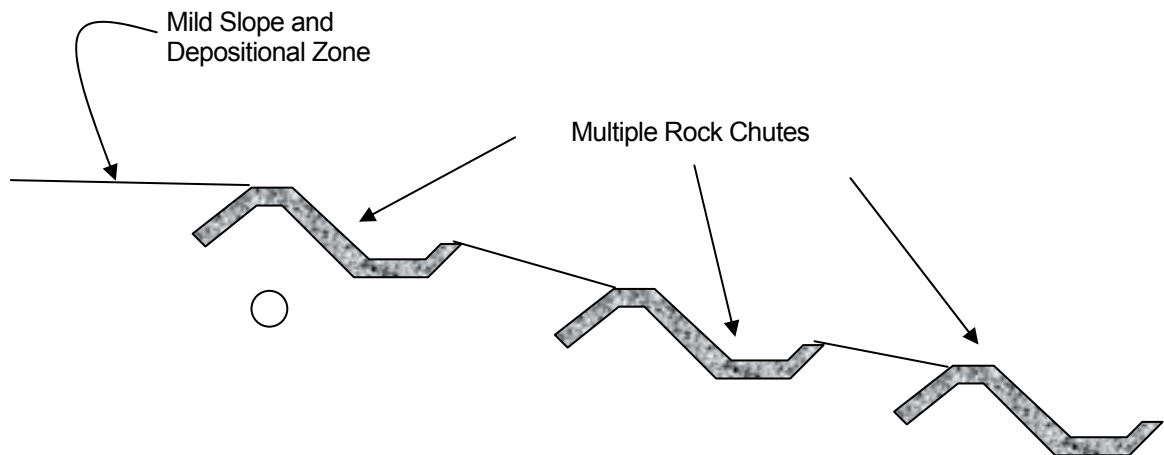


Figure 32. Multiple Rock Chutes.

REFERENCES

- Annable, W.K. 1994. Morphological relations of rural water courses in southeastern Ontario for use in natural channel design, Masters thesis, Univ. of Guelph, School of Engineering, Guelph, Ontario, Canada.
- Andrews, E.D. 1980. Effective and bankfull discharges of streams in the Yampa River Basin, Colorado and Wyoming, *Journal of Hydrology*, 46: 311-330.
- Annandale, G.W. 2006. *Scour Technology*, McGraw-Hill, New York.
- Annandale, G.W. 1995. Erodibility. *Journal of Hydraulic Research* 33:471-494.
- Chamani, M.R. and M.K. Beirami. "Flow Characteristics at Drops" *Journal of Hydraulic Engineering*, 128(8), 2002.
- Chang, Howard H. 1992. *Fluvial Processes in River Engineering*. Krieger Publishing Company. Malabar, Florida.
- Chang, Howard H. 1995. Inland Feeder Pipeline, San Bernardino Segment (Contract 3): Fluvial Study of City Creek for Pipeline Placement. Prepared for Dames and Moore.
- Gessler, J. 1971. *Beginning & Ceasing of Sediment Motion.* *River Mechanics*, H.W. Shen, ed Hsieh Wen Shen, Fort Collins, Colorado, 7, 1-22.
- Google Earth 2006. [Google Earth version 3.0.0762] 34° 07' 40.87" N, 117 ° 11' 20.50" W
- Haan C.T., B. J. Barfield, and J.C. Hayes. 1994. Design hydrology and sedimentology for small catchments. San Diego CA : Academic Press Inc.
- Haestad Methods, Inc. 2003. *FlowMaster* v.6.1 [computer software]. www.haestad.com.
- Lane, E.W. 1955. *The importance of fluvial morphology in hydraulic engineering*. American Society of Engineering, Proceedings. 81. Paper 745: 1-17.
- Leopold, Luna B. 1994. *A View of the River*. Cambridge, Massachusetts: Harvard University Press.
- Odgaard, A.J., "Meander Flow Model Parts I and II", *Journal of Hydraulic Engineering*, Vol. 112, No. 12, December 1986, ASCE, pp. 1117-1150.
- Pemberton, EL and JM Lara. 1984. Computing Degradation and Local Scour. Technical Guideline for Bureau of Reclamation. Denver, Colorado.
- Rosgen, David L. 1996. *Applied river morphology*. Pagosa Springs, CO : Wildland Hydrology.
- U.S. Army Corps of Engineers (USACE). 2001. *HEC-RAS River Analysis System* v. 3.3.1 [computer software]. www.hec.usace.army.mil.
- USGS, 2006 Gage 11055800 Annual Peak Streamflow Data for period of record. http://nwis.waterdata.usgs.gov/nwis/peaks/?site_no=11055800&agency_cd=USGS.

APPENDIX A – HYDROLOGY CALCULATIONS

Appendix A: HYDROLOGY

Objective

In the Chang Study (1995) provided by the Metropolitan Water District (MWD), a hydrologic study of the watershed was performed and the following recurrence interval discharges were reported: 10-year 24-hour, 50-year 24-hour, 100-year 3-hour, 100-year 24-hour, and the project flood. Although these discharges were used in our study, the discharge of interest in estimating the stability of the channel is the dominant discharge, in this case the two-year recurrence interval discharge.

In order to evaluate the two-year discharge, yearly peak discharge data was obtained from USGS gage 11055800 (2005) and analyzed using a Log Pearson III distribution (Haan & Barfield, 1994). The results of the Log Pearson III distribution were compared to the reported discharges in the Chang Study.

Assumptions

- All discharges reported in by Chang (1995) are considered accurate;
- There are no trends in the data;
- The data represent independent hydrologic events;
- The flows are from a single population; and
- Measurement errors are random, unbiased, and have a relatively small variance.

Calculations

To estimate the magnitude of the two-year storm and verify the values reported by Chang (1995), the yearly peak discharge data was obtained from USGS gage 11055800 located on City Creek approximately one mile upstream of the Inland Feeder Pipeline crossing (Figure A-1). This gage provided 85 years of historical annual peak discharge data (Table A-1).



Figure A-1: Location of USGS Streamflow Gage 11055800

Table A-1: Historical Annual Peak Discharge from USGS Gage 11055800

Year	Peak Discharge (cfs)
1920	350
1921	1320
1922	1090
1923	720
1924	345
1925	74
1926	2360
1927	1930
1928	369
1929	196
1930	78
1931	146
1932	442
1933	62
1934	374
1935	166
1936	580
1937	1500
1938	6900
1939	400
1940	378
1941	2420
1942	172
1943	2300
1944	1030
1945	940
1946	1000
1947	285
1948	250
1949	100
1950	198
1951	71
1952	937
1953	132
1954	631
1955	115
1956	862
1957	1650
1958	1350
1959	358
1960	42
1961	92
1962	648

Year	Peak Discharge (cfs)
1963	163
1964	64
1965	292
1966	1310
1967	3080
1968	217
1969	7000
1970	205
1971	100
1972	722
1973	492
1974	126
1975	103
1976	326
1977	860
1978	2510
1979	359
1980	3630
1981	103
1982	330
1983	1140
1984	287
1985	200
1986	530
1987	108
1988	108
1989	262
1990	175
1991	460
1992	853
1993	1910
1994	188
1995	2260
1996	445
1997	1360
1998	2210
1999	37
2000	162
2001	105
2002	8.7
2003	272
2004	8000

It is possible to estimate the magnitude of discharges for various recurrence intervals by fitting the data to a particular probability distribution. Four commonly used distributions are the following: Normal, Lognormal, Extreme Value 1, and Log Pearson III. Skewness, a measure of the symmetry of the data, is a good parameter to determine the best probability distribution to fit the data and the equation to calculate skewness can be seen below:

$$C_s = \frac{n \sum (X_i - \bar{X})^3}{(n-1)(n-2)S_x^3}. \quad (\text{A.1})$$

The skewness of the raw data set was calculated to be 3.3. Table A-2 provides the optimal skewness values for each probability distribution. To test the appropriateness of the Lognormal distribution, the coefficient of variance, C_v , must be determined:

$$C_v = \frac{S_x}{\bar{X}} \quad (\text{A.2})$$

where S_x is the standard deviation $\left(S_x = \sqrt{\frac{\sum X_i^2 - n\bar{X}^2}{n-1}} \right)$ and \bar{X} is the mean $\left(\bar{X} = \sum \frac{X_i}{n} \right)$.

C_v was calculated to be 1.57 and according to Table A-2 the appropriate skewness for the Lognormal distribution should be close to $3C_v + C_v^3$, which in this case is equal to 8.64.

Due to the magnitude of the skewness, the most appropriate probability distribution is the Log Pearson III (LPIII). The LPIII is capable of handling any skewness values a data set yields.

Table A-2 Appropriate Skewness Values for Possible Probability Distributions

Distribution	Skewness
Normal	0
Lognormal	$3C_v + C_v^3$
Extreme Value I	1.139
Log Pearson III	Any value

Following are the steps involved in using the LPIII distribution:

1. transform the n original observations, X_i , to logarithmic values, Y_i , by the relation

$$Y_i = \log X_i; \quad (\text{A.3})$$

2. compute the mean logarithm, \bar{Y}

$$\bar{Y} = \sum \frac{Y_i}{n}; \quad (\text{A.4})$$

3. compute the standard deviation of the logarithm, S_Y

$$S_y = \sqrt{\frac{\sum Y_i^2 - n\bar{Y}^2}{n-1}}; \quad (A.5)$$

4. compute the coefficient of skewness C_s from

$$C_s = \frac{n \sum (Y_i - \bar{Y})^3}{(n-1)(n-2)S_y^3}; \quad (A.6)$$

5. compute

$$Y_T = \bar{Y} + S_y K_T \quad (A.7)$$

where K_T is from the Frequency Factors for Pearson Type III Distribution Table for all desired recurrence intervals; and

6. calculate

$$X_T = \text{anti log } Y_T \quad (A.8)$$

Results

The magnitude of the 200, 100, 50, 25, 10, 5, 2, and 1.01 year discharges calculated using a LPIII distribution can be seen in Table 2 along with the 100, 50, and 10 year discharges reported in the Chang 1995 report. The discharges estimated using the LPIII distribution as well as those provided in the Chang Study are shown in Table A-3. All discharges used in our evaluation are highlighted in yellow.

Table A-3: City Creek Hydrology

	Log Pearson III	Dames & Moore 1995
Recurrence	Discharge (cfs)	Discharge (cfs)
Standard Project Flood	N/A	15000
100-yr (24-hr storm)	8548	10500
100-yr (3-hr storm)	N/A	13000
50-yr	5983	6600
25-yr	4021	N/A
10-yr	2174	2150
5-yr	1221	N/A
2-yr	400	N/A
1.0101-yr	19	N/A

References

Haan C.T., B. J. Barfield, and J.C. Hayes. 1994. *Design Hydrology and Sedimentology for Small Catchments*. San Diego CA: Academic Press Inc.

Chang, Howard H., 1995. *Inland Feeder Pipeline, San Bernardino Segment (Contract 3) Fluvial Study of City Creek for Pipeline Placement*. Rancho Santa Fe CA

USGS, 2006 Gage 11055800 Annual Peak Streamflow Data for period of record.
http://nwis.waterdata.usgs.gov/nwis/peaks/?site_no=11055800&agency_cd=USGS.

APPENDIX B – HEC-RAS MODEL

Appendix B: HEC-RAS Modeling

Introduction

HEC-RAS [Version 3.1.3] was used to determine the erosive capacity of City Creek and to quantify the anticipated hydraulic characteristics at the Inland Feeder Pipeline crossing.

The primary HEC-RAS model represents existing conditions (EXST). In addition to evaluating the hydraulic parameters for the existing conditions, three alternative HEC-RAS models were constructed to simulate construction of a trapezoidal channel with channel bottom widths of 50 ft (ALT50), 70 ft (ALT 70), or 100 ft (ALT100). All models were run in steady state. The cross-section for the pipeline crossing for all four models can be seen in Figure B-2.

Assumptions

General assumptions made for this model were:

- One Dimensional Flow: The system of equations used to solve the hydraulics of the channel in HEC-RAS only takes into account one dimensional flow. The hydraulics around the structures can be two and three dimensional.
- Hydrology: The magnitude of the 10-year, 50-year, 100-year 3-hour, 100-year 24-hour, and Standard Project Flood developed in Chang (1995) is assumed to still be valid for this site. This is a reasonable assumption as the creek discharges directly from the San Bernardino forest and no known changes have taken place in this area since execution of the previous study by Chang (1995).

Input

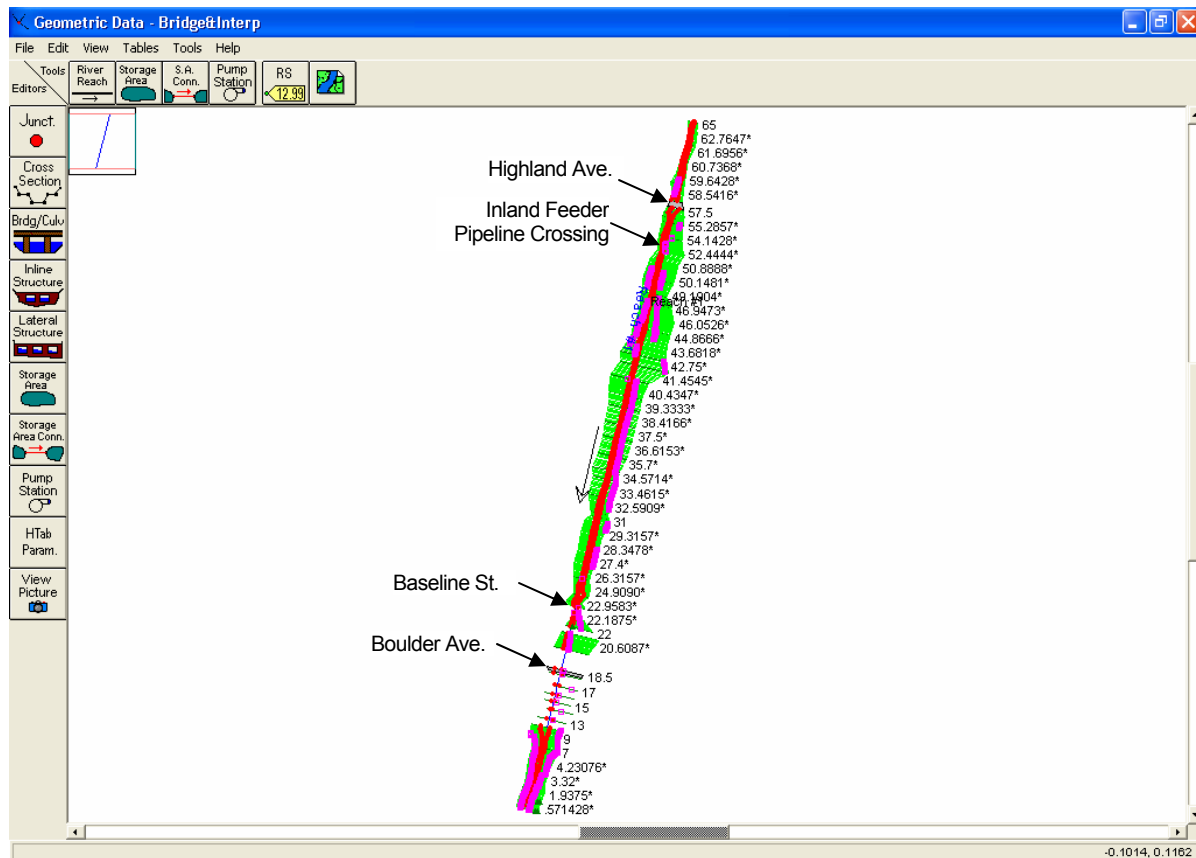


Figure B-1. Cross Section Locations for EXST, ALT50, ALT70, and ALT100

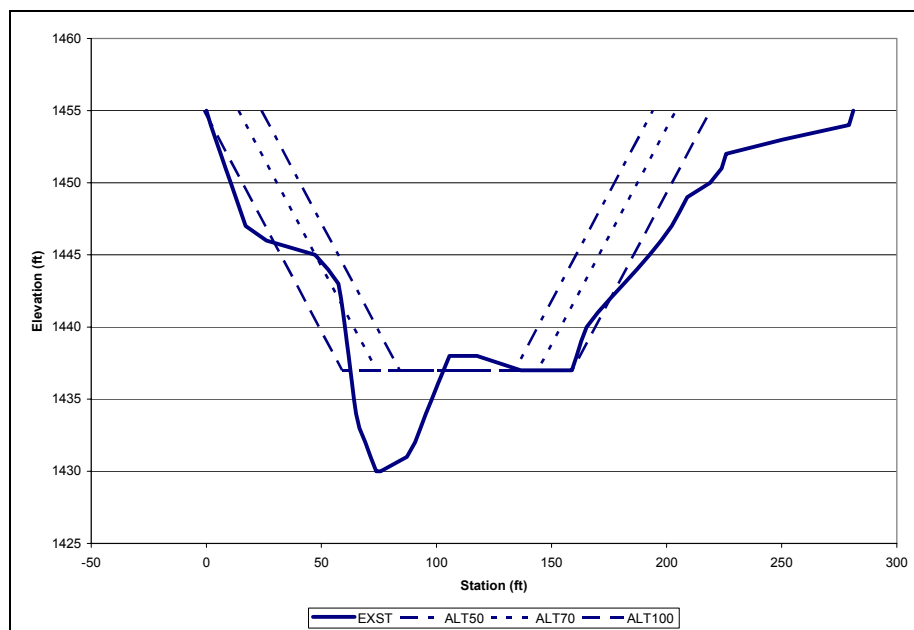


Figure B-2.: Pipeline Cross-sections Used for the HEC-RAS Models (looking upstream)

Edit Manning's n or k Values

River: Reach #1 ☐ Edit Interpolated XS's

Reach: Reach #1 All Regions

Selected Area Edit Options: Add Constant ... Multiply Factor ... Set Values ... Replace ...

River Station	Frctn (n/K)	n #1	n #2	n #3
1 65	n	0.03	0.03	0.03
2 64	n	0.03	0.03	0.03
3 63	n	0.03	0.03	0.03
4 62	n	0.03	0.03	0.03
5 61	n	0.03	0.03	0.03
6 60	n	0.03	0.03	0.03
7 59	n	0.03	0.03	0.03
8 58	n	0.015	0.015	0.015
9 57.75	Bridge			
10 57.5	n	0.015	0.015	0.015
11 57	n	0.015	0.015	0.015
12 56	n	0.03	0.03	0.03
13 55	n	0.03	0.03	0.03
14 54	n	0.03	0.03	0.03
15 53	n	0.03	0.03	0.03
16 52	n	0.03	0.03	0.03
17 51	n	0.03	0.03	0.03
18 50	n	0.03	0.03	0.03
19 49	n	0.03	0.03	0.03
20 48	n	0.03	0.03	0.03
21 47	n	0.03	0.03	0.03
22 46	n	0.03	0.03	0.03
23 45	n	0.03	0.03	0.03
24 44	n	0.03	0.03	0.03
25 43	n	0.03	0.03	0.03
26 42	n	0.03	0.03	0.03
27 41	n	0.03	0.03	0.03
28 40	n	0.03	0.03	0.03
29 39	n	0.03	0.03	0.03
30 38	n	0.03	0.03	0.03
31 37	n	0.03	0.03	0.03
32 36	n	0.03	0.03	0.03
33 35	n	0.03	0.03	0.03
34 34	n	0.03	0.03	0.03
35 33	n	0.03	0.03	0.03

OK Cancel Help

Edit Manning's n or k Values

River: Reach #1 ☐ Edit Interpolated XS's

Reach: Reach #1 All Regions

Selected Area Edit Options: Add Constant ... Multiply Factor ... Set Values ... Replace ...

River Station	Frctn (n/K)	n #1	n #2	n #3
36 32	n	0.03	0.03	0.03
37 31	n	0.03	0.03	0.03
38 30	n	0.03	0.03	0.03
39 29	n	0.03	0.03	0.03
40 28	n	0.03	0.03	0.03
41 27	n	0.03	0.03	0.03
42 26	n	0.03	0.03	0.03
43 25	n	0.03	0.03	0.03
44 24	n	0.03	0.03	0.03
45 23	n	0.03	0.03	0.03
46 22.75	n	0.03	0.03	0.03
47 22.7	n	0.015	0.015	0.015
48 22.5	Bridge			
49 22.3	n	0.015	0.015	0.015
50 22.25	n	0.03	0.03	0.03
51 22	n	0.03	0.03	0.03
52 21	n	0.03	0.03	0.03
53 20	n	0.03	0.03	0.03
54 18.5	n	0.03	0.03	0.03
55 18.25	Bridge			
56 18	n	0.03	0.03	0.03
57 17	n	0.03	0.03	0.03
58 16	n	0.03	0.03	0.03
59 15	n	0.03	0.03	0.03
60 14	n	0.03	0.03	0.03
61 13	n	0.03	0.03	0.03
62 12	n	0.03	0.03	0.03
63 11	n	0.03	0.03	0.03
64 10	n	0.03	0.03	0.03
65 9	n	0.03	0.03	0.03
66 8	n	0.03	0.03	0.03
67 7	n	0.03	0.03	0.03
68 6	n	0.03	0.03	0.03
69 5	n	0.03	0.03	0.03
70 4	n	0.03	0.03	0.03

OK Cancel Help

Figure B-3. Manning's n for All Models

Edit Downstream Reach Lengths

River: Reach #1 ☐ Edit Interpolated XS's

Reach: Reach #1

Selected Area Edit Options: Add Constant ... Multiply Factor ... Set Values ... Replace ...

River Station	LOB	Channel	ROB
1 65	91.7	90.6	89.4
2 64	55.56	57.06	57.24
3 63	154.02	164.22	160.82
4 62	235.52	224.02	217.58
5 61	174.23	185.06	175.94
6 60	143.78	137.62	133.56
7 59	215.76	234	263.76
8 58	103.2	104.65	106.61
9 57.75	Bridge		
10 57.5	86.56	72.79	42
11 57	62.93	61.53	62.51
12 56	64.47	62.65	63.35
13 55	194.67	201.81	202.65
14 54	100.87	102.41	110
15 53	67.23	81.09	72.9
16 52	140.56	138.32	116.49
17 51	265.68	264.87	270.81
18 50	191.73	200.76	198.03
19 49	112.64	105.93	105.16
20 48	23.88	21	19.35
21 47	175.75	189.24	189.24
22 46	168.84	173.7	175.5
23 45	147.9	143.4	138.45
24 44	212.74	212.08	213.18
25 43	150.6	143.55	139.35
26 42	182.91	204.54	196.14
27 41	231.38	225.17	222.18
28 40	160.14	164.73	168.81
29 39	236.64	237.36	237.36
30 38	190.57	189.81	190
31 37	250.25	244.75	239.75
32 36	203.6	196.8	198.2
33 35	125.06	127.92	117.13
34 34	250.25	250	251.25
35 33	214.5	216.05	216.26

OK Cancel Help

Edit Downstream Reach Lengths

River: Reach #1 ☐ Edit Interpolated XS's

Reach: Reach #1

Selected Area Edit Options: Add Constant ... Multiply Factor ... Set Values ... Replace ...

River Station	LOB	Channel	ROB
36 32	56.1	56.34	60.24
37 31	65.52	71.04	71.92
38 30	132.28	188.86	187.34
39 29	231.38	221.95	219.42
40 28	193.2	191.6	193.8
41 27	183.54	181.45	180.31
42 26	113.28	118.08	118.68
43 25	106.7	108.9	102.41
44 24	91.96	100.87	91.3
45 23	54.37	58.2	65.75
46 22.75	5.01	5.01	5.01
47 22.7	80	80	80
48 22.5	Bridge		
49 22.3	5.01	5.01	5.01
50 22.25	202	193	185.6
51 22	86.04	88.74	88.74
52 21	224.71	224.71	224.71
53 20	280.14	280.14	207.93
54 18.5	65.48	63	65.61
55 18.25	Bridge		
56 18	135.36	159.69	172.96
57 17	125.88	120	129.24
58 16	87.7	94.4	101.6
59 15	114.96	114.12	113.88
60 14	132.45	136.86	143.58
61 13	139.32	115.8	84.72
62 12	25.16	30.84	28.48
63 11	13.86	13.98	17.14
64 10	64.6	44.9	26.25
65 9	78.12	81.81	84.24
66 8	95.92	106.81	105.38
67 7	58.8	58.2	59.34
68 6	55.68	52.08	54.06
69 5	118.56	123.76	125.06
70 4	244.75	247	245.5

OK Cancel Help

Figure B-4. Reach Lengths for All Models

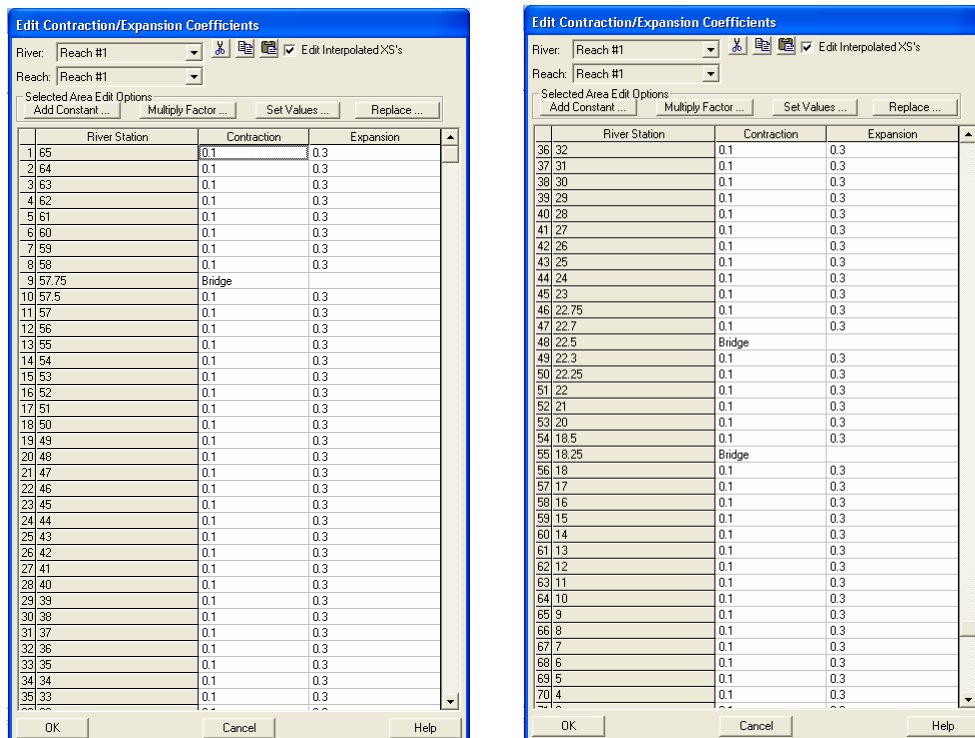


Figure B-5. Contraction/Expansion Coefficients for All Models

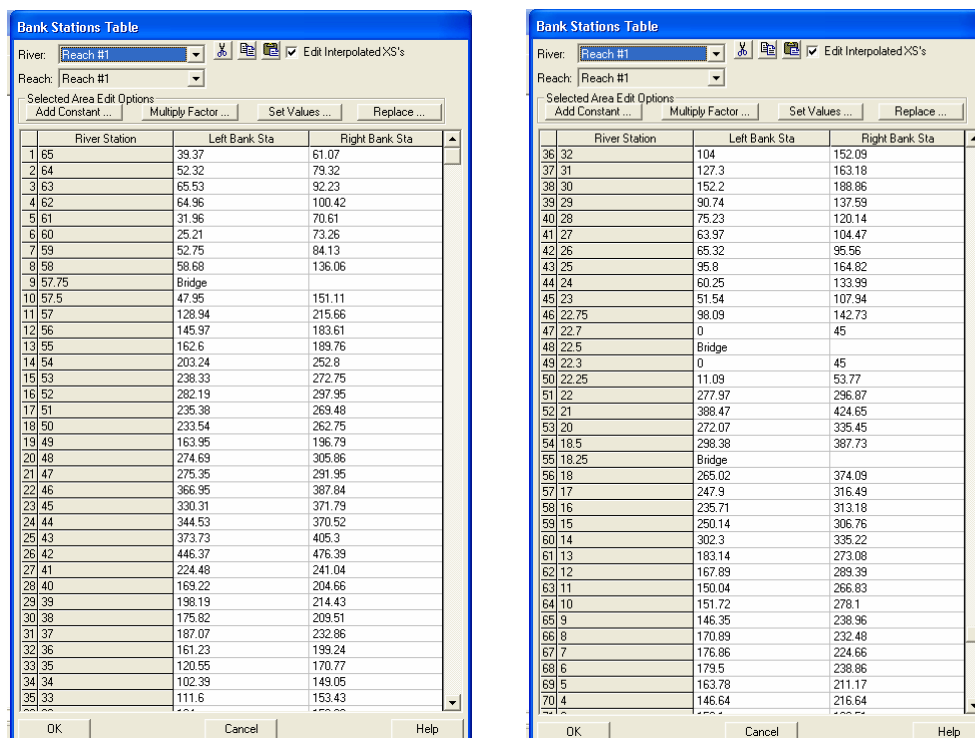


Figure B-6. Bank Stations for EXST

Bank Stations Table

River: Reach #1 ☐ Edit Interpolated X'S's

Reach: Reach #1

Selected Area Edit Options:

	River Station	Left Bank Sta	Right Bank Sta
9	57.75	Bridge	
10	57.5	47.95	151.11
11	57	128.94	215.66
12	56	145.97	183.61
13	55	60	110
14	54	60	110
15	53	60	110
16	52	60	110
17	51	60	110
18	50	60	110
19	49	60	110
20	48	60	110
21	47	60	110
22	46	60	110
23	45	330.31	371.79
24	44	344.53	370.52

Figure B-7. Bank Stations for ALT50

Bank Stations Table

River: Reach #1 ☐ Edit Interpolated X'S's

Reach: Reach #1

Selected Area Edit Options:

	River Station	Left Bank Sta	Right Bank Sta
9	57.75	Bridge	
10	57.5	47.95	151.11
11	57	128.94	215.66
12	56	145.97	183.61
13	55	60	130
14	54	60	130
15	53	60	130
16	52	60	130
17	51	60	130
18	50	60	130
19	49	60	130
20	48	60	130
21	47	60	130
22	46	60	130
23	45	330.31	371.79
24	44	344.53	370.52

Figure B-8. Bank Stations for ALT70

Bank Stations Table

River: Reach #1 ☐ Edit Interpolated X'S's

Reach: Reach #1

Selected Area Edit Options:

	River Station	Left Bank Sta	Right Bank Sta
9	57.75	Bridge	
10	57.5	47.95	151.11
11	57	128.94	215.66
12	56	145.97	183.61
13	55	60	160
14	54	60	160
15	53	60	160
16	52	60	160
17	51	60	160
18	50	60	160
19	49	60	160
20	48	60	160
21	47	60	160
22	46	60	160
23	45	330.31	371.79
24	44	344.53	370.52

Figure B-9. Bank Stations for ALT100

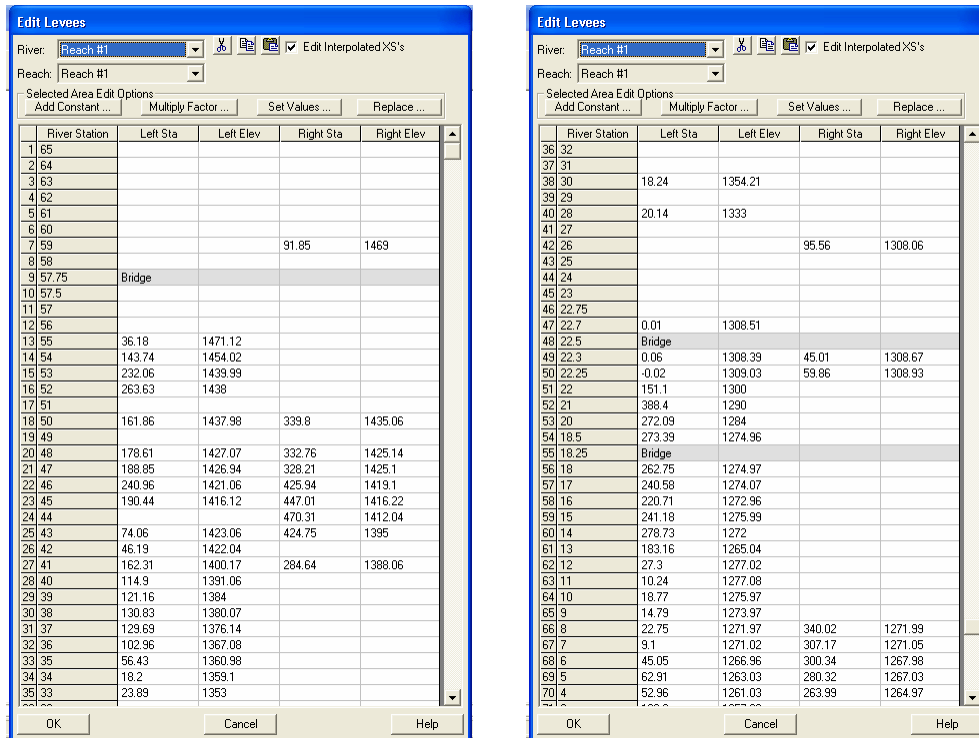


Figure B-10. Levee Stations for EXST

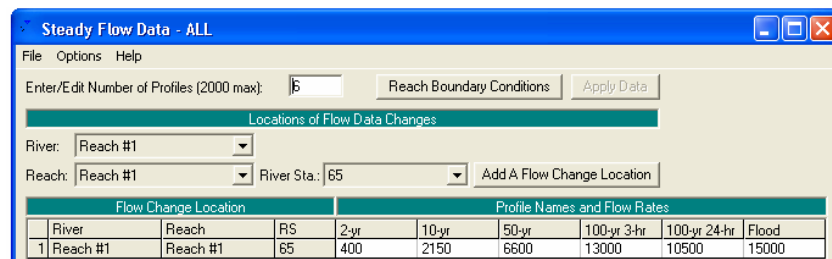


Figure B-11. Steady Flow Input File for All Models

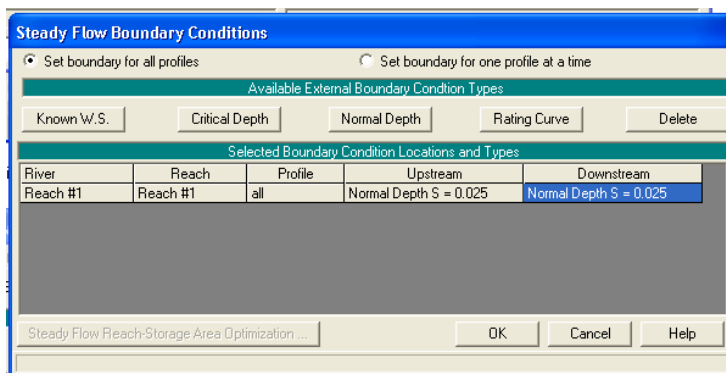


Figure B-12. Boundary Condition Input File for All Models

OUTPUTS

Overview

Figure B-13 thru Figure B-15 display the channel velocity, shear stress, and stream power for all four models (EXST, ALT50, ALT70, ALT100) for all six storm discharges.

The majority of the calculations were made using the 2-yr discharge for the various HEC-RAS models, Table B-1 thru Table B-4 display the 2-yr discharge output for the EXST, ALT50, ALT70, and ALT100 models.

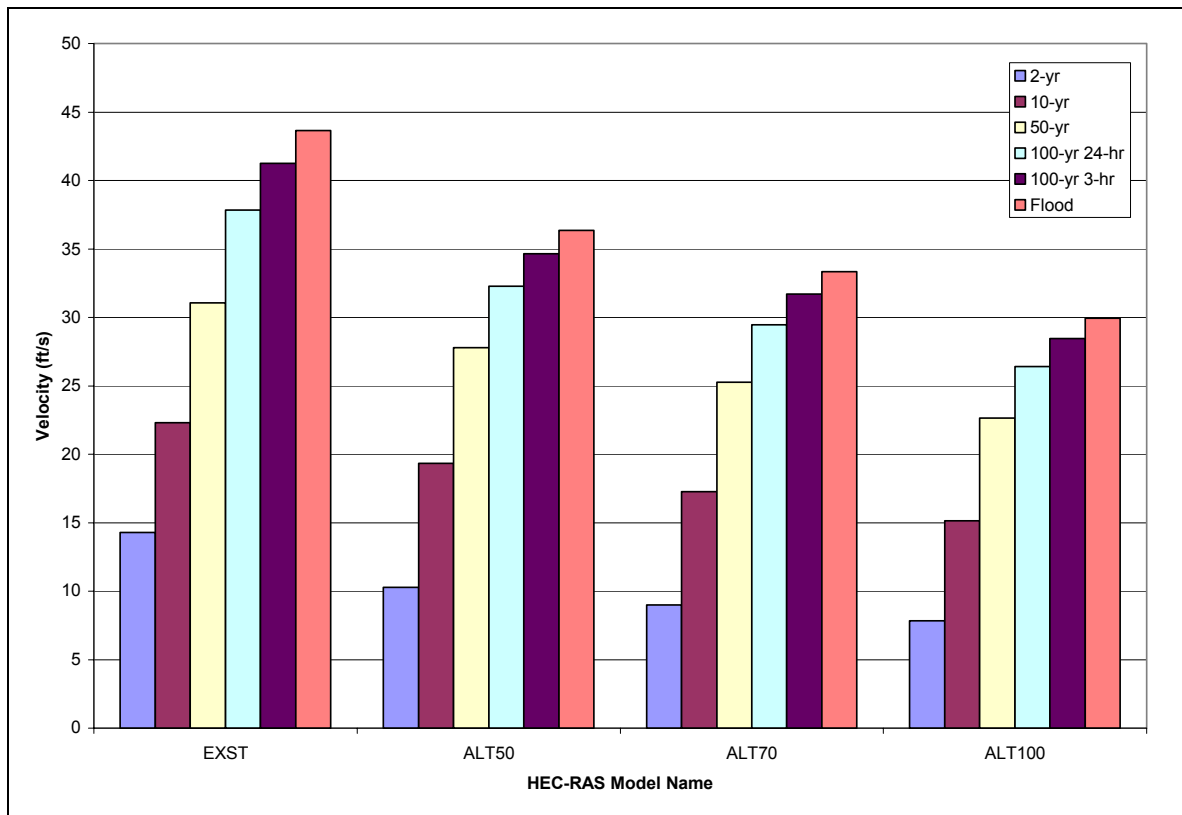


Figure B-13: Flow Velocities

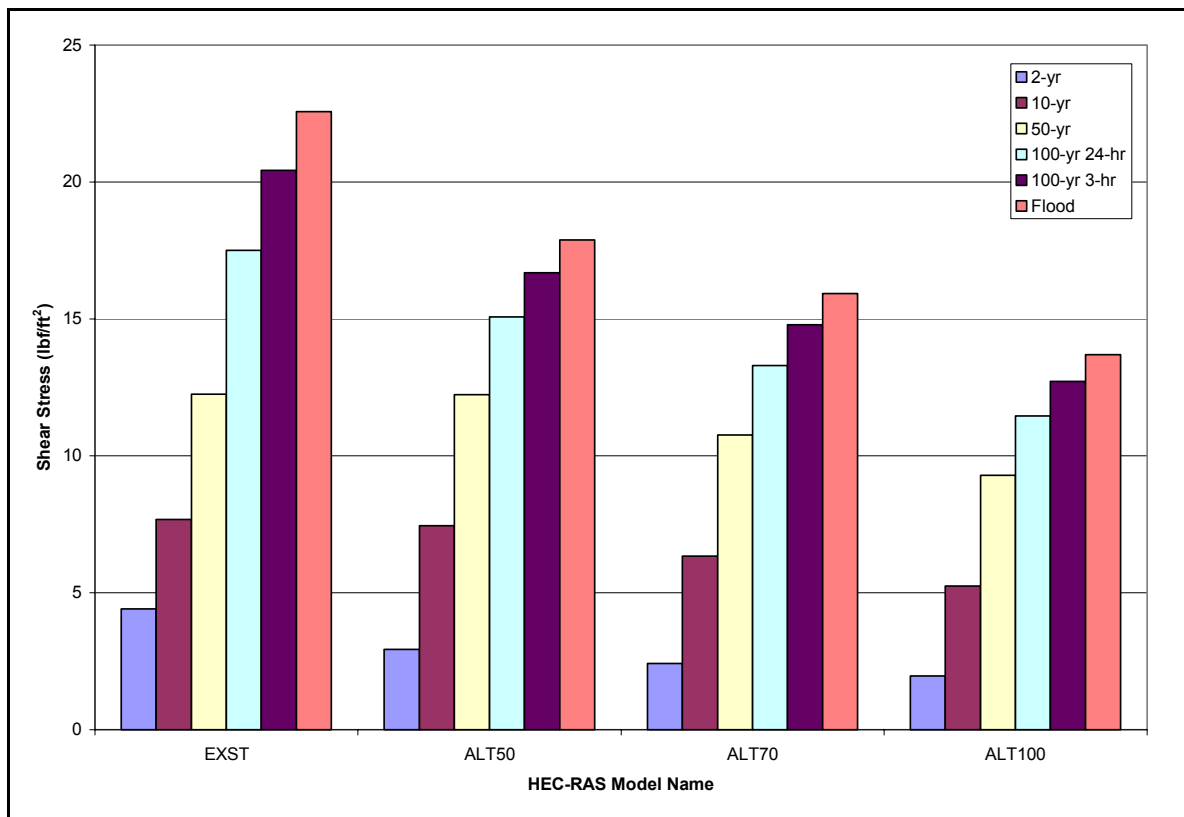


Figure B-14: Shear Stress at Channel Bottom

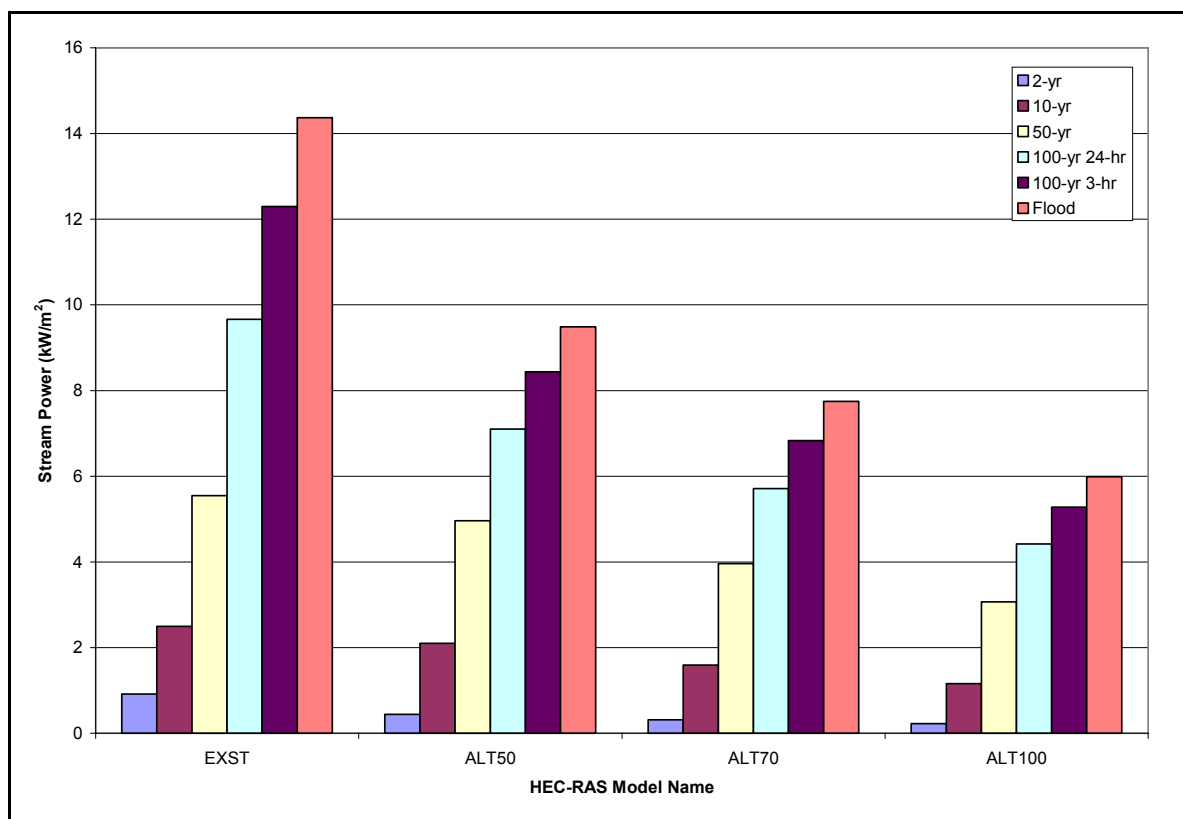


Figure B-15: Stream Power at Channel Bottom

Table B-1. EXST - Existing Conditions (2-yr Storm Event) Output

HEC-RAS Plan: EXST-Final River: Reach #1 Reach: Reach #1 Profile: 2-yr

River Sta	Profile	Q Total (cfs)	Min Ch EI (ft)	W.S. Elev (ft)	Crit W.S. (ft)	E.G. Elev (ft)	E.G. Slope (ft/ft)	Vel Chnl (ft/s)	Flow Area (sq ft)	Top Width (ft)	Froude # Chl	Shear Chan (lb/sq ft)	Power Chan (lb/ft s) (kW/m ²)	
65	2-yr	400	1490	1492.08	1492.60	1493.85	0.0250	10.84	38.54	27.30	1.49	2.54	27.56	0.40
64	2-yr	400	1488	1489.86	1490.33	1491.41	0.0287	10.25	41.83	39.15	1.55	2.42	24.78	0.36
63	2-yr	400	1484	1485.60	1486.38	1488.34	0.0646	13.39	30.61	30.84	2.25	4.42	59.22	0.86
62	2-yr	400	1480	1481.94	1482.28	1483.14	0.0261	8.96	46.85	45.45	1.45	1.93	17.30	0.25
61	2-yr	400	1475	1476.89	1477.14	1477.90	0.0215	8.20	50.84	48.21	1.32	1.61	13.21	0.19
60	2-yr	400	1470	1471.80	1472.09	1472.88	0.0262	8.34	47.95	45.01	1.42	1.74	14.48	0.21
59	2-yr	400	1465	1466.74	1467.22	1468.33	0.0319	10.18	39.97	34.49	1.61	2.46	25.01	0.36
58	2-yr	400	1462	1462.58	1462.89	1463.62	0.0149	8.37	49.79	95.81	1.94	0.54	4.48	0.07
57.75														
57.5	2-yr	400	1457	1457.78	1458.39	1460.71	0.0508	13.74	29.12	60.13	3.48	1.53	21.02	0.31
57	2-yr	400	1455	1455.44	1455.87	1457.10	0.0323	10.35	38.78	88.05	2.74	0.89	9.25	0.13
56	2-yr	400	1450	1451.45	1452.02	1453.22	0.0511	10.82	38.83	51.02	1.95	3.03	32.79	0.48
55	2-yr	400	1444	1446.30	1447.12	1449.11	0.0674	13.47	29.92	29.17	2.27	4.51	60.74	0.89
54	2-yr	400	1440	1441.50	1441.75	1442.49	0.0263	8.03	50.24	52.26	1.41	1.64	13.17	0.19
53	2-yr	400	1435	1437.65	1438.12	1439.10	0.0326	9.77	42.31	41.61	1.60	2.32	22.68	0.33
52	2-yr	400	1430	1432.11	1433.05	1435.13	0.0430	14.30	29.90	22.22	1.95	4.41	63.03	0.92
51	2-yr	400	1425	1427.08	1427.71	1429.13	0.0383	11.48	34.83	26.35	1.76	3.08	35.41	0.52
50	2-yr	400	1420	1421.82	1422.22	1423.11	0.0241	9.39	46.40	46.01	1.42	2.03	19.05	0.28
49	2-yr	400	1415	1416.76	1417.15	1418.05	0.0259	9.28	45.37	43.61	1.46	2.03	18.85	0.28
48	2-yr	400	1410	1412.23	1412.80	1414.04	0.0404	10.82	37.24	34.21	1.75	2.86	30.92	0.45
47	2-yr	400	1405	1407.94	1409.33	1412.53	0.0629	17.20	23.26	12.32	2.21	6.40	110.01	1.61
46	2-yr	400	1400	1402.84	1403.55	1405.17	0.0294	12.23	32.70	17.35	1.57	3.17	38.82	0.57
45	2-yr	400	1395	1397.78	1398.32	1399.44	0.0279	10.34	38.70	26.69	1.51	2.43	25.15	0.37
44	2-yr	400	1391	1392.91	1393.54	1395.00	0.0306	11.59	34.51	21.21	1.60	2.96	34.27	0.50
43	2-yr	400	1385	1387.31	1387.88	1389.24	0.0257	11.12	35.96	20.66	1.49	2.66	29.60	0.43
42	2-yr	400	1380	1382.24	1382.88	1384.29	0.0353	11.47	34.86	24.36	1.69	3.02	34.61	0.50
41	2-yr	400	1375	1377.53	1378.14	1379.63	0.0355	12.50	38.05	39.19	1.74	3.43	42.90	0.63
40	2-yr	400	1370	1372.17	1372.52	1373.45	0.0256	9.10	44.00	36.05	1.44	1.97	17.90	0.26
39	2-yr	400	1365	1367.45	1368.10	1369.47	0.0278	11.98	39.51	40.67	1.56	3.03	36.34	0.53
38	2-yr	400	1360	1362.23	1362.74	1363.92	0.0228	11.26	42.03	34.43	1.45	2.63	29.63	0.43
37	2-yr	400	1355	1357.48	1358.05	1359.10	0.0273	10.28	40.43	35.88	1.51	2.40	24.67	0.36
36	2-yr	400	1350	1351.70	1352.02	1352.83	0.0239	8.62	47.61	44.09	1.39	1.78	15.35	0.22
35	2-yr	400	1345	1346.59	1347.03	1347.99	0.0366	10.58	45.86	60.59	1.71	2.69	28.50	0.42
34	2-yr	400	1340	1341.99	1342.56	1343.80	0.0394	10.80	37.04	31.65	1.76	2.83	30.59	0.45
33	2-yr	400	1335	1336.87	1337.14	1337.89	0.0228	8.16	50.18	47.37	1.35	1.62	13.26	0.19
32	2-yr	400	1330	1331.54	1331.79	1332.51	0.0242	7.92	51.14	51.91	1.37	1.57	12.46	0.18
31	2-yr	400	1329	1330.20	1330.44	1331.16	0.0213	8.17	52.20	50.25	1.31	1.60	13.04	0.19
30	2-yr	400	1325	1327.24	1327.72	1328.79	0.0284	9.99	40.05	30.17	1.53	2.32	23.18	0.34
29	2-yr	400	1320	1322.87	1323.16	1323.94	0.0251	8.33	48.02	43.41	1.40	1.71	14.28	0.21
28	2-yr	400	1315	1316.95	1317.25	1318.03	0.0255	8.35	47.90	43.98	1.41	1.73	14.43	0.21
27	2-yr	400	1310	1312.28	1312.59	1313.37	0.0234	8.39	48.06	44.23	1.37	1.70	14.29	0.21
26	2-yr	400	1306	1308.14	1308.38	1309.00	0.0169	7.98	59.17	68.77	1.19	1.46	11.63	0.17
25	2-yr	400	1304	1305.76	1305.90	1306.41	0.0213	6.54	62.48	76.89	1.24	1.14	7.47	0.11
24	2-yr	400	1301	1302.67	1302.84	1303.40	0.0265	6.86	58.69	75.86	1.36	1.30	8.89	0.13
23	2-yr	400	1297	1299.68	1299.79	1300.40	0.0184	6.83	59.18	59.48	1.18	1.18	8.03	0.12
22.75	2-yr	400	1297	1299.65	1299.89	1299.89	0.0021	3.92	103.83	48.21	0.46	0.30	1.17	0.02
22.7	2-yr	400	1296.83	1297.61	1298.19	1299.65	0.0197	11.47	34.88	44.99	2.30	0.92	10.56	0.15
22.5														
22.3	2-yr	400	1295.49	1297.82	1296.83	1298.04	0.0006	3.82	104.62	45.00	0.44	0.07	0.28	0.00
22.25	2-yr	400	1295	1297.26	1297.26	1297.97	0.0125	6.77	59.13	43.05	1.01	1.06	7.15	0.10
22	2-yr	400	1291	1292.01	1292.01	1292.17	0.0025	1.75	127.67	97.30	0.40	0.09	0.16	0.00
21	2-yr	400	1288	1289.53	1290.00	1291.43	0.0436	11.06	36.15	32.26	1.84	3.01	33.33	0.49
20	2-yr	400	1283	1283.97	1284.00	1284.89	0.0315	7.72	51.79	62.75	1.50	1.62	12.51	0.18
18.5	2-yr	400	1273	1274.98	1274.67	1274.99	0.0002	0.81	442.34	339.81	0.13	0.02	0.01	0.00
18.25														
18	2-yr	400	1273	1273.99	1273.99	1274.37	0.0147	4.93	81.12	108.69	1.01	0.68	3.37	0.05
17	2-yr	400	1271	1271.51	1271.51	1271.79	0.0176	4.11	92.91	175.28	1.03	0.54	2.24	0.03
16	2-yr	400	1269	1270.26	1270.00	1270.55	0.0059	4.29	94.02	82.73	0.69	0.44	1.90	0.03
15	2-yr	400	1267	1269.07	1269.07	1269.74	0.0120	6.55	61.05	45.72	1.00	1.00	6.52	0.10
14	2-yr	400	1265	1265.33	1266.03	1267.25	0.0430	3.11	37.05	41.34	1.34	0.45	1.39	0.02
13	2-yr	400	1264	1265.04	1265.04	1265.31	0.0062	3.26	103.41	123.46	0.65	0.29	0.96	0.01
12	2-yr	400	1262	1263.53	1263.62	1264.04	0.0204	5.75	69.56	94.75	1.18	0.93	5.37	0.08
11	2-yr	400	1261	1262.66	1262.81	1263.25	0.0259	6.17	64.80	94.83	1.32	1.10	6.80	0.10
10	2-yr	400	1260	1262.52	1262.56	1262.97	0.0167	5.42	73.76	94.49	1.08	0.81	4.41	0.06
9	2-yr	400	1259	1260.42	1260.79	1261.64	0.0324	8.87	45.09	45.21	1.57	2.01	17.81	0.26
8	2-yr	400	1258	1259.96	1259.86	1260.45	0.0104	5.62	71.22	60.66	0.91	0.76	4.28	0.06
7	2-yr	400	1257	1258.87	1258.73	1259.21	0.0067	5.01	91.63	97.24	0.75	0.58	2.88	0.04
6	2-yr	400	1255	1257.54	1257.73	1258.37	0.0194	7.30	54.81	50.03	1.23	1.32	9.62	0.14
5	2-yr	400	1254	1256.70	1256.80	1257.50	0.0147	7.17	55.79	42.33	1.10	1.20	8.58	0.13
4	2-yr	400	1253	1255.11	1255.24	1255.88	0.0160	7.02	57.01	47.89	1.13	1.18	8.31	0.12
3	2-yr	400	1250	1251.61	1251.72	1252.22	0.0161	6.77	66.68	77.83	1.13	1.12	7.61	0.11
2	2-yr	400	1248	1250.15	1250.00	1250.57	0.0068	5.71	80.82	65.57	0.78	0.70	4.02	0.06
1	2-yr	400	1245	1247.54	1247.62	1248.20	0.0173	6.54	61.18	60.09	1.14	1.09	7.10	0.10
0	2-yr	400	1243	1245.05	1245.13	1245.62	0.0174	6.07	65.92	73.17	1.13	0.97	5.90	0.09

Table B-2. ALT50 (2-yr Storm Event) Output

HEC-RAS Plan: ALT50 River: Reach #1 Reach: Reach #1 Profile: 2-yr

River Sta	Profile	Q Total (cfs)	Min Ch EI (ft)	W.S. Elev (ft)	Crit W.S. (ft)	E.G. Elev (ft)	E.G. Slope (ft/ft)	Vel Chnl (ft/s)	Flow Area (sq ft)	Top Width (ft)	Froude # Chl	Shear Chan (lb/sq ft)	Power Chan (lb/ft s) (kW/m ²)	
55	2-yr	400	1444	1444.65	1445.23	1446.87	0.1058	12.06	33.66	53.89	2.64	4.28	51.60	0.75
54	2-yr	400	1440	1441.07	1441.23	1441.86	0.0195	7.22	56.75	56.40	1.23	1.30	9.37	0.14
53	2-yr	400	1435	1435.82	1436.23	1437.20	0.0484	9.52	42.82	54.90	1.86	2.47	23.46	0.34
52	2-yr	400	1430	1430.76	1431.23	1432.37	0.0621	10.27	39.64	54.55	2.08	2.94	30.19	0.44
51	2-yr	400	1425	1425.89	1426.23	1427.04	0.0362	8.71	46.85	55.34	1.63	2.01	17.49	0.26
50	2-yr	400	1420	1421.08	1421.23	1421.85	0.0185	7.11	57.63	56.49	1.20	1.25	8.91	0.13
49	2-yr	400	1415	1415.99	1416.23	1416.91	0.0249	7.77	52.62	55.96	1.37	1.54	11.98	0.17
48	2-yr	400	1410	1410.82	1411.23	1412.18	0.0472	9.45	43.14	54.93	1.84	2.42	22.89	0.33
47	2-yr	400	1405	1405.52	1406.23	1409.01	0.2210	15.07	26.86	53.13	3.68	7.19	108.29	1.58
46	2-yr	400	1400	1400.97	1401.23	1401.93	0.0266	7.94	51.52	55.84	1.42	1.62	12.83	0.19

Table B-3. ALT70 (2-yr Storm Event) Output

HEC-RAS Plan: ALT70 River: Reach #1 Reach: Reach #1 Profile: 2-yr

River Sta	Profile	Q Total (cfs)	Min Ch EI (ft)	W.S. Elev (ft)	Crit W.S. (ft)	E.G. Elev (ft)	E.G. Slope (ft/ft)	Vel Chnl (ft/s)	Flow Area (sq ft)	Top Width (ft)	Froude # Chl	Shear Chan (lb/sq ft)	Power Chan (lb/ft s) (kW/m ²)	
55	2-yr	400	1444	1444.53	1444.99	1446.27	0.1077	10.64	37.92	73.18	2.58	3.56	37.90	0.55
54	2-yr	400	1440	1440.87	1440.99	1441.50	0.0200	6.40	63.37	75.24	1.21	1.09	6.99	0.10
53	2-yr	400	1435	1435.67	1435.99	1436.75	0.0484	8.36	48.39	74.03	1.80	2.03	16.96	0.25
52	2-yr	400	1430	1430.62	1430.99	1431.87	0.0620	9.01	44.87	73.75	2.01	2.42	21.76	0.32
51	2-yr	400	1425	1425.73	1425.99	1426.63	0.0360	7.65	52.94	74.40	1.57	1.65	12.62	0.18
50	2-yr	400	1420	1420.88	1420.99	1421.50	0.0195	6.35	63.93	75.28	1.19	1.07	6.79	0.10
49	2-yr	400	1415	1415.82	1415.99	1416.53	0.0248	6.83	59.39	74.92	1.33	1.27	8.65	0.13
48	2-yr	400	1410	1410.68	1410.99	1411.73	0.0468	8.27	48.88	74.07	1.77	1.98	16.41	0.24
47	2-yr	400	1405	1405.42	1405.99	1408.22	0.2353	13.47	29.91	72.52	3.66	6.17	83.04	1.21
46	2-yr	400	1400	1400.80	1400.99	1401.55	0.0267	6.98	58.03	74.81	1.37	1.34	9.33	0.14

Table B-4. ALT100 (2-yr Storm Event) Output

HEC-RAS Plan: ALT100 River: Reach #1 Reach: Reach #1 Profile: 2-yr

River Sta	Profile	Q Total (cfs)	Min Ch EI (ft)	W.S. Elev (ft)	Crit W.S. (ft)	E.G. Elev (ft)	E.G. Slope (ft/ft)	Vel Chnl (ft/s)	Flow Area (sq ft)	Top Width (ft)	Froude # Chl	Shear Chan (lb/sq ft)	Power Chan (lb/ft s) (kW/m ²)	
55	2-yr	400	1444	1444.43	1444.78	1445.75	0.1076	9.24	43.49	102.58	2.49	2.88	26.65	0.39
54	2-yr	400	1440	1440.71	1440.78	1441.19	0.0201	5.58	72.27	104.25	1.17	0.89	4.96	0.07
53	2-yr	400	1435	1435.55	1435.78	1436.36	0.0482	7.26	55.43	103.27	1.73	1.64	11.93	0.17
52	2-yr	400	1430	1430.51	1430.78	1431.45	0.0621	7.84	51.35	103.04	1.94	1.96	15.36	0.22
51	2-yr	400	1425	1425.60	1425.78	1426.27	0.0355	6.62	60.85	103.59	1.51	1.32	8.76	0.13
50	2-yr	400	1420	1420.73	1420.78	1421.18	0.0183	5.42	74.39	104.37	1.12	0.83	4.51	0.07
49	2-yr	400	1415	1415.66	1415.78	1416.21	0.0250	5.96	67.68	103.98	1.29	1.03	6.16	0.09
48	2-yr	400	1410	1410.55	1410.78	1411.35	0.0473	7.22	55.75	103.29	1.72	1.62	11.70	0.17
47	2-yr	400	1405	1405.34	1405.78	1407.43	0.2302	11.62	34.56	102.05	3.50	4.91	57.12	0.83
46	2-yr	400	1400	1400.65	1400.78	1401.22	0.0268	6.09	66.22	103.90	1.33	1.09	6.62	0.10

References

Chang, Howard H. 1995. Inland Feeder Pipeline, San Bernardino Segment (Contract 3): Fluvial Study of City Creek for Pipeline Placement. Prepared for Dames and Moore.

U.S. Army Corps of Engineers (USACE). 2001. *HEC-RAS River Analysis System* v. 3.3.3 [computer software]. www.hec.usace.army.mil

BOSS International, Inc. 2000. *BOSS RMS for AutoCAD* version 2000 Windows [software package]. Madison, WI: BOSS International, Inc.

APPENDIX C – ERODIBILITY INDEX METHOD

Appendix C: Erodibility Index Calculations

Introduction

Through the use of the Erodibility Index Method, EIM, (Annandale 1995) and data provided in the Chang Study (1995), it was possible to evaluate the scour threshold of the existing material of City Creek. In addition, the EIM was used to determine the erosive threshold of the armor layer (Appendix D).

Methodology

The potential erodibility of the riverbanks and bed was determined by making use of the Erodibility Index Method (Annandale 1995; Annandale 2006). The Erodibility Index Method defines a threshold between erosion and non-erosion by relating the erosive power of water, expressed in terms of stream power, and the relative ability of earth material to resist erosion, expressed in terms of the erodibility index. The index is the scalar product of the values of its constituent parameters and takes the form:

$$K = M_s \cdot K_b \cdot K_d \cdot J_s \quad (C.1)$$

M_s = mass strength number

K_b = particle/block size number

K_d = discontinuity or inter-particle bond shear strength number = tangent of the angle of internal friction

J_s = relative ground structure number

M_s is based on the SPT count of non-cohesive material, and can be obtained by making use of Table C-1.

• Table C-1. Mass Strength Number (Annandale, 1995, 2006)

Soil Type	Consistency	Identification in Profile	SPT Blow Count	M_s
Non-cohesive	Very loose	Crumbles very easily when scraped with geologic pick	0-4	0.02
	Loose	Small resistance to penetration by sharp end of geologic pick	4-10	0.04
	Medium dense	Considerable resistance to penetration by sharp end of geologic pick	10-30	0.09
	Dense	Very high resistance to penetration of sharp end of geologic pick - requires many blows of pick for excavation	30-50	0.19
	Very dense	High resistance to repeated blows of geologic pick - requires power tools for excavation	50-80	0.41
			80+	see rock

For non-cohesive material, the particle/block size number, K_b is defined in terms of the median grain size, D_{50} (in meters) (Annandale 1995; 2006):

$$K_b = 1000 \cdot D_{50}^3 \quad (C.2)$$

The shear strength number, K_d was determined by:

$$K_d = \tan \phi_r \quad (C.3)$$

where ϕ_r the minimum friction angle (Annandale 1995; 2006). A typical value of ϕ_r for quartz sand is 32 degrees.

The orientation number $J_s = 1$ by convention if the material under investigation is other than jointed rock (Annandale 1995; 2006).

The erodibility threshold of a material can be calculated by the following:

$$P_R = K^{0.75} \quad \text{for } K > 0.1 \quad (C.4)$$

$$P_R = 0.48 \cdot K^{0.44} \quad \text{for } K \leq 0.1 \quad (C.5)$$

The Erodibility Index for a particular earth material can be used to determine the threshold stream power per unit area. If the stream power of the water is greater than the threshold stream power, the earth material will erode. If it is lower, the earth material will not erode. The stream power exerted by the water can be obtained from the HEC-RAS model for open channel flow conditions. It is quantified by analytical means for other flow conditions, such as those present at headcuts or hydraulic jumps (Annandale 2006).

Assumptions

- The grain size distribution reported for Highland Ave. in the Chang Study (1995) is still representative of the materials on site.

Input

The main input required for this site is the particle size at which 50% is finer, or the D_{50} . When looking at the erosive threshold of the armor layer particles, the average D_{50} was used.

Results

The erosive threshold for the existing bed material can be seen in Figure C-1. After the armor layer particle size was determined (Appendix D), the erosive threshold for the EXST, ALT50, ALT70, and ALT100 models was calculated at the pipeline crossing (Figure C-2). In addition the erosive threshold for the armor layers calculated at existing headcuts located at stations 64, 48, 31, and 25 was calculated as well (Figure C-3).

Figure C-1. Erodibility Index Method for Existing Bed Material

Ms	0.04
D₅₀ (mm)	25
Kb	0.016
Kd	0.62
Js	1
K	7.8E-04
Erosive Threshold (W/m²)	15.2

Figure C-2. Erodibility Index Method for Median Armor Layer Particle Size Calculated at the Pipeline Crossing

Parameter	At Pipeline Crossing			
	EXST	ALT50	ALT70	ALT100
Ms	0.09	0.09	0.09	0.09
D ₅₀ (mm)	436	224	183	156
Kb	82.8	11.3	6.1	3.8
Kd	0.6	0.6	0.6	0.6
Js	1	1	1	1
K	4.7	0.6	0.3	0.2
Erosive Threshold (W/m²)	944	392	301	244

Figure C-3. Erodibility Index Method for Median Armor Layer Particle Size Calculated for Active Headcuts

Parameter	Existing Headcut Station #'s			
	64	48	31	25
Ms	0.09	0.09	0.09	0.09
D ₅₀ (mm)	217	328	114	129
Kb	10.2	35.2	1.5	2.2
Kd	0.6	0.6	0.6	0.6
Js	1	1	1	1
K	0.6	2.0	0.1	0.1
Erosive Threshold (W/m²)	375	648	161	190

References

1. Annandale, G. W., (1995), Erodibility, Journal of Hydraulic Research, Journal of Hydraulic Research, Vol. 33, No. 4, pp. 471-494.

APPENDIX D – ARMOR LAYER

Appendix D: Armor Layer

Introduction

Degradation can be controlled by formation of an armor layer or by a stable slope. The formation of an armor layer will generally occur if the channel contains more than 10 percent coarse material which cannot be transported under dominant flow conditions. The Gessler method (1970) is an additional method for calculating armor layer that is not included in Pemberton and Lara (1984). The following six methods can be used for calculating armor layer formation:

- 1) Meyer-Peter, Muller (bedload transport equation);
- 2) Competent bottom velocity;
- 3) Lane's tractive force theory;
- 4) Shields diagram;
- 5) Yang incipient motion; and
- 6) Gessler method.

Assumptions

- The grain size distribution at Highland Ave. reported in the Chang study (1995) reflects the current bed gradation at the pipeline crossing.
- Clear water, i.e. no sediment is being transported from upstream;
- The two-year discharge of 400cfs is the dominant discharge, the flow effecting the ultimate shape and hydraulics of the channel;
- The degraded channel will have the same hydraulic conditions as the existing channel;
- The ultimate slope of the degraded channel will be equal to that of the existing channel

Input

All hydraulic input data obtained from HEC-RAS results (Table D-1 and Table D-2) and all gradation input obtained from the Highland Ave. grain size distribution (Figure D- 1) (Chang 1995).

Table D-1. Input Parameters for Armor Layer and Gessler Method Calculations for EXST, ALT50, SLT70, and ALT100

Method 1: Meyer-Peter, Muller					
Variable	EXST	ALT50	ALT70	ALT100	Comment
d_1	0.64 m	0.23 m	0.19 m	0.16 m	mean water depth at pipeline crossing
S_{E_1}	0.043 m/m	0.062 m/m	0.062 m/m	0.062 m/m	Energy gradient slope
n_{ls}	0.03	0.03	0.03	0.03	Manning's roughness for the channel bed
D_{90_1}	970 mm	970 mm	970 mm	970 mm	Particle size at which 90 percent of the bed material is finer
K_1	0.058	0.058	0.058	0.058	constant
Δp_1	0.15	0.22	0.24	0.26	Decimal percentage of original bed material larger than the armor size D_c
Method 2: Competent Bottom Velocity Method					
Variable	EXST	ALT50	ALT70	ALT100	Comment
V_m	4.36 m/s	3.08 m/s	2.719 m/s	2.37 m/s	mean channel velocity
Δp_2	0.17	0.25	0.29	0.33	Decimal percentage of original bed material larger than the armor size D_c
Method 3: Lane's Tractive Force Method					
Variable	EXST	ALT50	ALT70	ALT100	Comment
d	0.64 m	0.23 m	0.19 m	0.16 m	mean water depth at pipeline crossing
S	0.043 m/m	0.062 m/m	0.062 m/m	0.062 m/m	Energy gradient slope
Δp_3	n/a	0.3	0.34	0.35	Decimal percentage of original bed material larger than the armor size D_c
Method 4: Shields Method					
Variable	EXST	ALT50	ALT70	ALT100	Comment
T_{star}	0.047	0.047	0.047	0.047	Dimensionless shear stress
Δp_4	0.18	0.25	0.24	0.31	Decimal percentage of original bed material larger than the armor size D_c
Method 5: Yang Incipient Motion Method					
Variable	EXST	ALT50	ALT70	ALT100	Comment
Re	2.931×10^3	3.62×10^3	3.634×10^3	3.751×10^3	Reynold's number
ν	0.929×10^{-6} m ² /s	0.929×10^{-6} m ² /s	0.929×10^{-6} m ² /s	0.929×10^{-6} m ² /s	kinematic viscosity @ 25 deg. C
D_{50}	25 mm	25 mm	25 mm	25 mm	Particle size at which 50 percent of the bed material is finer
Δp_5	0.22	0.18	0.18	0.16	Decimal percentage of original bed material larger than the armor size D_c

Method 6: Gessler					
Variable	EXST	ALT50	ALT70	ALT100	Comment
D ₅₀	25 mm	25 mm	25 mm	25 mm	Particle size at which 50 percent of the bed material is finer
D ₉₀	970 mm	970 mm	970 mm	970 mm	Particle size at which 90 percent of the bed material is finer
Q	400 ft ³ /s	400 ft ³ /s	400 ft ³ /s	400 ft ³ /s	Flow rate
M	2.69	2.69	2.69	2.69	Approximate bank slope (MH:1V) at sample location
S	0.049	0.039	0.039	0.039	Approximate bed slope at sample location
b	17 ft	50 ft	70 ft	100 ft	Approximate bottom width of the channel at sample location
γ _s	25970 N/m ³	25970 N/m ³	25970 N/m ³	25970 N/m ³	Specific weight of sediment
γ	9800 N/m ³	9800 N/m ³	9800 N/m ³	9800 N/m ³	Specific weight of water
ρ	1000 kg/m ³	1000 kg/m ³	1000 kg/m ³	1000 kg/m ³	Density of water
ν	1.31x10 ⁻⁶ m ² /s	1.31x10 ⁻⁶ m ² /s	1.31x10 ⁻⁶ m ² /s	1.31x10 ⁻⁶ m ² /s	Kinematic viscosity of water
g	9.807 m/s ²	9.807 m/s ²	9.807 m/s ²	9.807 m/s ²	Acceleration due to gravity
h'	2.11 ft	0.76 ft	0.62 ft	0.51 ft	Depth of flow
f _s	0.03	0.03	0.03	0.03	Friction factor of the bank
R'	1.31 ft	0.72 ft	0.61 ft	0.5 ft	Hydraulic radius
R' _s	0.55 ft	0.36 ft	0.3 ft	0.24 ft	Hydraulic radius for channel sides
R' _b	1.64 ft	0.76 ft	0.62 ft	0.51 ft	Hydraulic radius of channel bottom
P'	22.84 ft	54.8 ft	73.95 ft	103.2 ft	Wetted Perimeter
P' _s	6.84 ft	4.8 ft	4 ft	3.2 ft	Wetted Perimeter for channel sides
A'	29.9 ft ²	39.64 ft ²	44.87 ft ²	51.35 ft ²	Cross sectional area
A' _s	3.63 ft ²	1.7 ft ²	1.2 ft ²	0.76 ft ²	Cross sectional area for channel sides
A' _b	26.27 ft ²	37.92 ft ²	43.7 ft ²	50.59 ft ²	Cross sectional area of channel bottom
U'	13.38 ft/s	10.09 ft/s	8.92 ft/s	7.79 ft/s	Average flow velocity
Δp _{A50}	0.15	0.19	0.19	0.21	Decimal percentage of original bed material larger than the armor size D _c

Table D-2. Input Parameters for Armor Layer Calculations for Active Headcuts

Method 1: Meyer-Peter, Muller					
Variable	#64	#48	#31	#25	Comment
d_1	0.567 m	0.68 m	0.366 m	0.536 m	mean water depth at pipeline crossing
S_{E_1}	0.0287 m/m	0.0404 m/m	0.0213 m/m	0.0213 m/m	Energy gradient slope
n_{ls}	0.03	0.03	0.03	0.03	Manning's roughness for the channel bed
D_{90_1}	970 mm	970 mm	970 mm	970 mm	Particle size at which 90 percent of the bed material is finer
K_1	0.058	0.058	0.058	0.058	constant
Δp_1	0.2	0.15	0.28	0.24	Decimal percentage of original bed material larger than the armor size D_c
Method 2: Competent Bottom Velocity Method					
Variable	#64	#48	#31	#25	Comment
V_m	2.914 m/s	3.27 m/s	2.34 m/s	1.95 m/s	mean channel velocity
Δp_2	0.26	0.24	0.31	0.36	Decimal percentage of original bed material larger than the armor size D_c
Method 3: Lane's Tractive Force Method					
Variable	#64	#48	#31	#25	Comment
d	0.567 m	0.68 m	0.366 m	0.536 m	mean water depth at pipeline crossing
S	0.0287 m/m	0.0404 m/m	0.0213 m/m	0.0213 m/m	Energy gradient slope
Δp_3	n/a	n/a	0.34	n/a	Decimal percentage of original bed material larger than the armor size D_c
Method 4: Shields Method					
Variable	#64	#48	#31	#25	Comment
T_{star}	0.047	0.047	0.047	0.047	Dimensionless shear stress
Δp_4	0.24	0.18	0.34	0.26	Decimal percentage of original bed material larger than the armor size D_c
Method 5: Yang Incipient Motion Method					
Variable	#64	#48	#31	#25	Comment
V_m	2.914 m/s	3.27 m/s	2.34 m/s	1.95 m/s	Particle size at which 50 percent of the bed material is finer
Δp_5	0.26	0.22	0.31	0.36	Decimal percentage of original bed material larger than the armor size D_c

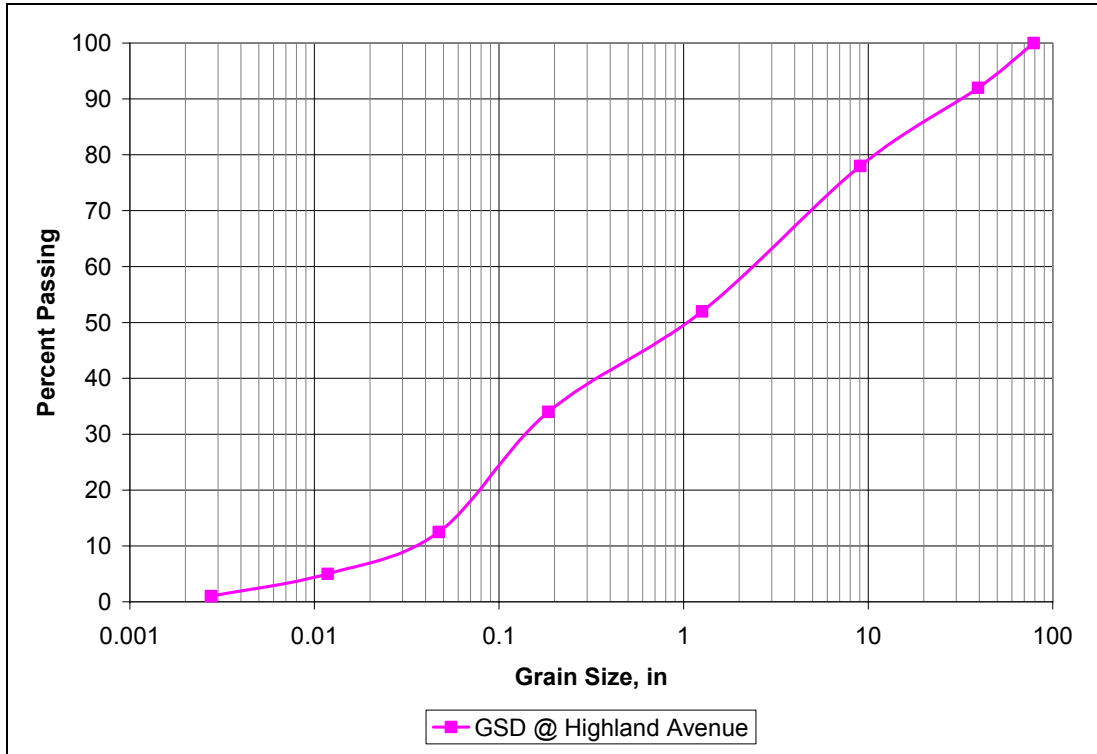


Figure D- 1. Highland Ave. Grain Size Distribution (Chang 1995)Calculations

Calculations

The hydraulic results for the two-year discharge for all four HEC-RAS models (EXST, ALT50, ALT70, and ALT100) were used to estimate the size of the armor layer particles, depth of degradation at the pipeline crossing, and new slope using the thalweg at Baseline St. as the control point. In addition, the armor layer, depth of degradation, and associated new slope were calculated using the hydraulic results for the 2-year discharge in the EXST model for four active head cuts at chainage: 91 ft, 2511 ft, 5486 ft, and 6568 ft with drop heights of 4 ft, 5 ft, 4 ft, and 3 ft, respectively (the Gessler Method was not used in these evaluations). By evaluating the expected armor layer formation and associated degradation at existing headcuts it is possible to estimate the slope of the channel as it reaches equilibrium.

All calculations were conducted using MathCAD. The EXST armor layer and Gessler Method MathCAD Calculations can be seen on the following pages, which serves as an example calculation. Calculations for the ALT50, ALT70, and ALT100 models and the four existing headcuts were conducted using the same MathCAD calculations. The results for all of the calculations can be seen in the Results section, Table D-1.

City Creek

Degradation Limited by Armoring

Created By: Amber Fuxan

Date: January 25th, 2006

Five methods are analyzed for computing the degradation limited by armoring for the Salt Creek channel (Pemberton and Lara, 1984). Calculations have been performed using the 2yr design discharge.

Method 1: Meyer-Peter, Muller

$d_1 := 0.64$	mean water depth at pipeline crossing (m)
$S_{E_1} := 0.043$	Energy Gradient slope (m/m)
$n_{1s} := 0.03$	Manning's roughness for the channel bed
$D_{90_1} := 970$	in (mm)
$K_1 := 0.058$	Constant (metric)

$$D_{c1} := \frac{d_1 \cdot S_{E_1}}{K_1 \cdot \left(\frac{n_{1s}}{\frac{1}{D_{90_1}^6}} \right)^{\frac{3}{2}}}$$

$$D_{c1} = 509.602$$

D_{c1} is in (mm)

Method 2: Competent Bottom Velocity Method

$V_m := 4.36$	mean channel velocity (m/s)
---------------	-----------------------------

$$D_{c2} := 20.2 \cdot V_m^2$$

$$D_{c2} = 383.994$$

D_{c2} is in (mm)

Method 3: Lane's Tractive Force Method

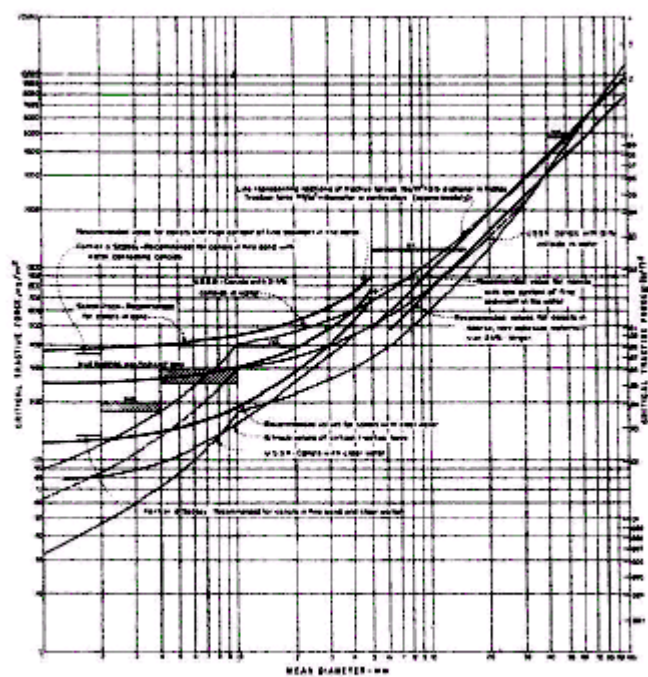


Figure 4. - Tractive force versus transportable sediment size (after Lane, 1952).

$$\gamma_{\text{W}} := 1000 \frac{\text{kg}}{\text{m}^3}$$

$$d := 0.64\text{m}$$

$$S := 0.043$$

$$T_c := \gamma_w \cdot d \cdot S$$

$$T_c = 27.52 \frac{\text{kg}}{\text{m}^2}$$

$D_{c3} := \text{off}$ OUT OF RANGE

Method 4: Shields Method

$$\gamma_s := 2650 \frac{\text{kg}}{\text{m}^3}$$

$$T_{\text{star}} := 0.047$$

This value for dimensionless shear stress obtained from stable slope calculations method 3.

$$D_{c4} := \frac{T_c}{T_{\text{star}} \cdot (\gamma_s - \gamma_w)}$$

$$D_{c4} = 354.868 \text{ mm}$$

Method 5: Yang Incipient Motion Method

$$V_m = 4.36$$

$$D_{c5} := 0.0216 V_m^2 \cdot 1000$$

$$D_{c5} = 410.607 \quad \text{Answer is in mm}$$

$$D_{c5} \cdot \text{mm} = 16.166 \text{ in}$$

Method 6: Gessler Approach Method

From the following file: G:\Projects\City Creek\Analysis\Gessler Armor Layer\Gessler Armor Layer - City Creek.xmcd

$$D_{A50} := 520 \text{ mm} \quad D_{A90} := 1300 \text{ mm}$$

Summary

$$D_{c1} = 509.602$$

$$D_{c2} = 383.994$$

$$D_{c3} := \text{■}$$

$$D_{c4} = 354.868\text{mm}$$

$$D_{c5} = 410.607$$

$$D_{A50} = 520\text{mm}$$
$$D_{\text{avg}} := \frac{D_{c1} + D_{c2} + \frac{D_{c4}}{\text{mm}} + \frac{D_{A50}}{\text{mm}} + D_{c5}}{5}$$

$$D_{\text{avg}} = 435.814 \quad \text{in mm}$$

Depth to Armor and Volume Computations

Meyer - Peter Muller Depth of Degradation

$$y_{a1} := 3 \cdot D_{c1} \cdot \text{mm}$$

Thickness of the armor layer, which equals two times the mean diameter of particles in the armor layer

$$y_{a1} = 1.529\text{m}$$

$$\Delta p_1 := 0.15$$

Decimal percentage of original bed material larger than the armor size D_c .

$$y_{d1} := y_{a1} \cdot \left(\frac{1}{\Delta p_1} - 1 \right)$$

$$y_{d1} = 8.663\text{m}$$

Competent Bottom Velocity Depth of Degradation

$$y_{a2} := 3 \cdot D_{c2} \cdot \text{mmr}$$

Thickness of the armor layer, which equals two times the mean diameter of particles in the armor layer

$$y_{a2} = 1.152\text{m}$$

$$\Delta p_2 := 0.17$$

Decimal percentage of original bed material larger than the armor size D_c .

$$y_{d2} := y_{a2} \cdot \left(\frac{1}{\Delta p_2} - 1 \right)$$

$$y_{d2} = 5.624\text{m}$$

Lane's Tractive Force Depth of Degradation

$$y_{a3} := 3 \cdot D_{c3} \cdot \text{mmr}$$

Thickness of the armor layer, which equals two times the mean diameter of particles in the armor layer

$$y_{a3} = \blacksquare$$

$$\Delta p_3 := \blacksquare$$

Decimal percentage of original bed material larger than the armor size D_c .

$$y_{d3} := y_{a3} \cdot \left(\frac{1}{\Delta p_3} - 1 \right)$$

$$y_{d3} = \blacksquare$$

OUT OF RANGE

Shields Diagram Depth of Degradation

$$y_{a4} := 3 \cdot D_{c4}$$

Thickness of the armor layer, which equals two times the mean diameter of particles in the armor layer

$$y_{a4} = 1.065 \text{ m}$$

$$\Delta p_4 := 0.18$$

Decimal percentage of original bed material larger than the armor size D_c .

$$y_{d4} := y_{a4} \cdot \left(\frac{1}{\Delta p_4} - 1 \right)$$

$$y_{d4} = 4.85 \text{ m}$$

Yang Incipient Motion Depth of Degradation

$$y_{a5} := 3 \cdot D_{c5} \cdot \text{mmr}$$

Thickness of the armor layer, which equals two times the mean diameter of particles in the armor layer

$$y_{a5} = 1.232 \text{ m}$$

$$\Delta p_5 := 0.16$$

Decimal percentage of original bed material larger than the armor size D_c .

$$y_{d5} := y_{a5} \cdot \left(\frac{1}{\Delta p_5} - 1 \right)$$

$$y_{d5} = 6.467 \text{ m}$$

$$y_{d5} = 21.217 \text{ ft}$$

Gessler D_{50} Depth of Degradation

$$y_{aA50} := 3 \cdot D_{A50}$$

Thickness of the armor layer, which equals two times the mean diameter of particles in the armor layer

$$y_{aA50} = 1.56 \text{ m}$$

$$\Delta p_{A50} := 0.15$$

Decimal percentage of original bed material larger than the armor size D_c .

$$y_{dA50} := y_{aA50} \cdot \left(\frac{1}{\Delta p_{A50}} - 1 \right)$$

$$y_{dA50} = 8.84 \text{ m}$$

D
w

Gessler D_{90} Depth of Degradation

$$y_{aA90} := 3 \cdot D_{A90}$$

Thickness of the armor layer, which equals two times the mean diameter of particles in the armor layer

$$y_{aA90} = 3.9 \text{ m}$$

$$\Delta p_{A90} := 0.08$$

Decimal percentage of original bed material larger than the armor size D_c .

$$y_{dA90} := y_{aA90} \cdot \left(\frac{1}{\Delta p_{A90}} - 1 \right)$$

$$y_{dA90} = 44.85 \text{ m}$$

Average Depth of Degradation

$$y_{aAVG} := 2 \cdot D_{avg} \cdot mn$$

Thickness of the armor layer, which equals two times the mean diameter of particles in the armor layer

$$y_{aAVG} = 0.872 \text{ m}$$

$$\Delta p_{AVG} := 0.17$$

Decimal percentage of original bed material larger than the armor size D_c .

$$y_{dAVG} := y_{aAVG} \cdot \left(\frac{1}{\Delta p_{AVG}} - 1 \right)$$

$$y_{dAVG} = 4.256 \text{ m}$$

City Creek

Armor Layer Calculations using the Gessler Approach (Gessler 1970)

Created By: Amber Fuxan

Date: January 25th, 2006

Calculations for Bed Material Location: Highland Avenue

Free-flowing Conditions: $Q = 400$ cfs

Particle Size Distribution

% finer d (mm)

All inputs are highlighted in yellow.

Read from Graph:

$D_{50} := 25\text{-mm}$

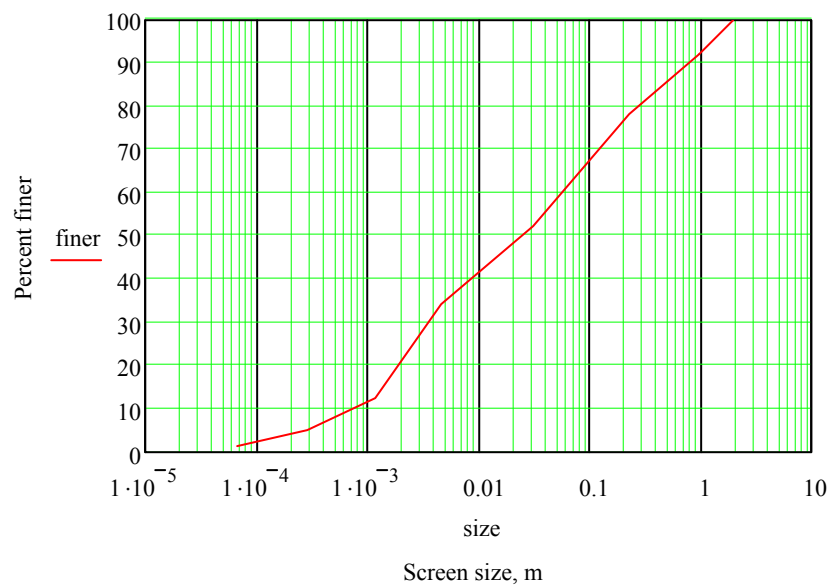
$D_{90} := 970\text{-mm}$

$\text{data}_s := \begin{pmatrix} 1 & 0.07 \\ 5 & .3 \\ 12.5 & 1.2 \\ 34 & 4.7 \\ 52 & 32 \\ 78 & 230 \\ 92 & 1000 \\ 100 & 2000 \end{pmatrix}$

$\text{finer} := \text{data}_s^{(0)}$

$\text{size} := \text{data}_s^{(1)} \cdot \text{mm}$

$i := 1..8$



Input Parameters:

$$Q := 400 \frac{\text{ft}^3}{\text{s}}$$

Flow rate

$$Q = 11.327 \text{m}^3 \cdot \text{s}^{-1}$$

$$M := 2.69$$

Approximate bank slope (MH:1V) at sample location

$$S := 0.049 \frac{\text{m}}{\text{m}}$$

Approximate bed slope at sample location

$$b := 17 \text{ft}$$

Approximate bottom width of the channel at sample location

$$\gamma_s := 25970 \frac{\text{N}}{\text{m}^3}$$

Specific weight of sediment

$$\gamma := 9800 \frac{\text{N}}{\text{m}^3}$$

Specific weight of water

$$\rho := 1000 \frac{\text{N} \cdot \text{s}^2}{\text{m}^4}$$

Density of water

$$\nu := 0.00000131 \frac{\text{m}^2}{\text{s}}$$

Kinematic viscosity of water

$$g = 9.807 \text{m} \cdot \text{s}^{-2}$$

Acceleration due to gravity

Calculated Input Parameters:

$$k_s := D_{90}$$

Controlling roughness for the bank

$$k_s = 0.97 \text{m}$$

$$P_b := b$$

Wetted perimeter of the bed

$$P_b = 5.182 \text{m}$$

$$f_b := \left(2.21 + 2.03 \log \left(\frac{0.0251}{S} \right) \right)^{-2}$$

Friction factor of the bed

$$f_b = 0.381$$

Input the known value or a guess value for each of the parameters below. Subscript (s) refers to the banks of the channel, subscript (b) refers to the bed of the channel, and variables without a subscript refer to the overall parameter for the system.

$$h' := 2.1 \text{ ft}$$

Depth of flow

$$f'_s := .03$$

Friction factor of the bank

$$R' := 1.3 \text{ ft}$$

$$R'_s := 0.55 \text{ ft}$$

Hydraulic radii

$$R'_b := 1.64 \text{ ft}$$

$$P' := 22.84 \text{ ft}$$

$$P'_s := 6.84 \text{ ft}$$

Wetted perimeters

$$A' := 29.9 \text{ ft}^2$$

$$A'_s := 3.63 \text{ ft}^2$$

Cross-sectional areas

$$A'_b := 26.27 \text{ ft}^2$$

$$U' := 13.38 \frac{\text{ft}}{\text{s}}$$

Average flow velocity (Calculations are very sensitive to this guess. If Mathcad does not calculate values below, try changing this guess.)

The following is the system of equations that provide the relationships required to solve for the parameters listed previously. Equations based on Darcy-Weisbach's flow equation and taken from Oehy (1999)

Given

$$U'^2 = \frac{8 \cdot g}{f'_s} \cdot R'_s \cdot S$$

$$R'_s = \frac{A'_s}{P'_s}$$

$$U'^2 = \frac{8 \cdot g}{f'_b} \cdot R'_b \cdot S$$

$$R'_b = \frac{A'_b}{P'_b}$$

$$f'_s = \left(2.21 + 2.03 \cdot \log \left(\frac{R'_s}{k_s} \right) \right)^{-2}$$

$$R' = \frac{A'}{P'}$$

$$P'_s = h' \cdot \sqrt{1 + M^2}$$

$$U' = \frac{Q}{A'}$$

$$P' = P'_b + 2 \cdot P'_s$$

$$A' = h' \cdot (b + M \cdot h')$$

$$A' = A'_b + 2 \cdot A'_s$$

$$\begin{pmatrix} h \\ f'_s \\ \underline{R} \\ R'_s \\ R'_b \\ P \\ P'_s \\ \underline{A} \\ A'_s \\ A'_b \\ U \end{pmatrix} := \text{Find}(h', f'_s, R', R'_s, R'_b, P', P'_s, A', A'_s, A'_b, U')$$

Solution to system of equations:

$h = 0.689\text{m}$	Depth of flow
$f_s = 0.365$	Friction factor of the bank
$R = 0.531\text{m}$	Overall hydraulic radius
$R_s = 0.518\text{m}$	Hydraulic radius for the banks
$R_b = 0.541\text{m}$	Hydraulic radius for the bed
$P = 9.137\text{m}$	Overall wetted perimeter
$P_s = 1.978\text{m}$	Wetted perimeter for the banks
$A = 4.849\text{m}^2$	Total cross-sectional area
$A_s = 1.024\text{m}^2$	The area of the bank subarea
$A_b = 2.802\text{m}^2$	The area of the bed subarea
$U = 2.336\text{m}\cdot\text{s}^{-1}$	Average flow velocity
$f := \frac{8 \cdot g}{U^2} \cdot R \cdot S$	$f = 0.374$ Average friction factor

Stress calculations:

$$\tau_b := \gamma \cdot R_b \cdot S$$

$$\tau_b = 259.644 \frac{\text{N}}{\text{m}^2}$$

Bed shear stress

$$u_b := \sqrt{\frac{\tau_b}{\rho}}$$

$$u_b = 0.51 \frac{\text{m}}{\text{s}}$$

Shear velocity, measure of the intensity of turbulent fluctuations.

$$r := 1..7$$

$$\text{davg}_r := \frac{\text{size}_r + \text{size}_{r-1}}{2}$$

Average grain sizes for gradation

$$\text{Re}_r := \frac{u_b \cdot \text{davg}_r}{\nu}$$

Reynold's Number for each size fraction in gradation

Below are equations that define of Shield's Diagram piecewise (τ_{s1} - τ_{s6}) and τ_{star} is an "if statement" to determine which portion of the diagram applies to a given Re value:

$$\tau_{s1_r} := .115 \left(\text{Re}_r \right)^{-.79279}$$

$$\begin{aligned} \tau_{s2_r} := & -2.65633 \cdot 10^{-5} \cdot \left(\text{Re}_r \right)^6 + 7.84922 \cdot 10^{-4} \cdot \left(\text{Re}_r \right)^5 - 9.23733 \cdot 10^{-3} \cdot \left(\text{Re}_r \right)^4 \dots \\ & + 5.47343 \cdot 10^{-2} \cdot \left(\text{Re}_r \right)^3 - 1.67934 \cdot 10^{-1} \cdot \left(\text{Re}_r \right)^2 + 2.35315 \cdot 10^{-1} \cdot \text{Re}_r - \left(4.75161 \cdot 10^{-2} \right) \end{aligned}$$

$$\tau_{s3_r} := .032$$

$$\tau_{s4_r} := \left[4.849216650181811 \cdot 10^{-9} \cdot \left(\text{Re}_r \right)^3 - 2.36934036367859 \cdot 10^{-6} \cdot \left(\text{Re}_r \right)^2 + 3.8048049563885 \cdot 10^{-4} \cdot \text{Re}_r \dots \right. \\ \left. + 2.5449950466873 \cdot 10^{-2} \right]$$

$$\tau_{s5_r} := .046$$

$$\tau_{s6_r} := .047$$

$$\tau_{star_r} := \text{if} \left[\text{Re}_r \leq 2, \tau_{s1_r}, \text{if} \left[\left(\text{Re}_r < 8 \right), \tau_{s2_r}, \text{if} \left(\text{Re}_r \leq 19, \tau_{s3_r}, \text{if} \left(\text{Re}_r < 217, \tau_{s4_r}, \text{if} \left(\text{Re}_r \leq 397, \tau_{s5_r}, .047 \right) \right) \right] \right] \right]$$

$d_{avg_r} =$	$Re_r =$	$\tau_{star_r} =$
1.85·10 ⁻⁴ m	71.96	0.042
7.5·10 ⁻⁴	291.729	0.046
2.95·10 ⁻³	1.147·10 ³	0.047
0.018	7.138·10 ³	0.047
0.131	5.096·10 ⁴	0.047
0.615	2.392·10 ⁵	0.047
1.5	5.835·10 ⁵	0.047

$$\tau_{c_r} := \tau_{star_{r-1}} \cdot d_{avg_r} \cdot (\gamma_s - \gamma) \quad \text{Critical shear stress for each size fraction in gradation}$$

$$\tau_{r-1} := \frac{\tau_{c_r}}{\tau_b} \quad \text{Ratio of critical shear stress of each size fraction to average shear stress in river}$$

Theoretical Armor Layer Calculations:

Probability that a grain of given size will not erode, fit from Gessler plot of q versus τ_c/τ_b :

$$q_r := \text{if } \tau_{r-1} < 2.8, \left[\begin{aligned} &0.0716545194773488(\tau_{r-1})^4 - 0.496929374396984(\tau_{r-1})^3 \dots \\ &+ 0.987737827575074(\tau_{r-1})^2 - 0.104758490295694\tau_{r-1} \dots \\ &+ 0.0527834049124749 \end{aligned} \right], 1.0$$

$$q\Delta P_r := q_r \cdot (\text{finer}_r - \text{finer}_{r-1}) \quad \text{Intermediate Calculation}$$

$\tau_{c_r} =$	$d_{avg_r} =$	$\tau_{r-1} =$	$q_r =$	$q\Delta P_r =$
0 m ⁻¹ ·kg·s ⁻²	1.85·10 ⁻⁴ m	0	0.053	0.211
0.514	7.5·10 ⁻⁴	1.979·10 ⁻³	0.053	0.394
2.194	2.95·10 ⁻³	8.451·10 ⁻³	0.052	1.117
13.946	0.018	0.054	0.05	0.899
99.559	0.131	0.383	0.131	3.416
467.394	0.615	1.8	0.919	12.861
1.14·10 ³	1.5	4.391	1	8

$$\Sigma q\Delta P := \sum_{r=1}^7 q\Delta P_r \quad \Sigma q\Delta P = 26.898 \quad \text{Summation of all } q\Delta P_0 \text{ terms for use in determining } \Delta P_A.$$

$$\Delta P_{A_r} := \frac{q\Delta P_r}{\Sigma q\Delta P} \quad \text{Incremental probability function of armor layer (missing probability = 0 for finest grain size).}$$

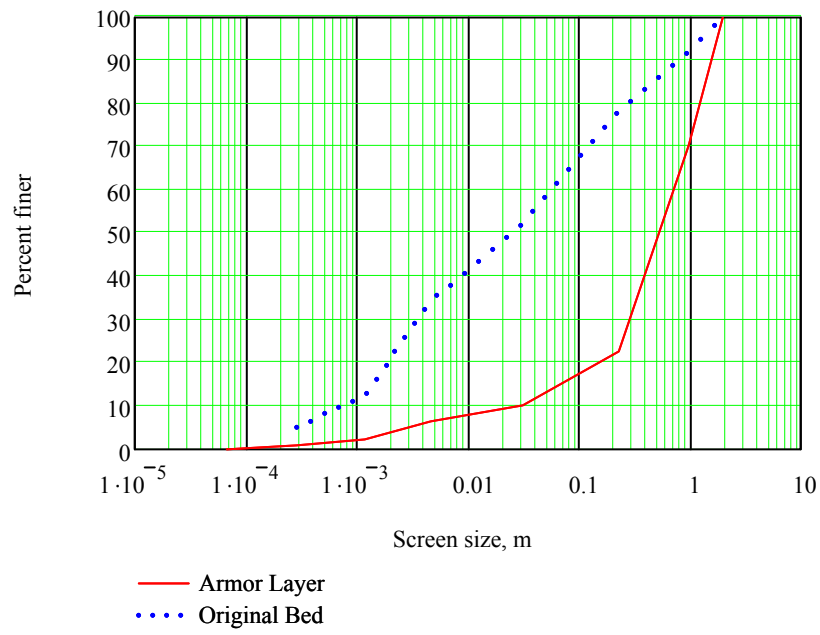
$$P_{A \text{ incomplete}}_r := \sum_{r=1}^r \Delta P_{A_r} \quad \text{Cumulative probability function of armor layer (missing probability = 0 for finest grain size). See following page for complete grain size distribution, } P_{A_r}.$$

$r := 0..7$ Increase counter variable to account for entire set of grain sizes given initially.

$$P_{A_r} := \left(\text{if}(r = 0, 0, P_{A \text{ incomplete}}_r) \right) \cdot 100 \quad \text{Add initial probability = 0 for finest grain size in armor layer distribution--COMPLETE ARMOR LAYER DISTRIBUTION expressed in percent.}$$

Resulting Armor Layer Particle Size Distribution:

size _r · mm =		
7·10 ⁻⁸	$\Delta P_{A_r} =$	$P_{A_r} =$
3·10 ⁻⁷	0	0
1.2·10 ⁻⁶	7.849·10 ⁻³	0.785
4.7·10 ⁻⁶	0.015	2.251
3.2·10 ⁻⁵	0.042	6.405
2.3·10 ⁻⁴	0.033	9.746
1·10 ⁻³	0.127	22.445
2·10 ⁻³	0.478	70.258
	0.297	100



Read from Graph: $D_{A50} := 520\text{ mm}$ $D_{A90} := 1300\text{ mm}$

Results

The armor layer particle diameter and depth of degradation results for the EXST, ALT50, ALT70, and ALT100 models at the pipeline crossing can be seen in Table D-3. Table D-4 reflects the armor layer and degradation results for four existing headcuts at stations 64, 48, 31, and 25.

Table D-3. Armor Layer Results for Two-Year Discharge for All Models

Method	Armor Layer Particle Diameter (in)			
	EXST	ALT50	ALT70	ALT100
Meyer-Peter, Muller	20	10	9	7
Competent Bottom Velocity	15	7.5	6	4
Lane's Tractive Force	Out of range	4	4	4
Shields Diagram	14	7	6	5
Yang Incipient Motion	16	8	6	5
Gessler D ₅₀	20	16	13	12
Average Particle Diameter	17	9	7	6

Method	Depth of Degradation (ft)			
	EXST	ALT50	ALT70	ALT100
Meyer-Peter, Muller	28	9	7	5
Competent Bottom Velocity	18	6	4	2
Lane's Tractive Force	- - -	2	2	2
Shields Diagram	16	5	5	3
Yang Incipient Motion	21	6	4	3
Gessler D ₅₀	29	8	6	4
Average Depth of Degradation	23	8	6	4

Table D-4. Armor Layer Results for Two-Year Discharge for Active Headcuts

Section #	64	48	31	25
Chainage (ft)	91	2511	5486	6568
Thalweg Elevation (ft)	1488	1405	1329	1301

Method	Armor Layer Particle Diameter (in)			
Meyer-Peter, Muller	12	20	6	8
Competent Bottom Velocity	7	9	4	3
Lane's Tractive Force	Out of range	Out of range	Out of range	Out of range
Shields Diagram	8	14	4	6
Yang Incipient Motion	7	9	5	3
Average	9	13	4	5

Method	Depth of Degradation (ft)			
Meyer-Peter, Muller	12	28	4	7
Competent Bottom Velocity	5	7	2	1
Lane's Tractive Force	---	---	---	---
Shields Diagram	7	16	2	4
Yang Incipient Motion	5	8	3	1
Average Depth of Degradation	7	15	3	3

References

- Chang, Howard H. 1995. *Inland Feeder Pipeline, San Bernardino Segment (Contract 3): Fluvial Study of City Creek for Pipeline Placement*. Prepared for Dames and Moore.
- Gessler, J. 1971. *Beginning & Ceasing of Sediment Motion.* *River Mechanics*, H.W. Shen, ed Hsieh Wen Shen, Fort Collins, Colorado, 7, 1-22.
- Pemberton, EL and JM Lara. 1984. *Computing Degradation and Local Scour*. Technical Guideline for Bureau of Reclamation. Denver, Colorado.
- U.S. Army Corps of Engineers (USACE). 2001. *HEC-RAS River Analysis System v. 3.3.3* [computer software]. www.hec.usace.army.mil

APPENDIX E – STABLE SLOPE

APPENDIX F – BEND SCOUR

APPENDIX G – HEADCUT HYDRAULICS

Appendix E: STABLE SLOPE

Introduction

Degradation limited by a stable slope is based on the degrading process controlled by zero or negligible transport of the material forming the bed of the stream channel. This method is applied to streams where the amount of coarse material is insufficient to form an armor layer. The methods used in Pemberton and Lara (1984) to calculate a stable slope are:

- 1)** Schoklitsch bedload equation;
- 2)** Meyer-Peter Muller bedload equation for beginning transport;
- 3)** Shields diagram for no motion; and
- 4)** Lane's relationship for critical tractive force assuming clear water-flow in canals.

Assumptions

- The grain size distribution at Highland Ave. reported in the Chang study (1995) reflects the current bed gradation at the pipeline crossing;
- Clear water, i.e. no sediment is being transported from upstream;
- The two-year discharge of 400cfs is the dominant discharge, the flow effecting the ultimate shape and hydraulics of the channel; and

Input

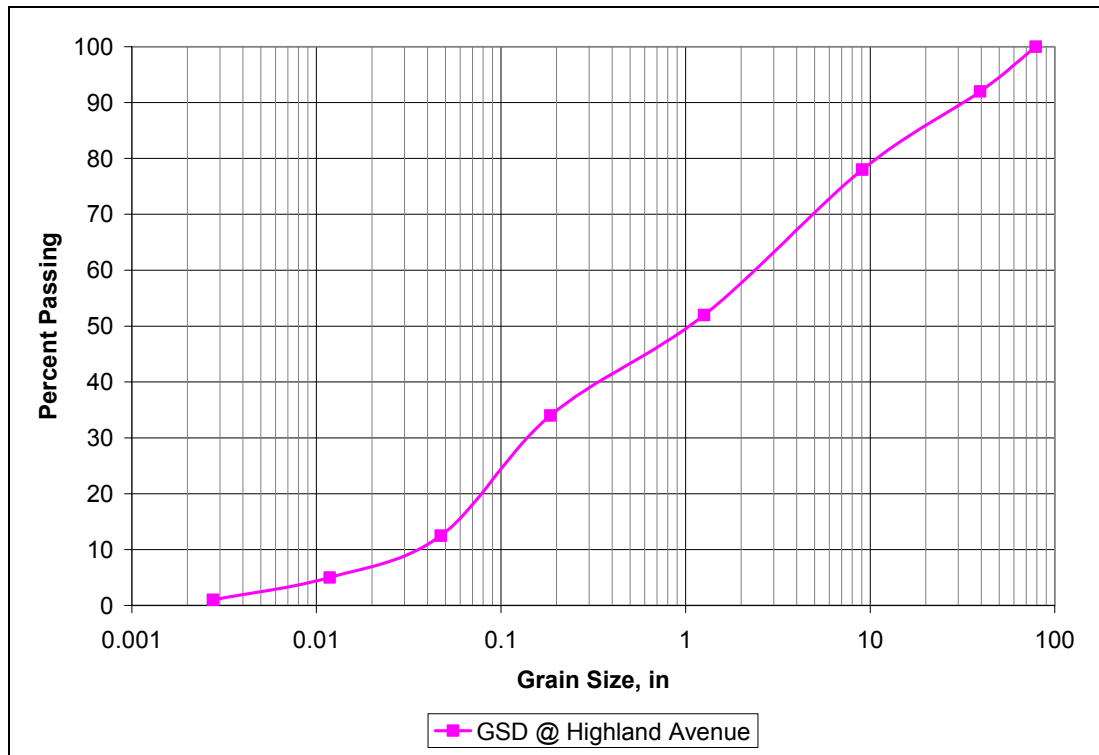
All hydraulic input data obtained from HEC-RAS results and all gradation input obtained from the Highland Ave. grain size distribution (Figure E-1).

• Table E-1. Stable Slope Input Parameters for EXST, ALT50, SLT70, and ALT100

All Methods					
Variable	EXST	ALT50	ALT70	ALT100	Comment
Q	400 cfs	400 cfs	400 cfs	400 cfs	Dominant discharge
Q _B	375.56 cfs	389.23 cfs	393.6 cfs	396.35 cfs	Average flow over bed of channel
B	17 ft	17 ft	17 ft	17 ft	Bottom width of channel
d	2.11 ft	0.76 ft	0.62 ft	0.51 ft	Average flow depth
R	1.31 ft	0.72 ft	0.61 ft	0.5ft	Average hydraulic radius
D ₅₀	25 mm	25 mm	25 mm	25 mm	Mean particle size
D ₉₀	970 mm	970 mm	970 mm	970 mm	Particle size at which 90% of bed material by weight is finer
n	0.03	0.03	0.03	0.03	Manning's roughness coefficient for bed of the channel
Method 1: Schoklitsch					
Variable	EXST	ALT50	ALT70	ALT100	Comment
K ₁	0.000293	0.000293	0.000293	0.000293	Constant (metric)
Method 2: Meyer-Peter, Muller					
Variable	EXST	ALT50	ALT70	ALT100	Comment
K ₂	0.058	0.058	0.058	0.058	Constant (metric)
Method 3: Shields Diagram					
Variable	EXST	ALT50	ALT70	ALT100	Comment
ν	0.929 x10 ⁻⁶ m ² /s	0.929x10 ⁻⁶ m ² /s	0.929x10 ⁻⁶ m ² /s	0.929x10 ⁻⁶ m ² /s	Kinematic viscosity of water @ 25 degrees C
ρ _w	997 kg/m ³	997 kg/m ³	997 kg/m ³	997 kg/m ³	Density of water @ 25 degrees C
ρ _s	2650 kg/m ³	2650 kg/m ³	2650 kg/m ³	2650 kg/m ³	Particle density
S	0.043 m/m	0.062 m/m	0.062 m/m	0.062 m/m	Energy gradient slope (first guess at stable slope)
Method 4: Lane's Tractive Force					
Variable	EXST	ALT50	ALT70	ALT100	Comment
T _c	2000 g/m ²	2000 g/m ²	2000 g/m ²	2000 g/m ²	Critical tractive force read from Lane Tractive Force diagram based on D ₅₀

• Table E-2. Description of Control Point and Degradation Life

Grade Control Structure Location:	Base Line Rd. Culvert
Elevation of Thalweg of Base Line Rd. Culvert:	1296 ft
Distance Between Pipeline and Base Line Rd.:	4947.18 ft
Current Thalweg Elevation at Pipeline Crossing:	1430 ft
Life of Degradation:	100 yr



• Figure E-1. Highland Ave. Grain Size Distribution (Chang 1995)

Calculations

The stable slope and depth of degradation were conducted using the two year (dominant) discharge for the EXST, ALT50, ALT70, and ALT100 HEC-RAS models. All the stable-slope equations use dominant discharge, which has been assumed as the 2-yr discharge for this site.

In order to calculate the new slope, identification of a downstream grade control or local baselevel is required. The local baselevel for City Creek is the Santa Ana River. However, for this investigation, we assumed that the culvert at Base Line Road would be maintained and that this will act as the grade control structure for the Pipeline crossing. The culvert, which is about 1 mile downstream of the crossing, will function as a grade control for the Pipeline crossing because all the flow in the creek is routed through a concrete box culvert. The depth of scour at the Pipeline crossing was calculated using this location as the grade control.

Salt Creek

Compute Long-Term Stable Slope (Grade Control @ Baseline Culvert)

Created By: Mike George Edited By: Amber Fuxan

Date: January 13th, 2006



Four methods are analyzed for computing the long-term stable slope for the future design of the Salt Creek channel (Pemberton and Lara, 1984). Calculations have been performed using the 2yr design discharge.

$Q := 400 \frac{\text{ft}^3}{\text{s}}$ Dominant discharge for City Creek based on Log Pearson III distribution applied to USGS gage 1105580 data

$Q_B := 375.56 \frac{\text{ft}^3}{\text{s}}$ Average flow over bed of channel (from HEC-RAS)

$B := 17\text{ft}$ Bottom width of channel

$d := 2.1\text{ft}$ Average flow depth in channel (from HEC-RAS)

$R_{\text{hw}} := 1.3\text{ft}$ Average hydraulic radius (from HEC-RAS)

$D_{50} := 25\text{mm}$ Mean particle size (based on gradations provided to E&H)

$D_{90} := 970\text{mm}$ Average particle size at which 90% of bed material by weight is finer (based on gradations provided to E&H)

$n := 0.03$ Manning's roughness coefficient for bed of the channel

Method 1: Scholitsch Method

$K_1 := 0.00029$ Constant

$$S_{L_1} := K_1 \cdot \left[\frac{\left(\frac{D_{50} \cdot 1000}{\text{SIUnitsOf}(D_{50})} \right) \cdot \frac{B}{\text{SIUnitsOf}(B)}}{\frac{Q}{\text{SIUnitsOf}(Q)}} \right]^{0.75}$$

D_{50} is in mm.

$$S_{L_1} = 1.822 \times 10^{-3}$$

Method 2: Meyer-Peter, Muller Method

$$K_2 := 0.05 \quad \text{Constant}$$

$$S_{L_2} := \frac{K_2 \cdot \left(\frac{Q}{\text{SIUnitsOf}(Q)} \right) \cdot \left(\frac{Q_B}{\text{SIUnitsOf}(Q_B)} \right) \cdot \left[\frac{n}{\left(\frac{D_{90} \cdot 1000}{\text{SIUnitsOf}(D_{90})} \right)^{\frac{1}{6}}} \right]^{\frac{3}{2}} \cdot \frac{D_{50} \cdot 1000}{\text{SIUnitsOf}(D_{50})}}{d}$$

SIUnitsOf(d)

D₅₀ and D₉₀ are in mm

$$S_{L_2} = 2.236 \times 10^{-3}$$

Method 3: Shields Diagram Method

$$\nu := 0.929 \times 10^{-6} \frac{\text{m}^2}{\text{s}} \quad \text{Kinematic viscosity of water @ 25 degrees C}$$

$$\rho_w := 997 \frac{\text{kg}}{\text{m}^3} \quad \text{Water density @ 25 degrees C}$$

$$\rho_s := 2650 \frac{\text{kg}}{\text{m}^3} \quad \text{Particle density}$$

$$S := 3.029 \times 10^{-3} \quad \text{Average energy slope, } S = 0.043 \text{ (first guess at stable slope)}$$

Calculate the Reynolds number:

$$Re := \frac{\sqrt{S \cdot R \cdot g} \cdot D_{50}}{\nu}$$

D₅₀ is in meters.

$$Re = 2.931 \times 10^3$$

Below are equations that define of Shield's Diagram piecewise (τ_{s1} - τ_{s6}) and τ_{star} is an "if statement" to determine which portion of the diagram applies to a given Re value:

$$\tau_{s1}(Re) := .115 Re^{-.79279}$$

$$\tau_{s2}(Re) := -2.65633 \cdot 10^{-5} \cdot Re^6 + 7.84922 \cdot 10^{-4} \cdot Re^5 - 9.23733 \cdot 10^{-3} \cdot Re^4 \dots \\ + 5.47343 \cdot 10^{-2} \cdot Re^3 - 1.67934 \cdot 10^{-1} \cdot Re^2 + 2.35315 \cdot 10^{-1} \cdot Re - (4.75161 \cdot 10^{-2})$$

$$\tau_{s3} := .032$$

$$\tau_{s4}(Re) := 4.849216650181811 \cdot 10^{-9} \cdot Re^3 - 2.36934036367859 \cdot 10^{-6} \cdot Re^2 + 3.80480495638856 \cdot 10^{-4} \cdot Re + 2.54499504668731 \cdot 10^{-2}$$

$$\tau_{s5} := .046$$

$$\tau_{s6} := .047$$

$$\tau_{star}(Re) := \text{if}[Re \leq 2, \tau_{s1}(Re), \text{if}[(Re < 8), \tau_{s2}(Re), \text{if}[(Re \leq 19, \tau_{s3}, \text{if}[(Re < 217, \tau_{s4}(Re), \text{if}[(Re \leq 397, \tau_{s5}, .047))]]]]]$$

$$\tau_{star}(Re) = 0.047$$

The stable slope may then be calculated as:

$$S_{L_3}(Re) := \frac{\tau_{star}(Re) \cdot (\rho_s - \rho_w) \cdot D_{50}}{\rho_w \cdot d}$$

Stable slope as calculated by Shields method.

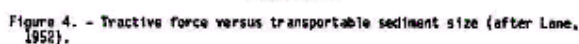
$$S_{L_3}(Re) = 3.029 \times 10^{-3}$$

Iterate this value by placing it in the "S" value above until a stable slope is reached.

Method 4: Lane's Tractive Force Method

The stable slope, S_L , can be determined by making use of the following figure. Read the corresponding tractive force based on the mean particle size (D_{50}).

$$D_{50} = 25 \text{ mm}$$



Read from graph depending on D_{50}

Stable slope as calculated by Lane's tractive force method

$$S_{L_4} = 3.119 \times 10^{-3}$$

Summary of Results

$$S_{L1} = 1.822 \times 10^{-3}$$

$$S_{L2} = 2.236 \times 10^{-3}$$

$$S_{L_3}(\text{Re}) = 3.029 \times 10^{-3}$$

$$\text{Average} := \frac{1}{4} \cdot (S_{L_1} + S_{L_2} + S_{L_3}(\text{Re}) + S_{L_4})$$

$$\text{Average} = 2.552 \times 10^{-3}$$

Results

The average slope of City Creek for current conditions is approximately 2.7×10^{-2} , which is anticipated to change to approximately 2.6×10^{-3} (the average of the estimated slopes for EXST in Table E-3) for developed conditions. This is approximately a 10 fold decrease in the estimated slope.

Based on the stated assumptions, it is estimated that the rate of scour is about 1-2 ft/yr if no remedial action is taken.

• Table E-3. Estimated Stable Slope, Total Degradation, and Rate of Scour at Pipeline Crossing

	Bottom Width (ft)	EXST	ALT50	ALT70	ALT100
Stable Slope	Schoklitsch	0.18%	0.41%	0.53%	0.69%
	Meyer-Peter, Muller	0.22%	0.60%	0.73%	0.88%
	Shields Diagram	0.30%	0.84%	1.00%	1.30%
	Lane's Tractive Force	0.31%	0.87%	1.10%	1.30%
	Average	0.26%	0.68%	0.84%	1.00%
Degradation @ Pipeline (ft)	Schoklitsch	125	114	108	100
	Meyer-Peter, Muller	123	104	98	91
	Shields Diagram	119	92	85	70
	Lane's Tractive Force	119	91	80	70
	Average	121	100	93	85
Average Scour Per Year (ft/yr)*		1.21	1.00	0.93	0.85

* Assumes 100 years for full degradation depth

References

- Chang, Howard H. 1995. Inland Feeder Pipeline, San Bernardino Segment (Contract 3): Fluvial Study of City Creek for Pipeline Placement. Prepared for Dames and Moore.
- Pemberton, EL and JM Lara. 1984. Computing Degradation and Local Scour. Technical Guideline for Bureau of Reclamation. Denver, Colorado.
- U.S. Army Corps of Engineers (USACE). 2001. *HEC-RAS River Analysis System* v. 3.3.3 [computer software]. www.hec.usace.army.mil

Appendix F: Bend Scour

Introduction

A channel bend exists in the vicinity of the pipeline crossing. It is necessary to investigate the additional scour that will occur due to the presence of this bend. To do so, the transverse stream power was investigated using the Chang method (1992) to evaluate the total stream power around the bend. If the magnitude of the stream power is greater than the erosive threshold of the bed material scour will occur and additional scour depth was evaluated using the Odgaard Method (1986).

The bend scour was only investigated for existing channel geometry (EXST) because the bend would most likely be removed if widening the channel was implemented.

Input

All hydraulic input parameters were obtained from the EXST 2-year discharge HEC-RAS model and bed gradation characteristics were obtained from the Highland Ave. grain size distribution in the Chang study (1995).

- Table F-1. Input Parameters for the Chang Method

Chang Input		
Variable	Value	Comment
D_{\max}	2.1 ft.	Maximum depth along bend
S_0	0.049 ft/ft	Average slope through bend
r_c	62.5 ft.	Radius of curvature along center line
Δr	22 ft.	Average width
R_h	1.3 ft.	Average hydraulic radius
L_{reach}	100 ft.	Length
V_{RM51}	14.3 ft/s	Maximum velocity
κ	0.4	von Karman's coefficient
η	0.03	Manning coefficient for roughness
ρ	1.94 slug/ft ³	Density of water
γ	62.4 pcf	Unit weight of water

- Table F-2. Input Parameters for the Odgaard Method

Odgaard Input		
Variable	Value	Comment
Q	400 ft ³ /s	Dominant discharge (2-year)
D	0.025 m	Size of bed material
S_0	0.049 ft/ft	Slope
r_c	62.5 ft.	Radius of curvature along center line
W	22 ft.	Average water surface width
d_c	2.1 ft.	Average flow depth
ν	1.1×10^{-6} m ² /s	Kinematic viscosity
EL_{ws}	1432.11 ft	Water surface elevation

Calculations

City Creek

Chang Method: Transverse Stream Power Around a Bend

Created By: Amber Fuxan

Date: January 25th, 2006

Parameters

$D_{max} := 2.1$	Maximum depth along bend [ft]
$S_0 := 0.049$	Average slope through the bend
$r_c := 62.5$	Radius of curvature along center line [ft]
$\Delta r := 22$	Essentially the average width [ft]
$R_h := 1.3$	Average hydraulic radius [ft]
$L_{reach} := 100$	Length from [ft]
$v_{RM51} := 14.3$	Should be a maximum velocity, used an average velocity because we didn't have a maximum velocity [ft/s].
$U := v_{RM51}$	
$\kappa := 0.4$	von Karman's coefficient
$\eta := 0.03$	Manning coefficient for roughness
$\rho := 1.94$	Density of water (slug/ft ³)
$\gamma := 62.4$	Unit weight of water (pcf)

The transverse velocity, v_t , can be considered a constant if known at the location of interest, i.e. at the point of maximum velocity within a particular bend. By assuming that the transverse flow velocity at the water surface in the cross section defines the magnitude of the transverse circulating velocity, the transverse velocity can be calculated with equations (8.87) and (8.88) in Chang, i.e.

$$f := \left(\frac{\eta}{0.093 R_h^{\frac{1}{6}}} \right)^2$$

$$m_I := \kappa \cdot \left(\frac{8}{f} \right)^{0.5}$$

Equation 8.31 from Chang p. 199.

Equation 8.88 from Chang p. 215

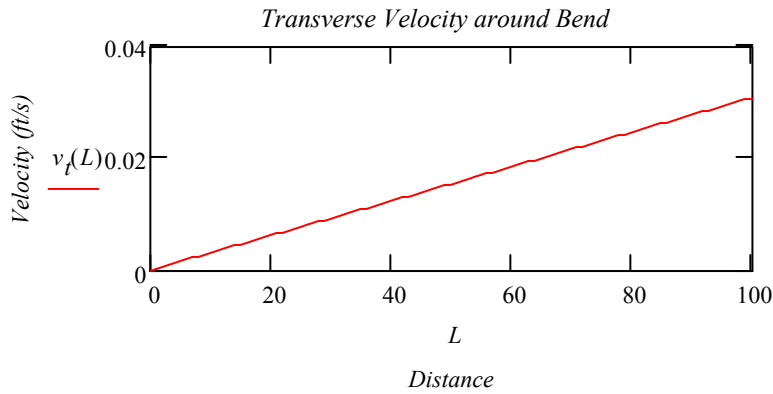
$$F_I := \left(\frac{f}{2}\right)^{0.5} \cdot \left[\left(\frac{10}{3}\right) - \left(\frac{1}{\kappa}\right) \left(\frac{5}{9}\right) \cdot \left(\frac{f}{2}\right)^{0.5} \right]$$

$$F_2 := \left(\frac{\kappa}{D_{max}}\right) \cdot \left(\frac{f}{2}\right)^{0.5} \cdot \left(\frac{m_I}{1+m_I}\right)$$

$$v_{t0} + \left(\int_0^L F_I \cdot \frac{U}{r_c} \cdot e^{\int_0^L F_2 ds} ds - \int_0^L F_2 ds \right) \cdot e^{\int_0^L F_2 ds} \quad \text{expand} \rightarrow v_{t0} + .15137125026831095056 \cdot e^{.32671626038048332459e-1 \cdot L} \cdot (-.32671626038048332459e-1) \cdot L$$

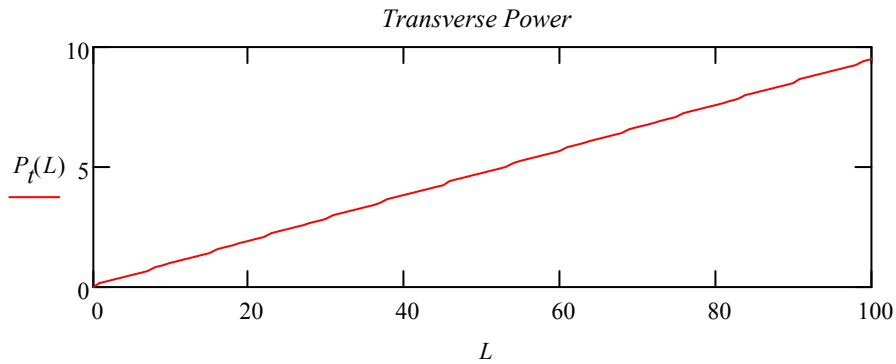
$$L := 0, 1..L_{reach} \quad v_{t0} := 0$$

$$v_t(L) := v_{t0} + 3.06893840100891456710^{-4} \cdot L \cdot \exp\left(4.54997825906743221010^{-3} \cdot L\right) \cdot \exp\left(-4.54997825906743221010^{-3} \cdot L\right)$$



$$P_t(L) := \frac{\rho \cdot v_t(L)}{r_c} \cdot \Delta r \cdot U^2 \cdot \left(\frac{1+m_I}{m_I}\right)^2 \cdot \frac{1}{1 + \left(\frac{2}{m_I}\right)} \cdot D_{max}$$

Transverse Power along the bend



$$P_l := \gamma D_{max} \cdot S_0 \cdot v_{RM51}$$

Longitudinal Power along the bend

$$P_l = 91.81973$$

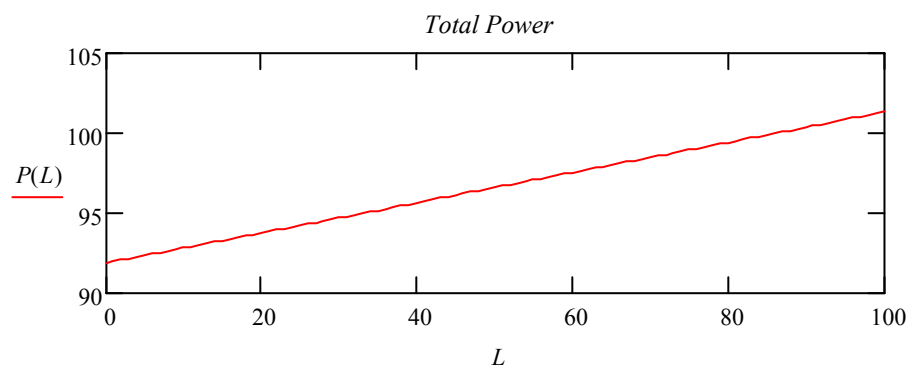
$$P_t(0) = 0$$

$$P(L) := P_l + P_t(L)$$

Total Power

$$P(95) = 100.781333$$

Total Power in lbf/fts. Need to multiply by .01459 to get kW/m2



$$v_t(s) = v_{t0} + \left(\int_0^s F_I \cdot \frac{U}{r_c} \cdot e^{\int_0^s F_2 ds} ds \right) \cdot e^{-\int_0^s F_2 ds}$$

$$Result := P(95) \cdot .01459$$

$$\boxed{Result = 1.47 \times 10^0}$$

City Creek

Odgaard Bend Scour

Created By: Dr. George Annandale

Date: January 25th, 2006

MEANDER FLOW MODEL - Constant Radius Reach Solution

The model in this Mathcad program is based on the paper by Odgaard, A.J., "Meander Flow Model Parts I and II", Journal of Hydraulic Engineering, Vol. 112, No. 12, December 1986, ASCE, pp. 1117-1150.

The model is valid for steady, subcritical, turbulent flow in alluvial channel curves with uniform bed sediment and accounts for development and decay of flow through a bend. Constraints are:

1. The channel width is assumed to be constant.
2. The centerline radius of curvature is assumed large compared to channel width.
3. The flow-depth is small compared with the width.
4. Cross-sectional velocity components are small compared with down-channel components
5. Turbulence is isotropic

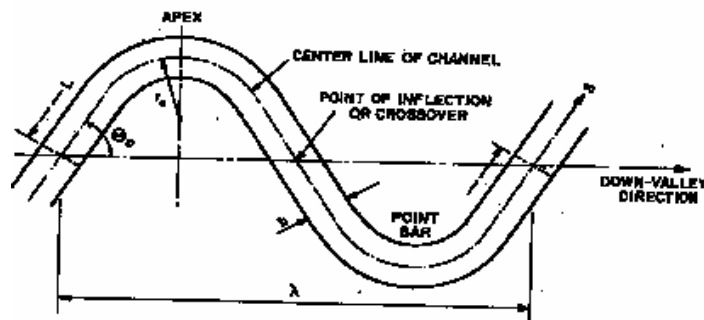


FIG. 1.—Definition Sketch of Meander Channel

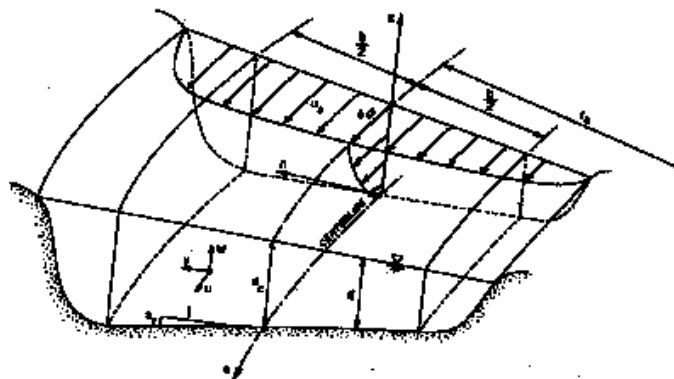


FIG. 2.—Definition Sketch of Channel Cross Section (Idealized)

The method has been tested with field data and was found to provide accurate representation of the long- and cross-sectional geometry of meandering rivers. The solution presented herewith is for constant radius bends. The solution for "sine-generated" meander curves is provided separately.

Input requirements:

$$Q := 400 \frac{\text{ft}^3}{\text{sec}} \quad D := 0.0250 \text{ m} \quad S_0 := 0.04\% \quad r_c := 62.5 \text{ ft}$$

(two-year flood)

$$W := 22 \text{ ft} \quad d_c := 2.1 \text{ ft} \quad \nu := 1 \cdot 10^{-6} \frac{\text{m}^2}{\text{sec}} \quad EL_{ws} := 1432.11 \text{ ft}$$

where Q = discharge; D = size of the bed material; S_0 = slope; W = average water surface width; d_c = average flow depth; ν = kinematic viscosity; r_c = radius of bend at centerline.

The effective water surface width, b , that is used in the calculations, is calculated as the average water surface width, W , less two times the average flow depth, d_c :

$$b := W - 2 \cdot d_c$$

$$b = 17.8 \text{ ft}$$

The average velocity at the center of the channel can therefore be calculated as:

$$u_c := \frac{Q}{b \cdot d_c}$$

$$u_c = 3.262 \frac{\text{m}}{\text{s}}$$

Assuming that the soil particle density (ρ_s) and the water density (ρ) is given by

$$\rho_s := 2650 \frac{\text{kg}}{\text{m}^3}$$

$$\rho := 1000 \frac{\text{kg}}{\text{m}^3}$$

the particle Froude Number at the centerline of the channel can be calculated as,

$$F_{Dc} := \frac{u_c}{\sqrt{\frac{(\rho_s - \rho) \cdot g \cdot D}{\rho}}}$$

$$F_{Dc} = 5.128$$

Shear velocity, u_* , is determined as,

$$u_{\text{star}} := \sqrt{g \cdot S_0 \cdot d_c}$$

$$u_{\text{star}} = 0.555 \frac{\text{m}}{\text{s}}$$

With von Karman's coefficient, κ , equal to

$$\kappa := 0.4$$

the friction factor m can be calculated as:

$$m_{\text{dash}} := \kappa \cdot \frac{u_c}{u_{\text{star}}}$$

$$m_{\text{dash}} = 2.352$$

and the particle Reynolds number is,

$$R_{\text{star}} := u_{\text{star}} \cdot \frac{D}{\nu}$$

$$R_{\text{star}} = 1.386 \times 10^4$$

N , a factor used in the calculation of the transverse velocity component, is equal to:

$$N := \frac{2 \cdot m_{\text{dash}} + 1}{2 \cdot \kappa^2 \cdot m_{\text{dash}}}$$

$$N = 7.578$$

The coefficient G that is used to calculate the variation in flow velocity along the distance s is determined as:

$$G := \frac{2 \cdot \kappa^2 \cdot b}{(m_{\text{dash}} + 1)^2 \cdot d_c}$$

$$G = 0.241$$

With an assumed value of the Shields parameter, θ , equal to

$$\theta := 0.047$$

and the particle shape parameter, α , equal to

$$\alpha := 1.27$$

it is possible to calculate the coefficients a_{dash} , b_{dash} and c_{dash} that are used to calculate the change in transverse bed slope in a bend as a function of curvilinear distance:

$$a_{\text{dash}} := \frac{(16 \cdot \kappa \cdot N) \cdot (m_{\text{dash}} + 2) \cdot d_c}{3 \cdot \alpha \cdot \sqrt{\theta} \cdot (m_{\text{dash}} + 1) \cdot F_{Dc} \cdot b}$$

$$a_{\text{dash}} = 1.754$$

$$b_{\text{dash}} := \frac{(32 \cdot \kappa^3 \cdot N) \cdot (m_{\text{dash}} + 2)}{3 \cdot \alpha \cdot \sqrt{\theta} \cdot (m_{\text{dash}} + 1)^2 \cdot F_{Dc}}$$

$$b_{\text{dash}} = 1.419$$

$$c_{\text{dash}} := \frac{16 \cdot \kappa^2 \cdot N \cdot d_c}{(m_{\text{dash}} + 1) \cdot r_c}$$

$$c_{\text{dash}} = 0.194$$

Calculation of Variation in Bed Topography as a Function of Distance along the Bend

The solution for the variation in the transverse bed slope in the stream can now be calculated by dividing the stream reach into straight and constant radius reaches, and performing the following calculations for each reach:

a. Identify the starting point for each reach computation, i.e. the section with known values of S_{TC} and dS_{TC}/ds (e.g. at the location where the cross-over between adjacent bends, where $S_{TC} = 0$, the derivative dS_{TC}/ds (or, in dimensionless form, $dS_{TC}/d\sigma$) may often be taken to be zero.

Additional Input Required are the following:

The transverse slope at the upstream end of the Constant Radius Reach is:

$$S_{TCi} := 0.00$$

It is also required to quantify the rate of change of the transverse slope at the upstream end of the Constant Radius Reach ($dS_{TC}/d\sigma$) represented by S_{TCRC0} , as follows:

$$S_{TCRC0} := 0$$

The value of the transverse bed slope for the fully developed, constant radius bend flow can be calculated as follows,

$$S_{Tc0} := \left(3 \cdot \frac{\alpha}{2} \right) \cdot \frac{(\sqrt{\theta}) \cdot (m_{\text{dash}} + 1) \cdot F_{Dc} \cdot d_c \cdot b}{\kappa \cdot (m_{\text{dash}} + 2) \cdot b \cdot r_c}$$

$$S_{Tc0} = 0.137$$

The progression of S_{Tc} depends on whether the system is over-, critically, or under-damped. The distinction as to whether the system is over- or critically damped, or whether it is under-damped can be made for the dimensionless distance, $\sigma = s/b$, along the bend, as follows (s = distance along centerline of channel, b = effective channel width):

For, $\alpha' := 90\text{deg}$

Inscribed angle along bend

$$s_{\text{max}} := r_c \cdot \alpha'$$

$$s_0 := \frac{s_{\text{max}}}{10}$$

$$s_1 := \frac{s_{\text{max}}}{10}, \frac{2s_{\text{max}}}{10} \dots s_{\text{max}}$$

$$\sigma(s_1) := \frac{s_1}{b}$$

$$\sigma_i := \frac{s_0}{b}$$

The remainder of the calculations can be completed as follows:

For

$$\psi := \frac{S_{TcRC0}}{S_{Tc0} - S_{Tci}}$$

$$\psi = 0$$

and,

$$\omega := 0.5 \cdot \sqrt{4 \cdot b_{\text{dash}} - a_{\text{dash}}^2}$$

$$\omega = 0.806$$

$$\phi := \text{atan} \left(\left(\frac{-\psi}{\omega} + \frac{a_{\text{dash}}}{2 \cdot \omega} \right) \right)$$

$$\phi = 0.827$$

and

$$\lambda_1 := 0.5 \left(-a_{\text{dash}} + \sqrt{a_{\text{dash}}^2 - 4 \cdot b_{\text{dash}}} \right)$$

$$\lambda_2 := 0.5 \left(-a_{\text{dash}} - \sqrt{a_{\text{dash}}^2 - 4 \cdot b_{\text{dash}}} \right)$$

$$\lambda_1 = -0.877 + 0.806i$$

$$\lambda_2 = -0.877 - 0.806i$$

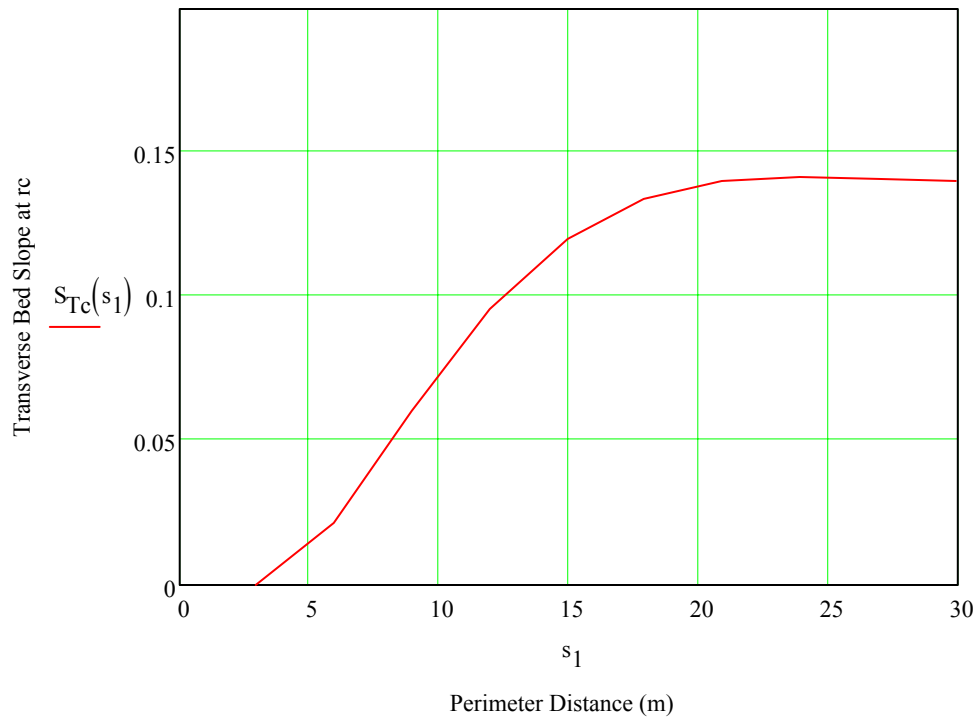
the value of the function E (equation 34 in the Odgaard paper) that is a function of the system's damping characteristics can be calculated as follows:

$$E(s_1) := \begin{cases} \left[\sqrt{1 + \left(\frac{\psi}{\omega} - \frac{a_{\text{dash}}}{2 \cdot \omega} \right)^2} \right] \cdot \left[\cos \left[\omega \cdot (\sigma(s_1) - \sigma_i) - \phi \right] \cdot e^{-0.5 \cdot a_{\text{dash}} \cdot (\sigma(s_1) - \sigma_i)} \right] & \text{if } a_{\text{dash}}^2 \leq 4 \cdot b_{\text{dash}} \\ \left[e^{\lambda_1 \cdot (\sigma(s_1) - \sigma_i)} \cdot \frac{\lambda_2 + \psi}{\lambda_2 - \lambda_1} \right] - \left[e^{\lambda_2 \cdot (\sigma(s_1) - \sigma_i)} \cdot \frac{\lambda_1 + \psi}{\lambda_2 - \lambda_1} \right] & \text{otherwise} \end{cases}$$

The change in transverse slope along the bend is therefore as follows:

$$S_{Tc}(s_1) := S_{Tc0} - (S_{Tc0} - S_{Tci}) \cdot E(s_1)$$

Transverse Slope S_{Tc} as a Function of Distance s



For a curved reach, the change in depth is:

$$\beta(s_1) := S_{Tc}(s_1) \cdot \frac{r_c}{d_c}$$

and,

$$d(r, s_1) := d_c \cdot \left(\frac{r}{r_c} \right)^{\beta(s_1)} \quad E_t(r, s_1) := EL_{ws} - d(r, s_1)$$

$$s_{max} := \frac{s_{max}}{UnitsOf(s_{max})}$$

$$r_c := \frac{r_c}{UnitsOf(r_c)}$$

$$d_c := \frac{d_c}{UnitsOf(d_c)}$$

$$b := \frac{b}{UnitsOf(b)}$$

$$N_1 := 10$$

$$Freeboard := 0\text{-ft}$$

Freeboard is difference between ELws and the ground surface

$$EL_{concave}(Freeboard) := EL_{ws} + Freeboard$$

assign ground surface on concave side of bend

$$EL_{conc} := EL_{concave}(Freeboard)$$

$$EL_{convex} := EL_{ws}$$

assign ground surface on convex side of bend

$$EL_{ws} := \frac{EL_{ws}}{UnitsOf(EL_{ws})}$$

$$EL_{conc} := \frac{EL_{conc}}{UnitsOf(EL_{conc})}$$

$$EL_{convex} := \frac{EL_{convex}}{UnitsOf(EL_{convex})}$$

```

( $\underline{d}$   $\underline{x}$   $\underline{y}$ ) := for  $k \in 1, 2.. N_1 \cdot 3$ 
    for  $r \in 1, 2.. N_1 \cdot 3$ 
         $d_{r,k} \leftarrow 0$ 
         $\theta_{r,k} \leftarrow 0$ 
         $x_{r,k} \leftarrow 0$ 
         $y_{r,k} \leftarrow 0$ 
         $EL_{g1} \leftarrow EL_{convex}$ 
         $EL_{g2} \leftarrow EL_{conc}$ 
    for  $k \in 1, 2.. N_1$ 
         $s_2 \leftarrow k \cdot \frac{s_{max}}{N_1}$ 
        for  $r \in 1, 2.. N_1$ 
             $r_2 \leftarrow r_c - \frac{b}{2} + r \cdot \frac{b}{N_1}$ 
             $\sigma \leftarrow \frac{s_2}{b}$ 
             $E \leftarrow \begin{cases} \left[ \sqrt{1 + \left( \frac{\psi}{\omega} - \frac{a_{dash}}{2 \cdot \omega} \right)^2} \right] \cdot \left[ \cos[\omega \cdot (\sigma - \sigma_i) - \phi] \cdot e^{-0.5 \cdot a_{dash} \cdot (\sigma - \sigma_i)} \right] & \text{if } a_{dash}^2 \leq 4 \cdot b_{dash} \\ \left[ e^{\frac{\lambda_1 \cdot (\sigma - \sigma_i)}{\lambda_2 - \lambda_1} \cdot \frac{\lambda_2 + \psi}{\lambda_2 - \lambda_1}} \right] - \left[ e^{\frac{\lambda_2 \cdot (\sigma - \sigma_i)}{\lambda_2 - \lambda_1} \cdot \frac{\lambda_1 + \psi}{\lambda_2 - \lambda_1}} \right] & \text{otherwise} \end{cases}$ 
             $S_{TC} \leftarrow S_{TC0} - (S_{TC0} - S_{TCi}) \cdot E$ 
             $\beta_1 \leftarrow S_{TC} \cdot \frac{r_c}{d_c}$ 
             $d_{r,k} \leftarrow d_c \cdot \left( \frac{r_2}{r_c} \right)^{\beta_1}$ 
             $d_{r,k} \leftarrow EL_{ws} - d_{r,k}$ 
             $\theta_{r,k} \leftarrow \frac{s_2}{r_c}$ 
             $x_{r,k} \leftarrow r_2 \cdot \cos(\theta_{r,k})$ 
             $y_{r,k} \leftarrow r_2 \cdot \sin(\theta_{r,k})$ 
        for  $k \in N_1 + 1, N_1 + 2.. 2 \cdot N_1$ 
             $k' \leftarrow k - N_1$ 
             $s_2 \leftarrow k' \cdot \frac{s_{max}}{N_1}$ 
            for  $r \in N_1 + 1, N_1 + 2.. 2 \cdot N_1$ 
                 $r_2 \leftarrow r_c - \frac{b}{2} - r \cdot \frac{r_c - \frac{b}{2}}{2 \cdot N_1 + 1}$ 
                 $d_{r,k} \leftarrow EL_{g1}$ 

```

$$X := \text{submatrix}(x, 1, N_1, 1, N_1)$$

$$Y := \text{submatrix}(y, 1, N_1, 1, N_1)$$

$$\underline{D} := \text{submatrix}(d, 1, N_1, 1, N_1)$$

$$X_2 := \text{submatrix}(x, N_1 + 1, 2N_1, N_1 + 1, 2N_1)$$

$$Y_2 := \text{submatrix}(y, N_1 + 1, 2N_1, N_1 + 1, 2N_1)$$

$$D_2 := \text{submatrix}(d, N_1 + 1, 2N_1, N_1 + 1, 2N_1)$$

$$X_3 := \text{submatrix}(x, 2 \cdot N_1 + 1, 3N_1, 2 \cdot N_1 + 1, 3N_1)$$

$$Y_3 := \text{submatrix}(y, 2 \cdot N_1 + 1, 3N_1, 2 \cdot N_1 + 1, 3N_1)$$

$$D_3 := \text{submatrix}(d, 2 \cdot N_1 + 1, 3N_1, 2 \cdot N_1 + 1, 3N_1)$$

$$DD := \text{stack}(D^{\langle 0 \rangle}, D^{\langle 1 \rangle}, D^{\langle 2 \rangle}, D^{\langle 3 \rangle}, D^{\langle 4 \rangle}, D^{\langle 5 \rangle}, D^{\langle 6 \rangle}, D^{\langle 7 \rangle}, D^{\langle 8 \rangle}, D^{\langle 9 \rangle})$$

$$DD_2 := \text{stack}(D_2^{\langle 0 \rangle}, D_2^{\langle 1 \rangle}, D_2^{\langle 2 \rangle}, D_2^{\langle 3 \rangle}, D_2^{\langle 4 \rangle}, D_2^{\langle 5 \rangle}, D_2^{\langle 6 \rangle}, D_2^{\langle 7 \rangle}, D_2^{\langle 8 \rangle}, D_2^{\langle 9 \rangle})$$

$$DD_3 := \text{stack}(D_3^{\langle 0 \rangle}, D_3^{\langle 1 \rangle}, D_3^{\langle 2 \rangle}, D_3^{\langle 3 \rangle}, D_3^{\langle 4 \rangle}, D_3^{\langle 5 \rangle}, D_3^{\langle 6 \rangle}, D_3^{\langle 7 \rangle}, D_3^{\langle 8 \rangle}, D_3^{\langle 9 \rangle})$$

$$XX := \text{stack}(X^{\langle 0 \rangle}, X^{\langle 1 \rangle}, X^{\langle 2 \rangle}, X^{\langle 3 \rangle}, X^{\langle 4 \rangle}, X^{\langle 5 \rangle}, X^{\langle 6 \rangle}, X^{\langle 7 \rangle}, X^{\langle 8 \rangle}, X^{\langle 9 \rangle})$$

$$XX_2 := \text{stack}(X_2^{\langle 0 \rangle}, X_2^{\langle 1 \rangle}, X_2^{\langle 2 \rangle}, X_2^{\langle 3 \rangle}, X_2^{\langle 4 \rangle}, X_2^{\langle 5 \rangle}, X_2^{\langle 6 \rangle}, X_2^{\langle 7 \rangle}, X_2^{\langle 8 \rangle}, X_2^{\langle 9 \rangle})$$

$$XX_3 := \text{stack}(X_3^{\langle 0 \rangle}, X_3^{\langle 1 \rangle}, X_3^{\langle 2 \rangle}, X_3^{\langle 3 \rangle}, X_3^{\langle 4 \rangle}, X_3^{\langle 5 \rangle}, X_3^{\langle 6 \rangle}, X_3^{\langle 7 \rangle}, X_3^{\langle 8 \rangle}, X_3^{\langle 9 \rangle})$$

$$YY := \text{stack}\left(Y^{\langle 0 \rangle}, Y^{\langle 1 \rangle}, Y^{\langle 2 \rangle}, Y^{\langle 3 \rangle}, Y^{\langle 4 \rangle}, Y^{\langle 5 \rangle}, Y^{\langle 6 \rangle}, Y^{\langle 7 \rangle}, Y^{\langle 8 \rangle}, Y^{\langle 9 \rangle}\right)$$

$$YY_2 := \text{stack}\left(Y_2^{\langle 0 \rangle}, Y_2^{\langle 1 \rangle}, Y_2^{\langle 2 \rangle}, Y_2^{\langle 3 \rangle}, Y_2^{\langle 4 \rangle}, Y_2^{\langle 5 \rangle}, Y_2^{\langle 6 \rangle}, Y_2^{\langle 7 \rangle}, Y_2^{\langle 8 \rangle}, Y_2^{\langle 9 \rangle}\right)$$

$$YY_3 := \text{stack}\left(Y_3^{\langle 0 \rangle}, Y_3^{\langle 1 \rangle}, Y_3^{\langle 2 \rangle}, Y_3^{\langle 3 \rangle}, Y_3^{\langle 4 \rangle}, Y_3^{\langle 5 \rangle}, Y_3^{\langle 6 \rangle}, Y_3^{\langle 7 \rangle}, Y_3^{\langle 8 \rangle}, Y_3^{\langle 9 \rangle}\right)$$

$$DD := \text{stack}\left(DD, DD_2, DD_3\right)$$

$$XX := \text{stack}\left(XX, XX_2, XX_3\right)$$

$$YY := \text{stack}\left(YY, YY_2, YY_3\right)$$

$$\text{Depth} := \text{augment}(XX, YY, DD)$$

$$\max(DD) = 436.507$$

$$S_0 := 0.04\%$$

$$r_{ax} := 62.5\text{ ft}$$

$$\max(XX) = 27.266$$

$$\max(YY) = 27.606$$

$$v := 1 \cdot 10^{-6} \cdot \frac{\text{m}^2}{\text{sec}}$$

$$\min(DD) = 435.386$$

$$\min(XX) = 0$$

$$\min(YY) = 0.122$$

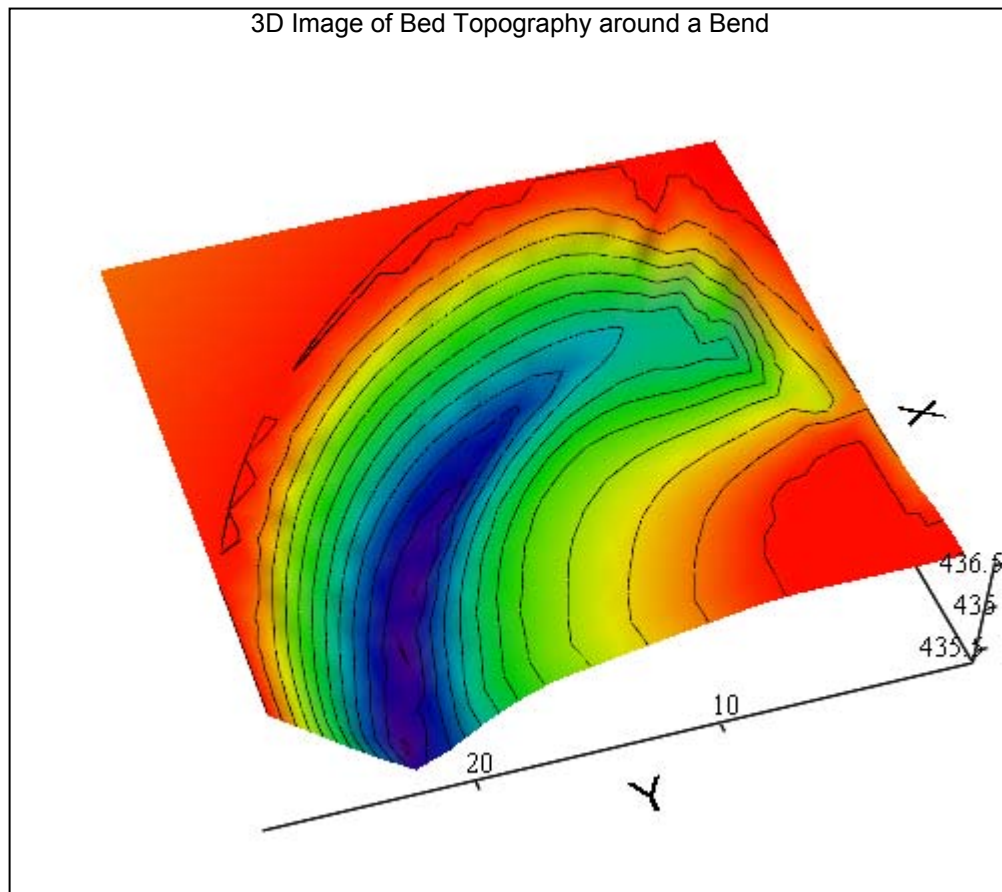
Scour Depth due to Bend:

$$\text{Scour} := \max(\text{DD}) - \min(\text{DD}) - \frac{d_c}{\text{SIUnitsOf}(d_c)}$$

$$\text{Scour}_{\max} := \text{Scour} \cdot m$$

$$\boxed{\text{Scour}_{\max} = 1.579\text{ft}} \quad \text{below the original river bed}$$

$$\text{mesh} := 100$$



(XX, YY, DD)

Results

Due to the fact that the total bend stream power exceeds the erosive threshold of the existing bed materials (15.2 W/m^2), scour can be expected around the bend. The expected stream power and additional scour due to the bend can be seen in Table F-3.

- Table F-3. Results for the Chang and Odgaard Methods

Chang		
Transverse Stream Power At end of Curve (95ft)	0.13	kW/m^2
Total Stream Power At end of Curve (95ft)	1.47	kW/m^2
Odgaard		
Depth of excess degradation at 95 ft through the bend:	1.578	ft

References

- Chang, Howard H. 1992. Fluvial Processes in River Engineering. Krieger Publishing Company. Malabar, Florida.
- Odgaard, A.J., "Meander Flow Model Parts I and II", Journal of Hydraulic Engineering, Vol. 112, No. 12, December 1986, ASCE, pp. 1117-1150.

Appendix G: Headcut Hydraulics

Introduction

Headcuts larger than 6 ft were observed during the site visit. It was deemed necessary to estimate the anticipated stream power produced by the impact of a jet falling over the head cut and the stream power of the back roller to adequately protect the pipeline from headcut migration. Supercritical flow was observed for all discharges and for all models in HEC-RAS, therefore, a procedure developed by Chamani and Beirami (2002) for supercritical flow over headcuts was utilized.

Assumptions

- The approach slope is equal to zero.
- A rectangular channel.
- It is a free overfall, the nappe is unsubmerged.
- The density is assumed constant throughout the calculation. The change in density due to aeration is neglected.
- Uniform velocity distribution throughout, $\alpha = 1$ and $\beta = 1$.
- Hydrostatic pressure distribution on the flow upstream, downstream, and at the pool.
- Friction losses are negligible.
- The jet angle where it hits the pool (ϕ) is equal to jet angle at the nappe base (β), see Figure 1.
- The retardation of jet velocity at the pool level affects only the vertical velocity component, not the horizontal.

Input

All hydraulic input parameters were obtained from the cross sections upstream of the headcuts in the EXST, ALT50, ALT70, and ALT100 2-year discharge HEC-RAS models.

- Table G-1. Input Parameters for the Headcut Calculations at the Pipeline Crossing

Headcut Hydraulics					
Variable	EXST	ALT50	ALT70	ALT100	Comment
q	25.2 ft ² /s	7.7 ft ² /s	5.6 ft ² /s	3.9 ft ² /s	Unit discharge (discharge/avg width)
H	15 ft	5 ft	4 ft	3 ft	Drop height (armor layer depth of degradation)
Fr ₁	1.95	2.08	2.01	1.94	Approach Froude number, upstream from drop

- Table G-2. Input Parameters for Existing Headcut Calculations

Headcut Hydraulics								
Variable	Cross-Section Station							Comment
	64	57	56	48	35	31	24	
q	19.8 ft ² /s	4.6 ft ² /s	15 ft ² /s	21.2 ft ² /s	11.9 ft ² /s	9.4 ft ² /s	5.3 ft ² /s	Unit discharge (discharge/avg width)
H	4 ft	3 ft	6 ft	5 ft	4 ft	4 ft	3 ft	Drop height (armor layer depth of degradation)
Fr ₁	1.55	2.74	1.95	1.75	1.41	1.31	1.24	Approach Froude number, upstream from drop

Calculations

The flow characteristics for each headcut analyzed were derived from HEC-RAS results at the location of the pipeline crossing and at the location of existing headcuts. The inputs for the stream power calculation are unit discharge, drop height, and approach Froude number. The unit discharge was found by dividing the discharge by the average width. The drop height used for the EXST, ALT50, ALT70, and ALT100 headcut calculations correlates to the expected average degradation due to armoring at the pipeline crossing. The drop heights for the existing headcuts are the current drop heights of the headcuts on site as seen in the topographic AutoCAD drawing. See attached MathCAD sheet for an example of the calculations.

City Creek

Supercritical flow Over Headcuts

Created By: Amber Fuxan

Date: January 25th, 2006

This sheet calculates the stream power in the backroller of a jet plunging over a headcut, with a supercritical approach flow. It also assumes that the downstream depth, Y_2 , is unknown.

Given: Unit discharge, drop height, approach Froude number.

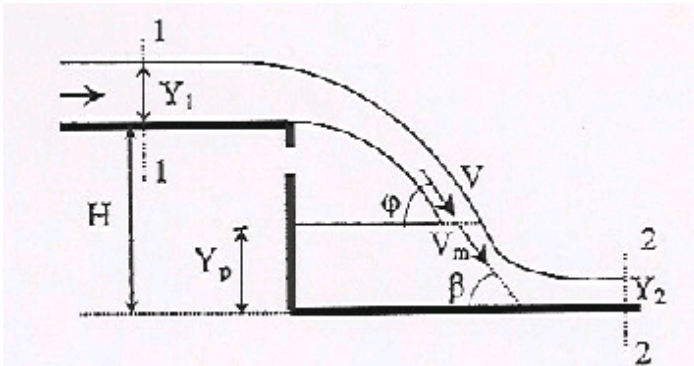
$$q := 18 \frac{\text{ft}^2}{\text{s}} \quad \text{Unit discharge}$$

$$\gamma := 9820 \frac{\text{N}}{\text{m}^3}$$

$$H := 15 \text{ ft} \quad \text{Drop height}$$

$$g = 9.807 \frac{\text{m}}{\text{s}^2}$$

$$Fr_1 := 1.95 \quad \text{Approach Froude Number, upstream from the drop.}$$



The upstream cross-section has the subscript 1. The downstream cross-section has the subscript 2. The pool characteristics have the subscript, P.

From given parameters calculate the critical depth, approach depth, and velocity. (Assuming a prismatic rectangular channel.)

$$y_c := \left(\frac{q^2}{g} \right)^{\frac{1}{3}}$$

$$y_c = 0.658 \text{ m}$$

Critical Depth (y_c)

$$Y_1 := \left(\frac{q^2}{g \cdot Fr_1^2} \right)^{\frac{1}{3}}$$

$$Y_1 = 1.384 \text{ ft}$$

Approach Depth (Y_1)

$$V_1 := \frac{q}{Y_1}$$

$$V_1 = 13.01 \frac{\text{ft}}{\text{s}}$$

Approach Velocity (V_1)

$$Y_{p1} := 1.018\text{m}$$

Estimated value, used in iteration.

$$A := \frac{2 \cdot Fr_1^2}{1 + 2Fr_1^2}$$

$$A = 0.884$$

A and B are defined and used by Chamani and Beirami(2002).

$$B := \sqrt{1 + 0.5 \cdot Fr_1^2 + \frac{H}{Y_1} - \frac{Y_{p1}}{Y_1}}$$

$$B = 3.366$$

$$\beta := \arccos\left(\left(\frac{-1 + \sqrt{1 + \frac{8A}{\sqrt{2} \cdot B}}}{2}\right)\right)$$

$$\beta = 1.278$$

β is the angle at which the jet strikes the downstream channel bed.

Gill (1979) used the momentum equation to show the reduction in flow velocity as the jet struck the pool. $V_m = 0.5V(1 - \cos(\beta))$. Where V is the jet velocity above the pool.

This equation combined with the energy equation is used by Chamani and Beirami (2002) to find the relationship between V and the pool depth, Y_p .

$$V_m := \frac{1}{2} \cdot (1 + \cos(\beta)) \cdot \sqrt{2 \cdot g \cdot \left[Y_1 \cdot \left(1 + 0.5 \cdot Fr_1^2 \right) + H - Y_{p1} \right]}$$

$$V_m = 6.235 \frac{\text{m}}{\text{s}}$$

The mean velocity of jet in mixing zone just below pool surface, V_m .

The downstream flow depth, Y_2 , can be found using Gill's method and the energy equation:

$$Y_2 := .02\text{-m}$$

Guess value, used for solve block below.

$$f(Y_2) := Y_2^3 - \left[\frac{1}{2 \cdot g} \cdot (V_m^2 + 2 \cdot g \cdot Y_{p1}) \cdot Y_2^2 \right] + \frac{q^2}{2g}$$

Given

$$f(Y_2) = 0$$

$$Y_2 := \text{Find}(Y_2)$$

$$Y_2 = 0.227\text{m}$$

Downstream flow depth (Y_2).

$$\text{Note: } 0 < Y_2 < y_c$$

$$y_c = 0.658\text{m} \quad y_c = 2.159\text{ft}$$

The pool depth, Y_p , can be calculated using the momentum and continuity principles for a control volume between cross-sections 1 and 2.

$$Y_p := Y_1 \cdot \sqrt{\left(\frac{Y_2}{Y_1} \right)^2 + 2 \cdot Fr_1^2 \cdot \left(\frac{Y_1}{Y_2} \right) - (2 \cdot Fr_1^2 + 1)}$$

$$Y_p = 1.018\text{m}$$

Iterate by changing Y_{p1} until error is minimized.

$$\text{error} := \frac{Y_p - Y_{p1}}{Y_p} \cdot 10 \quad \text{error} = 8.091 \times 10^{-3}$$

Minimize Error

Calculate change in energy between upstream and downstream of the drop.

$$\Delta E := H + \frac{\left(\frac{q}{Y_1} \right)^2}{2g} + Y_1 - Y_2 - \frac{\left(\frac{q}{Y_2} \right)^2}{2g}$$

$$\Delta E = 2.795\text{m}$$

Find the rate of energy dissipation at the downstream end of the jet (*Erodibility* eq. 2)

$$P_{\text{total}} := \gamma \cdot q \cdot \Delta E$$

$$P_{\text{total}} = 45.903 \frac{\text{kW}}{\text{m}}$$

Rate of energy dissipation at the downstream end of the jet.

Find the rate of energy dissipation in the backroller (*Erodibility* eq. 9).

$$q_3 := \frac{q \cdot (1 - \cos(\beta))}{1 + \cos(\beta)}$$

$$q_3 = 0.924 \frac{\text{m}^2}{\text{s}}$$

Unit discharge for the backroller.

$$P_{\text{backroller}} := \gamma \cdot q_3 \cdot \frac{V_m^2}{2g}$$

$$P_{\text{backroller}} = 17.984 \frac{\text{kW}}{\text{m}}$$

Rate of energy dissipation in the backroller.

Find the rate of energy dissipation for the jet impacting the pool/bed.

$$P_{\text{impact}} := P_{\text{total}} - P_{\text{backroller}}$$

$$P_{\text{impact}} = 27.92 \frac{\text{kW}}{\text{m}}$$

Rate of energy dissipation at jet impact.

To find the stream power per unit width, you need to divide by a length. For the back roller the length is (the depth of the pool plus the distance from the drop to jet impact). The location of the jet impact is needed.

$$\theta := 0$$

Take off angle from drop.

$$V_m = 6.235 \frac{\text{m}}{\text{s}}$$

Impact velocity, calculated above.

$$D_j := Y_1 \cdot \sqrt{\frac{V_1}{V_m}}$$

Dimensions of inner core of Jet (Ski-Jump Jet Hydraulics MathCAD worksheet).

$$K_2 := 1$$

Turbulence coefficient (Ski-Jump Jet Hydraulics MathCAD worksheet).

$$h_v := \frac{V_1^2}{2g}$$

$$h_v = 0.802 \text{ m}$$

$$L_t := \left[\tan(\theta) + \sqrt{\tan(\theta)^2 - \frac{(-1) \cdot H}{K_2 \cdot (Y_1 + h_v) \cdot \cos(\theta)^2}} \right] \cdot 2 \cdot K_2 \cdot (Y_1 + h_v) \cdot \cos(\theta)$$

$$L_t = 4.73 \text{ m}$$

Location where jet impacts the plunge pool, equation from Ski-Jump Hydraulics MathCAD worksheet.

$$L_{\text{backroller}} := (Y_p + L_t)$$

Length the backroller is in contact with.

$$L_{\text{backroller}} = 5.748 \text{ m}$$

With area and backroller stream power calculated, the stream power per unit width for the backroller can be calculated.

$$\frac{P_{\text{backroller}}}{L_{\text{backroller}}} = 3.12854 \frac{\text{kW}}{\text{m}^2}$$

Rate of energy dissipation per unit area in the backroller.

To find the stream power per unit width, you need to divide by an area. For the jet impact, the area is (unit width) times (dimensions of the inner core of the jet).

$$L_{\text{impact}} := D_j$$

$$L_{\text{impact}} = 0.336 \text{ m}$$

With area and impact stream power calculated, the stream power per unit width for the jet impact can be calculated.

$$\frac{P_{\text{impact}}}{L_{\text{impact}}} = 83.019 \frac{\text{kW}}{\text{m}^2}$$

Rate of energy dissipation per unit area at jet impact.

Results

Below, the headcut hydraulics associated with the hydraulics of the four HEC-RAS models (EXST, ALT50, ALT70, ALT100) and drop heights equal to the armor layer degradation depths for each model at the pipeline crossing (Table G-3).

- Table G-3. Results for the Headcut Calculations at the Pipeline Crossing

		Stream Power (kW/m ²)	
Model Name	Drop Height (ft)	Back Roller	Impact
EXST	15	4.0	89.4
ALT50	5	1.1	20.8
ALT70	4	0.8	14.5
ALT100	3	0.5	9.3

To determine the resistance of the existing bed material to headcut migration, it was necessary to calculate the stream power of the back roller of all of the existing head cuts. Below, is a table displaying the expected backroller and impact stream power magnitudes for the existing headcuts. The calculated erosive threshold) for the existing bed material is 0.02 kW/m² (Appendix C). Since the back roller stream power for all of the existing headcuts (Table G-4) is larger than the erosive threshold of the existing bed material, it is expected that all of these headcuts will migrate upstream

- Table G-4. Results for Existing Headcut Calculations

		Stream Power (kW/m ²)	
Cross Section Station	Drop Height (ft)	Back Roller	Impact
64	4	2.3	19.6
57	3	0.7	15.1
56	6	2.0	29.6
48	5	2.6	26.9
35	4	1.3	13.8
31	4	1.1	12.1
24	3	0.6	7.3

References

- Annandale, G.W. "Erodibility" *Journal of Hydraulic Research*, 33(4), 1995.
- Chamani, M.R. and M.K. Beirami. "Flow Characteristics at Drops" *Journal of Hydraulic Engineering*, 128(8), 2002.
- Gill, M.A. "Hydraulics of Rectangular Vertical Drop Structures" *Journal of Hydraulic Research*, 17(4), 1979.
- Moore, W.L. "Energy Loss at the Base of Free Overfall" *Transactions of ASCE*, 108, 1943.
- White, M.P. "Discussion of Moore (1943)" *Transactions of ASCE*, 108, 1943.
- Rouse, H. "Discussion of Moore (1943)" *Transactions of ASCE*, 108, 1943.

APPENDIX F-2

WEST Foothill Pipeline Scour Analysis Draft

DRAFT REPORT

SCOUR EVALUATION FOR THE FOOTHILL PIPELINE CROSSING CITY CREEK IN THE CITY OF HIGHLAND, CA

December 22, 2008



Prepared For:



SAN BERNARDINO VALLEY MUNICIPAL WATER DISTRICT
380 East Vanderbilt Way
SAN BERNARDINO, CA 92408
(909)-387-9200

Prepared By:



WEST CONSULTANTS, INC.
11440 W. BERNARDO COURT, SUITE 360
SAN DIEGO, CA 92127-1644
(858) 487-9378

TABLE OF CONTENTS

1.	Introduction.....	1-1
1.1.	Purpose.....	1-1
1.2.	Reach Description.....	1-2
1.3.	Data Collection	1-3
1.4.	Acknowledgments.....	1-4
2.	Hydrology	2-1
2.1.	Flood Frequency Discharge Data.....	2-1
2.2.	Historical Hydrograph	2-1
2.3.	100-Year Hydrograph	2-4
3.	Hydraulic Analysis.....	3-1
3.1.	Model Development.....	3-1
3.2.	Model Parameters	3-1
3.3.	Bridges and Culverts.....	3-1
4.	Sediment Transport Analysis.....	4-1
4.1.	General.....	4-1
4.2.	Sediment Parameters.....	4-2
4.3.	Bed Sediment Characteristics	4-2
4.4.	Sediment Boundary Conditions	4-6
4.5.	Quasi-Unsteady Flow Data.....	4-7
4.6.	Results.....	4-8
4.7.	Local Scour	4-10
4.8.	Total Scour.....	4-11
5.	References.....	5-1

LIST OF TABLES

Table 2-1.	Adopted Flood Frequency Results for City Creek.	2-1
Table 2-2.	89-year Historic Hydrograph (Mean Daily Flows).	2-2
Table 2-3.	25-year Precipitation Values.	2-4
Table 4-1.	Equilibrium Sediment Inflow Load.....	4-6
Table 4-2.	Estimated Antidune Scour.....	4-11
Table 4-3.	Total Predicted Scour at Pipeline Crossing.	4-11

LIST OF FIGURES

Figure 1-1. Location Map.	1-2
Figure 1-2. FEMA FIRM Panel No. 06071C8702H.....	1-3
Figure 2-1. USGS Gage No. 11055800 Record.....	2-2
Figure 2-2. Calculated 100-year Storm Hydrograph for City Creek.	2-4
Figure 3-1. City Creek HEC-RAS Cross Sections.	3-1
Figure 4-1. Sediment Sample Locations.....	4-3
Figure 4-2. Sediment Gradation Data (1).	4-4
Figure 4-3. Sediment Gradation Data (2).	4-5
Figure 4-4. Sediment Inflow Load Rating Curve.	4-7
Figure 4-5. Long-Term Invert Change at Pipeline Crossing - No Sediment Load.....	4-8
Figure 4-6. Long-Term Invert Change at Pipeline Crossing – 20% of Equilibrium Sediment Load (Laursen Method Failed to Provide Stable Solution).....	4-9
Figure 4-7. 100-Year Flood Invert Change at Pipeline Crossing - No Sediment Load.....	4-10

LIST OF APPENDICES

Appendix A: HEC-RAS Hydraulic Model Results

1. Introduction

1.1. Purpose

The purpose of this study is to perform a sediment transport, scour, and channel stability analysis for the City Creek Channel (Channel) near the San Bernardino Valley Municipal Water District (District) Foothill Pipeline. The pipeline is located about 1,000 ft downstream of Highland Avenue in the City of Highland, California. The results of this study will be utilized in the selection and design of the pipeline scour protection alternatives.

The pipeline crosses under the Channel along the base of the San Bernardino Mountains. At the Channel crossing, the pipeline is encased in reinforced concrete that is 2 feet thick on the top and 1 foot thick on the sides and bottom. When constructed, the pipeline had a minimum of 8 feet of cover within the Channel. During the winter of 2004/2005, the San Bernardino County Flood Control District (SBCFCD) changed the Channel's configuration from a wide, "braided" stream to a "single thread" earthen trapezoidal channel. This has changed the hydraulic characteristics of the channel. In April of 2006, the District visited the site and found that all of the cover had been removed from the pipeline and approximately 6 feet of the downstream side of the concrete encasement was exposed. Under emergency permits with the SBCFCD, the U.S. Army Corps of Engineers and the California Department of Fish and Game, the District arranged for the placement of large boulders on the downstream side of the pipeline to help prevent further erosion. Many of these rocks were later washed downstream which required the subsequent placement of larger rocks.

The Metropolitan Water District of Southern California (MWDSC) Inland Feeder Pipeline (Inland Feeder) also crosses the Channel just upstream from the Foothill pipeline. MWDSC was aware of this problem and had already completed a scour analysis. The MWDSC scour analysis concluded that "the channel has not yet achieved equilibrium" and will continue to erode. It also concluded that there was not yet enough field work to determine the extent of erosion. MWDSC and the District shared the cost to prepare a conceptual design report. However, this report also concluded that it is difficult to recommend an alternative not knowing the final extent of scour.

Given the importance of the Foothill pipeline as the foundation of regional water infrastructure in this area (it provides direct deliveries of water to four of the District's largest customers), the goal of this study is to:

- 1) Estimate the long-term (50 years or longer) configuration of the City Creek channel between Highland Avenue and Base Line Road.
- 2) Estimate the depth and width of potential erosion that will occur at the pipeline.
- 3) Prepare conceptual designs and cost estimates for one or more alternatives that would protect the pipeline.

1.2. Reach Description

The City Creek study reach extends from Highland Avenue to Base Line Road. The hydraulic and sediment transport model extends from about 4,000 ft upstream of Highland Avenue to 1,000 ft downstream of 5th Street in San Bernardino, California (see Figure 1-1). The pipeline crossing is located near Summertrail Place and Atlantic Avenue, about 1,000 ft downstream of Highland Avenue.



Figure 1-1. Location Map.

The portion of the study reach upstream of Highland Avenue features several sharp bends and a relatively narrow, steep channel. The Channel straightens past Highland Avenue and it flows southwesterly under Base Line Road, Boulder Avenue, 5th Street, Interstate 30 (I-30 and SR-210), and Alabama Avenue before joining with Plunge Creek, eventually reaching its confluence with the Santa Ana River. The Channel geometry is fairly consistent between Highland Avenue and Base Line Road (trapezoidal sand-bed channel with a straight to gentle serpentine morphology). The Channel widens past Base Line Road where the main channel shifts abruptly to the left side of the floodplain. Up to about 1,400 ft downstream of Base Line Road, the Channel gradually changes its alignment to recuperate its position on the right side of the floodplain. The FEMA Flood Insurance Rate Map (FIRM) No. 06071C8702H (FEMA, 2008) shows a levee on the right overbank starting just downstream of Boulder Avenue and ending upstream of Alabama Avenue.

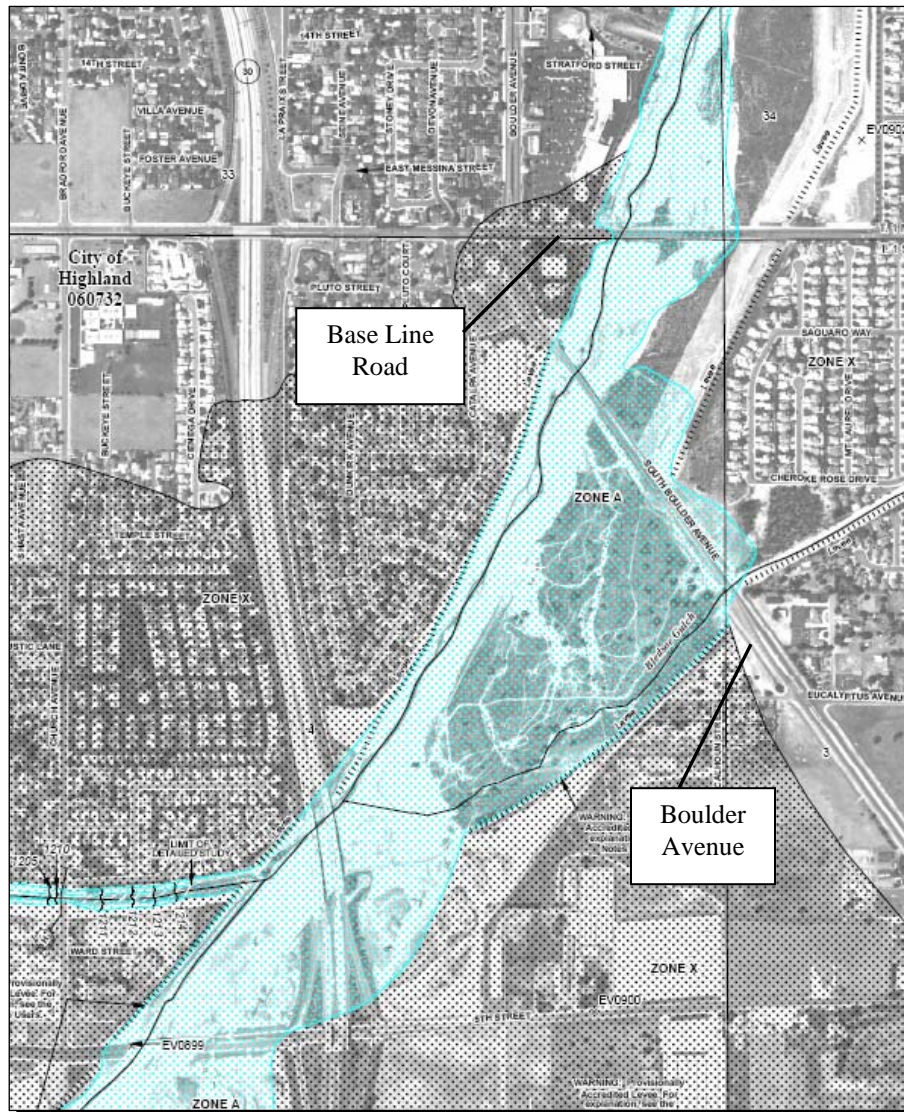


Figure 1-2. FEMA FIRM Panel No. 06071C8702H.

1.3. Data Collection

The digital topographic data for the portion of the Channel between 5th Street and 2,000 ft upstream of Base Line Road was obtained from Tetra Tech as 1-foot aerial contours (dated 2008) (Horizontal Datum: State Plane, California V, Feet. Vertical Datum: NAVD 88, Feet). A second set of digital 1-foot contours (dated 2006) extending from 2,000 ft upstream of Baseline Road to Highland Avenue was obtained from the District (Horizontal Datum: State Plane, California V, Feet. Vertical Datum: NGVD 29, Feet). Additional data for the portion of the Channel upstream of Highland Avenue was obtained from the District based on the October 2008 aerial mapping (Horizontal Datum: Local, Feet. Vertical Datum: NAVD 88, Feet).

INTRODUCTION

The flow frequency information for City Creek was found in the 2008 City Creek Levee report (Tetra Tech, 2008). Historical flows were downloaded from the Internet for the USGS Stream Gage No. 11055800 (City Creek, <http://waterdata.usgs.gov/nwis/uv?11055800>). No flow information for City Creek is indicated in the Flood Insurance Study (FIS) for San Bernardino County. The aerial images for the study reach were downloaded from the National Map Seamless Server (<http://seamless.usgs.gov/>).

WEST performed a field reconnaissance of the site on July 17, 2008 to document field conditions necessary for the development of the sediment transport model. The field inspection included an assessment of stream behavior and morphology in the vicinity of the pipeline crossing, existing and potential scour problems, and estimates of hydraulic parameters. Observations made regarding channel stability, aggradation/degradation, hydraulic roughness, bed material size, and hydraulic or sediment transport controls were used throughout this study. WEST also collected bed sediment samples to determine streambed characteristics (representative sediment grain sizes). NMG Geotechnical Inc. analyzed the sediment samples and developed gradation curves (discussed in Section 4.3 of this report) used in the sediment transport model.

1.4. Acknowledgments

Mr. Martin Teal, PE, PH, was the WEST project manager. Dr. Dragoslav Stefanovic, PE, was the lead hydraulic engineer who performed hydraulic, sediment transport, and scour analyses. Ms. Daniela Todesco, PE, assisted with the data collection and hydraulic analysis. The project manager for the District was Mr. Michael Esquer.

2. Hydrology

The flood frequency discharge data for the Channel were obtained from Tetra Tech (2008). The historic hydrograph (for the long-term sediment transport analysis) was based on the 89-year flow record at USGS Gage No. 11055800 (one mile upstream of the pipeline crossing). The 100-year event hydrograph was generated by WEST to match the 100-year peak flow obtained from the flood frequency analysis.

2.1. Flood Frequency Discharge Data

The flood frequency discharges for the City Creek were estimated by Tetra Tech (2008) as follows:

Table 2-1. Adopted Flood Frequency Results for City Creek.

PERCENT CHANCE EXCEEDANCE	RETURN FREQUENCY (YEAR)	COMPUTED PROBABILITY CURVE FLOW (CFS)		
		At USGS Stream Gauge 11055800	At Boulder Avenue	At 5 th Street
0.2	500	21,000	21,780	28,220
0.5	200	14,000	14,520	18,820
1.0	100	10,100	10,470	13,570
2.0	50	7,100	7,360	9,540
5.0	20	4,060	4,210	5,460
10.0	10	2,500	2,590	3,360
20.0	5	1,390	1,440	1,870

2.2. Historical Hydrograph

A continuous historical hydrograph for City Creek consisting of 89 years of mean daily flows was developed by WEST based on the records of USGS Gage No. 11055800 – City Creek at Highland Avenue (see Figure 2-1). Only days in which the gage had positive readings were considered. This historical hydrograph was prepared to simulate the long-term bed changes in the study reach as requested by the District.

The final hydrograph used in this study (see Table 2-2) was reduced to 424 days by eliminating those days in which the readings (or estimates) were less than 100 cfs (flows below 100 cfs were considered to have little influence on shaping the channel morphology).

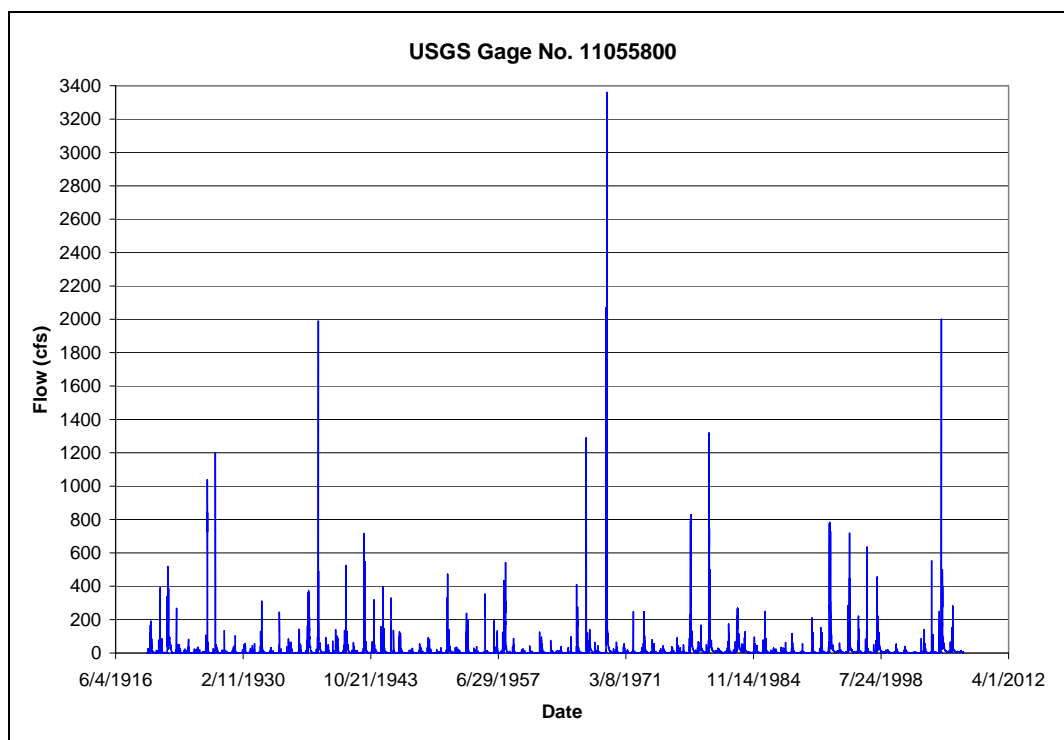


Figure 2-1. USGS Gage No. 11055800 Record.

Table 2-2. 89-year Historic Hydrograph (Mean Daily Flows).

Day	1	2	3	4	5	6	7	8	9	10	11	12	13
Q (cfs)	134	166	120	190	117	138	138	393	109	339	249	101	112
Day	14	15	16	17	18	19	20	21	22	23	24	25	26
Q (cfs)	247	149	101	520	227	137	104	216	385	288	191	143	119
Day	27	28	29	30	31	32	33	34	35	36	37	38	39
Q (cfs)	105	268	140	106	620	1040	725	840	330	157	258	628	1200
Day	40	41	42	43	44	45	46	47	48	49	50	51	52
Q (cfs)	365	191	116	134	104	129	135	310	172	131	245	142	129
Day	53	54	55	56	57	58	59	60	61	62	63	64	65
Q (cfs)	106	162	346	363	153	372	240	160	116	120	217	130	149
Day	66	67	68	69	70	71	72	73	74	75	76	77	78
Q (cfs)	115	170	254	1990	735	262	208	160	144	337	491	334	238
Day	79	80	81	82	83	84	85	86	87	88	89	90	91
Q (cfs)	192	153	123	105	140	104	136	525	507	200	110	176	203
Day	92	93	94	95	96	97	98	99	100	101	102	103	104
Q (cfs)	130	239	197	140	107	122	107	118	131	105	263	716	124
Day	105	106	107	108	109	110	111	112	113	114	115	116	117
Q (cfs)	119	294	234	122	422	547	250	150	105	318	124	131	157
Day	118	119	120	121	122	123	124	125	126	127	128	129	130
Q (cfs)	397	137	147	182	329	133	136	127	118	332	126	472	127
Day	131	132	133	134	135	136	137	138	139	140	141	142	143
Q (cfs)	134	113	140	126	119	238	153	199	150	101	221	352	192
Day	144	145	146	147	148	149	150	151	152	153	154	155	156

Table 2-2 (continued).

Q (cfs)	120	133	110	124	168	243	434	207	245	114	205	310	242
Day	157	158	159	160	161	162	163	164	165	166	167	168	169
Q (cfs)	541	328	202	170	190	158	127	115	104	125	322	409	144
Day	170	171	172	173	174	175	176	177	178	179	180	181	182
Q (cfs)	137	276	210	158	192	197	507	1290	320	142	120	140	120
Day	183	184	185	186	187	188	189	190	191	192	193	194	195
Q (cfs)	308	302	269	2070	1460	642	268	162	120	160	190	1020	3360
Day	196	197	198	199	200	201	202	203	204	205	206	207	208
Q (cfs)	2900	2220	1340	886	620	445	330	248	238	217	197	182	189
Day	209	210	211	212	213	214	215	216	217	218	219	220	221
Q (cfs)	166	155	148	138	136	134	134	132	123	104	118	105	104
Day	222	223	224	225	226	227	228	229	230	231	232	233	234
Q (cfs)	247	199	248	129	102	197	117	747	791	257	162	232	110
Day	235	236	237	238	239	240	241	242	243	244	245	246	247
Q (cfs)	122	411	725	408	829	740	317	226	170	138	114	126	116
Day	248	249	250	251	252	253	254	255	256	257	258	259	260
Q (cfs)	118	107	130	144	167	122	104	120	1320	291	226	331	760
Day	261	262	263	264	265	266	267	268	269	270	271	272	273
Q (cfs)	1170	741	615	645	746	474	370	280	213	170	139	120	256
Day	274	275	276	277	278	279	280	281	282	283	284	285	286
Q (cfs)	474	501	478	317	271	420	363	277	235	210	177	153	135
Day	287	288	289	290	291	292	293	294	295	296	297	298	299
Q (cfs)	118	110	104	105	176	112	115	222	124	264	145	243	269
Day	300	301	302	303	304	305	306	307	308	309	310	311	312
Q (cfs)	235	153	124	107	103	106	114	105	128	250	124	117	209
Day	313	314	315	316	317	318	319	320	321	322	323	324	325
Q (cfs)	124	152	120	109	775	364	131	168	284	260	737	783	621
Day	326	327	328	329	330	331	332	333	334	335	336	337	338
Q (cfs)	331	213	163	134	120	115	105	310	199	138	112	127	464
Day	339	340	341	342	343	344	345	346	347	348	349	350	351
Q (cfs)	728	301	215	231	224	185	169	168	150	135	125	117	110
Day	352	353	354	355	356	357	358	359	360	361	362	363	364
Q (cfs)	103	110	117	129	284	277	116	181	108	719	552	187	124
Day	365	366	367	368	369	370	371	372	373	374	375	376	377
Q (cfs)	449	264	168	132	112	103	109	102	208	222	144	135	634
Day	378	379	380	381	382	383	384	385	386	387	388	389	390
Q (cfs)	239	122	136	355	158	441	457	177	111	220	121	141	552
Day	391	392	393	394	395	396	397	398	399	400	401	402	403
Q (cfs)	110	250	195	492	1650	2000	1600	460	300	200	160	135	115
Day	404	405	406	407	408	409	410	411	412	413	414	415	416
Q (cfs)	200	150	105	182	160	500	275	400	200	150	128	120	112
Day	417	418	419	420	421	422	423	424					
Q (cfs)	105	151	152	281	140	222	117	170					

2.3. 100-Year Hydrograph

The 100-year storm hydrograph was developed by WEST following the San Bernardino County Hydrology Manual (Manual, 1986) procedures for the Unit Hydrograph Method. Because the 100-year peak flow of 10,470 cfs (at Boulder Avenue) was already estimated, WEST calibrated the Unit Hydrograph parameters to match the above peak flow.

The contributing subbasin area for Gage No. 11055800 was estimated at 20.7 square miles. Point precipitation values were obtained from an online version of NOAA Atlas 14 (<http://hdsc.nws.noaa.gov>) as presented in Table 2-3. WEST utilized the 25-year precipitation which SBCFCD has found to match the FEMA's 50-percent confidence level for calculating the 100-year peak flow.

Table 2-3. 25-year Precipitation Values.

25-year Precipitation (inches)					
5-minutes	15-minutes	1 hour	2 hours	3 hours	6 hours
0.48	0.91	1.52	2.15	2.70	4.12

The lag was estimated at 1.2 hours based on the stream length, centroidal stream length, and drainage slope using the empirical formula presented in the Manual and it was adjusted to 1.1125 hours to match the 100-year peak flow value of 10,470 cfs. The maximum loss rate was calculated as 0.33 in/hr based on studies from nearby basins (e.g., WEST 2009 – Daley Basin). Initial abstractions were omitted for conservative purposes. The S-graph for Mountain Conditions was used based on the Manual guidelines. A hydrologic model for the City Creek basin was created using HEC-HMS Version 3.3. The resulting 100-year hydrograph utilized in this study is shown in Figure 2-2.

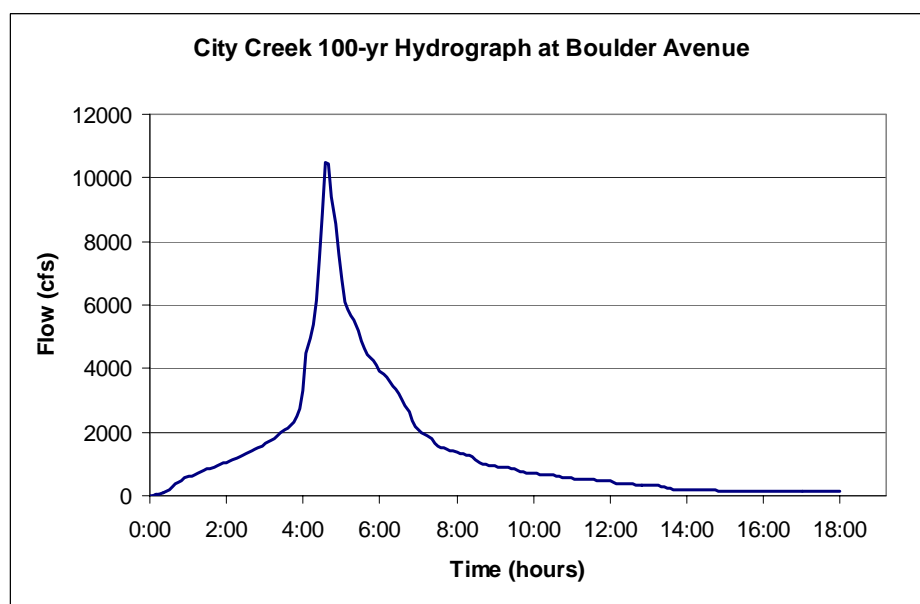


Figure 2-2. Calculated 100-year Storm Hydrograph for City Creek.

3. Hydraulic Analysis

3.1. Model Development

WEST combined the topographic data from Tetra Tech (2008), and the District (2006 and 2008) to generate a Triangular Irregular Network (TIN). The Vertical Datum for the Tetra Tech data is NAVD 88. The 2006 District data are referenced to the NGVD 29 vertical datum and had to be increased by 2.68 ft (obtained using Vertcon, NGS 2003) to account for the difference between the two vertical datums [Vertcon shows a difference between the datums of 0.822 m (2.7 ft) at Boulder Avenue and of 0.812 m (2.66 ft) at 5th Avenue; on average, the difference is 2.68 ft].

WEST utilized the ArcGIS program (Version 9.1) to extract the cross section profiles from the TIN in order to develop the hydraulic model of City Creek. Cross sections were then imported into the HEC-RAS (River Analysis System) computer program, Version 4.0 (USACE, 2008). All the elevations in the model and the computed water surface elevations are referenced to the NAVD 88 vertical datum. The upstream model end is located some 4,000 ft upstream from Highland Avenue, while the downstream end is located 1,200 ft downstream of 5th Avenue.

Cross sections were spaced approximately every 200 ft based on the locations of bends, bridges, and contraction/expansion areas along the reach. Shorter cross section spacing was generally avoided to ensure sediment transport model stability. Cross sections were cut at the upstream and downstream face of bridges in order to follow the bridge modeling approach of HEC-RAS.

A plan view of the HEC-RAS model with cross section locations is shown in Figure 3-1. The cross sections plots are provided in Appendix A.

3.2. Model Parameters

A subcritical flow regime was assumed in the hydraulic analysis. The downstream boundary condition was based on normal depth for a friction slope of 0.006 (i.e., average channel slope in the study reach near the downstream boundary).

Manning's n values representing the roughness of the main channel and the overbanks for the Channel were determined based upon field observations, aerial photographs, and reference to pertinent publications such as Cowan (1956) and Chow (1959). The Manning's n value of 0.03 (0.04 upstream of Highland Avenue) was used for the sand-bed channel without vegetation. The overbank Manning's n value was estimated to be 0.04 (0.05 upstream of Highland Avenue). These relatively low roughness coefficients are on the conservative side (maximizing scour) because they do not include increased resistance by larger bed material (cobbles and boulders) observed in the field.

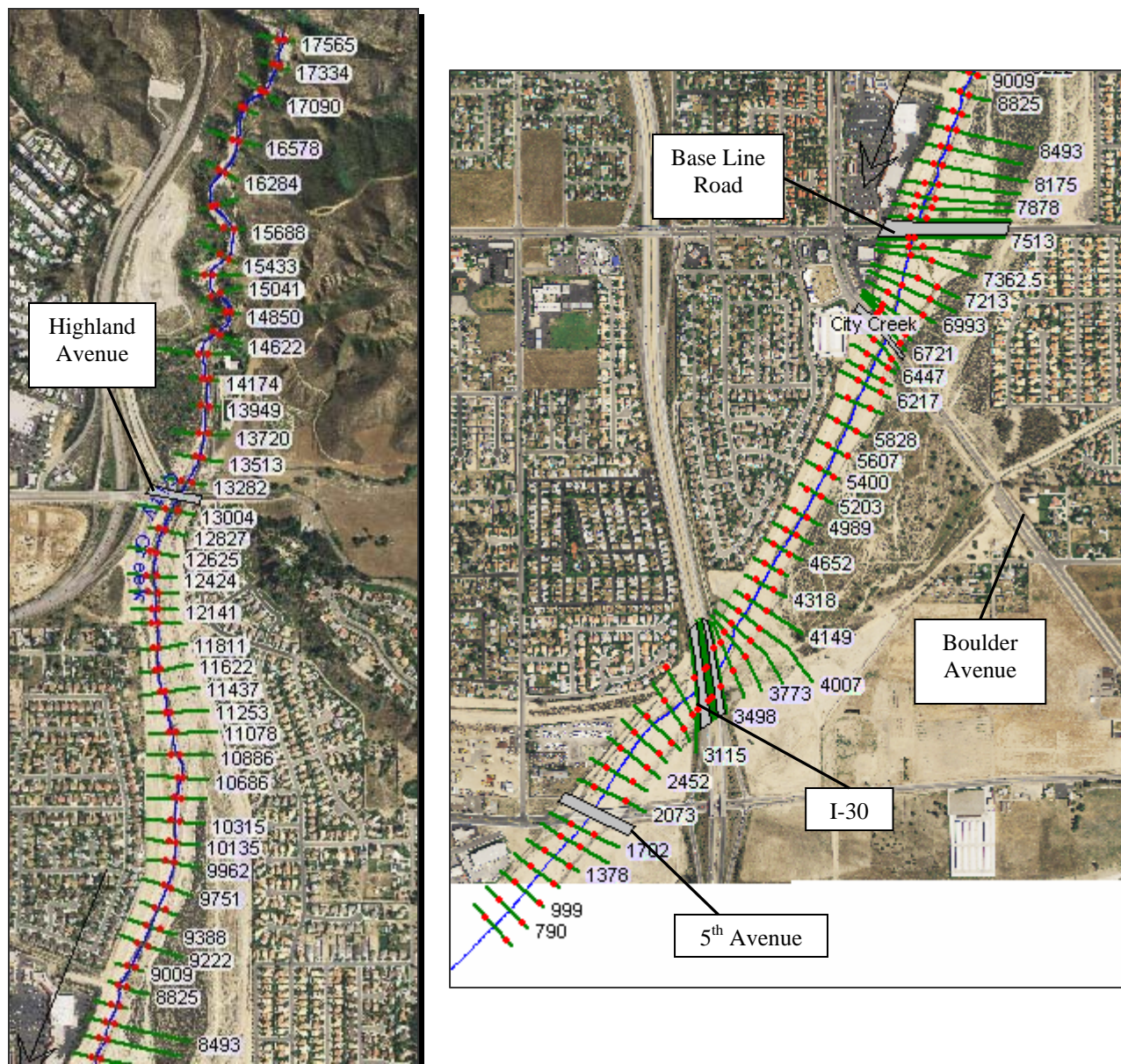


Figure 3-1. City Creek HEC-RAS Cross Sections.

3.3. Bridges and Culverts

There are four bridges in the study reach - Highland Avenue, Boulder Avenue, I-30, and 5th Street - and one set of culverts at Base Line Road. The Base Line Road culverts are low flow culverts. Bridge and culvert details such as low chord elevations, deck thickness, piers, and culvert dimensions were obtained from as-built construction drawings. Because all the bridges in the study area span the entire width of the Channel without causing constriction to the flow, ineffective flow limits were not needed at these locations. At the 100-year peak discharge, none of the bridges were overtopped. Only Base Line Road is overtopped, being a low crossing with insufficient capacity to convey the flow.

4. Sediment Transport Analysis

4.1. General

The objective of the sediment transport analysis is to identify baseline sediment transport characteristics of the Channel near the pipeline and to simulate its long-term bed elevation changes (degradation/aggradation). The local scour components (e.g., low-flow channel incision, flow concentration at severe stream bends and/or structures, antidune scour, etc.) were added to the long-term channel degradation to obtain the total scour depth at the pipeline crossing.

A baseline (existing) conditions sediment transport model was created using the geometry from the hydraulic model described in the previous section. The sediment transport module of HEC-RAS (Version 4.0) was used to conduct the numerical sediment transport modeling in this study. The sediment module requires a geometry file, a quasi-unsteady flow file, and a sediment file. The model first calculates the hydraulics of each discharge increment in a hydrograph to determine hydraulic parameters such as flow depth, water velocity, and effective flow width for each cross section. Then the sediment transport potential is computed at each cross section using the hydraulics of the main channel. Sediment contribution at the upstream end of the reach being modeled is simulated by the use of a sediment vs. discharge relation (rating curve), or equilibrium load, and is specified by the user. This load is compared to the sediment transport potential of the cross section. If the inflowing load is larger than the transport potential, the difference is deposited in the cross section. If the inflowing load is less than the transport potential, sediment is picked up (scoured) from the bed, taking into account the availability of material in the bed. The sediment load leaving the cross section then becomes the inflowing load to the next downstream cross section. This continues until the most downstream cross section is simulated. For the next discharge in the hydrograph, the hydraulics are again computed using the new bed geometry formed by the previous discharge. The cycle is repeated until the entire hydrograph is simulated.

The creation of the sediment transport model required the development/adjustment of the hydraulic model, hydraulic analysis for the water discharges being simulated, input of representative streambed material size distributions, selection of movable bed limits, creation of an inflowing sediment rating curve, and development of a design hydrograph (including the design single event and the representative long-term hydrograph). It is important to note that model limits should always be larger than the project limits both upstream and downstream (to minimize the influence of uncertain boundary conditions – starting water surface elevation at the downstream end and inflowing sediment load at the upstream end). Therefore, WEST located the downstream model boundary downstream of 5th Street. The upstream model boundary was located about 4,000 ft upstream of Highland Avenue, such that the entire study reach extends about 3 miles.

4.2. Sediment Parameters

Guidance from the U.S. Army Corps of Engineers computer program SAM (2002) and other references was used to select the most appropriate sediment transport relationship. Several transport functions were considered for the given range of hydraulic and sediment characteristics of the study reach: Yang, Toffaleti, Meyer-Peter and Muller, Ackers-White, Engelund-Hansen, and Laursen (Copeland). The following characteristics of the reach were identified: the median particle size D_{50} is between 1 mm and 40 mm (most samples have D_{50} less than 5 mm); the average bed slope is 0.025 ft/ft; the average flow velocity is between 5 and 15 ft/s; the average flow depth is between 1 and 10 ft; and the average channel width is between 30 and 100 ft.

Yang's method is highly applicable to sands up to 2 mm in size (Williams, 1995). It can also be used for gravel transport (extended formulation, included in HEC-RAS) up to 7 mm in size. The Ackers-White formulation was based on flume data and was found inapplicable to relatively larger flow depths (Williams, 1995). The Engelund-Hansen formulation is developed for finer sand (up to 1 mm). The Toffaleti function was developed for large rivers and generally applies to sand transport up to 2 mm in size. The Laursen (Copeland) function was originally developed for fine sand (up to 1 mm in size) and extended by Copeland to gravel sizes (up to 29 mm). The Meyer-Peter and Muller (MPM) function is recommended for gravel transport (up to 30 mm in size). Because the median grain size found in City Creek varies between 1 mm and 40 mm (predominantly below 5 mm), there is no single transport function that is the "best" for the entire range of sediment particles. Therefore, WEST investigated three sediment transport functions [Yang, Laursen (Copeland), and MPM] that are most appropriate for sand and gravel transport.

The vertical thickness of the sediment control volume is the "maximum depth" of sediment in the input data. This depth was set at 30-50 ft (to allow the development of maximum scour) for all cross sections except for Sta. 13282 and Sta. 13004 (upstream and downstream of Highland Avenue), where a concrete channel lining acts as a fixed-bed control (hard point).

Sediment dynamics tend to be more significant within the active channel, where the bed can either degrade or aggrade in response to erosion or deposition. The overbank areas tend to be more stable and normally are free of erosion, but can experience deposition. Therefore, movable bed (erosion) limits were roughly defined at the limits of the active channel which is formed by a dominant (channel-forming discharge). The dominant discharge for streams in arid regions corresponds to a less frequent event, on the order of the 5- to 10-year flood peak (RCE, 1994). In this study, the movable bed (erosion) limits generally correspond to a flow of 2,000 cfs based on the flood frequency analysis (Tetra Tech, 2008). At some locations which experience significant sediment deposition, these limits had to be widened to promote numerical stability. Deposition (but not erosion) was allowed outside of the movable bed limits using the Bed Change Option in the sediment data module of HEC-RAS.

4.3. Bed Sediment Characteristics

NMG Geotechnical Inc. provided gradation curves for nine sediment samples (S-1 through S-11, excluding S-3 and S-4) covering the study reach from Boulder Avenue to the upstream model limit. These samples were taken from the channel bed on July 17, 2008 by WEST (see Figure

4-1 for the location of the sediment samples). The material encountered was predominantly poorly graded sand with some gravel (see Figure 4-2 and Figure 4-3).

The particle size distributions were entered into the sediment data editor of HEC-RAS. Sediment sample S-2 was used as representative for the entire portion of the Channel upstream of Highland Avenue, while sediment sample S-11 was used for the portion of the Channel downstream of Boulder Avenue. The cross sections in the HEC-RAS model closest to the sample sediment locations were assigned the corresponding gradation curve, while a gradual transition was assumed for all the cross sections in between (for these cross sections, the “interpolated” option was selected in the HEC-RAS sediment editor).



Figure 4-1. Sediment Sample Locations.

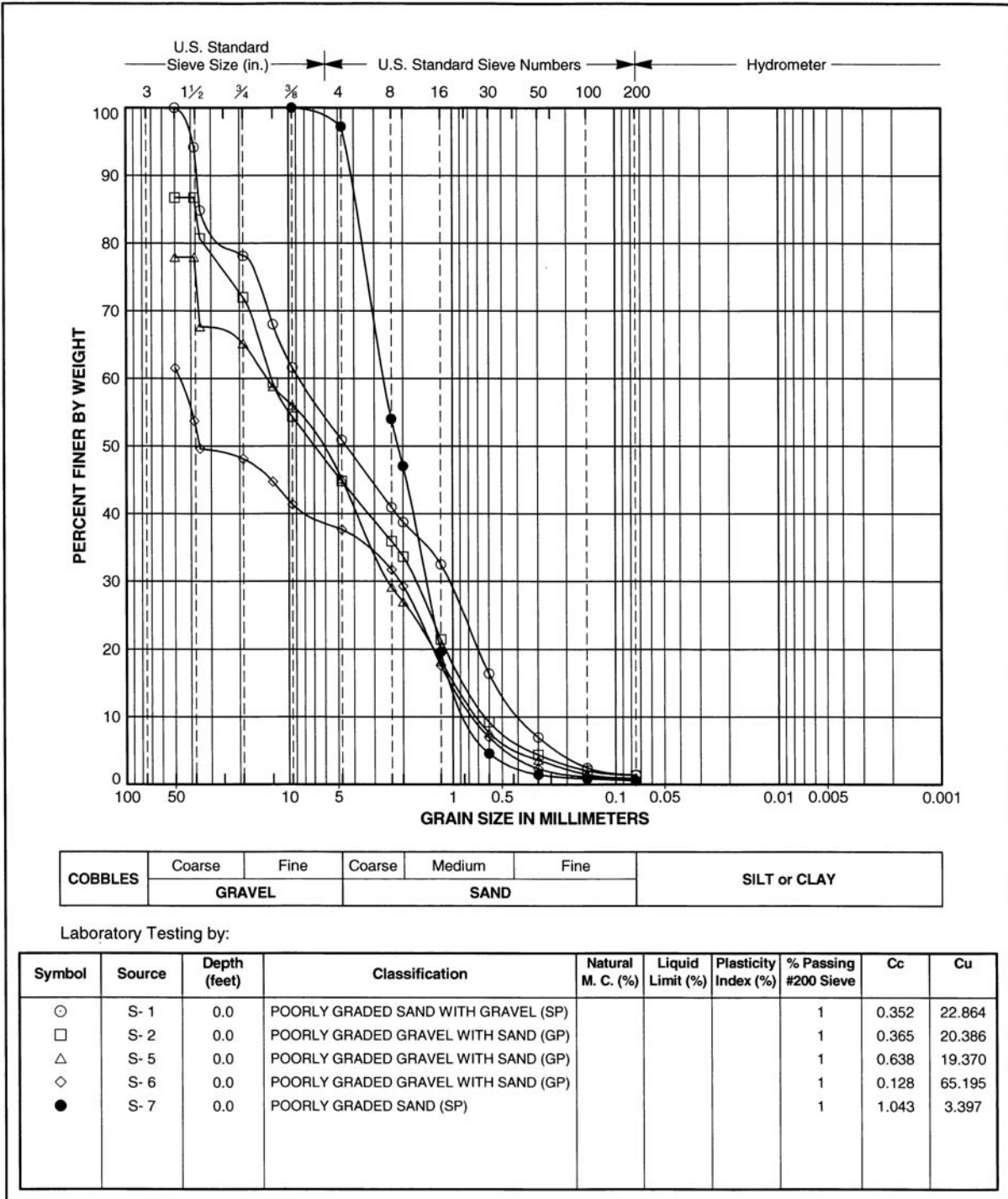


Figure 4-2. Sediment Gradation Data (1).

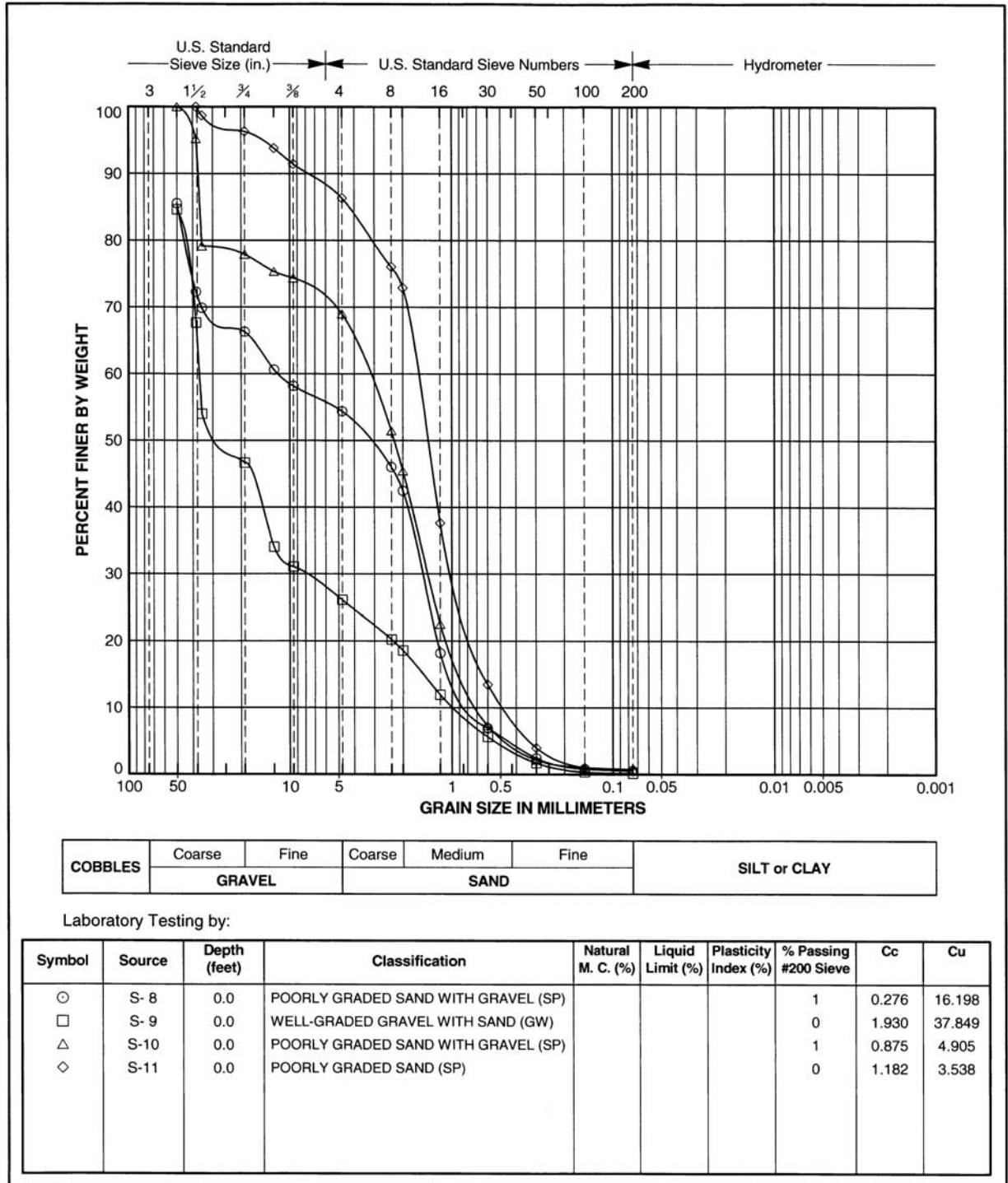


Figure 4-3. Sediment Gradation Data (2).

4.4. Sediment Boundary Conditions

Due to the lack of information on inflowing sediment load into the study reach, an equilibrium sediment load was determined. The load was developed for a range of discharges from 100 to 10,000 cfs by executing the HEC-6T sediment transport model (an advanced version of HEC-6) with the recirculation option applied to a supply reach upstream of Highland Avenue. Sediment sample S-2 was assumed representative of the supply reach. The recirculation option instructs the program to use the current sediment discharge at the downstream end of the supply reach (Sta. 17090) as the sediment inflow at the upstream end (Sta. 17565) for the subsequent time step; when quasi-equilibrium is attained, the sediment load entering the reach is about equal to the load leaving the reach, with no further changes in bed elevations along the supply reach. Simulations were run for three years (using the Yang transport method) with a time step of 2 hours. The resulting inflowing sediment load is shown in Table 4-1 and plotted in Figure 4-4. Table 4-1 also shows the fraction of inflowing load per sediment size class. This information was entered as the upstream sediment rating curve into the HEC-RAS sediment data editor.

Table 4-1. Equilibrium Sediment Inflow Load.

Classification	Q (cfs)	100	500	2,000	5,000	10,000
	Qsed (tons/day)	6,500	50,000	220,000	610,000	1,000,000
	Grain Size (mm)	<i>Fraction of inflowing load</i>				
VFS	0.088	0.289	0.201	0.359	0.159	0.166
FS	0.177	0.268	0.323	0.474	0.399	0.376
MS	0.354	0.157	0.148	0.063	0.182	0.229
CS	0.707	0.138	0.175	0.052	0.134	0.117
VCS	1.414	0.116	0.120	0.047	0.111	0.097
VFG	2.828	0.003	0.001	0.000	0.000	0.000
FG	5.657	0.005	0.002	0.000	0.000	0.000
MG	11.314	0.011	0.005	0.000	0.002	0.002
CG	22.627	0.007	0.006	0.000	0.002	0.003
VCG	45.255	0.000	0.012	0.001	0.007	0.007

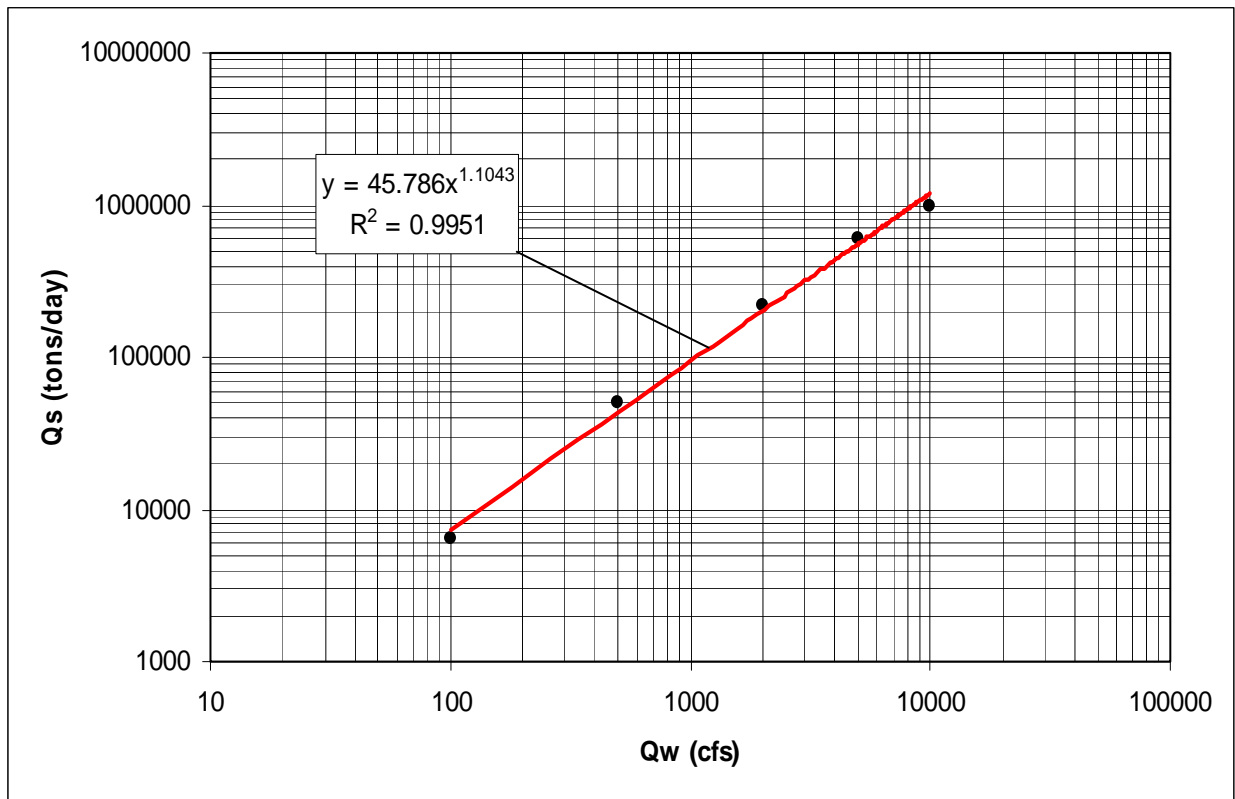


Figure 4-4. Sediment Inflow Load Rating Curve.

4.5. Quasi-Unsteady Flow Data

Sediment transport calculations in HEC-RAS (Version 4.0) are based on quasi-unsteady hydraulics. This approach approximates a flow hydrograph by a series of steady flow profiles associated with corresponding flow durations (HEC, 2008). Each flow series is specified by a flow value, corresponding flow duration, and computational increment.

A stage-discharge rating curve was developed for starting water surface elevations at the downstream boundary (Sta. 600) using a normal depth assumption (for a channel invert slope of 0.006 in the vicinity of the boundary). The hydraulic model described in Section 3 was used to determine the rating curve.

The historical inflow hydrograph described in Section 2 was used as input at the upstream boundary in the quasi-unsteady editor. The computational time increment was specified at 2 hours for the historical hydrograph, while it was set at 5 min for the 100-year single event (high flows require a finer time step for computational stability). These time steps were found to produce stable numerical results while still providing computationally efficient model runs.

4.6. Results

The sediment transport analysis results are presented using the time series plots of the channel invert (thalweg) change for the two hydrologic scenarios: 100-year single event and long-term (historical) flows. In order to maximize scour, no sediment inflow load (clear-water condition) was assumed at the upstream model boundary (Sta. 17565) for the 100-year flood event. For the long-term simulation with historical flows, the calculated equilibrium load (Section 4.4) was causing computational instabilities due to unrealistic deposition at Highland Avenue Bridge and particularly upstream of the Base Line Road low-flow culverts (equilibrium load was developed for the canyon reach upstream of Highland Avenue where the channel is relatively deep on a steep slope, capable of carrying sediment concentrations in excess of 40,000 mg/l). Therefore, the inflowing sediment load was reduced to only about 20 percent of the calculated equilibrium load and used for the long-term simulations, which enabled computational stability and at the same time provided a conservatively high estimate of scour. The long-term simulations also were performed with no sediment inflow load to assess the hypothetical scour maximum at the pipeline crossing for this highly improbable scenario (i.e., 424 days of flow without any inflowing sediment load).

Three sediment transport functions were utilized: Yang, Laursen (Copeland), and Meyer-Peter and Muller (MPM). All three methods predict a relatively large amount of ultimate long-term degradation (between 20 and 28 ft) with no sediment load (Figure 4-5). The Laursen function gives the most conservative result (largest amount of scour).

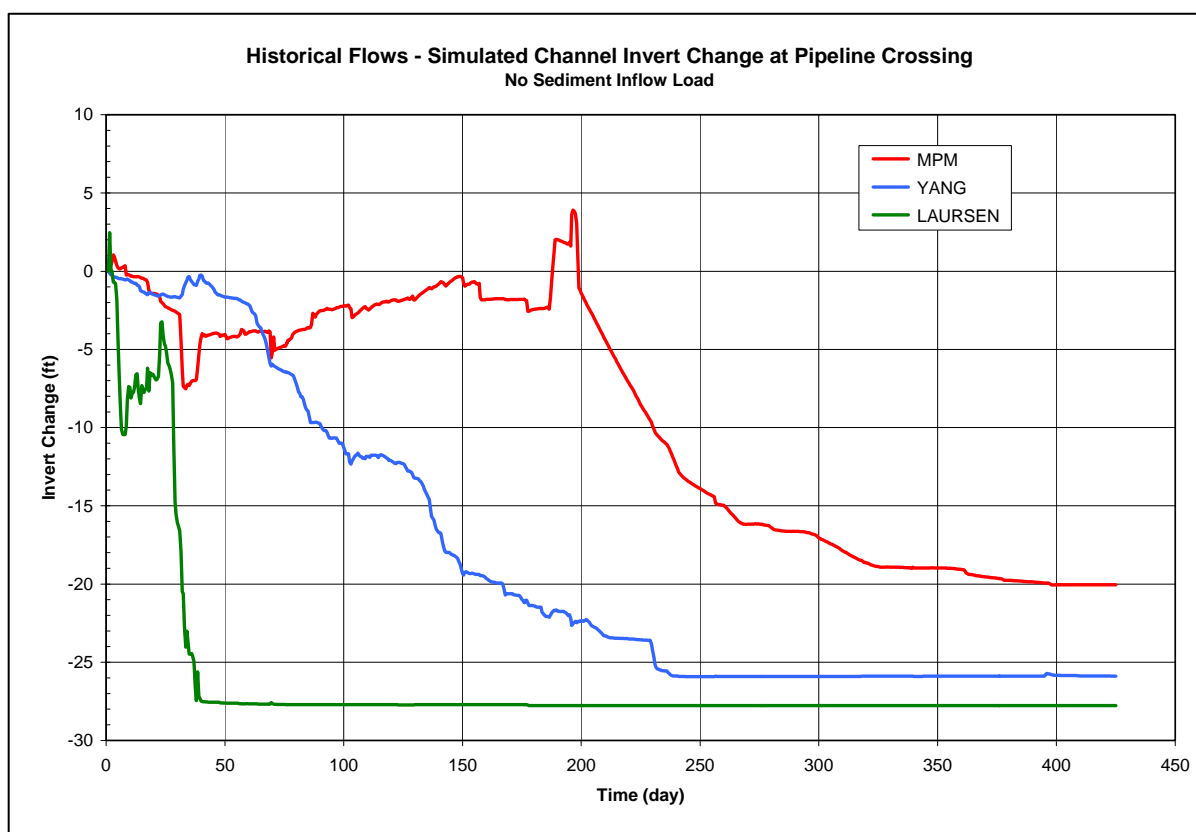


Figure 4-5. Long-Term Invert Change at Pipeline Crossing - No Sediment Load.

For a more realistic scenario with 20 percent of equilibrium sediment load (Figure 4-6), the Laursen method failed to produce a computationally stable solution. The MPM method experienced unrealistic deposition at the upstream boundary and predicted more scour with the sediment inflow load than for clear-water conditions (this result is questionable). It appears that the Yang transport function provides the physically most realistic result for this scenario.

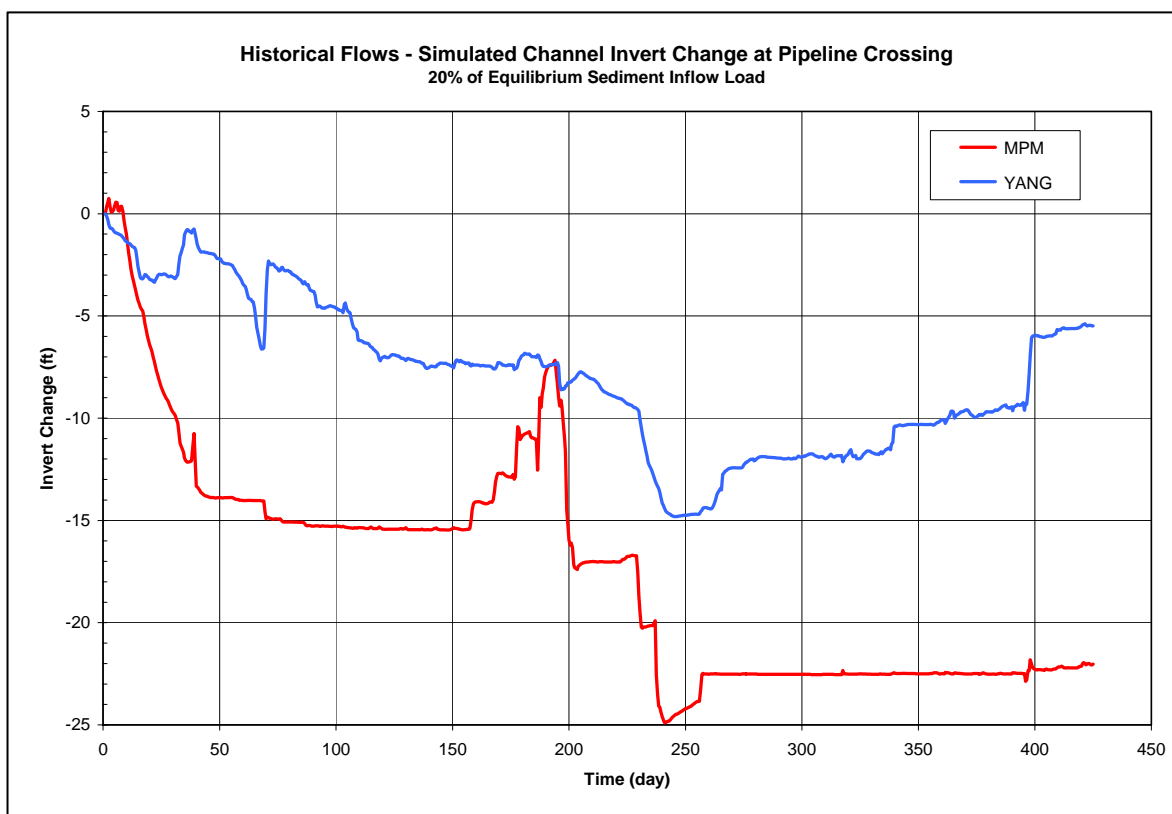


Figure 4-6. Long-Term Invert Change at Pipeline Crossing – 20% of Equilibrium Sediment Load (Laursen Method Failed to Provide Stable Solution).

For the 100-year single flood event (Figure 4-7), the Yang transport function surprisingly does not predict any significant scour. The MPM formulation shows degradation of 1.5 ft at the end of the flood. The Laursen method gives the most conservative prediction of 7.5 feet of scour.

It should be noted that several levels of conservatism are reflected in the above scour results: 1) All the simulations were carried out neglecting the presence of large boulders that the District placed on the downstream side of the pipeline to help prevent further erosion. This was done in case the boulders are washed away as it was the case in the past; 2) The erosion limits were fixed in place (approximately at the bank stations corresponding to the channel-forming discharge) during simulations, which also maximizes scour. In reality, large channel degradation predicted by the model would cause exceedence of the maximum stable bank height, which would lead to mass failure and lateral bankline retreat; 3) Sediment samples taken in the field are generally skewed toward sand particle sizes, neglecting the observed larger material that would likely provide additional armoring of the channel bed; 4) Roughness coefficients for sand-bed used in the model are relatively low and do not account for increased resistance by larger bed material.

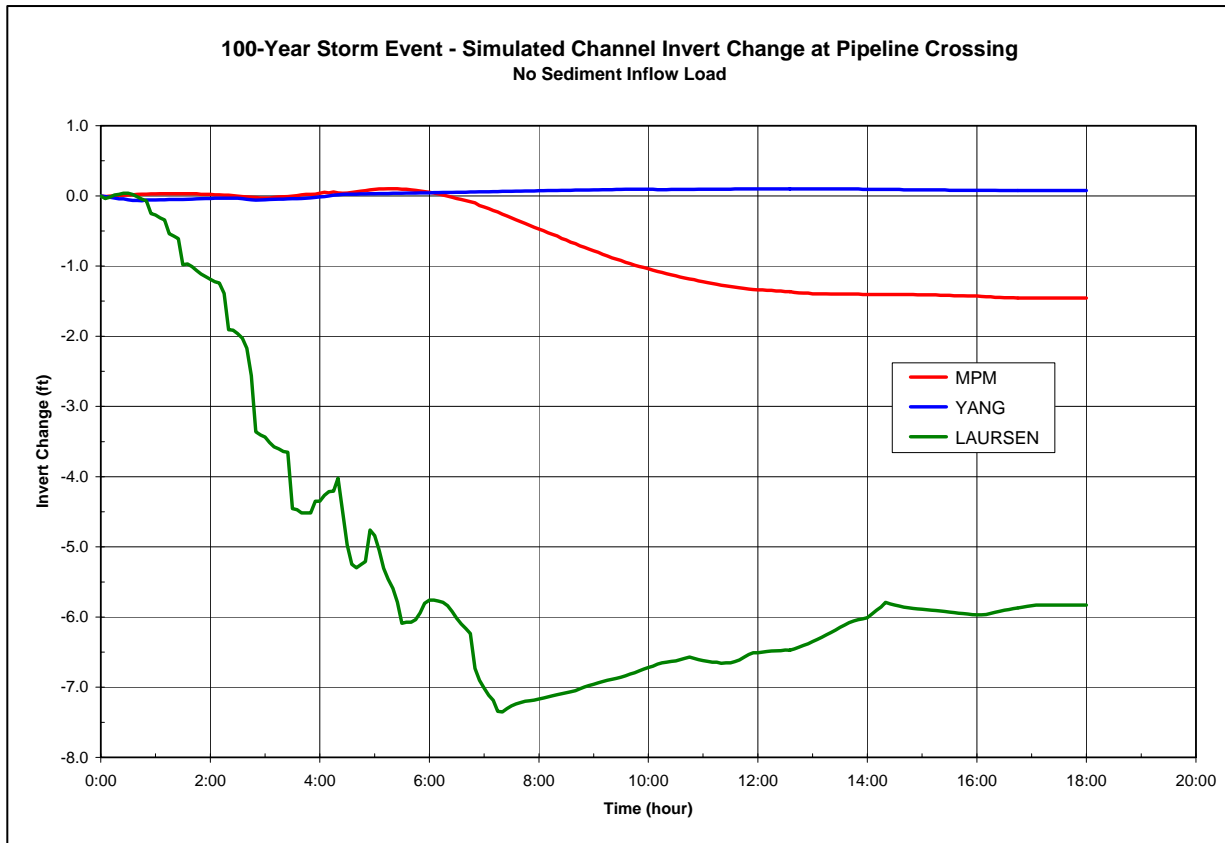


Figure 4-7. 100-Year Flood Invert Change at Pipeline Crossing - No Sediment Load.

4.7. Local Scour

Two local scour components also were considered in addition to the long-term channel degradation and 100-year scour: 1) antidune scour that occurs in steep, sand-bed channels during high flows (passage of antidunes past a point in the channel can increase the magnitude of scour); 2) potential channel incision during low-flows.

The antidune scour is generally determined as one-half the antidune height which can be estimated as follows (RCE, 1994):

$$h_a = 0.28 \pi y F_R^2 < y$$

Where:

h_a = antidune height

y = hydraulic depth of flow

F_R = Froude number = 1.0 (assuming subcritical flow)

The antidune scour was estimated for the 100-year flood peak (10,500 cfs) and the maximum flow in the historical flow record (3,400 cfs). The antidune scour corresponding to these two discharges is given in Table 4-2. The low-flow channel incision is estimated at 2.0 ft.

Table 4-2. Estimated Antidune Scour.

Discharge (cfs)	Depth y (ft)	Antidune Height h_a (ft)	Scour (ft)
3,400	5	4.4	2.5
10,500	10	8.8	4.5

4.8. Total Scour

Total scour is found as a combination of the long-term degradation or the single storm event scour and local scour components. The results are summarized in Table 4-3 (rounded up to the nearest foot). The sediment transport model scour (Degradation) is based on the Yang function for the long-term scenario, and on the Laursen (Copeland) function for the 100-year flood. The amount of scour in scenario 1 is the anticipated ultimate scour at the pipeline crossing using historical flow conditions if no scour mitigation alternative is in place. The predicted scour in scenario 2 is the maximum scour that may be expected during the 100-year flood event in any given year (having a 1 percent chance of being equaled or exceeded) if no scour protection is in place.

Table 4-3. Total Predicted Scour at Pipeline Crossing.

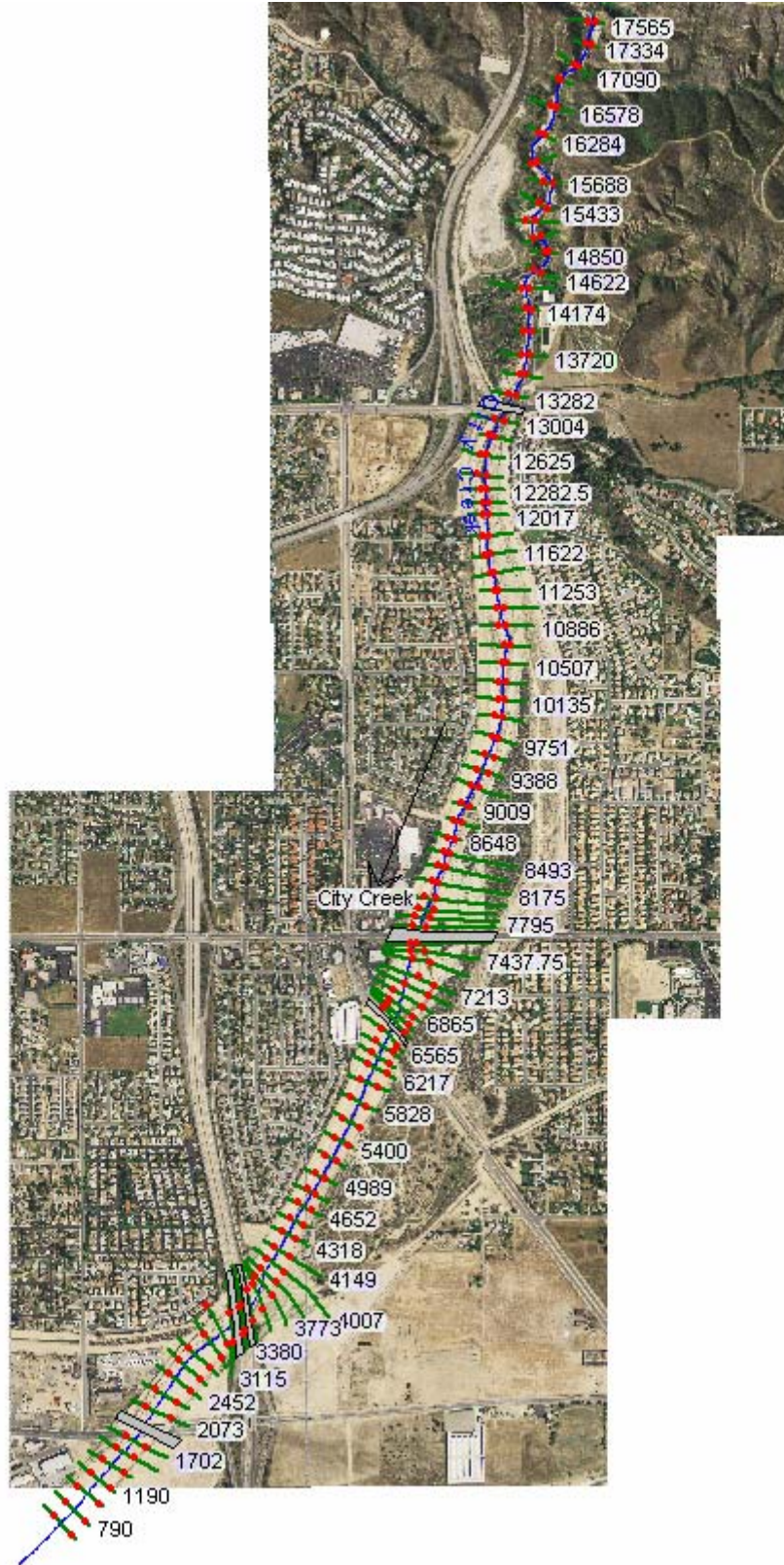
Scenario/Scour	Degradation (ft)	Antidune (ft)	Low-Flow Incision (ft)	Total (ft)
1) Long-Term	15.0	2.5	2.0	20.0
2) 100-Year Flood	7.5	4.5	2.0	14.0

5. References

- Flood Emergency Management Agency (FEMA). *Flood Insurance Study, San Bernardino County, California, and Incorporated Areas*, August 28, 2008.
- Hydrologic Engineering Center (HEC). *HEC-GeoRAS – GIS Tools for support of HEC-RAS using ArcGIS– User’s Manual*. Version 4, U.S. Army Corps of Engineers, Hydrologic Engineering Center, Davis, California, September 2005.
- Hydrologic Engineering Center (HEC). *HEC-RAS River Analysis System – User’s Manual*. Version 4.0, U.S. Army Corps of Engineers, Hydrologic Engineering Center, Davis, California, March 2008.
- National Geodetic Survey (NGS). *VERTCON - North American Vertical Datum Conversion Utility*, <http://www.ngs.noaa.gov/TOOLS/Vertcon/vertcon.html>, 2003.
- Tetra Tech (2008). *City Creek Levee Hydrologic and Hydraulic Analyses*, Draft Report, February 2008.
- Cowan, W.L. Estimating Hydraulic Roughness Coefficients, *Agricultural Engineering*, Vol. 37, No. 7, pp. 473-475, 1956.
- Resource Consultants & Engineers, Inc. (RCE). *Sediment and Erosion Design Guide*. Prepared for Albuquerque Metropolitan Arroyo Flood Control Authority (AMAFCA), November 1994.
- San Bernardino County. *Hydrology Manual*, August 1986.
- U.S. Army Corps of Engineers. SAM Hydraulic Design Package for Channels. Coastal and Hydraulics Laboratory, U.S. Army Engineer Research and Development Center, Vicksburg, Mississippi, 2002.
- WEST Consultants, Inc. *FEMA Map Revision for City Creek and Plunge Creek*, September 2008.
- WEST Consultants, Inc. *San Bernardino County FEMA Levee Certification*, August 2009.
- Williams, D.T. *Selection and Predictability of Sand Transport Relations Based upon a Numerical Index*, Doctoral Dissertation, Colorado State University, Fort Collins, CO, 1995.

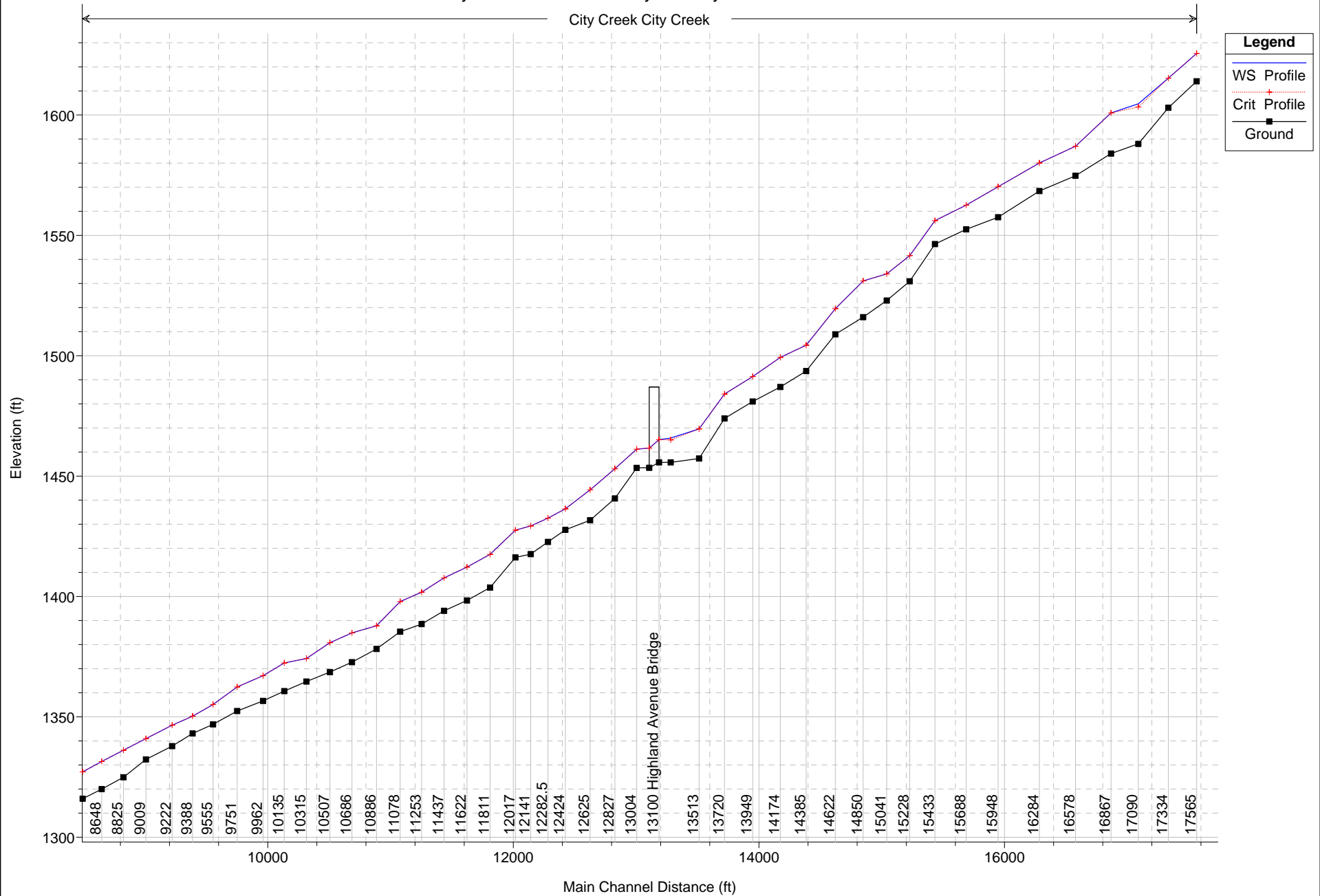
APPENDIX A

HEC-RAS Hydraulic Model Results



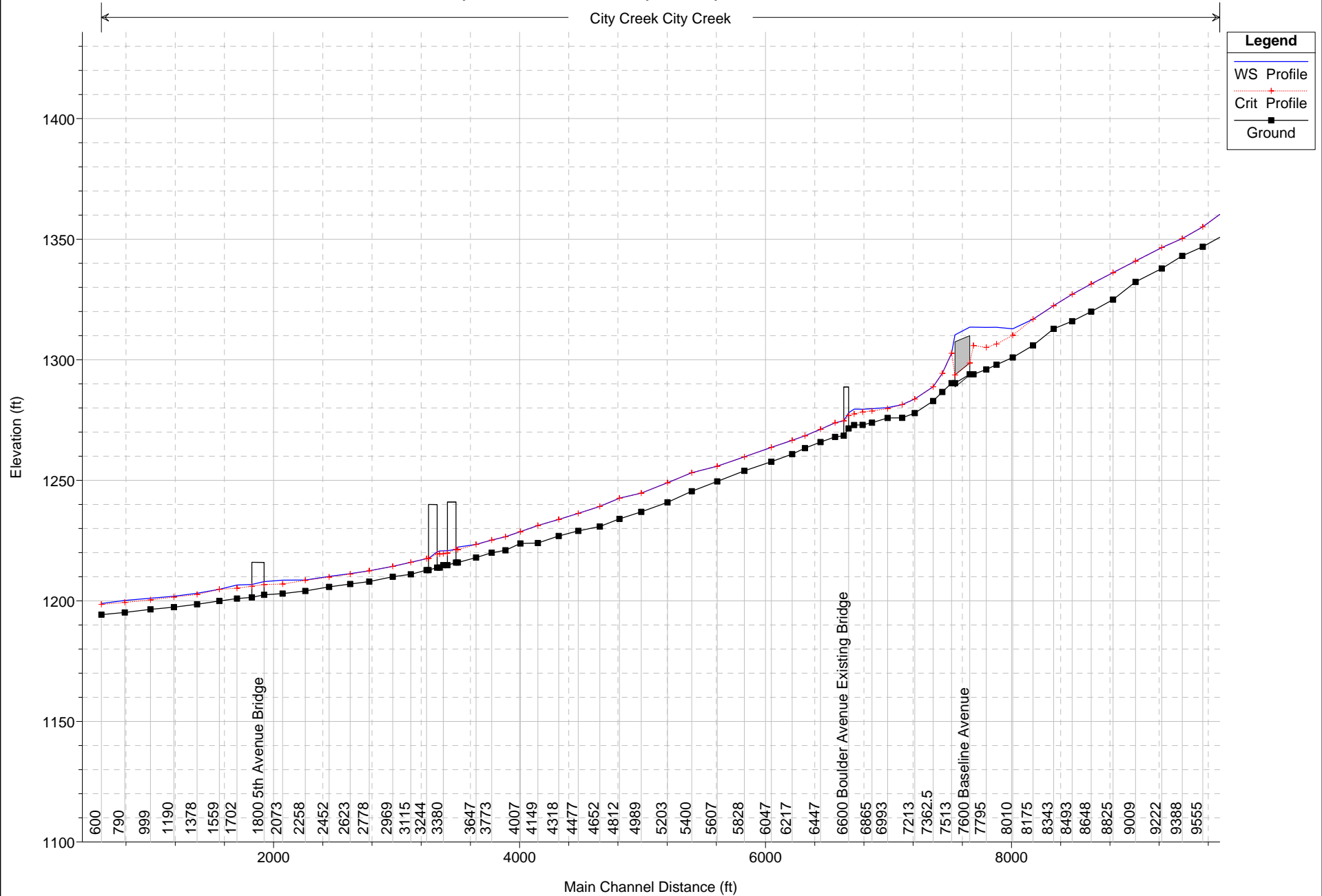
City Creek Plan: 100-yr Steady RAS 12/22/2008

City Creek City Creek



City Creek Plan: 100-yr Steady RAS 12/22/2008

City Creek City Creek

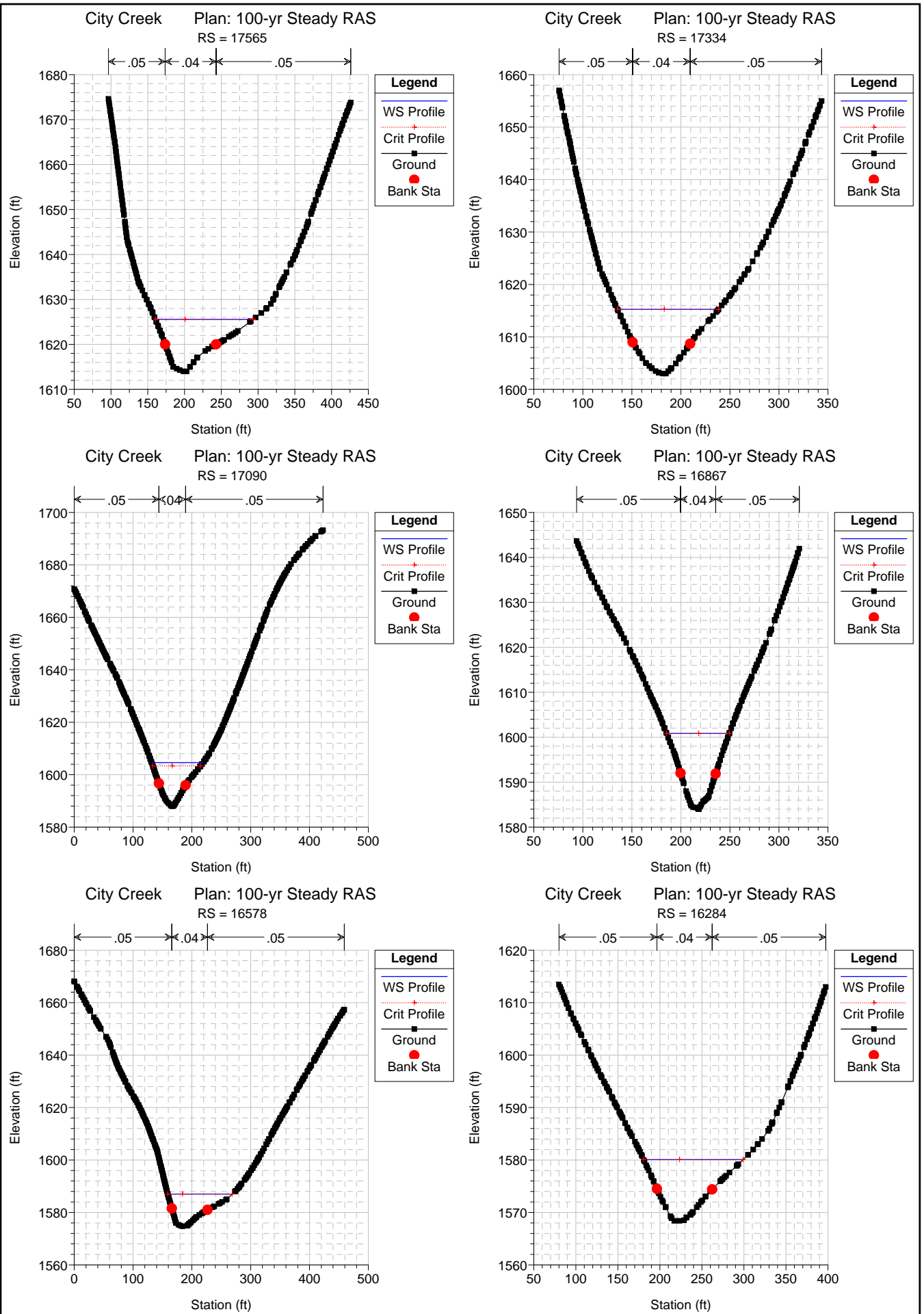


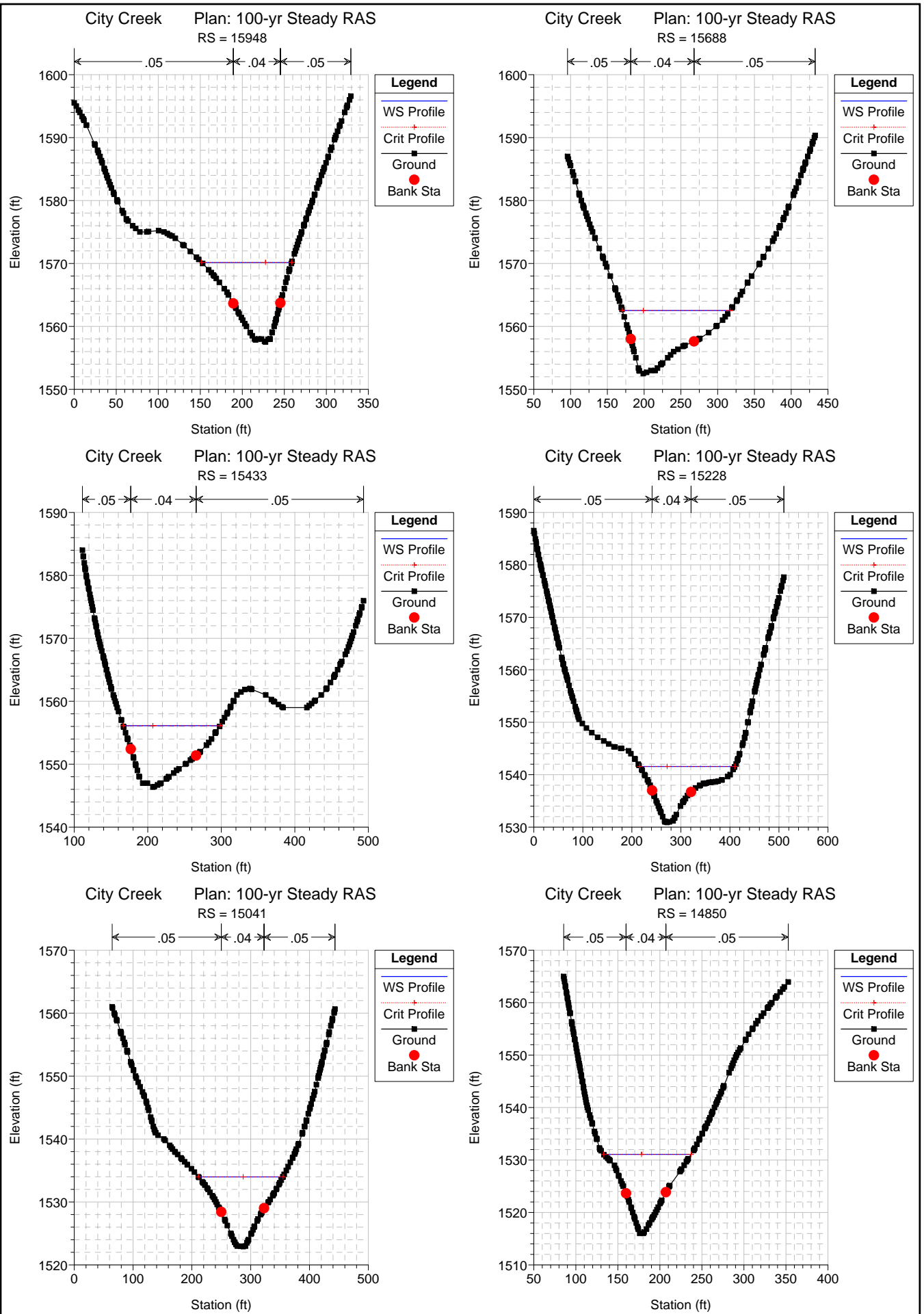
HEC-RAS Plan: 100-yr Steady River: City Creek Reach: City Creek Profile: Profile

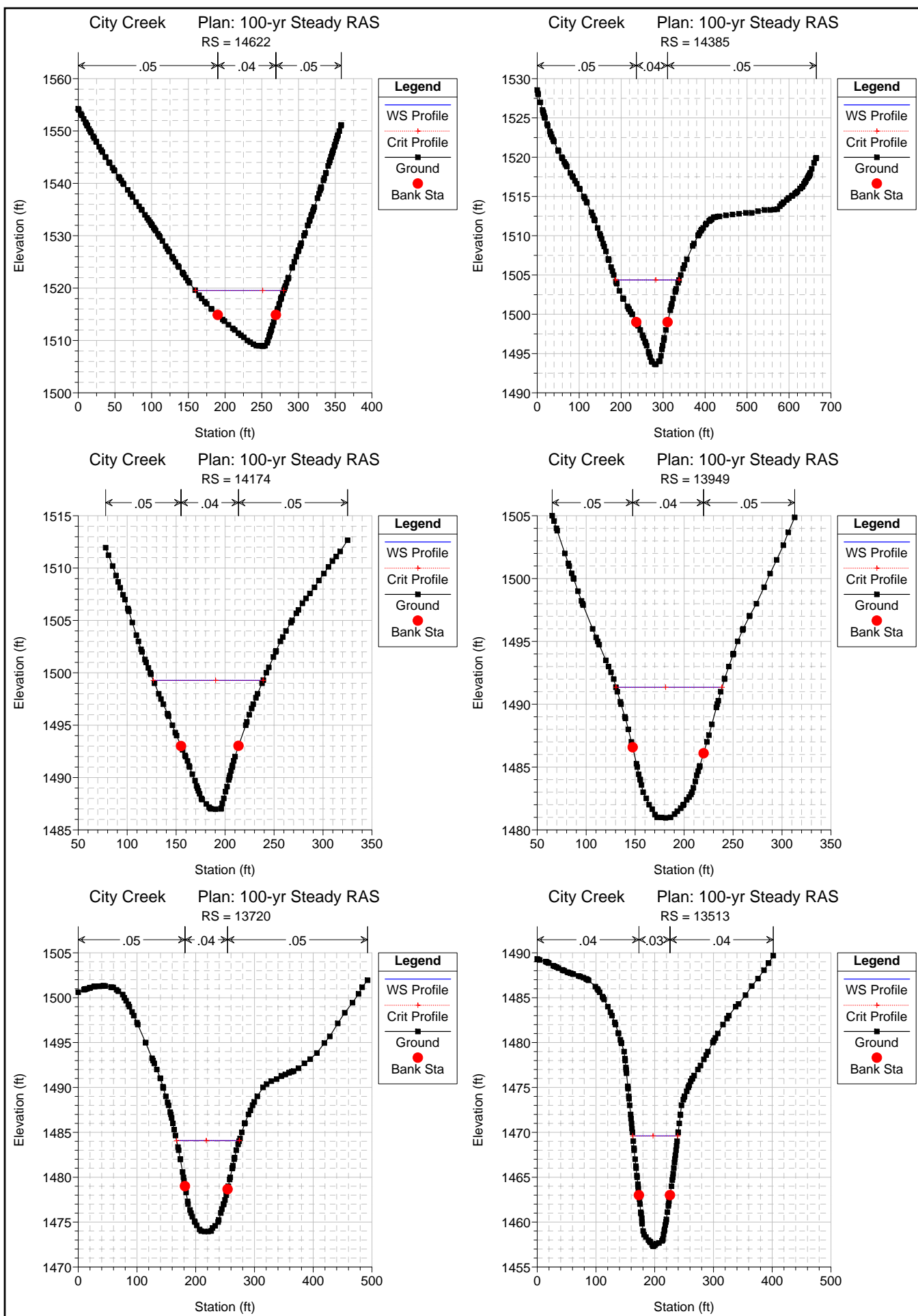
Reach	River Sta	Q Total (cfs)	Min Ch El (ft)	W.S. Elev (ft)	Crit W.S. (ft)	E.G. Elev (ft)	E.G. Slope (ft/ft)	Vel Chnl (ft/s)	Flow Area (sq ft)	Top Width (ft)	Froude # Chl
City Creek	17565	10470.00	1614.00	1625.55	1625.55	1628.87	0.009589	15.32	797.05	132.79	0.91
City Creek	17334	10470.00	1603.00	1615.27	1615.27	1619.15	0.009320	16.40	727.44	103.20	0.91
City Creek	17090	10470.00	1588.00	1604.64	1603.32	1608.14	0.006243	15.68	779.04	87.61	0.76
City Creek	16867	10470.00	1584.00	1600.83	1600.83	1606.25	0.009423	19.36	618.62	63.97	0.91
City Creek	16578	10470.00	1574.73	1586.99	1586.99	1590.70	0.009662	16.12	747.08	109.73	0.91
City Creek	16284	10470.00	1568.41	1580.07	1580.07	1583.66	0.009491	15.77	757.93	118.32	0.91
City Creek	15948	10470.00	1557.51	1570.18	1570.18	1574.09	0.009108	16.50	734.40	107.23	0.90
City Creek	15688	10470.00	1552.50	1562.55	1562.55	1565.55	0.010423	14.50	820.97	146.66	0.93
City Creek	15433	10470.00	1546.37	1556.12	1556.12	1559.32	0.010738	14.71	776.71	131.65	0.94
City Creek	15228	10470.00	1530.90	1541.55	1541.55	1544.11	0.008665	13.78	946.88	193.86	0.85
City Creek	15041	10470.00	1522.91	1533.98	1533.98	1537.20	0.009383	15.03	814.25	143.72	0.90
City Creek	14850	10470.00	1516.00	1531.07	1531.07	1535.13	0.008602	16.99	737.23	103.89	0.88
City Creek	14622	10470.00	1508.88	1519.54	1519.54	1522.97	0.010307	15.21	753.02	120.25	0.93
City Creek	14385	10470.00	1493.63	1504.37	1504.37	1507.43	0.009392	14.78	839.77	151.60	0.90
City Creek	14174	10470.00	1486.98	1499.28	1499.28	1503.03	0.009197	16.21	750.05	112.17	0.90
City Creek	13949	10470.00	1480.96	1491.35	1491.35	1495.04	0.010156	15.74	723.66	108.36	0.94
City Creek	13720	10470.00	1473.94	1484.07	1484.07	1487.82	0.010332	15.84	717.27	106.80	0.95
City Creek	13513	10470.00	1457.30	1469.60	1469.60	1474.25	0.005685	17.66	647.32	76.60	0.95
City Creek	13282	10470.00	1455.71	1465.79	1465.03	1468.39	0.004078	13.21	879.22	144.59	0.79
City Creek	13100	Bridge									
City Creek	13004	10470.00	1453.41	1461.20	1461.20	1464.58	0.006851	14.80	722.64	112.77	0.99
City Creek	12827	10470.00	1440.71	1453.04	1453.04	1457.06	0.004778	16.36	713.88	106.16	0.88
City Creek	12625	10470.00	1431.64	1444.27	1444.27	1448.52	0.005768	16.90	680.84	89.75	0.94
City Creek	12424	10470.00	1427.68	1436.41	1436.41	1439.90	0.006578	15.10	719.62	110.11	0.98
City Creek	12282.5	10470.00	1422.64	1432.54	1432.54	1436.38	0.006089	15.93	697.94	100.13	0.96
City Creek	12141	10470.00	1417.59	1429.27	1429.27	1433.29	0.005259	16.55	716.68	100.47	0.91
City Creek	12017	10470.00	1416.21	1427.56	1427.56	1431.18	0.005212	16.15	772.32	112.43	0.90
City Creek	11811	10470.00	1403.71	1417.48	1417.48	1422.35	0.005574	18.23	650.10	76.16	0.90
City Creek	11622	10470.00	1398.35	1412.20	1412.20	1416.25	0.004976	17.05	742.50	110.59	0.85
City Creek	11437	10470.00	1394.03	1407.73	1407.73	1412.06	0.005218	17.70	742.42	110.44	0.88
City Creek	11253	10470.00	1388.51	1401.78	1401.78	1405.82	0.004875	17.13	769.94	118.31	0.87
City Creek	11078	10470.00	1385.37	1397.88	1397.88	1401.44	0.004878	15.67	786.66	131.79	0.86
City Creek	10886	10470.00	1378.20	1387.81	1387.81	1391.50	0.006023	15.66	717.37	105.95	0.96
City Creek	10686	10470.00	1372.70	1384.86	1384.86	1389.45	0.005572	17.56	654.59	79.88	0.93
City Creek	10507	10470.00	1368.59	1380.77	1380.77	1384.88	0.005376	16.74	713.28	102.17	0.90
City Creek	10315	10470.00	1364.66	1374.20	1374.20	1378.23	0.006463	16.19	665.88	89.73	0.97
City Creek	10135	10470.00	1360.69	1372.41	1372.41	1376.61	0.005799	16.76	677.76	89.25	0.94
City Creek	9962	10470.00	1356.62	1367.09	1367.09	1370.96	0.006312	15.93	686.80	95.57	0.96
City Creek	9751	10470.00	1352.41	1362.43	1362.43	1366.13	0.005753	15.71	724.94	108.87	0.93
City Creek	9555	10470.00	1346.87	1355.11	1355.11	1358.65	0.006456	15.19	716.06	111.20	0.97
City Creek	9388	10470.00	1343.10	1350.26	1350.26	1353.25	0.007116	13.91	763.17	131.67	0.99
City Creek	9222	10470.00	1337.82	1346.52	1346.52	1349.94	0.006121	15.04	742.50	119.00	0.95
City Creek	9009	10470.00	1332.30	1340.93	1340.93	1344.67	0.006572	15.62	691.78	97.82	0.98
City Creek	8825	10470.00	1324.92	1336.14	1336.14	1339.94	0.006608	15.74	689.10	96.97	0.98
City Creek	8648	10470.00	1319.96	1331.44	1331.44	1335.26	0.005852	15.88	705.91	104.48	0.94
City Creek	8493	10470.00	1316.00	1327.15	1327.15	1331.13	0.005707	16.19	694.82	101.80	0.92
City Creek	8343	10470.00	1312.82	1322.44	1322.44	1326.61	0.006277	16.54	667.35	89.29	0.97
City Creek	8175	10470.00	1305.94	1316.82	1316.82	1320.93	0.006680	16.32	654.57	84.99	0.98
City Creek	8010	10470.00	1300.96	1312.81	1310.13	1314.54	0.002706	10.55	992.11	114.24	0.63
City Creek	7878	10470.00	1297.92	1313.46	1306.54	1314.03	0.000660	6.08	1803.18	470.25	0.32
City Creek	7795	10470.00	1295.97	1313.42	1305.10	1313.97	0.000646	5.99	1836.96	498.96	0.32
City Creek	7691	10470.00	1293.95	1313.50	1305.90	1313.86	0.000482	5.39	3021.31	733.50	0.28
City Creek	7600	Culvert									
City Creek	7513	10470.00	1290.30	1302.66	1302.66	1307.02	0.005459	17.06	673.27	89.21	0.92
City Creek	7437.75	10470.00	1286.64	1294.38	1294.38	1297.38	0.007092	13.96	764.96	136.22	0.99
City Creek	7362.5	10470.00	1282.90	1288.81	1288.81	1291.03	0.007651	12.03	892.60	216.52	0.98
City Creek	7213	10470.00	1277.86	1283.71	1283.71	1285.26	0.005591	10.59	1213.39	394.98	0.85
City Creek	7111	10470.00	1275.91	1281.37	1281.37	1282.84	0.008137	10.14	1138.38	383.09	0.96
City Creek	6993	10470.00	1275.87	1280.16	1279.73	1281.25	0.005579	8.46	1281.58	399.70	0.80
City Creek	6865	10470.00	1273.89	1279.68	1278.72	1280.64	0.003679	7.87	1348.12	328.89	0.67
City Creek	6789	10470.00	1272.98	1279.47	1278.31	1280.36	0.003196	7.60	1393.75	323.56	0.63
City Creek	6721	10470.00	1272.91	1279.50	1277.57	1280.11	0.001832	6.29	1677.69	336.64	0.49
City Creek	6600	Bridge									
City Creek	6565	10470.00	1268.00	1273.83	1273.83	1275.63	0.007728	11.00	1018.68	294.73	0.97
City Creek	6447	10470.00	1265.86	1271.16	1271.16	1273.11	0.007634	11.34	968.07	256.11	0.97
City Creek	6320	10470.00	1263.34	1268.44	1268.44	1270.34	0.007606	11.26	990.65	272.83	0.97
City Creek	6217	10470.00	1260.86	1266.57	1266.57	1268.43	0.007831	11.08	992.15	277.18	0.97
City Creek	6047	10470.00	1257.73	1263.65	1263.65	1265.45	0.007797	11.20	1032.46	297.35	0.97
City Creek	5828	10470.00	1253.90	1259.70	1259.70	1261.63	0.007572	11.60	996.97	264.17	0.97
City Creek	5607	10470.00	1249.51	1255.86	1255.86	1258.02	0.007783	11.87	902.35	215.10	0.99
City Creek	5400	10470.00	1245.45	1253.15	1253.15	1255.75	0.007294	13.07	839.93	180.38	0.99
City Creek	5203	10470.00	1240.83	1249.00	1249.00	1251.53	0.006567	13.06	868.67	180.94	0.95
City Creek	4989	10470.00	1236.92	1244.69	1244.69	1247.24	0.006528	13.18	871.88	181.12	0.95
City Creek	4812	10470.00	1234.00	1242.57	1242.57	1245.30	0.005983	13.72	860.08	168.00	0.93
City Creek	4652	10470.00	1230.86	1239.18	1239.18	1241.61	0.007247	12.67	865.06	186.91	0.98

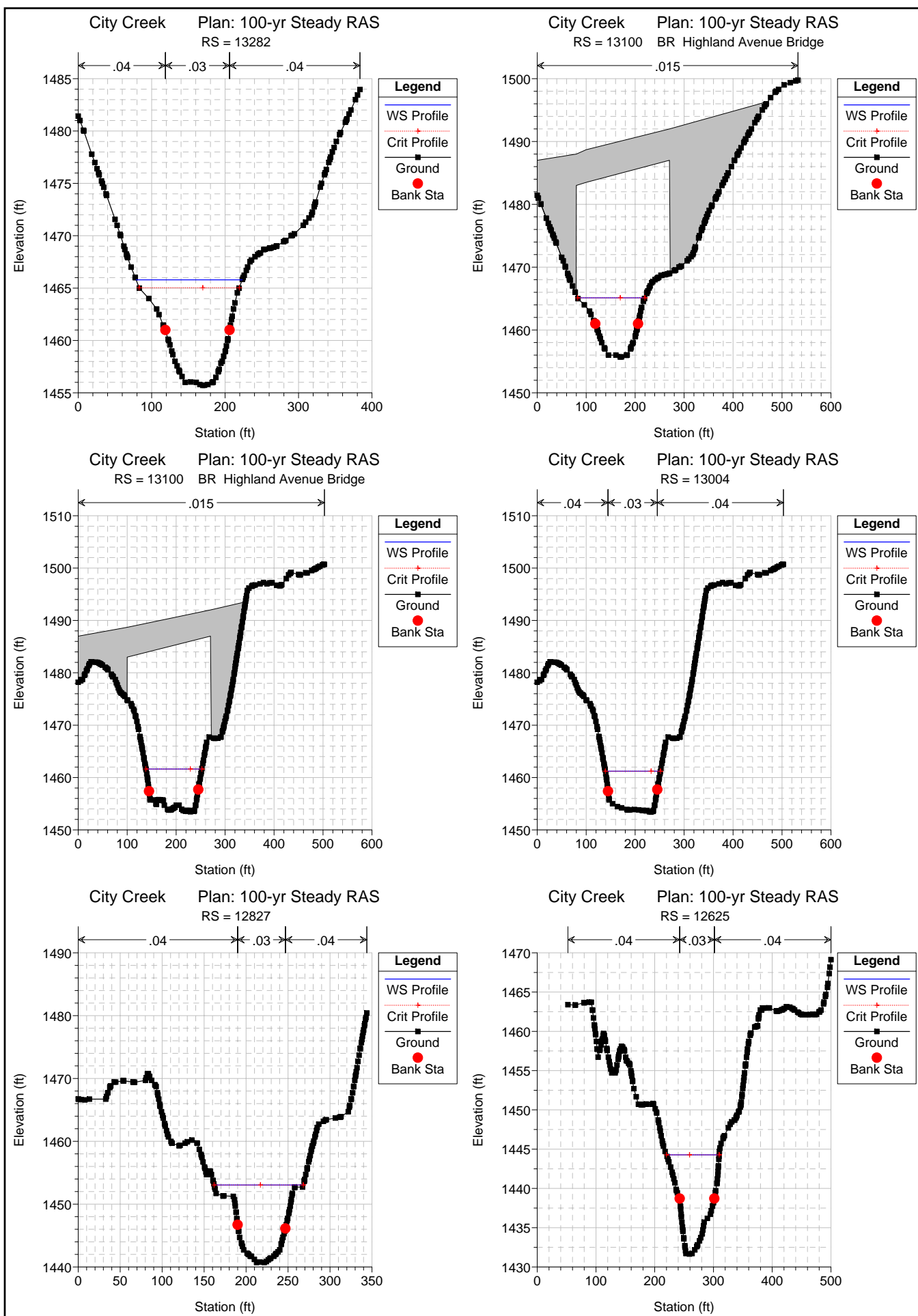
HEC-RAS Plan: 100-yr Steady River: City Creek Reach: City Creek Profile: Profile (Continued)

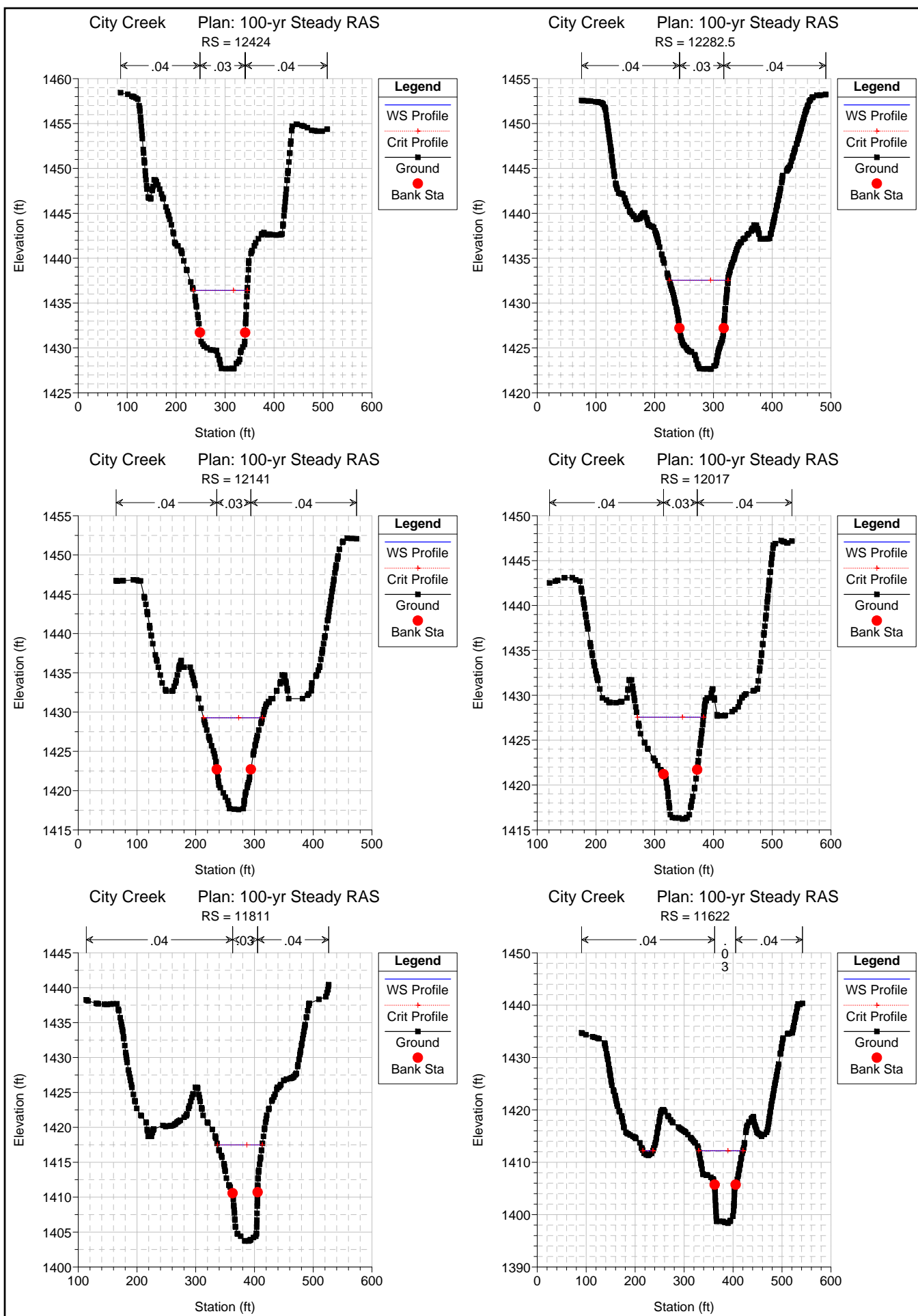
Reach	River Sta	Q Total (cfs)	Min Ch El (ft)	W.S. Elev (ft)	Crit W.S. (ft)	E.G. Elev (ft)	E.G. Slope (ft/ft)	Vel Chnl (ft/s)	Flow Area (sq ft)	Top Width (ft)	Froude # Chl
City Creek	4477	10470.00	1229.00	1236.26	1236.26	1238.73	0.007286	12.73	855.63	183.66	0.98
City Creek	4318	10470.00	1226.90	1233.76	1233.76	1235.98	0.007008	12.16	917.28	218.23	0.95
City Creek	4149	10470.00	1223.97	1231.26	1231.26	1233.26	0.007668	11.55	957.84	247.73	0.98
City Creek	4007	10470.00	1223.80	1228.70	1228.70	1229.87	0.006945	9.69	1400.84	580.12	0.90
City Creek	3885	10470.00	1220.99	1226.61	1226.61	1227.73	0.006527	9.59	1464.53	622.40	0.88
City Creek	3773	10470.00	1219.95	1225.21	1225.21	1226.62	0.007246	9.86	1208.01	467.99	0.92
City Creek	3647	10470.00	1217.95	1223.39	1223.39	1224.89	0.007619	10.23	1156.26	407.24	0.94
City Creek	3498	10470.00	1215.91	1222.31	1221.23	1223.13	0.003176	7.29	1483.21	389.95	0.62
City Creek	3470	Bridge									
City Creek	3380	10470.00	1214.79	1220.74	1219.60	1221.50	0.002685	7.32	1649.80	446.83	0.59
City Creek	3350	10470.00	1213.80	1220.71	1219.35	1221.40	0.002299	6.95	1671.29	394.98	0.55
City Creek	3340	Bridge									
City Creek	3244	10470.00	1212.74	1217.48	1217.48	1218.98	0.007606	10.01	1126.32	385.92	0.94
City Creek	3115	10470.00	1211.00	1215.99	1215.99	1217.61	0.008725	10.26	1035.34	324.32	0.99
City Creek	2969	10470.00	1210.00	1214.28	1214.28	1215.96	0.008644	10.46	1026.72	319.70	1.00
City Creek	2778	10470.00	1208.00	1212.46	1212.45	1214.14	0.008872	10.41	1011.11	309.22	1.00
City Creek	2623	10470.00	1207.00	1211.28	1211.11	1212.85	0.007365	10.08	1047.12	300.66	0.93
City Creek	2452	10470.00	1205.79	1210.16	1209.85	1211.65	0.006478	9.82	1078.83	312.76	0.88
City Creek	2258	10470.00	1204.12	1208.64	1208.47	1210.31	0.007202	10.42	1025.04	282.56	0.93
City Creek	2073	10470.00	1203.00	1208.57	1206.97	1209.33	0.002351	7.00	1530.26	327.85	0.55
City Creek	1800	Bridge									
City Creek	1702	10470.00	1200.93	1206.56	1205.27	1207.75	0.003320	8.76	1200.90	226.87	0.66
City Creek	1559	10470.00	1199.95	1204.79	1204.79	1206.96	0.007573	11.94	909.83	219.43	0.98
City Creek	1378	10470.00	1198.57	1203.13	1202.63	1204.59	0.005547	9.73	1089.43	266.26	0.83
City Creek	1190	10470.00	1197.38	1201.91	1201.60	1203.47	0.006396	10.03	1056.08	275.66	0.88
City Creek	999	10470.00	1196.48	1201.07	1200.42	1202.32	0.004836	8.99	1186.61	301.77	0.77
City Creek	790	10470.00	1195.18	1200.20	1199.36	1201.35	0.004183	8.65	1231.35	298.02	0.72
City Creek	600	10470.00	1194.27	1198.90	1198.54	1200.38	0.006006	9.82	1095.36	290.93	0.86

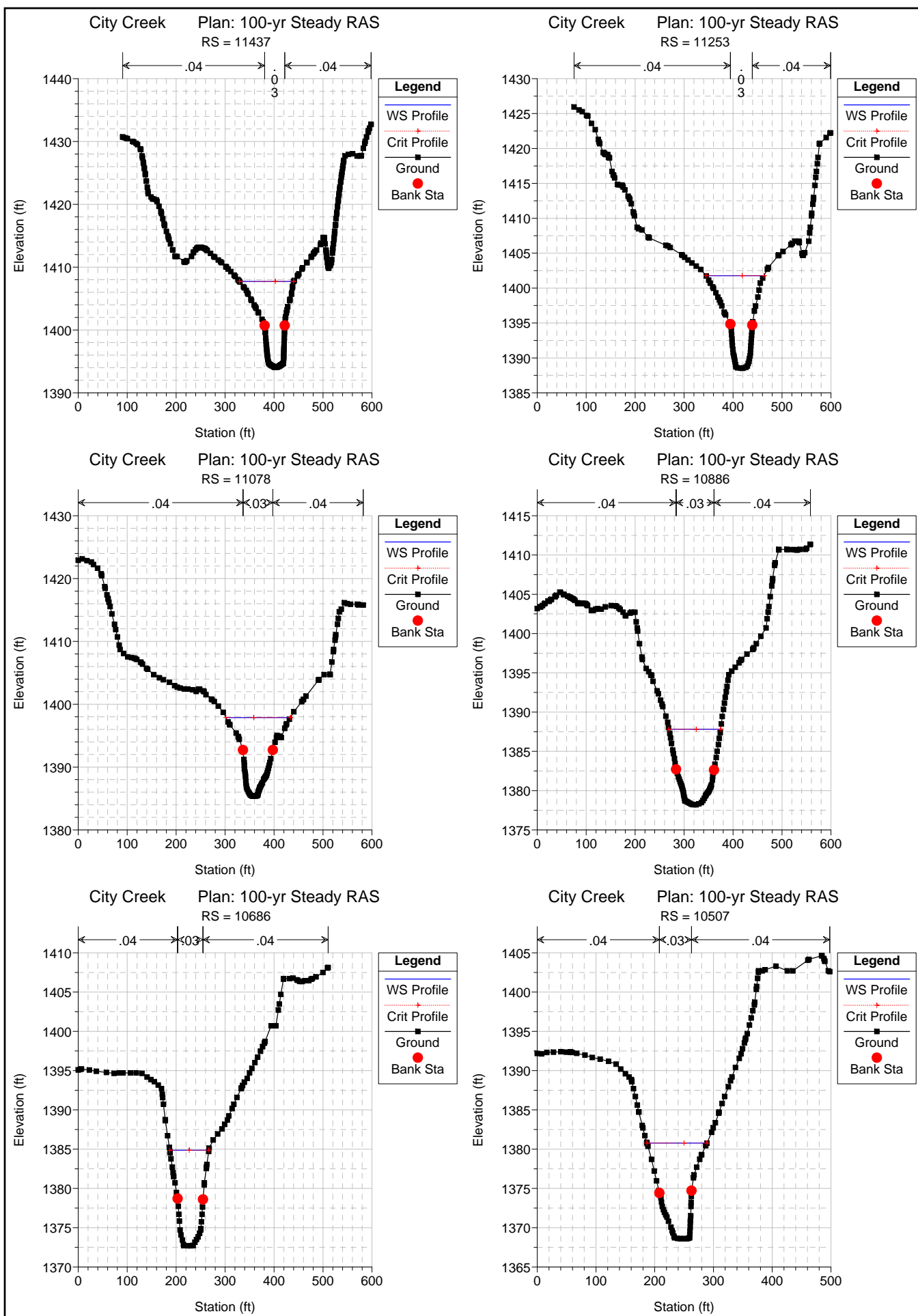


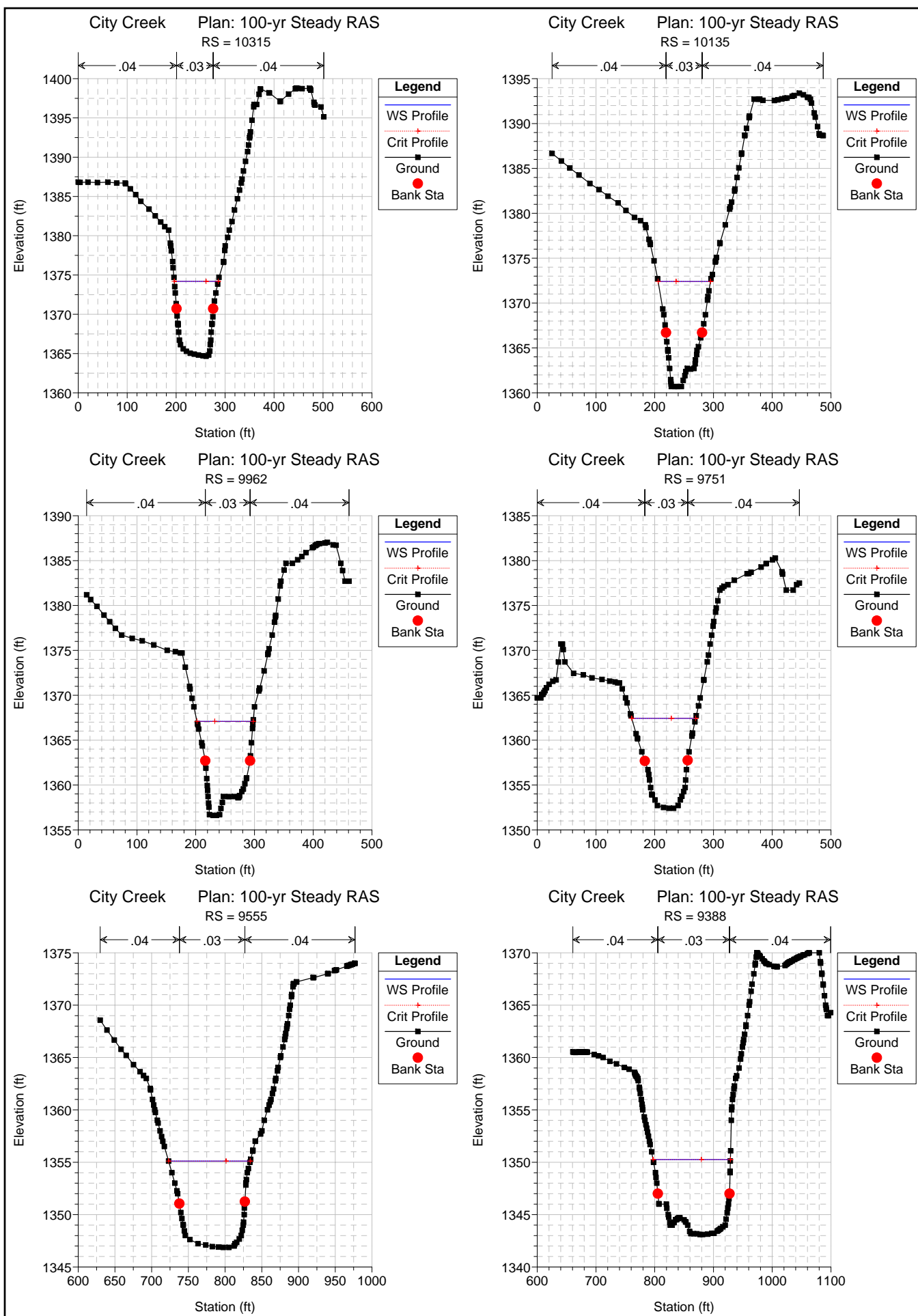


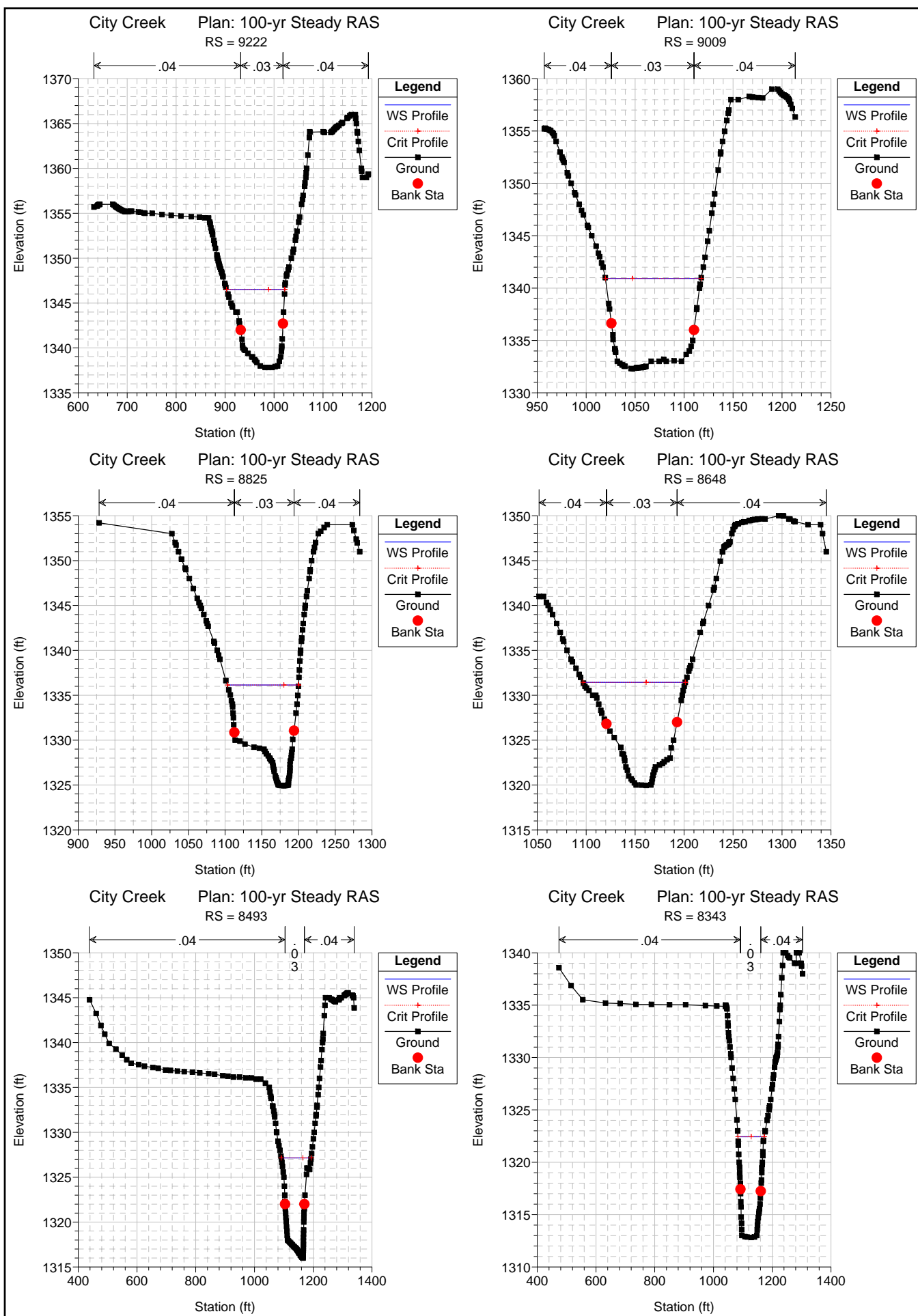


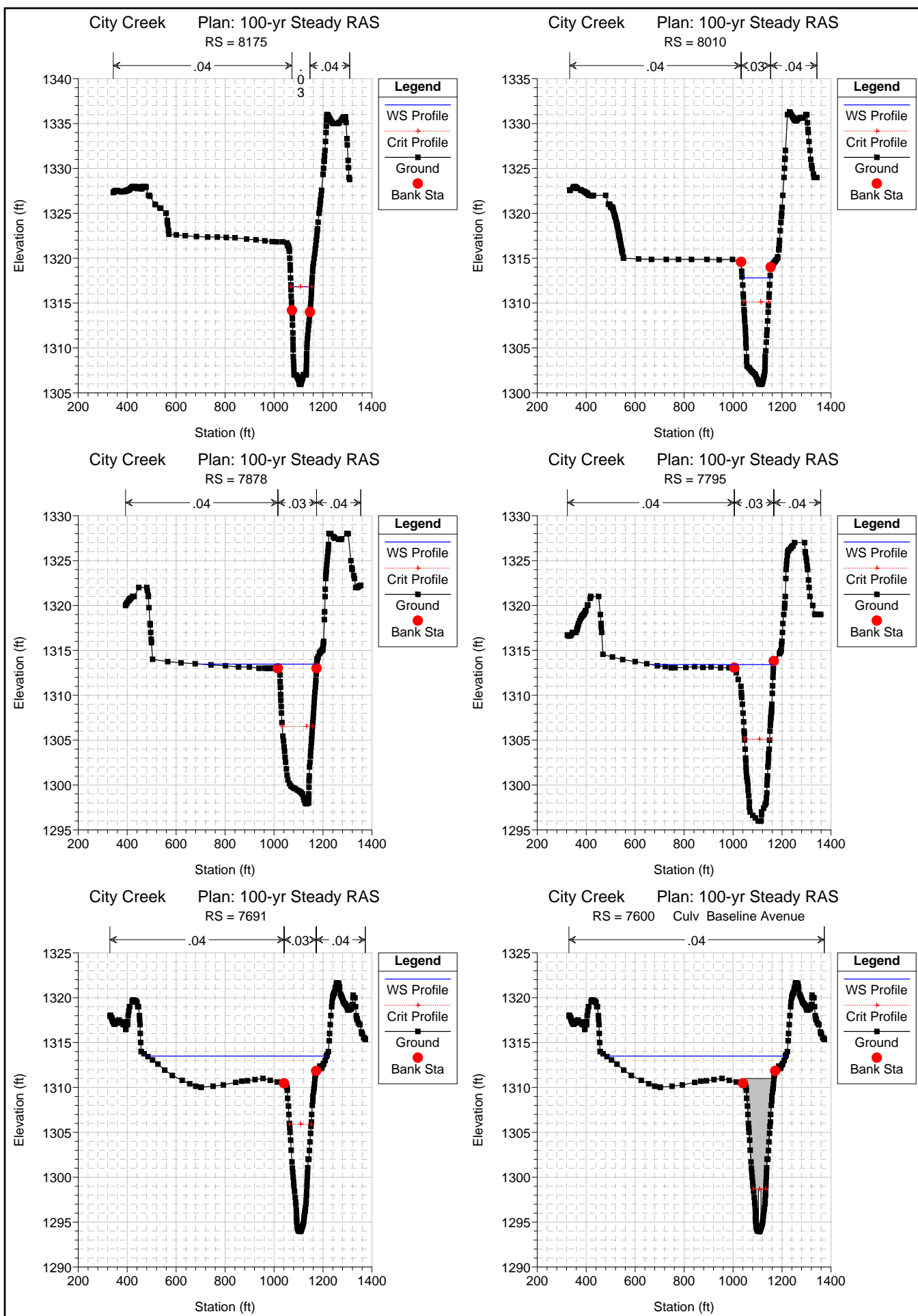


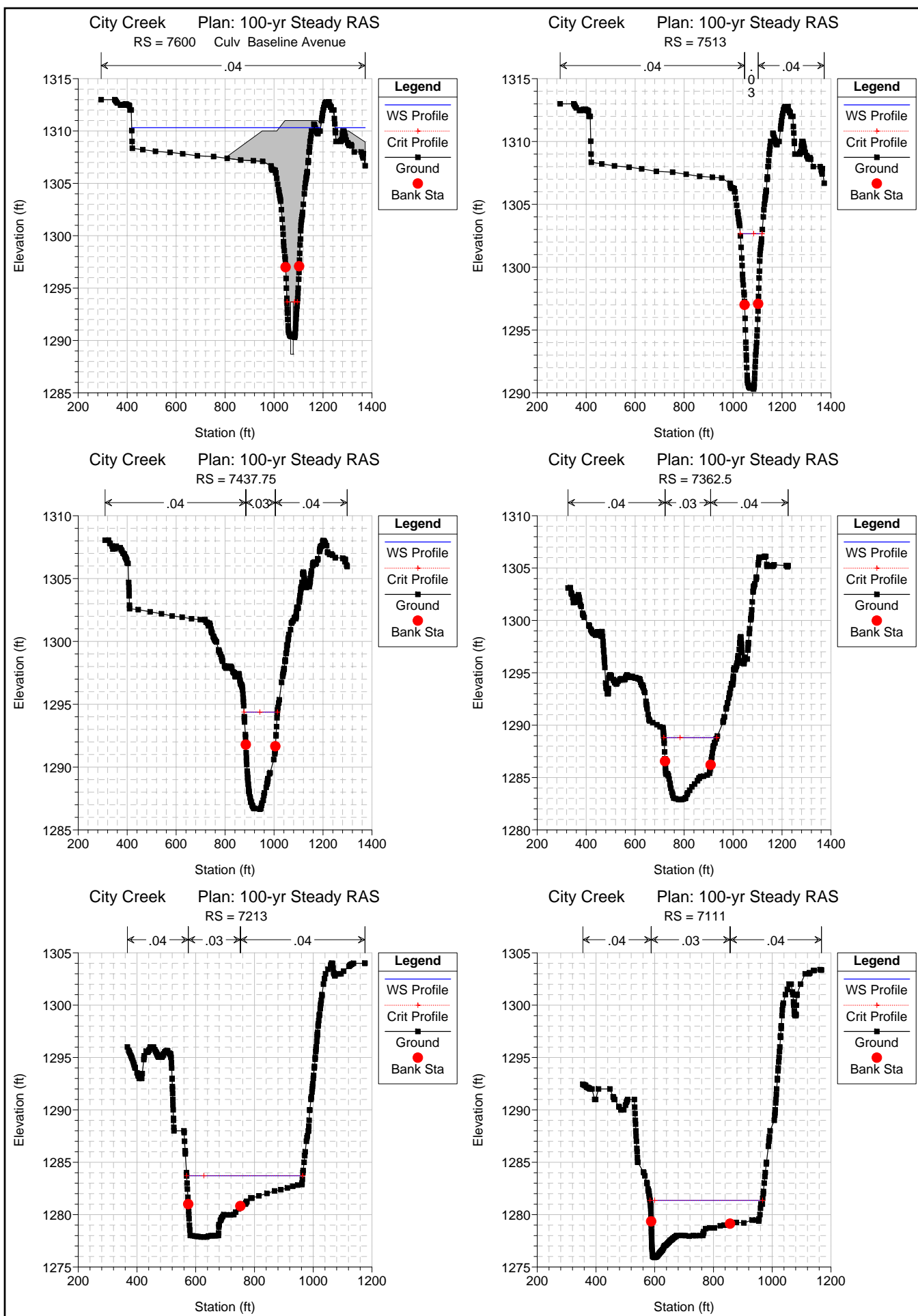


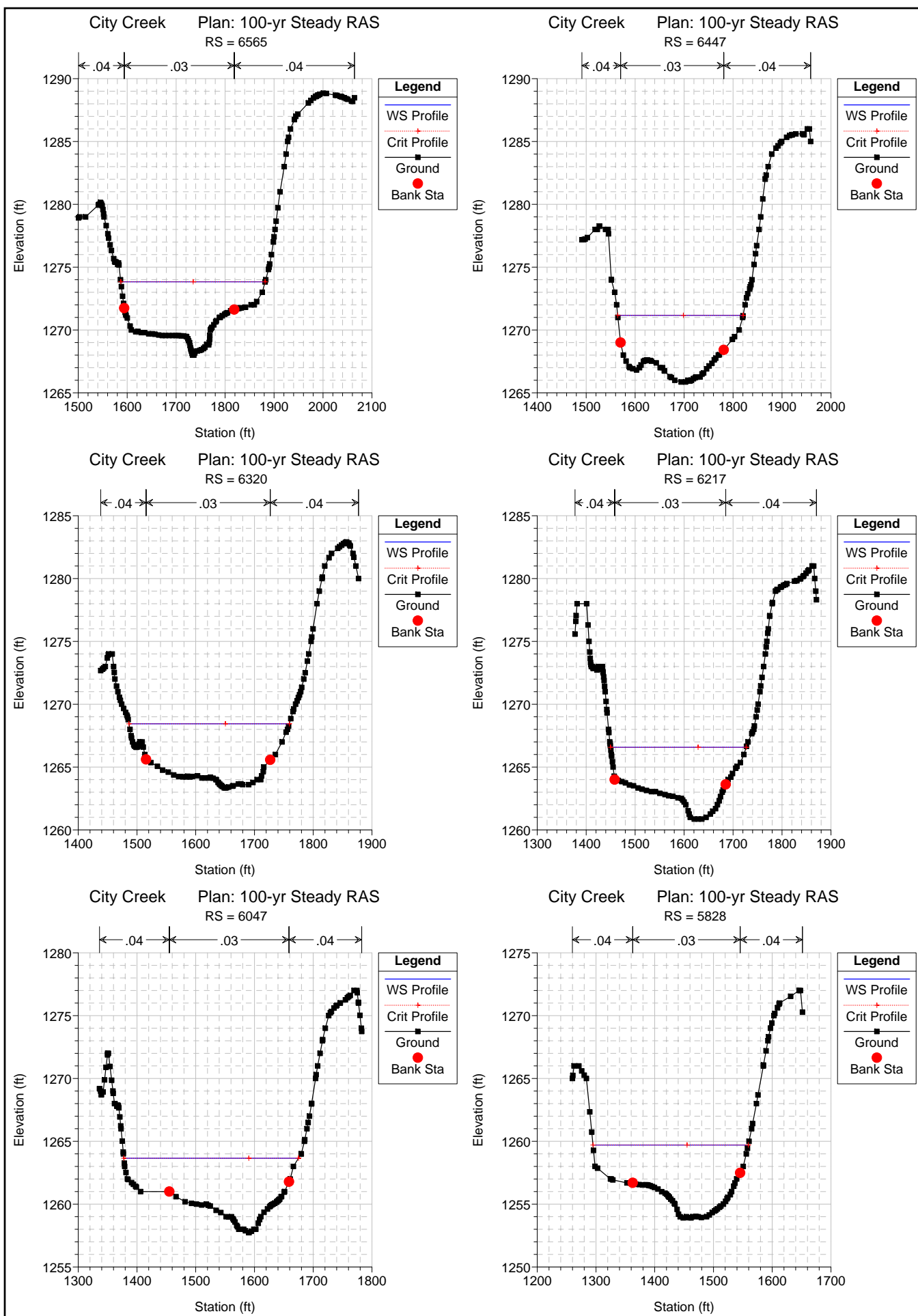


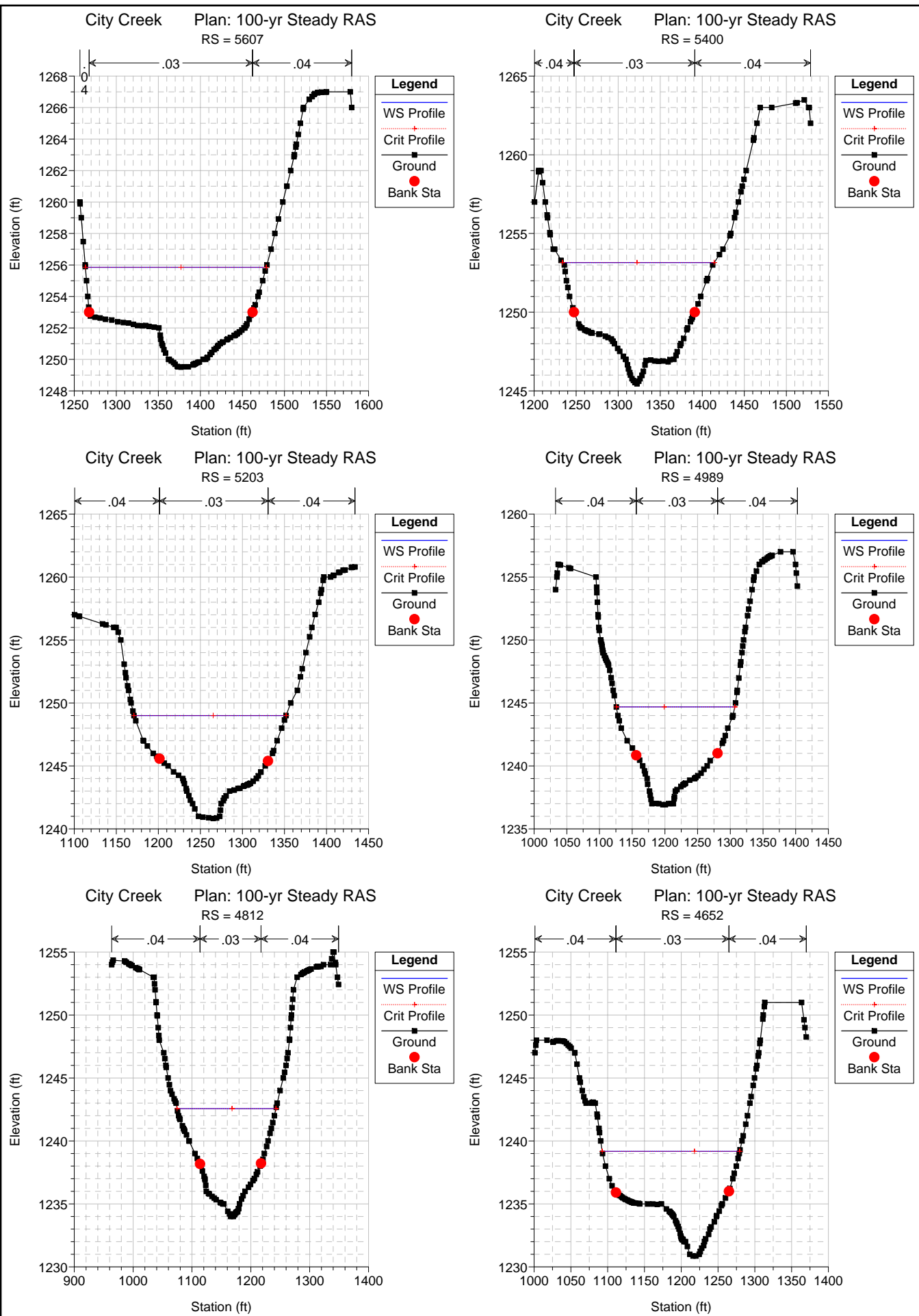


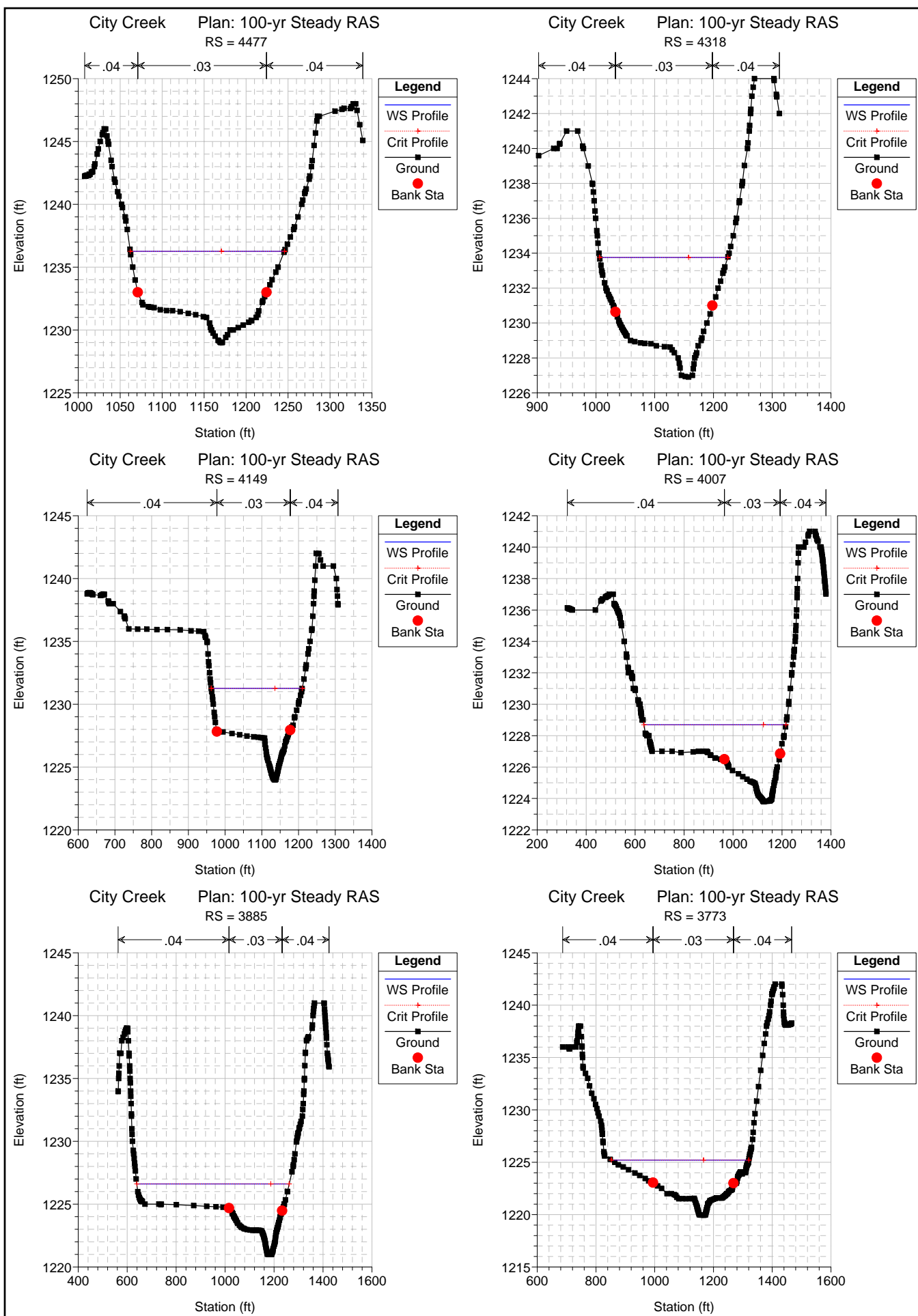


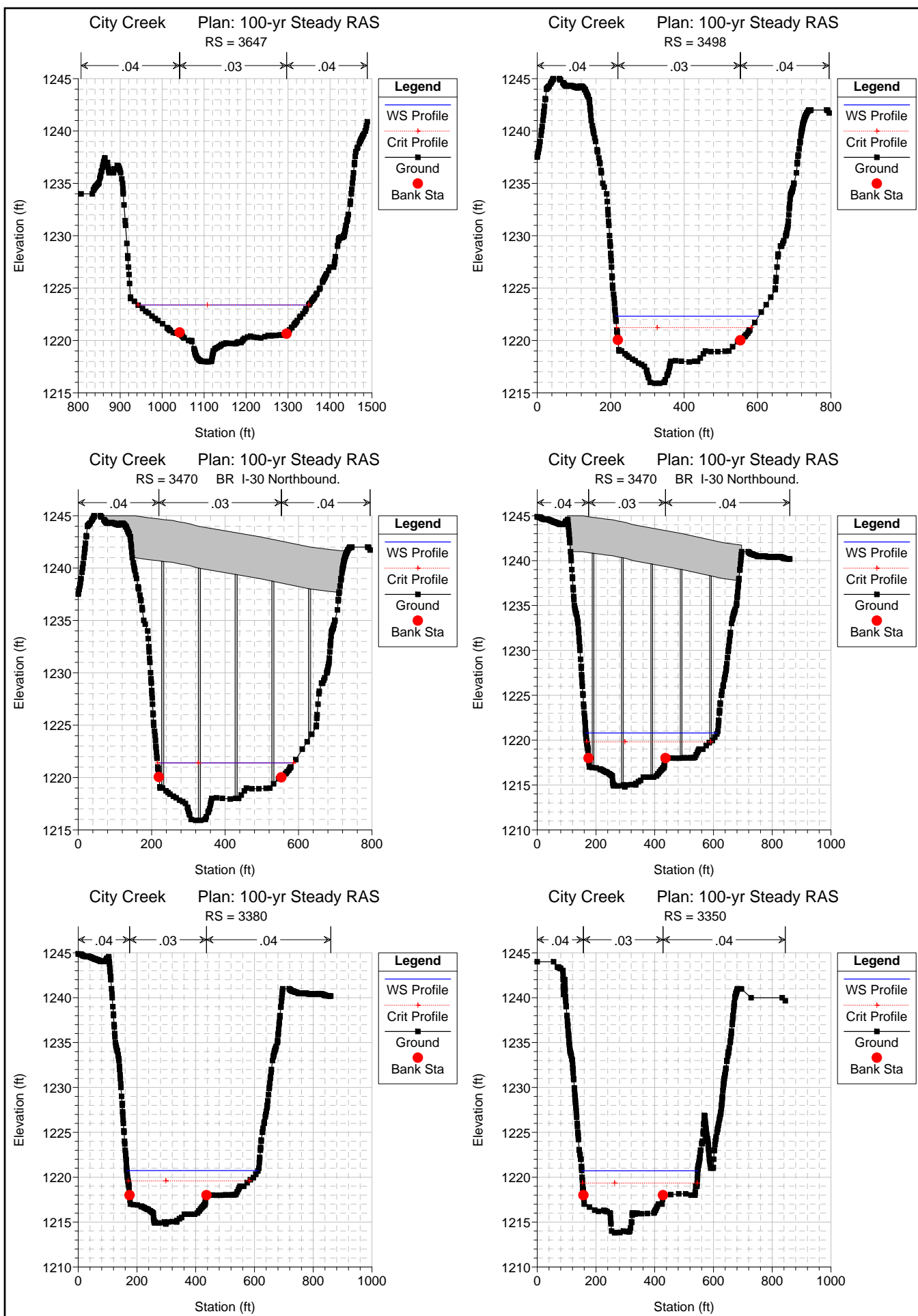


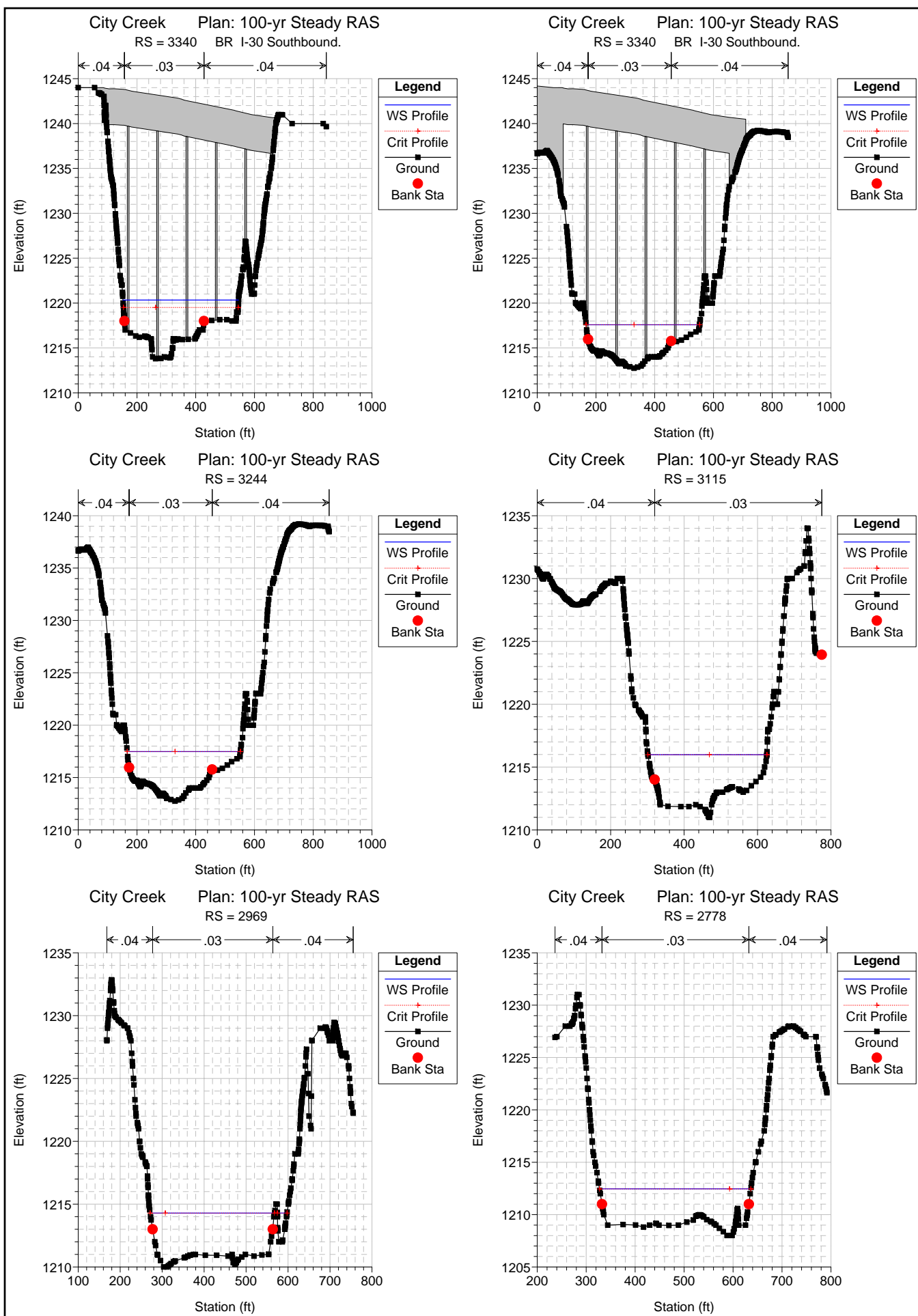


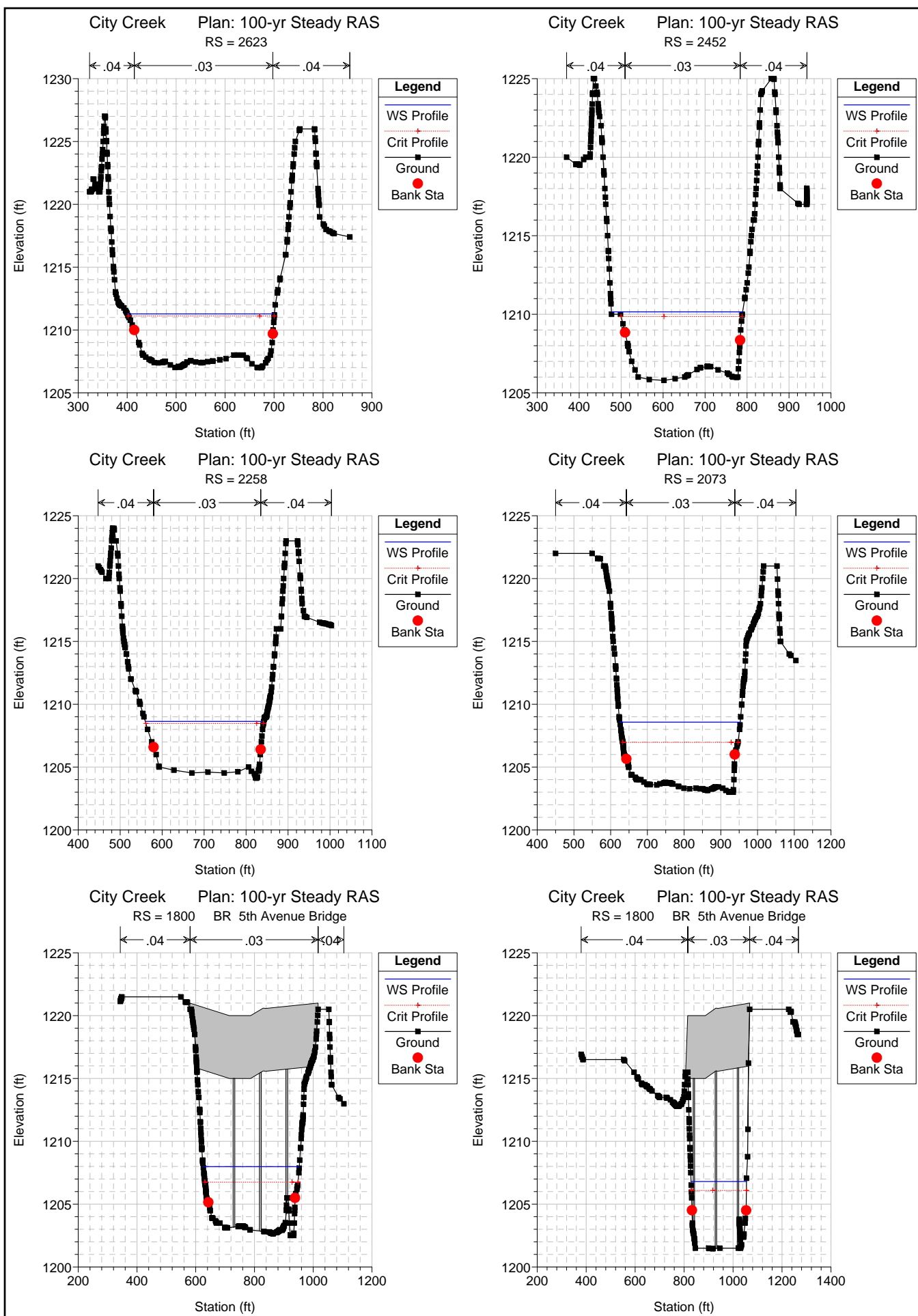


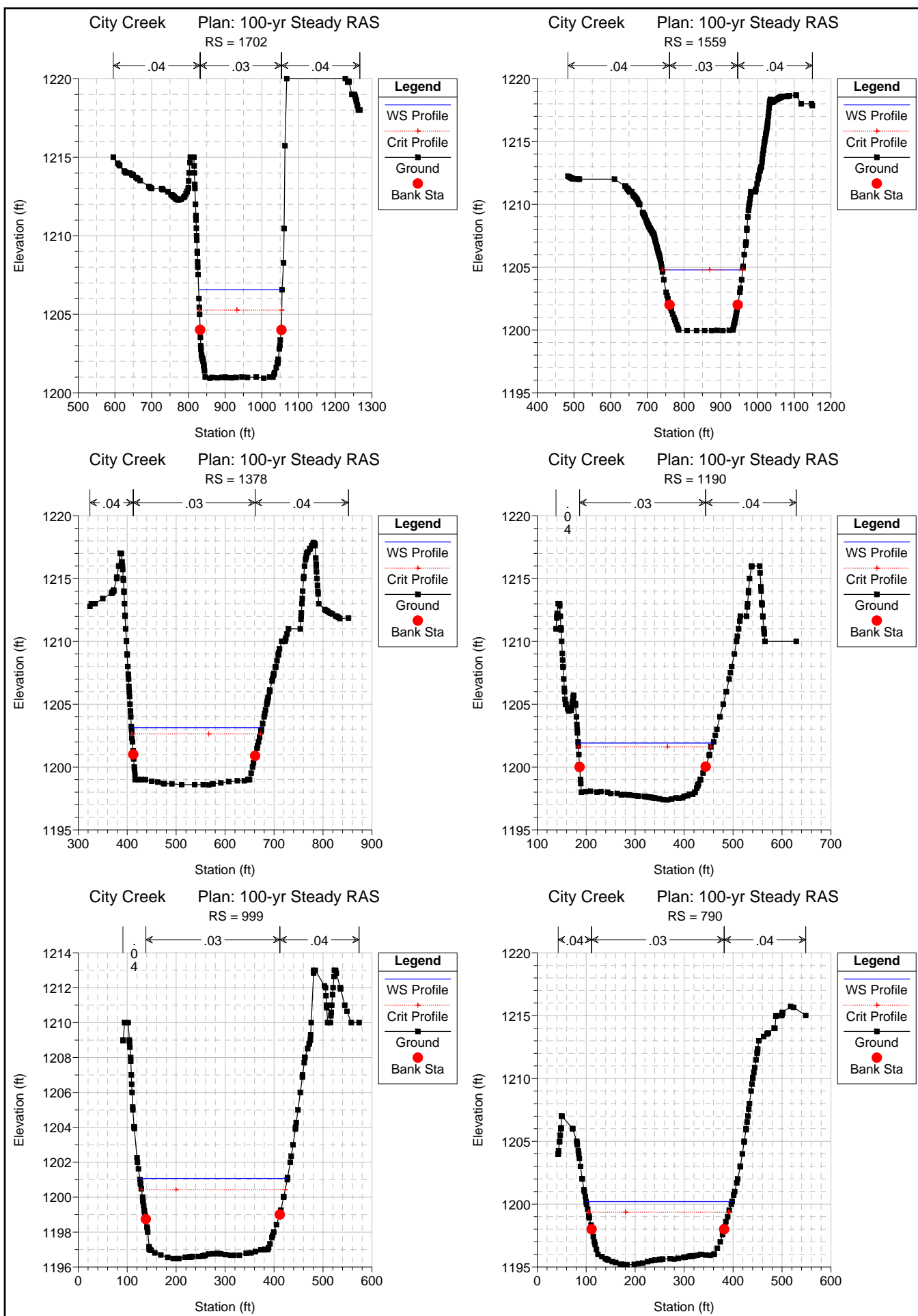






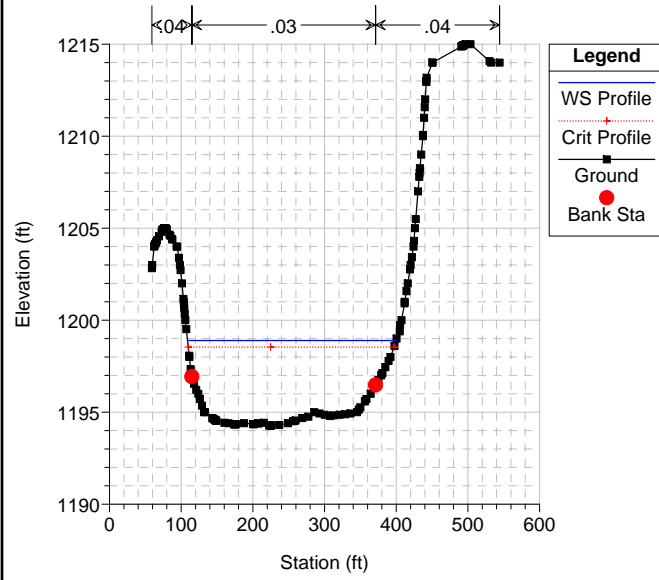






City Creek Plan: 100-yr Steady RAS

RS = 600



APPENDIX F-3

Upper SAR HCP Approved Covered Activities

San Bernardino County Flood Control District

Rialto Channel Regional Flood Control System (ID: FC.1)

The Rialto Channel project would increase channel capacity and reduce impediments to flow between Cactus Basins, Interstate-10 (I-10), and the Santa Ana River. Covered activities are based upon the hydraulic needs to convey the flow. The final design for each reach may change once an alternative analysis is performed

Reach 1 – Santa Ana River to Agua Mansa Road

This reach involves constructing a new high flow concrete rectangular channel parallel to an existing trapezoidal channel with rock side slopes and a 30-foot wide earthen bottom. Improvements involve widening an existing concrete trapezoidal channel immediately upstream of Agua Mansa Road to convey high flows into the new concrete channel. The new channel will be constructed in an upland area. Initial storm flows will continue to drain into the earthen channel downstream of Agua Mansa Road. Modifications to the existing flood control channel to concentrate the high flows into the parallel channel would improve sucker habitat by minimizing flow velocities and increases in flows by future connections to the system.

The lining of this section will not have any impact on the peak flow rates downstream. Although there is a constriction removal at Riverside Avenue, the flows in Rialto Channel are still limited by the box culvert beneath the I-10 Freeway. The net infiltration rate into the Rialto channel will be unchanged for nuisance flows as flows will be carried down to the unlined portion of the channel downstream of the petrochemical tank farm (just upstream of Santa Ana Avenue) and it is not planned to be lined.

Some specific activities that are expected within the existing portion of Rialto Channel for this reach includes removal of sediment, removal of trash and debris, railing maintenance, invert stabilization and repairs, weed abatement, and general control of existing and planned lateral connections.

Collectively, Flood Control estimates no new permanent ground disturbance for the Santa Ana River to Agua Mansa Road reach only 4 acres of temporary impacts.

Reach 2 – Agua Mansa Road to Santa Ana Avenue

This reach involves improving an approximately half mile of existing concrete trapezoidal channel with a 20-foot wide bottom. Existing improvements include a culvert crossing located mid- reach consisting of construction of floodwalls at east and west portions of the right of way. Improvements involve the paving of access roads with asphalt or concrete, new floodwalls at the top of the existing channel and replacement of the mentioned existing concrete box culvert approximately 1,130 feet upstream of Agua Mansa Road. This culvert is within the existing concrete channel section and is used as a bridge to get to the other side of the channel.

Flood Control estimates that these activities would result in no of new permanent ground disturbance as no additional concrete is proposed with the channel bed.

Reach 3 – Santa Ana Avenue to Sycamore Avenue

This reach involves approximately a half mile of composite material trapezoidal channel with 20-foot wide bottom. The channel is lined with concrete on the westerly side-slope and rock lined on the easterly side-slope. The invert is rock and gravel. Improvements involve widening and stabilizing the earthen bottom section from 300 feet downstream of Santa Ana Avenue to Sycamore Avenue. Improvements may involve construction of a concreted rock slope protection on the southwest side only and construction of concreted rock grade control structures at intervals along the reach.

The existing channel conveys the entire Q100 storm flow but is prone to scour and the side-slopes may collapse if they are undermined. The project will conduct channel and bank stabilization work designed to convey the ultimate condition Q100 flow of over 10,000 cfs through the area. The proposed configuration and material has not yet been determined. However, concrete-lining would not occur. The area immediately downstream of the concrete may be expanded in width in order to hold a pool. Vegetation would be allowed to establish and water would flow naturally over a soft bottom to the concrete portion located near the Rialto wastewater treatment plant (WWTP) outfall. Construction would consist of stabilizing the invert and side-slopes with grouted and non-grouted rock slope segments. Habitat restoration may be included in order to offset work on upstream segments.

Flood Control estimates that these activities would result in 1 acre of new permanent ground disturbance.

Reach 5 – Slover Avenue to Riverside Avenue

Improvements include approximately 300 feet of the existing 15-foot by 15-foot box culvert under Riverside Avenue and Cameron Way including expansion of the channel capacity under Riverside Avenue which is currently a single box culvert. At Riverside Avenue, the proposed project would install a proposed concrete rectangular channel designed to convey the ultimate condition Q100 flow of 9,563 cfs.

Flood Control estimates that these activities would result in 0.1 acres of new permanent ground disturbance.

Reach 6 – Riverside Avenue to I-10 Freeway

This reach involves approximately 650-foot earthen trapezoidal channel from Riverside Avenue to the location of the I-10 Freeway at a railroad culvert and a paved access road from Interstate 10 Freeway and Union Pacific Railroad south to Riverside Avenue.

Currently, ongoing maintenance needs within this area are extensive due to buildup of debris, erosion, weeds, and trash associated with human trespass. Flood events often result in damage to the system that require timely repair. Riparian vegetation (native and non-native species) and sediment would be permanently removed in order to concrete-line the channel and better convey nuisance runoff flow downstream of the railroad yard. This portion of the project site currently includes an existing earthen bottom channel with rock rip-rap sides. Coarse sediment may be periodically placed into this location in order to provide a source of material to replenish the supply of gravels and cobbles downstream within occupied Santa Ana Sucker habitat. Trucks carrying the coarse material would use existing roads and staging areas within the rail yard to access the input location.

Flood Control estimates that these activities would result in 1 acre of new permanent ground disturbance.

Reach 7 – Bulkhead Removal

This project involves removal of an existing bulkhead at the northern opening of the culvert under the I-10 Freeway. The previously mentioned downstream facilities are either undersized or not stable enough to convey the Q100 flow in the area. Therefore, one side of an existing double 15 foot wide by 15 foot wide box culvert is blocked to limit flows into these reaches. Therefore, the existing culvert is purposely operating at half capacity. The removal of the bulkhead will allow for new connections to the system upstream of the freeway and alleviate flooding through the area north of the freeway and the freeway itself. Once the downstream channel is able to accommodate greater flows, the bulkhead at the I-10 Freeway would be removed.

Flood Control estimates that this activity would result in 0.1 acres of temporary ground disturbance and no permanent ground disturbance.

Reach 8 – Willow Avenue to Metrolink Railroad

The Rialto Channel project includes several components within this reach of the Rialto Channel which includes approximately 1.75 miles of earthen trapezoidal channel with loose rock lining and culvert crossings at San Bernardino Avenue and Lilac Avenue, Bloomington Avenue, Randall Avenue, and Merrill Avenue. The design may include redirection of runoff from roadways and development areas within Rialto into the Rialto Channel for conveyance downstream. Overall, this will be an improved channel designed to alleviate flooding in the surrounding area and be able to convey the ultimate condition Q100 flow ranging from 4,281 cfs to 6,708 cfs. The channel configuration and lining type have not yet been determined. The new design could include a concrete box culvert being installed underneath the existing Flood Control access road. The box would convey peak flow during large storm events. Normal flow would be within the earthen bottom portion of Rialto Channel to Willow Avenue where the channel becomes concrete lined. The current capacity of the channel ranges from a couple hundred cfs second to several hundred cfs.

Channel improvements (or storm drain improvements) are proposed from Willow Avenue to the Metrolink railroad crossing. Construction involves ultimate concrete channels, culverts, bio swales, and paved access roads. Flood Control estimates that these activities would result in approximately 8 acres of new permanent ground disturbance.

Reach 9 – Metrolink Railroad to 2nd Street

Improvements to this reach would include improvements to existing culvert crossings at Cactus Avenue, the Metrolink railroad spur, Rialto Avenue, the railroad, and Second Street. This reach includes approximately 0.5 mile of earthen trapezoidal channel with loose rock lining. Improvements include constructing ultimate concrete channels, culverts, bio swales, and paved access roads. Flood Control estimates that these activities would result in approximately 2 acres of new permanent ground disturbance. Refer to the discussion for Reach 8 for additional detail regarding design and flow direction for this reach.

Reach 10 – 2nd Street to Etiwanda Avenue

Improvements to this reach include approximately 1 mile of earthen trapezoidal channel with loose rock lining at the Foothill Boulevard and Etiwanda Avenue culvert crossings. Concrete channels, culverts, bio swales, and paved access roads may ultimately be constructed in this location.

Flood Control estimates that these activities would result in approximately 2 acres of new permanent ground disturbance. Refer to the discussion for Reach 8 for additional detail regarding design and flow direction for this reach.

Reach 11 – Cactus Recharge Basins 1 & 2

This reach involves an area contained within two existing flood control basins with earthen bottom and slopes, concrete spillways, channels, culverts, and rock slope protection. Construction improvements involve potential excavation to provide additional storm flow attenuation. Flood Control will permanently remove vegetation and sediment from the recharge basins and construct new low flow outlets.

Flood Control estimates that these activities would result in 24 acres of temporary ground disturbance and less than 0.5 acres of permanent ground disturbance.

Maintenance

See Section 2.3.2, Routine Operations and Maintenance for general operations and maintenance conducted by the Flood Control District for their existing or planned facilities.